ADVANCES IN
VAGAL AFFERENT NEUROBIOLOGY

FRONTIERS IN NEUROSCIENCE

Series Editors
Sidney A. Simon, Ph.D.
Miguel A.L. Nicolelis, M.D., Ph.D.

Published Titles

Apoptosis in Neurobiology
Yusuf A. Hannun, M.D., Professor of Biomedical Research and Chairman/Department of Biochemistry and Molecular Biology, Medical University of South Carolina
Rose-Mary Boustany, M.D., tenured Associate Professor of Pediatrics and Neurobiology, Duke University Medical Center

Methods for Neural Ensemble Recordings
Miguel A.L. Nicolelis, M.D., Ph.D., Professor of Neurobiology and Biomedical Engineering, Duke University Medical Center

Methods of Behavioral Analysis in Neuroscience
Jerry J. Buccafusco, Ph.D., Alzheimer's Research Center, Professor of Pharmacology and Toxicology, Professor of Psychiatry and Health Behavior, Medical College of Georgia

Neural Prostheses for Restoration of Sensory and Motor Function
John K. Chapin, Ph.D., Professor of Physiology and Pharmacology, State University of New York Health Science Center
Karen A. Moxon, Ph.D., Assistant Professor/School of Biomedical Engineering, Science, and Health Systems, Drexel University

Computational Neuroscience: Realistic Modeling for Experimentalists
Eric DeSchutter, M.D., Ph.D., Professor/Department of Medicine, University of Antwerp

Methods in Pain Research
Lawrence Kruger, Ph.D., Professor of Neurobiology (Emeritus), UCLA School of Medicine and Brain Research Institute

Motor Neurobiology of the Spinal Cord
Timothy C. Cope, Ph.D., Professor of Physiology, Emory University School of Medicine

Nicotinic Receptors in the Nervous System
Edward D. Levin, Ph.D., Associate Professor/Department of Psychiatry and Pharmacology and Molecular Cancer Biology and Department of Psychiatry and Behavioral Sciences, Duke University School of Medicine

Methods in Genomic Neuroscience
Helmin R. Chin, Ph.D., Genetics Research Branch, NIMH, NIH
Steven O. Moldin, Ph.D, Genetics Research Branch, NIMH, NIH

Methods in Chemosensory Research
Sidney A. Simon, Ph.D., Professor of Neurobiology, Biomedical Engineering, and Anesthesiology, Duke University
Miguel A.L. Nicolelis, M.D., Ph.D., Professor of Neurobiology and Biomedical Engineering, Duke University

The Somatosensory System: Deciphering the Brain's Own Body Image
Randall J. Nelson, Ph.D., Professor of Anatomy and Neurobiology,
    University of Tennessee Health Sciences Center

The Superior Colliculus: New Approaches for Studying Sensorimotor Integration
William C. Hall, Ph.D., Department of Neuroscience, Duke University
Adonis Moschovakis, Ph.D., Institute of Applied and Computational Mathematics, Crete

New Concepts in Cerebral Ischemia
Rick C. S. Lin, Ph.D., Professor of Anatomy, University of Mississippi Medical Center

DNA Arrays: Technologies and Experimental Strategies
Elena Grigorenko, Ph.D., Technology Development Group, Millennium Pharmaceuticals

Methods for Alcohol-Related Neuroscience Research
Yuan Liu, Ph.D., National Institute of Neurological Disorders and Stroke, National Institutes
    of Health
David M. Lovinger, Ph.D., Laboratory of Integrative Neuroscience, NIAAA

***In Vivo* Optical Imaging of Brain Function**
Ron Frostig, Ph.D., Associate Professor/Department of Psychobiology,
    University of California, Irvine

Primate Audition: Behavior and Neurobiology
Asif A. Ghazanfar, Ph.D., Primate Cognitive Neuroscience Lab, Harvard University

Methods in Drug Abuse Research: Cellular and Circuit Level Analyses
Dr. Barry D. Waterhouse, Ph.D., MCP-Hahnemann University

Functional and Neural Mechanisms of Interval Timing
Warren H. Meck, Ph.D., Professor of Psychology, Duke University

Biomedical Imaging in Experimental Neuroscience
Nick Van Bruggen, Ph.D., Department of Neuroscience Genentech, Inc.,
    South San Francisco
Timothy P.L. Roberts, Ph.D., Associate Professor, University of Toronto

The Primate Visual System
John H. Kaas, Department of Psychology, Vanderbilt University
Christine Collins, Department of Psychology, Vanderbilt University

Neurosteroid Effects in the Central Nervous System
Sheryl S. Smith, Ph.D., Department of Physiology, SUNY Health Science Center

Modern Neurosurgery: Clinical Translation of Neuroscience Advances
Dennis A. Turner, Department of Surgery, Division of Neurosurgery, Duke University
    Medical Center

Sleep: Circuits and Functions
Pierre-Hervé Luoou, Université Claude Bernard Lyon I, Lyon, France

Methods in Insect Sensory Neuroscience
Thomas A. Christensen, Arizona Research Laboratories, Division of Neurobiology, University
    of Arizona, Tucson, AZ

Motor Cortex in Voluntary Movements
Alexa Riehle, INCM-CNRS, Marseille, France
Eilon Vaadia, The Hebrew University, Jeruselum, Israel

Advances in Vagal Afferent Neurobiology
Bradley J. Undem, Johns Hopkins Asthma Center, Baltimore, MD
Daniel Weinreich, University of Maryland, Baltimore, MD

ADVANCES IN
VAGAL AFFERENT NEUROBIOLOGY

Edited by

Bradley J. Undem
Johns Hopkins Asthma Center
Baltimore, MD

Daniel Weinreich
University of Maryland
Baltimore, MD

CRC Taylor & Francis
Taylor & Francis Group

Boca Raton   London   New York   Singapore

Dedication

*This volume is devoted to
the loving memory of Dr. Cinda Helke*

Series Preface

The Frontiers in Neuroscience series presents the insights of experts on emerging experimental techniques and theoretical concepts that are or will be at the vanguard of neuroscience. Books in the series cover topics ranging from methods to investigate apoptosis to modern techniques for neural ensemble recordings in behaving animals. The series also covers new and exciting multidisciplinary areas of brain research, such as computational neuroscience and neuroengineering, and describes breakthroughs in fields like insect sensory neuroscience, primate audition, and biomedical engineering. The goal is for this series to be the reference that every neuroscientist uses in order to get acquainted with new methodologies in brain research. These books can be given to graduate students and postdoctoral fellows when they are looking for guidance to start a new line of research.

Each book is edited by an expert and consists of chapters written by the leaders in a particular field. Books are richly illustrated and contain comprehensive bibliographies. Chapters provide substantial background material relevant to the particular subject. Hence, they are not the usual type of method books. They contain detailed "tricks of the trade" and information as to where these methods can be safely applied. In addition, they include information about where to buy equipment and web sites helpful in solving both practical and theoretical problems. Finally, they present detailed discussions of the present knowledge of the field and where it should go.

We hope that, as the volumes become available, the effort put in by us, the publisher, the book editors, and the individual authors will contribute to the further development of brain research. The extent to which we achieve this goal will be determined by the utility of these books.

Sidney A. Simon, Ph.D.
Miguel A.L. Nicolelis, M.D., Ph.D.
Series Editors

Preface

Vagus is a Latin word with a root that also gives us the term *vague*. This is appropriate, as much of what we know about vagal sensory neuroscience remains vague and imprecise. This is partly due to a decided lack of information. The number of scientific studies aimed directly at investigating the primary afferent nerves within the vagi pale in comparison with the somatosensory nerves of the dorsal roots. Given the pivotal role they play in visceral physiology as well as pathophysiology, one could reasonably argue that vagal sensory nerves are relatively understudied by today's standards. As a surrogate for direct information, it is often tempting to infer knowledge about vagal afferent nerves from the many elegant studies carried out on somatosensory nerves. Beyond some basic fundamental principles, however, this practice may lead to more confusion than clarity. This is because sensory nerve phenotype is directed from embryological "top down" signals as well as from tissue-derived "bottom up" signals. The vagal sensory neurons have their own unique embryological history and the tissues within the visceral organs they innervate provide another set of signals that render the nerves dissimilar in many ways to their somatosensory cousins.

Also contributing to the lack of focus in vagal neuroscience is the fact that investigators in this field are spread across many disciplines. The vagus meanders through the viscera, providing important regulatory influences over the thoracic and abdominal organs. This leads to a situation in which experts in vagal neurobiology are often "organo-centric" presenting their work in organ-specific journals and discussing their findings within their own organ-specific meetings. One of the purposes of this book is to present coherent summaries of vagal afferent neuroscience obtained within the body's organ systems. By juxtaposing these chapters in a single text, it is anticipated that cross-fertilization of ideas will provide new insights and focus on this important topic.

In Latin, the term *vagus* also means wandering. In this context, this book can be considered *vagal*. There have been outstanding resources published on specific aspects of vagal neuroscience, but there are few, if any, publications that provide a broad overview of vagal sensory neurobiology. With this in mind, this volume has been designed with chapters that wander through all aspects of vagal sensory nerve biology. This occurs on a lateral scale with chapters that deal with vagal nerves in the central nervous system (CNS), lungs, esophagus, heart, and gastrointestinal tract. The book also wanders on a vertical scale as it covers critical aspects ranging from vagus nerves in the embryo to vagus nerves in the adult, and from activity in individual neurons to whole animal studies of the reflexes and sensations such activity engenders. It is hoped that by painting vagal afferent biology with the broadest brush possible, this book will be a unique and useful resource for the

student, as well as for the established neuroscientist interested in the visceral nervous system.

Such nonreductionism runs the risk of failing for lack of discriminating detail. This is not the case here. In each chapter, experts cover a particular area of vagal afferent neuroscience. The authors provide an overview of the given topic and, in many cases, details pertaining to specific experiments and techniques. This approach has resulted in an informative reference for the vagal sensory neurobiologist.

Bradley J. Undem
Daniel Weinreich

Contributors

K.D. Alfrey
Biomedical Engineering Program
Purdue School of Engineering and
  Technology
Indiana University/Purdue University
Indianapolis, Indiana

Clare V.H. Baker
Department of Anatomy
University of Cambridge
United Kingdom

Michael J. Beyak
Department of Biomedical Science
University of Sheffield
Sheffield, United Kingdom
  and Gastrointestinal Diseases
  Research Unit
Queen's University
Kingston, Ontario, Canada

Ann C. Bonham
Department of Pharmacology
School of Medicine
University of California, Davis
Davis, California

Simon J.H. Brookes
Department of Human Physiology and
  Centre for Neuroscience
Flinders University
Adelaide, South Australia

Brendan J. Canning
Johns Hopkins Asthma and Allergy
  Center
Baltimore, Maryland

Michael J. Carr
GlaxoSmithKline
King of Prussia, Pennsylvania

Chao-Yin Chen
Department of Pharmacology
School of Medicine
University of California, Davis
Davis, California

Marcello Costa
Department of Human Physiology and
  Centre for Neuroscience
Flinders University
Adelaide, South Australia

James Deuchars
Department of Physiology
School of Medical Sciences
University of Leeds
Leeds, United Kingdom

David Grundy
Department of Biomedical Science
University of Sheffield
Sheffield, United Kingdom

Musa A. Haxhiu
Department of Physiology and
  Biophysics
Specialized Neuroscience Research
  Program
Howard University College of
  Medicine
Washington, D.C.

Cinda J. Helke
Department of Pharmacology and
  Neuroscience Program
Uniformed Services University of the
  Health Sciences
Bethesda, Maryland

Wilfrid Jänig
Department of Physiology
Christian-Albrechts-Universität zu Kiel
Kiel, Germany

Sergey Kasparov
Department of Physiology
School of Medical Sciences
University of Bristol
Bristol, United Kingdom

Prabha Kc
Department of Physiology and
  Biophysics
Specialized Neuroscience Research
  Program
Howard University College of
  Medicine
Washington, D.C.

Lu-Yuan Lee
Deparment of Physiology
University of Kentucky Medical
  Center
Lexington, Kentucky

B.Y. Li
Biomedical Engineering Program
Purdue School of Engineering and
  Technology
Indiana University/Purdue University
Indianapolis, Indiana

Stuart B. Mazzone
Department of Neurobiology
Howard Florey Institute
University of Melbourne
Melbourne, Australia

Constance T. Moore
Department of Physiology and
  Biophysics
Specialized Neuroscience Research
  Program
Howard University College of Medicine
Washington, D.C.

Julian F.R. Paton
Department of Physiology
School of Medical Sciences
University of Bristol
Bristol, United Kingdom

Robert J. Phillips
Department of Psychological Sciences
  and Integrative Neuroscience Program
Purdue University
West Lafayette, Indiana

Giovanni Piedimonte
Departments of Pediatrics, Medicine,
  and Molecular/Cellular Pharmacology
University of Miami School of
  Medicine
Miami, Florida

Terry L. Powley
Department of Psychological Sciences
  and Integrative Neuroscience Program
Purdue University
West Lafayette, Indiana

Steven C. Schachter
Department of Neurology
Beth Israel Deaconess Medical Center
Harvard Medical School
Boston, Massachusetts

J.H. Schild
Biomedical Engineering Program
Purdue School of Engineering and
  Technology
Indiana University/Purdue University
Indianapolis, Indiana

Harold D. Schultz
Department of Cellular and Integrative
  Physiology
University of Nebraska College of
  Medicine
Omaha, Nebraska

Jyoti N. Sengupta
Division of Gastroenterology and
  Hepatology
Medical College of Wisconsin
Milwaukee, Wisconsin

Reza Shaker
Professor and Chief
Division of Gastroenterology and
  Hepatology
Medical College of Wisconsin
Milwaukee, Wisconsin

Bradley J. Undem
Department of Medicine
Johns Hopkins Asthma and Allergy
  Center
Baltimore, Maryland

Sheng Wang
Department of Physiology
School of Medical Sciences
University of Bristol
Bristol, United Kingdom

Danny Weinreich
Department of Pharmacology and
  Experimental Therapeutics
University of Maryland
Baltimore, Maryland

Vladimir P. Zagorodnyuk
Department of Human Physiology and
  Centre for Neuroscience
Flinders University
Adelaide, South Australia

Contents

Part I

Development and Plasticity

1 The Embryology of Vagal Sensory Neurons

Clare V. H. Baker

CONTENTS

1.1   INTRODUCTION

The sensory neurons of the vagal nerve (cranial nerve X) are collected into two separate ganglia, the nodose and jugular ganglia. The neurons in these ganglia are functionally distinct: visceral sensory neurons are found only in the nodose ganglion, while somatic sensory neurons are found only in the jugular ganglion. These two different types of neuron are formed during embryogenesis from two different embryonic cell populations. The nodose placodes, paired bilateral patches of thickened surface ectoderm by the hindbrain (the most caudal in a series of "epibranchial" placodes), give rise to the visceral sensory neurons of the nodose ganglion. The neural crest, a migratory population of cells that delaminates from the neuroepithelium to migrate throughout the embryo, gives rise to the somatic sensory neurons of the jugular ganglion. In the embryo, these two types of neuron are also morphologically distinct: placode-derived nodose neurons are large in diameter, while neural crest-derived jugular neurons are small.

This chapter provides an introduction to the embryology of nodose and jugular neurons. Relatively little is known about the formation of nodose and jugular neurons specifically, while much more is known about the formation of placode-derived and neural crest-derived sensory neurons in general. Hence, this chapter will necessarily take a fairly general approach, but will emphasize nodose and jugular neurons where possible. Section 1.1 gives a brief general introduction to cranial ectodermal placodes and the neural crest. Section 1.2 describes what is currently known about nodose neuron development, embedded in a general outline of epibranchial placode formation and neurogenesis. Finally, Section 1.3 covers jugular neurons, with a general description of neural crest formation, and sensory neurogenesis within the neural crest.

1.1.1   THE SPATIAL SEGREGATION OF FUNCTIONALLY DISTINCT CRANIAL SENSORY NEURONS REFLECTS THEIR DIFFERENT EMBRYONIC ORIGINS

As described previously, vagal sensory neurons fall into two general functional classes that are spatially segregated in distinct ganglia on the vagal nerve (cranial nerve X). Somatic sensory neurons are found only in the jugular ganglion (Figure 1.1). General visceral and special visceral (gustatory) sensory neurons are found only in the nodose ganglion (Figure 1.1). This segregation reflects the different
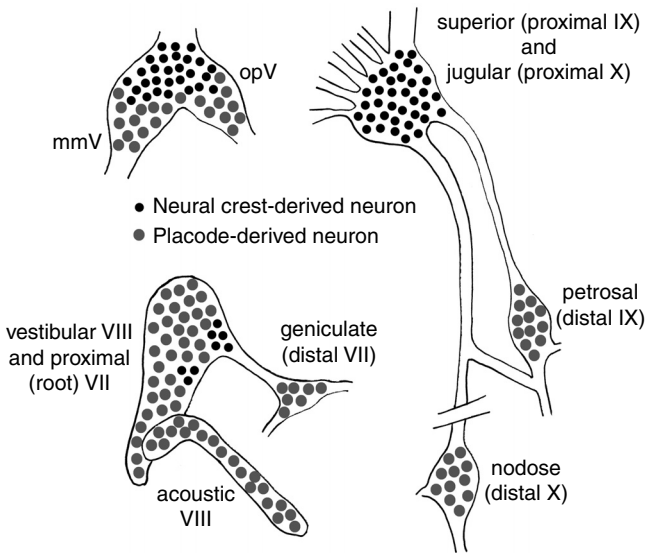
FIGURE 1.1 Schematic to show the distribution of large placode-derived neurons (grey circles) in distal sensory ganglia, and small neural crest-derived neurons (black circles) in proximal sensory ganglia, in a 12-day chick embryo. All the satellite glial cells in the ganglia, and Schwann cells lining the nerves, are derived from the neural crest. Roman numerals indicate the appropriate cranial nerve. The superior and jugular ganglia, and the vestibular (VIII) and proximal (root) ganglion of cranial nerve VII, are fused in the chick. mmV, maxillomandibular lobe of the trigeminal ganglion (cranial nerve V); opV, ophthalmic lobe of the trigeminal ganglion (cranial nerve V). (Modified from D'Amico-Martel, A. and Noden, D.M., *Am. J. Anat.*, 166, 445, 1983.)

embryonic origins of these neurons: the somatic sensory neurons in the jugular ganglion are derived from the neural crest, while the general and special visceral sensory neurons in the nodose ganglion are derived from cranial ectodermal placodes, specifically the nodose placodes (the third and more caudal placodes in the epibranchial series of placodes) (Figure 1.2). The neural crest and cranial placodes are both migratory cell populations that arise from ectoderm at the border between the prospective neural plate (which will eventually form the brain and spinal cord) and the prospective epidermis (skin). Together, neural crest and cranial placodes form the entire peripheral nervous system (reviewed in References 1 and 2).

The same spatial segregation of somatic sensory neurons in proximal ganglia ("root" ganglia, close to the brain), and general visceral and special visceral (gustatory) sensory neurons in distal ganglia ("trunk" ganglia, further from the brain), is also seen for the sensory neurons of cranial nerves VII (facial) and IX (glossopharyngeal) (Figure 1.1). Again, the spatial segregation of functionally distinct neurons into proximal and distal ganglia reflects their different embryonic origins. Just as for the vagal nerve, the proximal ganglia of the facial and glossopharyngeal nerves (root of VII and superior respectively) contain neural crest-derived somatic sensory neurons, while the distal ganglia (geniculate and petrosal respectively) contain placode-derived visceral sensory neurons (Figure 1.1 and Figure 1.2B).
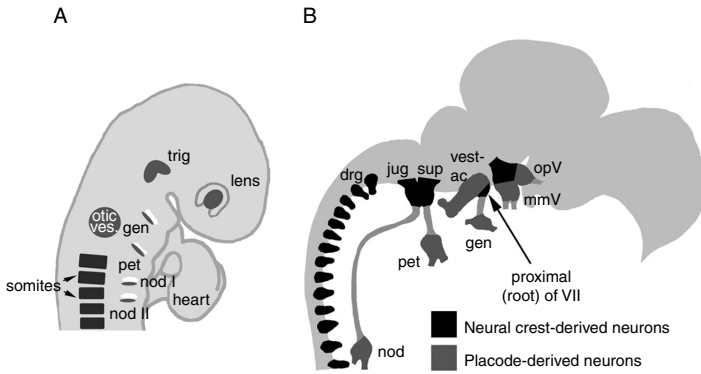
FIGURE 1.2 (**A**) Schematic to show the location of cranial ectodermal placodes in a 3-day chick embryo. Each of the four epibranchial placodes (geniculate, petrosal, and two nodose placodes) is located just caudal to a pharyngeal cleft. The bi-lobed trigeminal ganglion is already forming. gen, geniculate placode; nod, nodose placode; pet, petrosal placode; ves, vesicle. (Adapted from Le Douarin, N.M., Fontaine-Pérus, J., and Couly, G., *Trends Neurosci.*, 9, 175, 1986, and from Abu-Elmagd, M. et al., *Dev. Biol.*, 237, 258, 2001.) (**B**) Schematic to show the distribution of placode-derived (dark grey) and neural crest-derived (black) sensory neurons in an 8-day chick embryo. Roman numerals indicate the appropriate cranial nerve. drg, dorsal root ganglion; gen, geniculate ganglion; mmV, maxillomandibular lobe of the trigeminal ganglion; opV, ophthalmic lobe of the trigeminal ganglion; pet, petrosal ganglion; and vest-ac, vestibulo-acoustic ganglion. (Adapted from Le Douarin, N.M., Fontaine-Perus, J., and Couly, G., *Trends Neurosci.*, 9, 175, 1986.)

Most other cranial sensory neurons are placode-derived. The olfactory receptor neurons in the olfactory epithelium are formed by the olfactory placode. The special sensory neurons in the vestibuloacoustic (VIII) and lateral line ganglia (in anamniotes), which provide afferent innervation to the sensory hair cells of the inner ear and lateral line system respectively, are derived from the otic and lateral line placodes respectively (Figure 1.1 and Figure 1.2B). The somatic sensory neurons in the trigeminal ganglion are "mixed" in origin, with neurons derived both from the neural crest and from the two trigeminal placodes (the ophthalmic and maxillomandibular trigeminal placodes). However, neurons of different origin within the trigeminal ganglion are spatially segregated, with small neural crest-derived neurons proximally and large placode-derived neurons distally (Figure 1.1 and Figure 1.2B). (Note that there is no relationship between the different size classes of neuron in the embryonic ganglion and the different cytological classes of neuron in the mature ganglion.[3]). Both neural crest- and placode-derived neurons in the trigeminal ganglion are somatic sensory neurons, proving an exception to the general rule that placode-derived neurons mainly form special sensory (olfactory, otic, lateral line), special visceral (gustatory) and general visceral sensory neurons.

The precise embryonic origin of the neurons in cranial sensory ganglia (i.e., neural crest, placode, or both) was debated for decades (e.g., References 4 through 9). Ablation of one or the other cell population was first used to attack the question, but this was superseded by cell labeling techniques, in particular the permanent label

afforded by grafting quail tissue into chick hosts.[10] The quail-chick chimera method enabled precise and unequivocal labeling of either neural crest or placodes in avian embryos, and was used to demonstrate conclusively the picture of cranial sensory ganglion development outlined above.[8,11,12]

1.1.2 Cranial Ectodermal Placodes: An Introduction

Cranial ectodermal placodes are transitory patches of thickened, columnar epithelium in the embryonic head (Figure 1.2A).[2,13,14] Although hairs, feathers and teeth also arise from focal ectodermal thickenings called placodes, the term "cranial placodes" here refers only to those placodes that arise from ectoderm at the neural plate border in the head and that are associated with the sensory nervous system. As a group, cranial placodes form a wide variety of derivatives, primarily associated with the paired sense organs, but also including the endocrine cells of the adenohypophysis (anterior pituitary gland). Different cell types formed by cranial placodes include ciliated sensory receptor cells, sensory neurons, endocrine and neuroendocrine cells, and supporting cells, including some glial cells (olfactory ensheathing cells). Placodes are vital for the formation of the paired sense organs. The entire olfactory epithelium, the lens of the eye, the entire inner ear and, in anamniotes, the lateral line system, are all derived from different placodes (olfactory, lens, otic and lateral line placodes respectively). Most of the neurons in cranial sensory ganglia are also placode-derived (see Section 1.1.1) (Figure 1.1 and Figure 1.2B). In addition to forming the inner ear, the otic placode forms the afferent innervating neurons for inner ear hair cells collected in the vestibuloacoustic ganglion (cranial nerve VIII). Similarly, in anamniotes, the lateral line placodes form not only the mechanosensory and electroreceptive hair cells of the lateral line system, but also their afferent innervating neurons, collected in the lateral line ganglia. Two trigeminal placodes (ophthalmic and maxillomandibular) give rise to somatic sensory neurons in the distal regions of the eponymous lobes of the trigeminal ganglion (V) (Figure 1.2). Finally, and most relevant for this chapter, a series of epibranchial placodes (geniculate, petrosal and nodose) gives rise to all the general visceral and special visceral sensory neurons of the distal sensory ganglia of cranial nerves VII (geniculate), IX (petrosal) and X (nodose) (Figure 1.2). Clearly, cranial ectodermal placodes are essential for the formation of the majority of the peripheral sensory nervous system in the vertebrate head.

1.1.3 The Neural Crest: An Introduction

Neural crest cells are formed from ectoderm at the lateral borders of the neural plate, which are lifted up during neurulation to form the neural folds. The neural folds ultimately fuse, leading to formation of the neural tube from what was originally the flat neural plate, and bringing most neural crest cell precursors to the dorsal midline ("crest") of the neural tube. Some neural crest cells, particularly cranial neural crest cells, may delaminate from the neuroepithelium before neural fold fusion occurs so they are never part of the neural tube proper. Neural crest cells delaminate in a rostrocaudal wave, and migrate along well-defined pathways in both head and

trunk to form an enormous variety of derivatives.[1] These include most peripheral neurons and glia, with the exception of placode-derived cranial sensory neurons and olfactory ensheathing cells. They also form melanocytes, various endocrine cell types (e.g., adrenal chromaffin cells), most craniofacial bones and cartilages, and teeth. They give rise to all the somatic sensory neurons of the proximal sensory ganglia of cranial nerves VII (root), IX (superior) and X (jugular), together with somatic sensory neurons in the proximal region of the trigeminal ganglion (V) (Figure 1.1 and Figure 1.2B). All the glial cells of the cranial sensory ganglia originate from the neural crest, so neural crest cells are required for the formation or maintenance of even the vestibuloacoustic, lateral line, geniculate, petrosal and nodose ganglia, whose neurons are entirely placode-derived.

1.1.4 PLACODE AND NEURAL CREST FORMATION AT THE NEURAL PLATE BORDER

All fate-mapping studies to date have demonstrated that both neural crest and cranial placodes originate from ectoderm at the border between the prospective neural plate (future central nervous system) and the prospective epidermis (reviewed in References 1 and 2). Current molecular models for the induction of the neural plate are reviewed in Reference 15. Older fate maps (e.g., References 16 and 17) show the neural crest- and placode-forming regions as distinct, segregated strips of ectoderm, with prospective neural crest cells lying just lateral to the neural plate, and placodes lying between the neural crest and the epidermis (see Reference 2). However, more careful recent analyses, involving the labeling either of single cells or small groups of cells at the neural plate border, have shown that this view is greatly over-simplified. Individual cells at the trunk neural plate border can form epidermis, neural crest, and neural tube derivatives,[18] while at the cranial neural plate border, precursors of epidermis, placodes, neural crest, and neural tube are intermingled.[19] Although prospective placodal territory reaches further laterally than prospective neural crest territory, placodal and neural crest precursors are intermingled more medially.[19] Therefore, it is incorrect to think of prospective placode and neural crest territories as being completely segregated from one another at neural plate stages of development.

1.2 NODOSE NEURONS: PLACODE DEVELOPMENT AND NEUROGENESIS

Nodose neurons are derived from the nodose placode, the most caudal of the epibranchial series of placodes that forms above the pharyngeal (branchial) clefts (Figure 1.2, see Section 1.2.4). In this section, the formation of placodes in general, and the epibranchial placodes in particular, are described, followed by a discussion of our current understanding of the control of neurogenesis within the epibranchial placodes (geniculate, petrosal and nodose). As will be seen, nothing is currently known that distinguishes nodose placode neurogenesis from neurogenesis in the other epibranchial placodes.

1.2.1   EVIDENCE FOR A PAN-PLACODAL PRIMORDIUM AT THE NEURAL PLATE BORDER

Despite the intermingling of precursors of neural tube, neural crest, placodes, and epidermis at the neural plate border (see Section 1.1.4), there is increasing evidence to support the existence of a preplacodal field, or panplacodal primordium, around the anterior neural plate (for a more detailed discussion, see Reference 2). This field is delineated by the expression of several genes, mainly encoding transcription factors implicated in placode development, in a "horseshoe" around the anterior neural plate. These genes include the homeodomain transcription factors Dlx3, Dlx5, Dlx7, Six1 and Six4, the HMG-domain transcription factor Sox3 (also expressed in the neural plate), and the transcription co-factors Eya1 and Eya2 (for original references, see Reference 2). In the chick, these genes are expressed in a series of overlapping domains, rather than being strictly coincident.[19]

Fate-mapping data show that the preplacodal domain correlates neither with the site of origin of all placodal precursor cells, nor with determination toward a placodal fate. For example, not all otic placode precursors originate from the *Six4+* domain, and some cells within the *Six4+* domain form neural crest, epidermis or neural tube derivatives, rather than placodal derivatives.[19] What, therefore, is the significance of the preplacodal "horseshoe" of gene expression? It is possible that it represents a zone of ectoderm that is competent to respond to specific placode-inducing signals, although as yet there is no functional evidence to support this. There is a large amount of ectodermal cell movement at the neural plate border.[19,20] Precursors of a given placode, such as the zebrafish olfactory placode[20] or the chick otic placode,[19] arise from a relatively large ectodermal region at the anterior neural plate border that subsequently converges to form the placode proper. This may suggest a model in which cells moving into the preplacodal gene expression domain upregulate preplacodal genes, while cells leaving the domain downregulate these genes. Expression of a sufficient complement of preplacodal genes may render cells competent to respond to signals that induce the formation of specific placodes. However, the fate that is ultimately adopted by a particular cell within the preplacodal domain will be determined by the specific combination of signals it subsequently receives. Hence, despite being competent to contribute to a placode, it may instead form epidermis or neural crest.

1.2.2   FORMATION OF INDIVIDUAL PLACODES: INVOLVEMENT OF THE PAX/SIX/EYA/DACH REGULATORY NETWORK?

Members of the Pax family of paired domain, homeodomain transcription factors are expressed in different combinations in virtually all placodes. *Pax6* is found in the olfactory and lens placodes, *Pax3* in the ophthalmic trigeminal placode, *Pax2/5/8* in the otic placode, and *Pax2* in the epibranchial placodes (reviewed in Reference 2). Knockout studies in mice have shown that *Pax6* is required for proper olfactory and lens placode development, while *Pax2* is essential for various features of otic placode development (reviewed in Reference 2). Given the above, it is fascinating that several of the genes expressed in the preplacodal domain are members of the

Six and *Eya* gene families. Pax, Six, and Eya family members, together with the transcription co-factor Dach, act in an intricate cross-regulatory network in both eye and muscle development (see Reference 21). Dach family members are expressed in part of the preplacodal domain and in various placodes.[22–25] It is intriguing to speculate that expression of *Six*, *Eya*, and perhaps also *Dach* genes within the preplacodal domain may provide a pan-placodal regulatory module. Different Pax family members are induced in different locations within the preplacodal domain by specific placode-inducing signals from neighboring tissues (for a comprehensive review of known placode-inducing tissues and signals, see Reference 2). The different Pax proteins might then interact with Six, Eya and Dach members to specify the identities of individual placodes. There is currently no real evidence for this model, but it is eminently testable.

1.2.3 MANY INDIVIDUAL PLACODES, INCLUDING THE NODOSE PLACODE, ORIGINATE FROM DISTINCT MULTI-PLACODAL PRIMORDIA

The previous section discussed a model in which placodes become "individualized" within the preplacodal domain of ectoderm by receiving different inducing signals from adjacent tissues. However, in many or most species, discrete domains of thickened ectoderm are found that ultimately give rise to two or more placodes (the ectoderm in between the final placodes usually seems to become thin). This is certainly the case for the epibranchial placodes, which form the special visceral (gustatory) and general visceral sensory neurons in the geniculate, petrosal and nodose ganglia. In *Xenopus* embryos, the lateral line and otic (and possibly epibranchial) placodes seem to originate from a common "dorsolateral placode area" that expresses a common set of molecular markers, including Pax2.[26,27]

Data from both zebrafish and chick embryos support the origin of the epibranchial placodes from a molecularly and morphologically distinct region of ectoderm that includes the otic placode. In the zebrafish, the winged-helix transcription factor Foxi1, which is necessary for both otic and epibranchial placode formation[28,29] is expressed in a "lateral cranial placodal domain" that encompasses the otic and epibranchial placodes.[29] In the chick embryo, *Pax2* is expressed in a broad region of ectoderm that includes both otic and epibranchial placode precursors.[19,30] Furthermore, fate-map data combined with the expression of the pan-placodal marker gene *Sox3*, which generally correlates with the location of thickened ectoderm, suggest that the geniculate and otic placodes arise from a common domain of *Sox3* expression, while the petrosal and the two nodose placodes (see Figure 1.2A) arise from a second, more caudal domain of *Sox3* expression.[31,32] The ectoderm lying between the epibranchial placodes subsequently thins, while the ectoderm that will ultimately form the placodes remains thick and maintains *Sox3* expression.[31,32] Taken together, these results suggest that a broad domain of thickened ectoderm near the hindbrain initially shares a set of common molecular markers, including *Pax2* and *Foxi1*, and is subsequently partitioned into multiple individual placodes. This partitioning is likely to involve the maintenance of some molecular markers (such as *Sox3*) and

the induction of new placode-specific genes, by signals from adjacent tissues. Models of individual placode formation, therefore, must take these data into account.

1.2.4 INDUCTION OF THE EPIBRANCHIAL PLACODES (GENICULATE, PETROSAL, AND NODOSE)

The epibranchial placodes form above the pharyngeal (branchial) clefts (Figure 1.2A). These clefts are formed by the outpocketing of pharyngeal (foregut) endoderm as a series of pouches that fuse with the overlying ectoderm to form slits in the wall of the pharynx. The pharyngeal (branchial) arches represent the tissue between the successive pharyngeal clefts; the number of arches (and clefts) is variable between different vertebrates. In aquatic vertebrates, the pharyngeal clefts form the gill slits and the pharyngeal (gill) arches support gills. The first pharyngeal cleft in tetrapods forms the cavity of the middle ear; the first arch in all jawed vertebrates forms the jaw. Cranial neural crest cells migrate into the pharyngeal arches to fill the subectodermal space around the core of paraxial mesoderm (Figure 1.3); they form all the skeletal elements of the arches, and the connective components of the striated muscles formed by the paraxial mesoderm core.
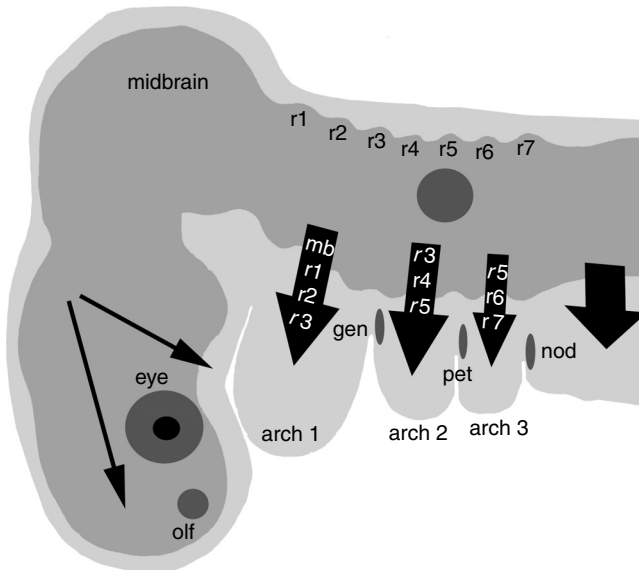
FIGURE 1.3 Schematic to show the migration pathways of cranial neural crest cells (black arrows) from the caudal diencephalon, midbrain and hindbrain, into the pharyngeal arches, relative to the location of the epibranchial placodes, in a 2-day-old chick embryo. The source of neural crest cells migrating into each arch is indicated by the white text on the black arrows. Neural crest cells from the postotic hindbrain contribute neurons to the jugular ganglion; gen, geniculate placode; mb, midbrain; nod, nodose placode; olf, olfactory pit; pet, petrosal placode; and r, rhombomere. (Adapted from Helms, J.A. and Schneider, R.A., *Nature*, 423, 326, 2003, and from Trainor, P.A. and Krumlauf, R., *Curr. Opin. Cell Biol.*, 13, 698, 2001.)

The first epibranchial placode (geniculate or facial) arises above the first pharyngeal cleft, and forms special visceral (gustatory) and general visceral sensory neurons in the distal (geniculate) ganglion of the facial nerve (cranial nerve VII) (Figure 1.2). The second epibranchial placode (petrosal or glossopharyngeal) arises above the second pharyngeal cleft, and forms special visceral (gustatory) and general visceral sensory neurons in the distal (petrosal) ganglion of the glossopharyngeal nerve (cranial nerve IX) (Figure 1.2). The third epibranchial placode (nodose or vagal) arises above the third pharyngeal cleft, and forms special visceral (gustatory) and general visceral sensory neurons in the distal (nodose) ganglion of the vagal nerve (cranial nerve X) (Figure 1.2). Additional nodose (vagal) epibranchial placodes arise above more posterior pharyngeal clefts, where these are present, and contribute neurons to the nodose ganglion or ganglia (see References 2 and 32). In the chick, for example, there are two nodose placodes that each contribute neurons to the nodose ganglion[32] (Figure 1.2A). The neural crest, as described previously, gives rise to all the satellite glial cells in these ganglia.[8,12]

The close association of epibranchial placode formation with pharyngeal cleft and arch formation, in both space and time, raises at least two possibilities for the source of epibranchial placode-inducing signals, or perhaps more accurately, for those signals that maintain, for example, *Sox3* and *Pax2* expression and upregulate epibranchial placode-specific gene expression (see Section 1.2.3). Firstly, there may be signals from the outpouching pharyngeal endoderm and/or the overlying surface ectoderm. Secondly, there may be signals from the migrating neural crest streams that enter the pharyngeal arches between the forming pharyngeal clefts (Figure 1.3). By mechanically ablating or genetically removing neural crest cells, various studies have shown that neural crest cells are not required for epibranchial placode formation.[5,33,34] In contrast, *in vitro* co-culture experiments in the chick demonstrated that pharyngeal endoderm is sufficient to induce epibranchial (*Phox2a*-positive) neurons in nonplacode-forming cranial ectoderm [5,33,34] (see Section 1.2.5).

1.2.5 Neurogenesis within the Epibranchial Placodes

1.2.5.1 Proneural Genes and Notch Signaling in Neurogenesis: A Brief Outline

Before discussing the genes currently known to be involved in neurogenesis within the epibranchial placodes, a brief introduction to the general classes of genes that control neurogenesis is required. In vertebrates and in *Drosophila*, where they were first discovered, the expression of proneural basic helix-loop-helix (bHLH) transcription factors bestows neuronal potential and specifies the identity of neural progenitor cells (reviewed in Reference 35). Proneural transcription factors activate the expression of ligands of the Notch receptor, such as Delta, Serrate, and Jagged. Cells with low levels of Notch activity, i.e., cells that are not receiving Notch ligands from surrounding cells or that have inherited intrinsic Notch inhibitors via asymmetric cell division, adopt a "primary" cell fate, e.g., differentiate as neurons (e.g.,

Reference 36). Cells with high levels of Notch activity, that is, whose neighbors are secreting high levels of Notch ligands, downregulate their own expression of Notch ligands (thus signal less to surrounding cells) and adopt a "secondary" cell fate, for example, differentiate as supporting or glial cells.

Two classes of proneural genes operate in the *Drosophila* peripheral nervous system: the *achaete-scute* complex and *atonal* (reviewed in Reference 37). The homologues of the *achaete-scute* complex in vertebrates include *ash1* (*Mash1* in mice, *Cash1* in chick, etc.) plus various species-specific genes (e.g., *Mash2* in mice, *Cash4* in chick). The homologues of the *atonal* class in vertebrates are much more numerous, and can be divided into different subfamilies (reviewed in Reference 35). One of these families comprises the *neurogenin*s (*ngn*s), which are particularly relevant here, as they are essential for the sensory lineage in both placodes and neural crest cells.

1.2.5.2 Neurogenins Are Required for Neurogenesis in the Epibranchial Placodes

Section 1.2.3 mentioned that the winged helix transcription factor Foxi1, which is expressed in a "lateral cranial domain" that includes the prospective otic and epibranchial placodes, is required for both otic and epibranchial placode formation in the zebrafish.[28,29] Foxi1 is essential for the expression of *neurogenin1* (*ngn1*) in the epibranchial placodes.[29] Ngn1 is also expressed in the neural crest, and after Ngn1 function is abrogated in zebrafish using antisense morpholinos, all peripheral sensory ganglia are lost.[38]

In the mouse and chick, two different *Neurogenin* genes (*Ngn1* and *Ngn2*) partition between them the functions apparently encompassed by *ngn1* alone in the zebrafish. In the chick, *Ngn1* alone is expressed in the epibranchial placodes.[39] In the mouse, *Ngn2* is expressed at higher levels, and *Ngn1* at lower levels, in the epibranchial placodes and cells delaminating from them, before neuronal differentiation occurs.[40] When *Ngn2* is knocked out genetically in mice, cells in the geniculate and petrosal placodes fail to delaminate, migrate or differentiate as neurons.[40] At the molecular level, they fail to express *Ngn1* and other bHLH genes in the cascade leading to neuronal differentiation, such as *Math3*, *NeuroD* and *Nscl1*.[40] The block in geniculate ganglion formation is only transient, however, as a geniculate ganglion eventually forms; the authors suggest that neural crest cells compensate for the loss of geniculate placode-derived neurons [40] (see Section 1.2.6). The nodose placode develops normally in *Ngn2* mutants, and it is thought that *Ngn1*, which is still present in the nodose placode (though at lower levels than normal) may compensate for the loss of *Ngn2* expression.[40,41]

In all the epibranchial placodes, *Ngn2* is necessary for the expression of the Notch ligand Delta-like1, suggesting that neurogenesis in the epibranchial placodes involves Notch-Delta signalling[40] (see Section 1.2.5.1). Interestingly, expression of the epibranchial neuron marker *Phox2a* (see next section) is unaffected by the loss of *Ngn2*,[40] suggesting that *Phox2a* and *Ngn2* expression are regulated independently.

1.2.5.3 Phox2a and Phox2b Confer Neuronal Subtype Identity and Are Required for Neuronal Survival

As described in Section 1.2.4, pharyngeal endoderm can induce *Phox2a*^{+} neurons in nonplacodal cranial ectoderm.[33] BMP7, which is produced by pharyngeal endoderm, is able to substitute for pharyngeal endoderm in this assay.[33] Furthermore, a BMP7 inhibitor (follistatin) decreases the neuron-inducing activity of the pharyngeal endoderm *in vitro*,[33] supporting the hypothesis that pharyngeal endoderm-derived BMP7 is involved in neurogenesis in the epibranchial placodes *in vivo*.

Phox2a is a paired-like homeodomain transcription factor that is required for the development of the noradrenergic phenotype (reviewed in References 42 and 43). It is expressed by a subset of cells within domains of *Ngn2*^{+} expression in the epibranchial placodes (indeed, seemingly only in the cells with the highest levels of *Ngn2* expression); it is also expressed in most *Ngn2*^{+} cells delaminating from the placodes, and in all epibranchial placode-derived neurons.[33,39,44,45] Both Phox2a and a related transcription factor, Phox2b, directly activate the promoter of the gene encoding the catecholamine synthesis pathway enzyme dopamine β-hydroxylase (DBH) (reviewed in References 42 and 43. Epibranchial placode-derived neurons transiently express both DBH and another enzyme in the catecholamine synthesis pathway, tyrosine hydroxylase (TH) (e.g., References 46 and 47).

In epibranchial placode-derived ganglia, *Phox2a* lies genetically upstream of *Phox2b*, which is in turn required for *DBH* expression.[44,45] *Phox2a* is neither required for the delamination or aggregation of epibranchial placode-derived cells, nor for their differentiation as neurons, but it is required for *DBH* expression, and also expression of the gene encoding the receptor tyrosine kinase cRet.[47] *Phox2a* is therefore probably required for neuronal survival in response to the Ret ligand, GDNF (glial cell line-derived neurotrophic factor).[47] Indeed, in *Phox2a*-mutant mice, the nodose and petrosal ganglia are severely atrophied through apoptosis: it is possible that the geniculate ganglion, which develops relatively normally, is rescued by redundancy with Phox2b.[47]

Phox2b is expressed later than *Phox2a*, in cells that have already delaminated from the placodes.[39,48] Like *Phox2a*, *Phox2b* is required for the survival of the epibranchial placode-derived ganglia, which are all severely atrophied in *Phox2b*-null mice.[44] Since the visceral sensory neurons derived from the epibranchial placodes provide afferent innervation to the heart, lungs and other visceral organs, they are required for medullary autonomic reflexes. Remarkably, *Phox2b*-null mice (but not *Phox2a*-null mice) lack all of the neural circuits underlying medullary autonomic reflexes (see References 42, 43, and 49). Phox2b therefore appears to be a true pan-autonomic marker.

In summary, Phox2a and Phox2b are not required for neurogenesis within the epibranchial placodes. However, they may determine the neuronal subtype identity of epibranchial placode-derived neurons, and are required for their survival.

1.2.6 NEURAL CREST CELLS ARE REQUIRED FOR THE FORMATION OF CENTRAL CONNECTIONS BY EPIBRANCHIAL NEURONS

As described previously (Section 1.2.4), ablation experiments in chick and mouse have demonstrated that epibranchial placode formation, neurogenesis and gangliogenesis proceed essentially as normal in the absence of neural crest cells.[5,33,34] In mice double mutant for *Hoxa1* and *Hoxb1*, loss of rhombomere 4-derived neural crest cells in the second pharyngeal arch has no apparent effect on the formation of either the geniculate or petrosal ganglia (see Figure 1.3).[34] Mechanical ablation of second-arch neural crest cells results in delayed delamination of cells from the geniculate placode, and in the formation of aberrant central projections from the displaced ganglion that eventually forms.[50] Thus, the presence of migrating neural crest streams from the hindbrain (see Figure 1.3) may play a role in guiding the central projections of epibranchial placode-derived neurons.

Neural crest cells may initially contribute neurons to the epibranchial ganglia in the chick,[51] but these presumably die, as they are not seen at later stages.[12] It has been suggested (though not proven) that neural crest cells contribute neurons to the geniculate ganglion in *Ngn2*-null mice, which lack epibranchial placode-derived neurons (see Section 1.2.5.2) but in which the geniculate ganglion eventually forms.[40] Also, when the nodose placode is mechanically ablated, neural crest cells from the same axial level form neurons in the nodose ganglion.[52] However, the heart does not function properly in nodose placode-ablated embryos,[52] suggesting that neural crest-derived neurons in the nodose ganglion are unable to substitute fully for nodose placode-derived neurons.

1.2.7 SUMMARY OF NODOSE NEURON DEVELOPMENT

Nodose neurons are derived from the nodose placodes, bilateral patches of thickened surface ectoderm at the level of the postotic hindbrain. These are the most caudal in a series of epibranchial placodes that form above the pharyngeal (branchial) clefts: the geniculate, petrosal and nodose placodes. These form all the neurons in the eponymous sensory ganglia on cranial nerves VII, IX and X, respectively. All placodes originate from ectoderm at the neural plate border. There is increasing evidence to suggest the existence of a preplacodal domain or panplacodal primordium in a horseshoe around the anterior neural plate, from which all placodes arise. This domain is characterized by a specific suite of overlapping transcription factor gene expression domains, including *Sox3*, plus *Six*, *Eya*, and *Dlx* family members. The epibranchial placodes form via the partitioning of a larger region of thickened ectoderm adjacent to the hindbrain that includes the otic placodes, and is characterized by *Sox3*, *Pax2* and *Foxi1* expression. The individual epibranchial placodes form above the pharyngeal clefts, shortly before or concomitant with pharyngeal cleft formation via outpocketing and fusion of pharyngeal endoderm with overlying surface ectoderm. The neural crest cells that migrate into the pharyngeal arches, between the pharyngeal clefts, are not required for neurogenesis within the epibranchial placodes, although they do seem to be necessary for appropriate for-

mation of the central connections of epibranchial-derived neurons. *Foxi1* is necessary for expression of the proneural gene *neurogenin1* in the epibranchial placodes in zebrafish. Neurogenins are essential for epibranchial neurogenesis. In both zebrafish and chick, *Ngn1* seems to be required, while in the mouse, *Ngn2* is required, although in the nodose placode, *Ngn1* seems able to compensate for loss of *Ngn2*. *Phox2a* and *Phox2b* are also expressed (independently of the *Ngn*s) in epibranchial neurons; they are required for transient noradrenergic marker expression (and thus neuronal subtype identity) and neuronal survival. BMP7 may be the pharyngeal endoderm-derived signal that induces *Phox2a*+ neurons within the epibranchial placodes.

As may be seen from the above, a general picture of the tissues and molecules involved in epibranchial placode development is beginning to take shape. Very little is known about how (or, indeed, whether) the different epibranchial placodes (geniculate, petrosal and nodose) become distinct from one another. The transcription factor Hoxb5 is expressed specifically in the nodose placode and nodose neurons, as well as in neural crest cells in the caudalmost pharyngeal arches.[53] This is the only molecule identified to date that shows a differential pattern of expression within the epibranchial placodes, but it does not seem to be necessary for the formation of nodose neurons.[54] Given that the geniculate, petrosal and nodose ganglia contain broadly similar neuronal subtypes (general visceral and gustatory sensory neurons), though in different proportions depending on their peripheral targets, it is possible that few or no differences in their embryology will be discovered. Hence, our understanding of the embryology of nodose neurons is, at least to date, identical to our understanding of the embryology of all epibranchial placode-derived neurons.

1.3 JUGULAR NEURONS: NEURAL CREST DEVELOPMENT AND SENSORY NEUROGENESIS

Jugular neurons arise from neural crest cells that emigrate from the postotic hindbrain, at the level of the first three somites[8,12] (see Figure 1.2A and Figure 1.3). In this section, a brief description is given of our current understanding of neural crest induction at the neural plate border, followed by a general discussion of lineage diversification within the neural crest. Finally, recent progress in elucidating the mechanisms underlying neural crest cell adoption of a sensory neuronal fate is described.

1.3.1 INDUCTION OF THE NEURAL CREST

The mechanisms and molecules thought to underlie neural crest induction have been exhaustively reviewed in recent years.[55–60] A brief summary is given here.

Neural crest induction can be divided into three main steps. Step 1 is the formation of the neural plate border region, which seems to be dependent on specific levels of bone morphogenetic protein (BMP) activity (e.g., References 56 and 61–64). The positioning of the neural plate border also seems to be dependent on the activity of Dlx transcription factors during gastrulation.[65,66] However, neither specific BMP activity levels nor Dlx activity is sufficient to induce neural crest cells alone.[61,67]

Step 2 of neural crest induction is the posteriorization of the neural plate border and induction of neural crest cell precursors within it. These processes can be experimentally uncoupled (e.g., References 68 and 69), but the Wnt and fibroblast growth factor (FGF) signaling pathways are implicated in both processes.[60,69,70] Wnts are both necessary and sufficient to induce neural crest cells from neuralized ectoderm (reviewed in Reference 60), and Wnt family members are expressed both in epidermis and paraxial mesoderm, tissues that have long been implicated in neural crest induction (for a historical review, see Reference 71). FGF signaling is required for the induction of neural crest cells by paraxial mesoderm in *Xenopus*,[69] however, so FGF involvement in neural crest induction cannot be ruled out. It is likely that the transcription factors AP2α, Sox9 and Sox10 are crucial downstream targets of BMP and Wnt/FGF signals in the formation of neural crest precursors.[72–74] AP2α seems to be upstream of Sox9, which in turn induces the expression of multiple other neural crest precursor markers, including the transcription factors Slug and FoxD3.

Step 3 of neural crest cell induction is the epithelial-mesenchymal transition that transforms a (potential) neural crest precursor within the dorsal neural tube, into a *bona fide* neural crest cell that has moved from the neuroepithelium into the periphery. Therefore, induction of delamination is the final step in neural crest cell induction. FoxD3 and Slug can promote delamination,[75,76] but when both genes are induced in ventral neural tube cells by Sox9 overexpression, the *Slug⁺FoxD3⁺* cells fail to delaminate, suggesting an additional signal in the dorsal neural tube is required.[73] Perhaps relevant to the nature of this additional signal, there is strong evidence that BMP activity in the dorsal neural tube is both necessary and sufficient to promote neural crest cell delamination.[77–79] A recent review of the molecular mechanisms underlying neural crest cell delamination can be found in Reference 80.

The control of neural crest cell migration is beyond the scope of this chapter, but numerous recent reviews may be consulted on this topic (e.g., References 80 and 81). The remainder of the chapter concentrates on how neural crest cells adopt a sensory neuronal fate, beginning with a general discussion of neural crest lineage diversification.

1.3.2 NEURAL CREST LINEAGE DIVERSIFICATION: GENERAL PRINCIPLES

Neural crest cells clearly give rise to an enormous variety of derivatives, from cartilage to pigment cells to neurons. Here, we are concerned with the formation specifically of sensory neurons. The sensory neurons of the jugular ganglion are derived from neural crest cells emigrating from the postotic hindbrain, at the level of the first three somites (see Figure 1.2A and Figure 1.3).[8,12]

Two different developmental questions arise when considering the extraordinary lineage diversification of neural crest cells and how, for example, sensory neurons develop.[82] Firstly, neural crest cells emigrating at different axial levels do not all form sensory neurons during normal development. Indeed, neural crest cells from different rostrocaudal levels of the neuraxis give rise to very different subsets of derivatives, a phenomenon called axial fate restriction. For example, cranial neural crest cells do not form sympathetic neurons, while trunk neural crest cells do not

form cartilage. What mechanisms underlie axial fate restriction? Are neural crest cells that emigrate at different axial levels intrinsically different, such that they only have the potential to form the derivatives they are fated to form, or do cells that emigrate at different axial levels encounter different environments, and thus different instructive differentiation cues? Secondly, neural crest cells that emigrate at the same or adjacent axial levels form multiple derivatives. For example, the "vagal" neural crest cells that emigrate from the postotic hindbrain at the level of the first 7 somites, give rise not only to sensory neurons in the superior and jugular ganglia and the most rostral dorsal root ganglia, but also to parasympathetic neurons, sympathetic neurons, enteric neurons, Schwann cells, satellite glial cells, calcitonin-producing cells, the carotid body, and the aorticopulmonary septum of the heart. How is this lineage diversification achieved from cells at the same axial level? Are emigrating neural crest cells totally naïve, responding to whichever differentiation cues they encounter, or are they a heterogeneous collection of predetermined cells?

The results of numerous heterotopic grafting experiments have shown that axial fate restriction does not seem to reflect axial-specific restrictions in potential, rather, it reflects axial-specific differences in the environmental signals encountered by neural crest cells (reviewed in Reference 1). For example, cranial neural crest cells grafted into the trunk will readily form sympathetic neurons. Indeed, recent experiments suggest that the most longstanding apparent exception to the rule, namely that trunk neural crest cells lack the potential to form cartilage, may finally have been removed.[83] Most current evidence, therefore, suggests that neural crest cells are fairly malleable, at least at the population level, and that there are no insurmountable restrictions associated with their rostrocaudal level of origin.

Lineage diversification at the same axial level could in theory be accounted for by two opposing hypotheses: instruction and selection. The first (instruction) proposes that neural crest cells emigrate as a homogeneous population of naïve cells that are instructed to differentiate into particular derivatives depending on where they end up. The second (selection) proposes that emigrating neural crest cells are a heterogeneous collection of determined cells that only form particular derivatives and that are eliminated from inappropriate environments. Both are compatible with the heterotopic grafting experiments used to attack the problem of axial fate restriction. The evidence, as so often in such cases, suggests that the truth lies somewhere in-between. Single cell lineage analysis, both *in vivo* and *in vitro*, suggests the existence of multipotent neural crest cells with the capacity to form multiple derivatives in response to instructive signals (reviewed in References 1, 84, and 85). Furthermore, several such instructive signals have been identified in recent years, such as BMPs for sympathetic neurons[86]; neuregulin 1 type II (glial growth factor) for satellite glial cells[87–89]; neuregulin 1 type III for Schwann cells[89]; and Wnts for both melanocytes[90] and sensory neurons[91] (see Section 1.3.3.1).

However, fate-restricted neural crest cells have also been identified, even in neural crest cell populations that have just left the neural tube, suggesting that the migrating neural crest cell population is indeed heterogeneous (reviewed in References 82 and 92). Neural crest precursors are, of course, exposed to environmental cues while they are within the neural tube: for example, Wnt family members are expressed in the dorsal neural tube, and these can instructively promote melanocyte and sensory

neural fates[90,91] (see Section 1.3.3.1). It seems likely that early exposure to instructive cues, plus community effects (neural crest cell-cell interactions) that lead to early fate restrictions (e.g., Reference 93), together underlie the heterogeneity seen in the migrating neural crest cell population. It is important to note, however, that restriction in fate does not necessarily imply restriction in potential: this can only be tested experimentally, by challenging the cell with a different environment, ideally *in vivo*.

1.3.3 SENSORY NEUROGENESIS WITHIN THE NEURAL CREST

1.3.3.1 Wnt Signaling Instructively Promotes Adoption of a Sensory Neuron Fate

The signaling molecule Wnt1 is expressed in the dorsal midline of the entire developing central nervous system except the telencephalon, throughout the period of neural crest cell emigration (see Reference 94). Neural crest cells do not themselves express *Wnt1* mRNA, but they are derived from *Wnt1*-expressing precursors in the dorsal midline of the neural tube, and the *Wnt1* promoter can be used to drive gene expression in neural crest cells[94] (also see References 91, 95, and 96). Genetic ablation of β-catenin, an essential component of the canonical Wnt signaling pathway (reviewed in Reference 97), in neural crest precursors and migrating neural crest cells (under the control of the *Wnt1* promoter) results in a complete lack of melanocytes and a severe reduction in sensory neural cells (both neurons and satellite cells) in peripheral sensory ganglia.[98] Mutant neural crest cells fail to form dorsal root ganglia and instead contribute to sympathetic and enteric ganglia.[98] These results suggested that Wnt signaling is essential for adoption of both sensory neural and pigment cell fates.

Conversely, expression of constitutively active β-catenin in neural crest precursors and migrating neural crest cells (again under the control of the *Wnt1* promoter) leads to the formation of sensory neurons at the expense of almost all other neural crest derivatives.[91] Clonally cultured early mammalian neural crest cells respond to Wnt1 primarily by generating small (fewer than 5 cells) clones of sensory neurons (over half formed a single sensory neuron),[91] while β-catenin-deficient neural crest stem cells do not form sensory neurons in response to Wnt1.[91] Taken together, these results strongly suggest that Wnt signaling instructively promotes the adoption of a sensory neuron fate by early neural crest cells.

The additional requirement for Wnt signaling for melanocyte formation[90,98] may reflect Wnt action at different times during development (see Reference 99). It is possible that Wnt signaling promotes a sensory fate in neural crest precursors, but a pigment cell fate in neural crest cells at a later stage of development.[99] In zebrafish, injection of mRNA encoding a constitutively active β-catenin, into neural crest precursors normally fated to form neurons, leads them to adopt a pigment cell fate.[90] This seems to contradict the results described previously in mice. The difference seen may reflect a delay in the production and accumulation of constitutively active β-catenin after mRNA injection, such that the cells respond by forming pigment cells instead; however, this hypothesis remains to be tested. Given that both *Wnt1* and *Wnt3a* are expressed in the dorsal neural tube (and indeed that neural crest cells

are formed from *Wnt1*-expressing precursor cells), the question also arises as to why only a subset of neural crest cells adopts a sensory neural fate. Community effects (i.e., interactions among neighbor neural crest precursors or neural crest cells) and the presence of other competing signals are likely to be important here, but much work remains to be done to clarify our understanding of these processes.

1.3.3.2 Sensory-Fated and Sensory-Committed Precursors Are Present in the Migrating Neural Crest Population

As described in the preceding section, Wnt signaling instructively promotes a sensory neuronal fate in early neural crest cells.[91] Wnts are expressed in the dorsal neural tube, suggesting that at least some neural crest precursors are likely to be specified toward a sensory fate even prior to delamination. Indeed, clonal analysis of migrating neural crest cells in the chick showed that some clones (which included both neurons and glia) were restricted either to dorsal root ganglia or sympathetic ganglia, suggesting that the fate of some cells and their progeny is restricted to either a sensory or an autonomic fate.[100] Furthermore, it appears that the migrating mammalian trunk neural crest cell population already contains cells that are committed to a sensory fate. Even when cultured in the presence of a potent autonomic neurogenic signal, BMP2, some proliferating rat trunk neural crest cells form sensory neurons.[101] This early commitment to a sensory neuronal fate may, therefore, reflect prior exposure of some neural crest precursors to Wnts in the dorsal neural tube.[91]

1.3.3.3 Neurogenin2 Biases Trunk Neural Crest Cells to a Sensory Fate

In the mouse, the proneural transcription factor Neurogenin2 (Ngn2; see Section 1.2.5.1) is expressed both in cells in the dorsal neural tube, and in a subpopulation of migrating trunk neural crest cells; it is maintained into the early stages of dorsal root ganglion formation.[102] Elegant genetic experiments have shown that the *Ngn2*+ subpopulation of migrating neural crest cells is not absolutely committed to a sensory fate, but is strongly biased toward it.[96] *Ngn2* is not expressed in cranial neural crest cells, however, and all neural crest-derived cranial sensory ganglia are normal in *Ngn2*-mutant mice.[40]

1.3.3.4 Neurogenin1 Is Required for the Formation of Jugular Neurons

All peripheral sensory ganglia are missing in zebrafish where Ngn1 function has been abrogated using antisense morpholinos (in fish, Ngn1 seems to encompass all functions of amniote Ngn1 and Ngn2).[38] In *Ngn1* mutant mice, the superior-jugular complex and the trigeminal ganglion are entirely missing.[41] The bHLH cascade that leads to neurogenesis is abrogated in neural crest cells that populate the nascent superior-jugular and trigeminal ganglia in *Ngn1*-mutant mice, as neither *NeuroD* nor *Math3* are detected, and no neurons form.[41] Hence, Ngn1 function is essential for the formation of jugular neurons.

1.3.3.5 Inhibition of Notch Signaling Is Required for Sensory Neuron Differentiation

Neuronal differentiation within the dorsal root ganglia depends on the inhibition of signaling through the transmembrane receptor Notch; conversely, glial differentiation depends on Notch activation (see Section 1.2.5.1).[103,104] In the dorsal root ganglia, dividing cells on the ganglionic periphery preferentially express Notch1, while the Notch ligand, Delta1, is expressed by differentiating neurons in the ganglionic core.[103] Constitutive activation of Notch signaling in quail trunk neural crest cells *in vitro* inhibits neuronal differentiation and transiently increases cell division, suggesting that Notch activity must be inhibited for neurogenesis to take place.[103] Asymmetric inheritance of the Notch antagonist Numb may be important for determining which cells within the ganglion form neurons and which continue to cycle and/or form satellite glial cells.[103] When Numb is knocked out genetically in mice, sensory neurons fail to form in the dorsal root ganglia,[104] providing additional support for this model. Cranial sensory neurons were not explicitly examined in this study, although apparently neurogenesis in the trigeminal ganglion was normal.[104] Hence, it is unclear how important the asymmetric inheritance of Numb is for sensory neurogenesis in the cranial sensory ganglia.

Although there is little or no information specifically on the importance of Notch inhibition for the formation of neural crest-derived cranial sensory neurons, studies of placodal neurogenesis have shown that Ngn1 (see previous section) is required for expression of the Notch ligand Delta1.[41] Since all cranial neural crest-derived sensory neurons are missing when Ngn1 function is abrogated,[38,41] and given the importance of Notch inhibition for sensory neurogenesis in the dorsal root ganglia, it seems likely that Notch inhibition is also required for sensory neurogenesis in cranial sensory ganglia.

1.3.4 SUMMARY OF JUGULAR NEURON DEVELOPMENT

Jugular neurons are derived from the neural crest, a population of ectodermal cells that originates from ectoderm at the lateral borders of the neural plate. Neurulation, that is, the rolling up of the neural plate to form the neural tube, brings neural crest precursors to the "crest" of the future brain and spinal cord. Neural crest cells subsequently delaminate and migrate throughout the embryo on stereotypical migration pathways. Neural crest cells that form jugular neurons migrate from the postotic hindbrain, at the level of the first three somites. Neural crest cells are induced in three steps:

1. Formation of the neural plate border
2. Posteriorization of the neural plate border and induction of neural crest precursors within it
3. Epithelial-mesenchymal transition to form migrating neural crest cells

Neural crest cells form an enormous array of different derivatives. Lineage diversification is achieved by a combination of instructive environmental cues and

early fate-restrictions (probably due to neural crest cell-cell interactions, i.e., community effects) that mean the migrating neural crest is a heterogeneous population of multipotent and fate-restricted cells. Wnt signaling instructively promotes adoption of a sensory neuronal fate within the early neural crest. Wnts are expressed in the dorsal neural tube, and at least some early migrating neural crest cells are already restricted to a sensory fate. The proneural basic helix-loop-helix transcription factor Neurogenin1 is required for the formation of neurons in all proximal cranial sensory ganglia, including the jugular ganglion. It is likely that inhibition of the Notch signaling pathway, which is necessary for neurogenesis in dorsal root ganglia, is also required for neurogenesis in cranial sensory ganglia.

REFERENCES

1. Le Douarin, N.M. and Kalcheim, C., *The Neural Crest,* 2nd ed., Cambridge University Press, Cambridge, 1999.
2. Baker, C.V.H. and Bronner-Fraser, M., Vertebrate cranial placodes I. Embryonic induction*, Dev. Biol.*, 232, 1, 2001.
3. D'Amico-Martel, A. and Noden, D.M., An autoradiographic analysis of the development of the chick trigeminal ganglion*, J. Embryol. Exp. Morphol.*, 55, 167, 1980.
4. Landacre, F.L., The origin of the cranial ganglia in *Ameiurus., J. Comp. Neurol.*, 20, 309, 1910.
5. Yntema, C.L., Experiments on the origin of the sensory ganglia of the facial nerve in the chick.*, J. Comp. Neurol.*, 81, 147, 1944.
6. Hamburger, V., Experimental analysis of the dual origin of the trigeminal ganglion in the chick embryo*, J. Exp. Zool.*, 148, 91, 1961.
7. Johnston, M.C., A radioautographic study of the migration and fate of cranial neural crest cells in the chick embryo*, Anat. Rec.*, 156, 143, 1966.
8. Narayanan, C.H. and Narayanan, Y., Neural crest and placodal contributions in the development of the glossopharyngeal-vagal complex in the chick*, Anat. Rec.*, 196, 71, 1980.
9. Levi-Montalcini, R., Richerche sperimentali sulla determinazione del placode otico nell'embrione di pollo*, Accad. Naz. Lincei Rendic. Cl. Sci. fis-mat. e nat., Ser. VIII*, 1, 443, 1946.
10. Le Douarin, N.M., A biological cell labelling technique and its use in experimental embryology.*, Dev. Biol.*, 30, 217, 1973.
11. Noden, D.M., The control of avian cephalic neural crest cytodifferentiation. II. Neural tissues*, Dev. Biol.*, 67, 313, 1978.
12. D'Amico-Martel, A. and Noden, D.M., Contributions of placodal and neural crest cells to avian cranial peripheral ganglia*, Am. J. Anat.*, 166, 445, 1983.
13. Webb, J.F. and Noden, D.M., Ectodermal placodes: contributions to the development of the vertebrate head*, Amer. Zool.*, 33, 434, 1993.
14. Begbie, J. and Graham, A., The ectodermal placodes: a dysfunctional family*, Philos. Trans. R. Soc. Lond. B*, 356, 1655, 2001.
15. Bally-Cuif, L. and Hammerschmidt, M., Induction and patterning of neuronal development, and its connection to cell cycle control*, Curr. Opin. Neurobiol.*, 13, 16, 2003.
16. Vogt, W., Gestaltungsanalyse am Amphibienkeim mit örtlicher Vitalfärbung Vorwort über Wege une Ziele. II: Gastrulation und Mesodermbildung bei Urodelen und Anuren*, Wilhelm Roux Arch. EntwMech. Org.*, 120, 384, 1929.

17. Rosenquist, G.C., Epiblast origin and early migration of neural crest cells in the chick embryo, *Dev. Biol.*, 87, 201, 1981.
18. Selleck, M.A. and Bronner-Fraser, M., Origins of the avian neural crest: the role of neural plate-epidermal interactions, *Development*, 121, 525, 1995.
19. Streit, A., Extensive cell movements accompany formation of the otic placode, *Dev. Biol.*, 249, 237, 2002.
20. Whitlock, K.E. and Westerfield, M., The olfactory placodes of the zebrafish form by convergence of cellular fields at the edge of the neural plate, *Development*, 127, 3645, 2000.
21. Wawersik, S. and Maas, R.L., Vertebrate eye development as modeled in *Drosophila, Hum. Mol. Genet.*, 9, 917, 2000.
22. Davis, R.J. et al., Characterization of mouse *Dach2*, a homologue of *Drosophila dachshund, Mech. Dev.*, 102, 169, 2001.
23. Hammond, K.L. et al., Isolation of three zebrafish *dachshund* homologues and their expression in sensory organs, the central nervous system and pectoral fin buds, *Mech. Dev.*, 112, 183, 2002.
24. Heanue, T.A. et al., *Dach1*, a vertebrate homologue of *Drosophila dachshund*, is expressed in the developing eye and ear of both chick and mouse and is regulated independently of *Pax* and *Eya* genes, *Mech. Dev.*, 111, 75, 2002.
25. Loosli, F., Mardon, G. and Wittbrodt, J., Cloning and expression of medaka *Dachshund, Mech. Dev.*, 112, 203, 2002.
26. Schlosser, G. and Northcutt, R.G., Development of neurogenic placodes in *Xenopus laevis, J. Comp. Neurol.*, 418, 121, 2000.
27. Schlosser, G., Development and evolution of lateral line placodes in amphibians. I. Development, *Zoology*, 105, 119, 2002.
28. Solomon, K.S. et al., Zebrafish *foxi1* mediates otic placode formation and jaw development, *Development*, 130, 929, 2003.
29. Lee, S.A. et al., The zebrafish forkhead transcription factor Foxi1 specifies epibranchial placode-derived sensory neurons, *Development*, 130, 2669, 2003.
30. Groves, A.K. and Bronner-Fraser, M., Competence, specification and commitment in otic placode induction, *Development*, 127, 3489, 2000.
31. Ishii, Y., Abu-Elmagd, M. and Scotting, P.J., *Sox3* expression defines a common primordium for the epibranchial placodes in chick, *Dev. Biol.*, 236, 344, 2001.
32. Abu-Elmagd, M. et al., cSox3 expression and neurogenesis in the epibranchial placodes, *Dev. Biol.*, 237, 258, 2001.
33. Begbie, J. et al., Induction of the epibranchial placodes, *Development*, 126, 895, 1999.
34. Gavalas, A. et al., Synergy between *Hoxa1* and *Hoxb1*: the relationship between arch patterning and the generation of cranial neural crest, *Development*, 128, 3017, 2001.
35. Bertrand, N., Castro, D.S., and Guillemot, F., Proneural genes and the specification of neural cell types, *Nat. Rev. Neurosci.*, 3, 517, 2002.
36. Gaiano, N. and Fishell, G., The role of Notch in promoting glial and neural stem cell fates, *Annu. Rev. Neurosci.*, 25, 471, 2002.
37. Skaer, N. et al., Gene duplication at the *achaete-scute* complex and morphological complexity of the peripheral nervous system in Diptera, *Trends Genet.*, 18, 399, 2002.
38. Andermann, P., Ungos, J., and Raible, D.W., Neurogenin1 defines zebrafish cranial sensory ganglia precursors, *Dev. Biol.*, 251, 45, 2002.
39. Begbie, J., Ballivet, M. and Graham, A., Early steps in the production of sensory neurons by the neurogenic placodes, *Mol. Cell. Neurosci.*, 21, 502, 2002.
40. Fode, C. et al., The bHLH protein NEUROGENIN 2 is a determination factor for epibranchial placode-derived sensory neurons, *Neuron*, 20, 483, 1998.

41. Ma, Q. et al., *neurogenin1* is essential for the determination of neuronal precursors for proximal cranial sensory ganglia, *Neuron*, 20, 469, 1998.

42. Brunet, J.F. and Pattyn, A., *Phox2* genes — from patterning to connectivity, *Curr. Opin. Genet. Dev.*, 12, 435, 2002.

43. Goridis, C. and Rohrer, H., Specification of catecholaminergic and serotonergic neurons, *Nat. Rev. Neurosci.*, 3, 531, 2002.

44. Pattyn, A. et al., The homeobox gene *Phox2b* is essential for the development of autonomic neural crest derivatives, *Nature*, 399, 366, 1999.

45. Pattyn, A., Goridis, C., and Brunet, J.-F., Specification of the central noradrenergic phenotype by the homeobox gene *Phox2b., Mol. Cell. Neurosci.*, 15, 235, 2000.

46. Katz, D.M. and Erb, M.J., Developmental regulation of tyrosine hydroxylase expression in primary sensory neurons of the rat, *Dev. Biol.*, 137, 233, 1990.

47. Morin, X. et al., Defects in sensory and autonomic ganglia and absence of locus coeruleus in mice deficient for the homeobox gene *Phox2a., Neuron*, 18, 411, 1997.

48. Pattyn, A. et al., Expression and interactions of the two closely related homeobox genes *Phox2a* and *Phox2b* during neurogenesis, *Development*, 124, 4065, 1997.

49. Dauger, S. et al., Phox2b controls the development of peripheral chemoreceptors and afferent visceral pathways, *Development*, 130, 6635, 2003.

50. Begbie, J. and Graham, A., Integration between the epibranchial placodes and the hindbrain, *Science*, 294, 595, 2001.

51. Kious, B.M. et al., Identification and characterization of a calcium channel gamma subunit expressed in differentiating neurons and myoblasts, *Dev. Biol.*, 243, 249, 2002.

52. Harrison, T.A. et al., Compensatory responses and development of the nodose ganglion following ablation of placodal precursors in the embryonic chick (*Gallus domesticus*), *Cell Tissue Res.*, 281, 379, 1995.

53. Kuratani, S.C. and Wall, N.A., Expression of Hox 2.1 protein in restricted populations of neural crest cells and pharyngeal ectoderm, *Dev. Dyn.*, 195, 15, 1992.

54. Rancourt, D.E., Tsuzuki, T., and Capecchi, M.R., Genetic interaction between *hoxb-5* and *hoxb-6* is revealed by nonallelic noncomplementation, *Genes Dev.*, 9, 108, 1995.

55. Knecht, A.K. and Bronner-Fraser, M., Induction of the neural crest: a multigene process, *Nat. Rev. Genet.*, 3, 453, 2002.

56. Mayor, R. and Aybar, M.J., Induction and development of neural crest in *Xenopus laevis., Cell Tissue Res.*, 305, 203, 2001.

57. Kalcheim, C., Mechanisms of early neural crest development: from cell specification to migration, *Int. Rev. Cytol.*, 200, 143, 2000.

58. LaBonne, C. and Bronner-Fraser, M., Molecular mechanisms of neural crest formation, *Annu. Rev. Cell Dev. Biol.*, 15, 81, 1999.

59. Gammill, L.S. and Bronner-Fraser, M., Neural crest specification: migrating into genomics, *Nat. Rev. Neurosci.*, 4, 795, 2003.

60. Wu, J., Saint-Jeannet, J.-P. and Klein, P.S., Wnt-frizzled signaling in neural crest formation, *Trends Neurosci.*, 26, 40, 2003.

61. LaBonne, C. and Bronner-Fraser, M., Neural crest induction in *Xenopus*: evidence for a two-signal model, *Development*, 125, 2403, 1998.

62. Nguyen, V.H. et al., Ventral and lateral regions of the zebrafish gastrula, including the neural crest progenitors, are established by a *bmp2b/swirl* pathway of genes, *Dev. Biol.*, 199, 93, 1998.

63. Streit, A. and Stern, C.D., Establishment and maintenance of the border of the neural plate in the chick: involvement of FGF and BMP activity, *Mech. Dev.*, 82, 51, 1999.

64. Villanueva, S. et al., Posteriorization by FGF, Wnt, and retinoic acid is required for neural crest induction, *Dev. Biol.*, 241, 289, 2002.

65. McLarren, K.W., Litsiou, A. and Streit, A., DLX5 positions the neural crest and preplacode region at the border of the neural plate, *Dev. Biol.*, 259, 34, 2003.
66. Woda, J.M. et al., Dlx proteins position the neural plate border and determine adjacent cell fates, *Development*, 130, 331, 2003.
67. Wilson, P.A. et al., Concentration-dependent patterning of the *Xenopus* ectoderm by BMP4 and its signal transducer Smad1, *Development*, 124, 3177, 1997.
68. Chang, C. and Hemmati-Brivanlou, A., Neural crest induction by *Xwnt7B* in *Xenopus.*, *Dev Biol*, 194, 129, 1998.
69. Monsoro-Burq, A.H., Fletcher, R.B., and Harland, R.M., Neural crest induction by paraxial mesoderm in *Xenopus* embryos requires FGF signals, *Development*, 130, 3111, 2003.
70. Nordström, U., Jessell, T.M. and Edlund, T., Progressive induction of caudal neural character by graded Wnt signaling, *Nat. Neurosci.*, 5, 525, 2002.
71. Baker, C.V.H. and Bronner-Fraser, M., The origins of the neural crest. Part I: Embryonic induction, *Mech. Dev.*, 69, 3, 1997.
72. Spokony, R.F. et al., The transcription factor Sox9 is required for cranial neural crest development in *Xenopus, Development*, 129, 421, 2002.
73. Cheung, M. and Briscoe, J., Neural crest development is regulated by the transcription factor Sox9, *Development*, 130, 5681, 2003.
74. Luo, T. et al., Induction of neural crest in *Xenopus* by transcription factor AP2alpha, *Proc. Natl. Acad. Sci. USA*, 100, 532, 2003.
75. Dottori, M. et al., The winged-helix transcription factor Foxd3 suppresses interneuron differentiation and promotes neural crest cell fate, *Development*, 128, 4127, 2001.
76. del Barrio, M.G. and Nieto, M.A., Overexpression of Snail family members highlights their ability to promote chick neural crest formation, *Development*, 129, 1583, 2002.
77. Sela-Donenfeld, D. and Kalcheim, C., Regulation of the onset of neural crest migration by coordinated activity of BMP4 and Noggin in the dorsal neural tube, *Development*, 126, 4749, 1999.
78. Sela-Donenfeld, D. and Kalcheim, C., Inhibition of noggin expression in the dorsal neural tube by somitogenesis: a mechanism for coordinating the timing of neural crest emigration, *Development*, 127, 4845, 2000.
79. Kanzler, B. et al., BMP signaling is essential for development of skeletogenic and neurogenic cranial neural crest, *Development*, 127, 1095, 2000.
80. Halloran, M.C. and Berndt, J.D., Current progress in neural crest cell motility and migration and future prospects for the zebrafish model system, *Dev. Dyn.*, 228, 497, 2003.
81. Krull, C.E., Segmental organization of neural crest migration, *Mech. Dev.*, 105, 37, 2001.
82. Anderson, D.J., Genes, lineages and the neural crest: a speculative review, *Phil. Trans. R. Soc. Lond. B*, 355, 953, 2000.
83. McGonnell, I.M. and Graham, A., Trunk neural crest has skeletogenic potential, *Curr. Biol.*, 12, 767, 2002.
84. Sommer, L., Context-dependent regulation of fate decisions in multipotent progenitor cells of the peripheral nervous system, *Cell Tissue Res.*, 305, 211, 2001.
85. Anderson, D.J., Cellular and molecular biology of neural crest cell lineage determination, *Trends Genet.*, 13, 276, 1997.
86. Shah, N.M., Groves, A.K., and Anderson, D.J., Alternative neural crest cell fates are instructively promoted by TGFβ superfamily members, *Cell*, 85, 331, 1996.
87. Shah, N.M. et al., Glial growth factor restricts mammalian neural crest stem cells to a glial fate, *Cell*, 77, 349, 1994.

88. Hagedorn, L. et al., The Ets domain transcription factor Erm distinguishes rat satellite glia from Schwann cells and is regulated in satellite cells by neuregulin signaling, *Dev. Biol.*, 219, 44, 2000.

89. Leimeroth, R. et al., Membrane-bound neuregulin1 type III actively promotes Schwann cell differentiation of multipotent progenitor cells, *Dev. Biol.*, 246, 245, 2002.

90. Dorsky, R.I., Moon, R.T., and Raible, D.W., Control of neural crest cell fate by the Wnt signalling pathway, *Nature*, 396, 370, 1998.

91. Lee, H.Y. et al., Instructive role of Wnt/beta-catenin in sensory fate specification in neural crest stem cells, *Science*, 303, 1020, 2004.

92. Dorsky, R.I., Moon, R.T., and Raible, D.W., Environmental signals and cell fate specification in premigratory neural crest, *BioEssays*, 22, 708, 2000.

93. Henion, P.D. and Weston, J.A., Timing and pattern of cell fate restrictions in the neural crest lineage, *Development*, 124, 4351, 1997.

94. Echelard, Y., Vassileva, G. and McMahon, A.P., Cis-acting regulatory sequences governing Wnt-1 expression in the developing mouse CNS, *Development*, 120, 2213, 1994.

95. Serbedzija, G.N. and McMahon, A.P., Analysis of neural crest cell migration in *Splotch* mice using a neural crest-specific LacZ reporter, *Dev. Biol.*, 185, 139, 1997.

96. Zirlinger, M. et al., Transient expression of the bHLH factor neurogenin-2 marks a subpopulation of neural crest cells biased for a sensory but not a neuronal fate, *Proc. Natl. Acad. Sci. USA*, 99, 8084, 2002.

97. Nusse, R., Wnts and Hedgehogs: lipid-modified proteins and similarities in signaling mechanisms at the cell surface, *Development*, 130, 5297, 2003.

98. Hari, L. et al., Lineage-specific requirements of beta-catenin in neural crest development, *J. Cell Biol.*, 159, 867, 2002.

99. Bronner-Fraser, M., Making sense of the sensory lineage, *Science*, 303, 966, 2004.

100. Fraser, S.E. and Bronner-Fraser, M., Migrating neural crest cells in the trunk of the avian embryo are multipotent, *Development*, 112, 913, 1991.

101. Greenwood, A.L., Turner, E.E. and Anderson, D.J., Identification of dividing, determined sensory neuron precursors in the mammalian neural crest, *Development*, 126, 3545, 1999.

102. Ma, Q. et al., NEUROGENIN1 and NEUROGENIN2 control two distinct waves of neurogenesis in developing dorsal root ganglia, *Genes Dev.*, 13, 1717, 1999.

103. Wakamatsu, Y., Maynard, T.M., and Weston, J.A., Fate determination of neural crest cells by NOTCH-mediated lateral inhibition and asymmetrical cell division during gangliogenesis, *Development*, 127, 2811, 2000.

104. Zilian, O. et al., Multiple roles of mouse Numb in tuning developmental cell fates, *Curr. Biol.*, 11, 494, 2001.

2 Vagal Afferent Neurons: Neurotrophic Factors and Epigenetic Influences

Cinda J. Helke

CONTENTS

2.1 INTRODUCTION

Visceral afferent neurons, including vagal and glossopharyngeal afferent neurons, are critical to autonomic and visceral homeostasis. Establishing and maintaining the appropriate functions of these neurons is thus necessary to the integrity of visceral afferent signals to the brain and subsequent influences on autonomic reflexes. Developmental influences on afferent neurons and the ways in which mature visceral afferent neurons respond to injury or neuropathic insults are likely to be important in determining the success or failure of the neurons to maintain visceral afferent reflexes. The functions of these neurons are altered in chronic disease states such as hypertension (chronic overloading of baroreceptors) and congestive heart failure (chronic overloading of cardiac stretch receptors).[164,258] Injury to visceral afferent nerves can occur from chemical agents (antineoplastic agents), trauma, tumors, and disease (e.g., diabetes mellitus, Guillain-Barre syndrome).[165,166,223]

Numerous alterations in the neuronal phenotype, growth, regenerative capacity, and survival are evident during the life span of these neurons, from development through maturity. Knowledge of the influences of trophic factors, injury, and other epigenetic influences on visceral afferent neurons is growing but remains incomplete. Knowledge of the regulatory influences on visceral afferent neurons is essential to understanding the responses of the neurons to deprivation of target-derived factors, and the potential roles of neurotrophins in alleviating specific dysfunctions of these neurons. Moreover, understanding neurotrophic receptor activation, transport, and actions in this important neuronal system will extend our ability to safely and wisely use neurotrophic factors as therapeutic agents in a variety of neuropathic and degenerative disorders affecting the autonomic nervous system.

This chapter provides current information on the neurotrophic and other influences affecting these important visceral afferent neurons.

2.2 EPIGENETIC INFLUENCES ON DEVELOPMENT/SURVIVAL OF VAGAL AFFERENT NEURONS

2.2.1 NEUROTROPHINS IN DEVELOPMENT

The best-studied neurotrophic responses are those of the neurotrophin family of neurotrophic factors. The neurotrophins, a structurally related group of polypeptide neurotrophic factors, include nerve growth factor (NGF), brain-derived neurotrophic factor (BDNF), neurotrophin-3 (NT-3), and neurotrophin-4/5 (NT-4). Nodose ganglion neurons express two classes of transmembrane neurotrophin receptors, which display pharmacologically distinct neurotrophin binding sites. Neurotrophin receptors include the low-affinity p75 receptor and the Trk family of receptor tyrosine kinases. NGF is the preferred ligand for TrkA, whereas TrkB is activated by both BDNF and NT-4, and NT-3 is the preferred ligand for TrkC.[30,68,122]

During development, nodose ganglion neurons are dependent for survival on BDNF, NT-3, and NT-4 but less, if at all, dependent on NGF.[32,142,213] Studies of mice with targeted mutations of the neurotrophin genes reveal the dependence of developing nodose ganglion neurons on BDNF, NT-3, and NT-4; however, NGF gene knockout mice and rodents autoimmune to NGF show deficits of nodose ganglion neurons only in narrow developmental periods.[213]

2.2.1.1 NGF and TrkA

NGF mRNA is not detected in E13 to E18 rat nodose or petrosal ganglia.[53] TrkA mRNA is present in the nodose/petrosal ganglia as early as E11 and peaks at E18. As development progresses, the TrkA labeling becomes isolated in the larger cells in the nodose ganglion and becomes less intense.[75] Modest labeling of TrkA mRNA in the nodose and petrosal ganglia is noted at postnatal day 1 (Figure 2.1).[252]

Most studies suggest that NGF has little, if any, effect on survival of developing nodose ganglion neurons. Many studies report that NGF has no trophic effect on cultured nodose ganglion neurons.[108,141,142,155,186] Studies using NGF gene knockout mice and rodents autoimmune to NGF also show no deficits of nodose ganglion neurons.[108,186,213]

In contrast to the numerous studies not showing an NGF dependence of developing nodose ganglion neurons, recent studies suggest that NGF may play a role at specific developmental stages in the survival of ganglion neurons. Katz et al. (see Reference 117) showed that NGF supports a small percentage of placode-derived neurons in explant culture for a narrow embryologic period (E13.5 to E14.5). Mice rendered NGF deficient had fewer neurons at middle to late (E16 and E18) embryologic stages and an increase in dying cells at middle stages (E16) only.[63] NGF promotes neuronal survival in cultured E12 and E13, as well as P1 nodose/petrosal ganglia, but has no effect on the embryologic stages in between.[63] Moreover, NGF increased the total dendritic growth in newborn nodose ganglion neurons.[41]

The presence of NGF in neonatal nodose ganglion cultures increases the amount of the neuropeptides calcitonin gene-related peptide (CGRP) and substance P (SP)
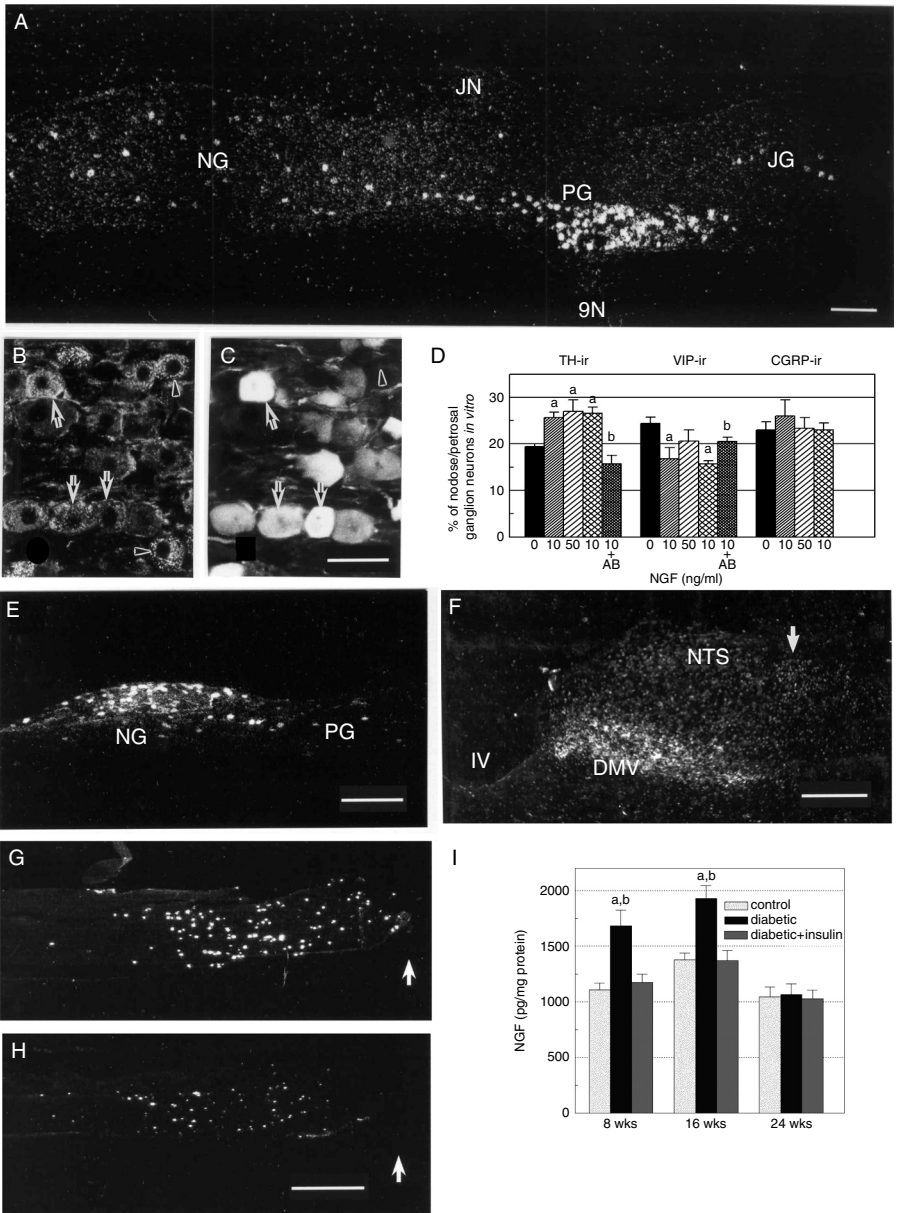
FIGURE 2.1 NGF, TrkA, and vagal afferents. (**A**) Dark-field photomicrographs showing adult nodose (NG), petrosal (PG), and jugular (JG) ganglia hybridized *in situ* with an ^{35}S-labeled antisense oligonucleotide probe for TrkA mRNA. Bar = 250 μm. (Adapted from Zhuo and Helke, 1996.) (**B** and **C**) Double immunofluorescent photomicrographs for TrkA-ir (**B**) and calbindin D-28k-ir (**C**) in the rat nodose ganglion. Arrows indicate neurons labeled for both TrkA-and calbindin D-28k-ir; arrowheads indicate TrkA neurons lacking calbindin D-28k-ir. Bar = 50 μm. (Adapted from Ichikawa and Helke, 1999.) *(continued)*

expressed by the neurons.[155,156] Nodose ganglion neurons cultured in the presence of NGF have double the amount of SP. The increased amount of CGRP in these neurons is variable, little change to 50% increase, with each experiment compared with those nodose ganglion neurons cultured without NGF present.[153,155] Newborn nodose ganglion neurons cultured with NGF show an increase in the amount of SP-immunoreactivity (ir) in normally expressing cells and in the total number of cells expressing SP.[154] In more recent studies, the level of TH mRNA in the nodose/petrosal ganglia is not affected by NGF deficiency,[63] but addition of NGF doubles the percentage of tyrosine hydroxylase (TH)-positive neurons at both E14.5 and E16.5.[114]

2.2.1.2 BDNF, NT-4, and TrkB

Numerous studies support the role for BDNF and many studies support a role for NT-4 in the development of nodose ganglion neurons. In addition, there appears to be an interactive relationship between these two neurotrophins, and among these agents and other trophic factors during development (Figure 2.2).

BDNF mRNA is found in the E13 to E18 rat nodose ganglion, but not in the petrosal ganglion.[53] BDNF mRNA and protein are first detected in the nodose/petrosal at E16.5 and the levels increase until P0.[18] BDNF is expressed transiently in nodose/petrosal target tissues coincident with sensory innervation and nodose/petrosal neuronal dependence on BDNF *in vitro*.[18] BDNF is expressed in hindbrain and heart (central and peripheral targets) prior to arrival of the earliest sensory axon.[197]

TrkB mRNA is detected in 1-day-old neonatal rat nodose and petrosal ganglia.[76,252] TrkB mRNA is first detected in the chick nodose ganglion at E21 and its level continues to rise to E24 (no measurement performed at later stages), while p75 mRNA is first detected at E20 and its level continues to rise to E24.[197] The addition

FIGURE 2.1 (CONTINUED) (**D**) Bar graph showing the percent of enriched dissociated mature nodose/petrosal ganglia neurons immunoreactive for tyrosine hydroxylase (TH), vasoactive intestinal peptide (VIP), and calcitonin gene-related protein (CGRP) after 5 days in cultures treated with NGF at 0, 50, 100 ng/ml or 100 ng/ml in the presence of an NGF neutralizing antibody (+AB). Neurotrophins and neutralizing antibodies were present throughout the 5-day culture period. a = P<0.05 compared with control, b = P<0.05 compared with corresponding 100 ng/ml data. (Adapted from Helke and Verdier-Pinard, 2000.) (**E and F**) Low power dark-field photomicrographs of the ipsilateral nodose ganglion (**E**) and nucleus of the solitary tract (NTS) (**F**) showing the retrogradely transported autoradiographic labeling of cell bodies in the NG and terminals in the NTS (-13.2 caudal to bregma) and cell bodies in the dorsal motor nucleus of the vagus (DMV) after application of ^{125}I-NGF to the cervical vagus nerve. IV = 4th ventricle, arrow indicates ipsilateral solitary tract. Note absence of labeling in the petrosal ganglion. Bar in E = 500 μm; bar in F = 200 μm. (Adapted from Helke et al., 1998.) (**G and H**) Dark-field photomicrographs showing the *in situ* hybridization labeling of mRNAs for NGF (**G**) and TrkA (**H**) in the proximal stump of the transected cervical vagus nerve 1 day after axotomy. Arrows indicate the site of transection. Bar = 500 μm. (Adapted from Lee et al., 2001a.) (**I**) Bar graph showing the effect of streptozotocin (STZ)-induced diabetes on NGF content of the intact right cervical vagus nerve at the 8-, 16-, and 24-week time points. a = P<0.05 compared with control, b = P<0.05 compared with diabetic+insulin-treated counterparts. (Adapted from Lee et al., 2001b.)
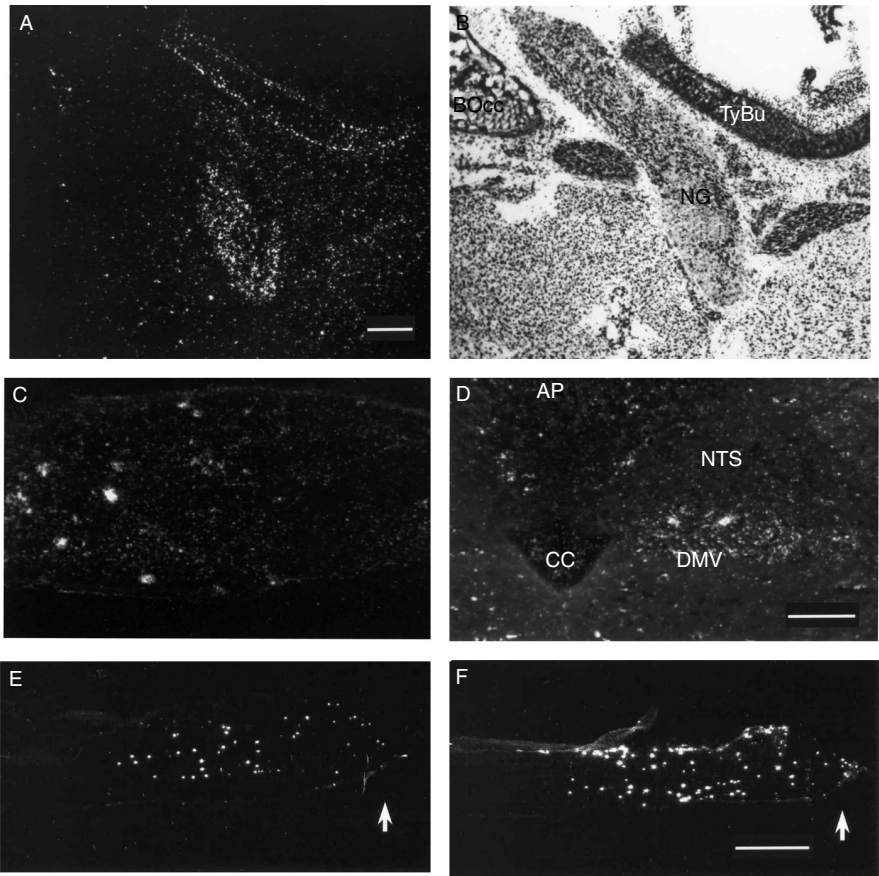
FIGURE 2.2 BDNF, TrkB, and vagal afferents. (**A** and **B**) Dark-field photomicrographs (**A**) and bright-field (**B**) showing autoradiographic labeling of the nodose ganglion (NG) in neonatal (P1) rats using ^{35}S-labeled antisense oligonucleotide probe for TrkB mRNA. BOcc = basioccipital bone; TyBU= tympanic bulla. Bar = 250 µm. (Adapted from Zhuo and Helke, 1996.) (**C** and **D**) Dark-field photomicrographs of the ipsilateral nodose ganglion (**C**) and nucleus of the solitary tract (NTS) (**D**) showing the small number retrogradely transported autoradiographic labeling of cell bodies in the NG and absence of terminals in the NTS (-13.2 caudal to bregma) after application of ^{125}I-BDNF to the cervical vagus nerve. Note the cellular labeling in vagal efferent neurons in the dorsal motor nucleus of the vagus (DMV). CC = central canal; AP = area postrema. Bar = 200 µm. (Adapted from Helke et al., 1998.) (**E** and **F**) Dark-field photomicrographs showing the *in situ* hybridization labeling of mRNAs for BDNF (**E**) and TrkB (**F**) in the proximal stump of the transected cervical vagus nerve 1 day after axotomy. Arrows indicate the site of transection. Bar = 500 µm. (Adapted from Lee et al., 2001a.)

of BDNF to the cultured medium increases TrkB mRNA only after 48 hours.[197] There is no difference in the amount of TrkB mRNA between BDNF-deficient, BDNF-heterozygous, and wild-type mouse nodose ganglia.[98]

During development, BDNF and NT-4 promote nodose neuronal survival *in vitro*[18,51,52,63,95,105,137,171,199,212,237,238] and *in vivo*.[51,93] BDNF increases nodose ganglion

neurite outgrowth in E12 chick nodose ganglion,[16] both the neurite length and density of late embryologic stage and newborn rat nodose ganglion explants.[160,180] Although early studies reported that NT-4/NT-5 had little effect on nodose ganglion neurons,[15,74] later studies report that NT-4 supports cultured developing nodose ganglion neurons[86] and induces neurite outgrowth from the cultured adult nodose ganglion.[245]

Studies in mice rendered neurotrophin-deficient reveal a distinct dependency of developing nodose or petrosal ganglion neurons to BDNF and NT-4.[32,51,52,110,144] Deficiencies in BDNF or NT-4 affect the nodose/petrosal neuronal number at different stages in development. A deficiency in BDNF has no effect on the neuronal survival of nodose/petrosal from E11 and E12 mouse embryos; however, addition of exogenous BDNF increases neuronal survival in both mutant and wild-type mice.[98] BDNF added to the culture of E3.5 chick nodose ganglion neurons for 72 hours has no effect on neuronal survival compared with control, and these neurons die faster than control after discontinuation of the BDNF treatment.[237] Mice deficient for BDNF have increased neuronal loss and increased apoptosis in the nodose/petrosal ganglia at later embryologic stages (E14 to P1).[49] From this, it is apparent that BDNF's role in nodose/petrosal neuronal development comes at later stages. Nodose ganglion neuronal dependence on BDNF is accelerated by a 12-hour pulse of BDNF added to the culture of E3.5 chick nodose ganglion neurons after 48 hours. Once the BDNF is removed at 60 hours, these neurons die faster than controls.[237] A 12-hour pulse prior to 48 hours in culture has no effect on BDNF dependence;[237] thus, the nodose neurons are only responsive to BDNF at certain embryologic developmental stages. In transgenic mice that overexpress BDNF in epithelial target tissues of sensory neurons, a 38% increase in neurons comprising the placode-derived nodose–petrosal complex occurred.[135]

Mice deficient in NT-4 lack 55% of vagal sensory neurons, yet are viable.[32,144] Mice deficient in NT-4 have increased neuronal loss, more apoptosis, and less proliferation in the nodose/petrosal ganglia at middle embryologic stages (E12 to E14).[49] NT-4 deficient mice show severe loss of vagal afferent structures from the duodenum and ileum but not the stomach.[64] Knockout of BDNF, NT-4, or both decreases the neonatal nodose/petrosal neuronal survival.[49–51,136] NT-3 and BDNF together rescue 90% of these neurons from death.[94] Almost all nodose/petrosal neurons are lost in newborn mice lacking functioning TrkB receptors.[51]

BDNF and NT-4 have nonredundant, but compensatory, actions in the nodose/petrosal ganglion, and each target separates subpopulations of the ganglia.[51] Without functioning BDNF or NT-4 there is a loss of about 50% in nodose/petrosal neuronal number, and with neither there is a loss of about 90%.[51] A large subpopulation of nodose/petrosal neurons can be supported by NT-4 when BDNF is not available, which suggests that NT-4 can compensate for the lack of BDNF during development.[51] The number of surviving neurons is proportional to the number of functioning BDNF alleles. In contrast, a single functioning NT-4 allele can support a large population of neurons.[51]

An organ-specific loss associated with a neurotrophin deficiency occurs in BDNF mutants wherein arterial chemoreceptors in the carotid body and baroreceptors (a class of mechanoreceptors) in the carotid sinus are lost.[18,51] Thus, receptors of two modalities but of the same organ system (arterial beds) are affected by loss of BDNF

during development. *In vivo* chemoafferents are selectively supported by treatment with TrkB ligands (BDNF and NT-4), whereas NGF and NT-3 had no effect.[86] In the absence of target tissues, a large proportion of carotid body afferents is rescued by implants containing BDNF.[86]

2.2.1.3 NT-3 and TrkC

NT-3 mRNA is found in the E13 to E18 rat petrosal ganglion, but not in the nodose ganglion.[53] TrkC mRNA is detected in the nodose but not petrosal ganglion of the embryologic chick[246] and rat.[53] The nodose and petrosal ganglia from 1-day-old neonates expressed TrkC mRNA (Figure 2.3).[252]

Embryologic nodose neurons are responsive to NT-3.[105] In nodose ganglion, a small population of neurons exclusively responds to NT-3 and a larger population of nodose ganglion neurons that can be supported by NT-3 or by BDNF.[136] The presence of NT-3 supports the survival of 30% of embryologic nodose ganglion neurons, NT-3 and BDNF together rescue 90% of these neurons from death.[94] NT-3 increases nodose ganglion neurite outgrowth in E12 chick nodose ganglion,[16] and both the neurite length and density of late embryologic stage and newborn rat nodose ganglion explants.[160,180]

NT-3 can rescue nodose neurons that are without functioning TrkC receptors only at earlier embryologic development stages, while BDNF can rescue these neurons throughout fetal development. E14 and E18 TrkC-/- mice have less than 10% of their nodose ganglion neurons surviving after 36 to 48 hours in culture.[40] At E14, both BDNF and NT-3 increase the neuronal survival to 60 to 70% after 36 to 48 hours. At E18, BDNF increases the percent of surviving neurons after 36 to 48 hours to 70%, while NT-3 only increases the percent survival to 15%.[40] At E14, increasing concentrations of NT-3 in culture increase the percent of surviving nodose neurons, whether the neurons are wild-type or TrkC-/-, while at E18, even with high concentrations of NT-3, the percent survival does not go above 20% in either the wild-type or the TrkC-deficient neurons.[40] These data indicate that, during mid-embryologic developmental stages, NT-3 can act via receptors other than TrkC, notably TrkA and TrkB.

NT-3 deficient mice have fewer nodose/petrosal neurons than wild-type mice.[57] Mice deficient for NT-3 have increased neuronal loss, more apoptosis, and less proliferation in the nodose/petrosal ganglia at early embryologic stages (up to E14).[49] In newborn single mutant mice, heterozygotes have fewer neurons in the nodose/petrosal ganglia than wild-type and the fewest neurons are in the homozygotes.[49] Newborn mice deficient in BDNF, NT-3, or NT-4 have 30 to 66% fewer neurons in the nodose ganglia compared with wild-type and the effect is additive in triple-deficient mice where there were 96% fewer neurons in the nodose ganglia compared with wild-type.[145] Vagal afferent structures in the esophagus are reduced in adult mice deficient for NT-3 or TrkC.[191]

BDNF acts only via the TrkB receptor during nodose neuronal development, while NT-3 acts via both the TrkB and TrkC receptors during nodose neuronal development. The percent survival in E13 nodose neurons after 36 to 48 hours is less than 10% in the presence of BDNF or NT-3 when TrkB is not functional and
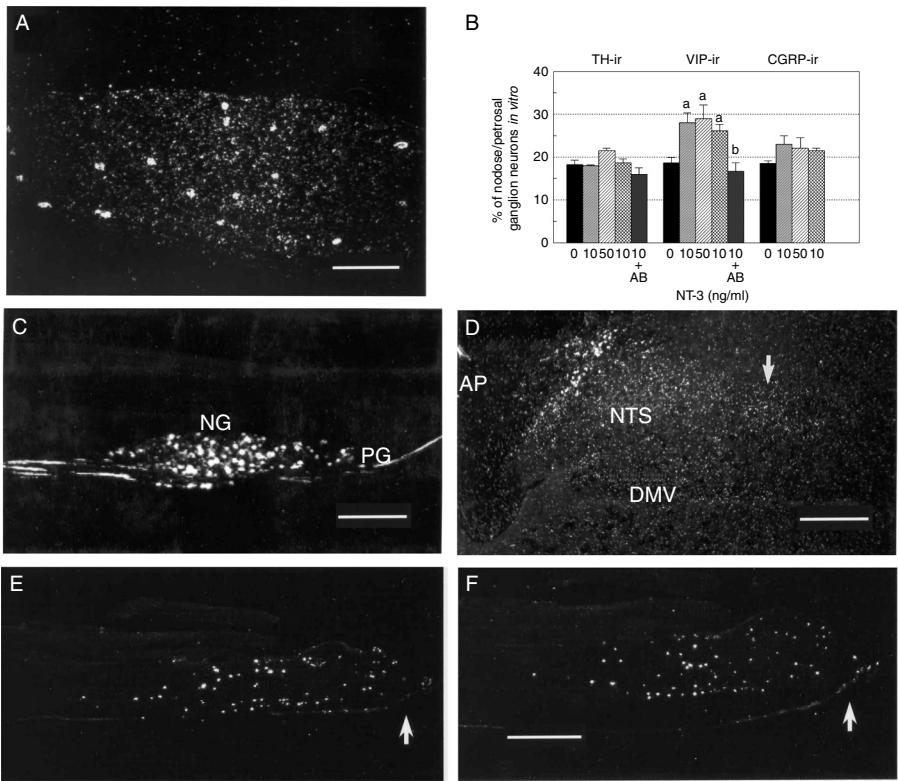
FIGURE 2.3 NT-3, TrkC, and vagal afferents. (**A**) Dark-field photomicrographs showing adult nodose ganglion hybridized *in situ* with an ^{35}S-labeled antisense oligonucleotide probe for TrkC mRNA. Bar = 250 μm. (Adapted from Zhuo and Helke, 1996.) (**B**) Bar graphs showing the percent of nodose/petrosal ganglia neurons immunoreactive for tyrosine hydroxylase (TH), vasoactive intestinal peptide (VIP), and calcitonin gene-related peptide (CGRP) after 5 days in dissociated enriched neuronal cultures treated with NT-3 at 0, 50, 100 ng/ml or 100 ng/ml in the presence of NT-3 neutralizing antibody (+AB). Neurotrophins and neutralizing antibodies were present from the time of plating, throughout the 5-day culture period. a = P<0.05 compared with control, b = P<0.05 compared with corresponding 100 ng/ml data. (Adapted from Helke and Verdier-Pinard, 2000.) (**C** and **D**) Low-power dark-field photomicrographs of the ipsilateral nodose ganglion (**C**) and nucleus of the solitary tract (NTS) (**D**) showing the retrogradely transported autoradiographic labeling of cell bodies in the NG and terminals in the NTS (-13.5 caudal to bregma) after application of ^{125}I-NT-3 to the cervical vagus nerve. AP = area postrema, arrow indicates ipsilateral solitary tract. Note absence of labeling in the petrosal ganglion and in the dorsal motor nucleus of the vagus (DMV). Bar in C = 500 μm, bar in D = 200 μm. (Adapted from Helke et al., 1998.) (**E** and **F**) Dark-field photomicrographs showing the *in situ* hybridization labeling of mRNAs for NT-3 (**E**) and TrkC (**F**) in the proximal stump of the transected cervical vagus nerve 1 day after axotomy. Arrows indicate the site of transection. Bar = 500 μm. (Adapted from Lee et al., 2001a.)

regardless of the TrkC genotype.[40] Seventy-five to eighty percent of the E13 nodose neurons survive in the presence of BDNF with functioning TrkB receptors, regardless of TrkC genotype, and 55 to 60% of the nodose neurons survive in the presence of BDNF with the heterozygous (+/−) TrkB genotype, regardless of TrkC genotype.[40]

Fifty to fifty-five percent of the E13 nodose neurons survive in the presence of NT-3 with functioning TrkB receptors, regardless of TrkC genotype. NT-3 promotes levels of survival in neurons with heterozygous TrkB receptors that are similar to the wild-type TrkB numbers as long as there is a functioning TrkC receptor. The percent survival of the neurons decreases by about 20% with heterozygous TrkC receptors and by about 50% with homozygous −/− receptors.[40]

The presence of BDNF during neuronal development can alter the transmitter phenotype of nodose and/or petrosal ganglion neurons. BDNF attenuates the carotid body glomectomy-induced catecholaminergic cell loss in the petrosal ganglion of newborn rats.[86,87] The absence of BDNF produces a loss in dopaminergic petrosal ganglion neurons between E14.5 and P0.[50] Mice deficient for BDNF had about half as many TH-ir neurons at P0 than wild-type, whereas mice deficient for NT-3 and NT-4 have similar TH-ir in nodose neurons in all embryological stages.[49] Moreover, all TH-ir neurons in the newborn petrosal ganglion are BDNF-ir.[18]

2.2.2   OTHER NEUROTROPHIC FACTORS/RECEPTORS IN DEVELOPING GANGLIA

Other neurotrophic factors, including glial cell line-derived neurotrophic factor (GDNF), ciliary neurotrophic factor (CNTF), and leukemia inhibitory factor (LIF), also have trophic actions on visceral sensory neurons.

2.2.2.1 Glial Cell Line-Derived Neurotrophic Factor (GDNF) Family

GDNF, originally isolated from the rat glial cell line B49, is found in many peripheral tissues, such as heart, lung, liver, kidney, spleen, blood,[217] and CNS.[214] The GDNF family includes GDNF, persephin, neurturin, and artemin.[8] GDNF exerts it actions by binding to the transmembrane tyrosine kinase Ret and GDNF family receptors GFR alpha 1, 2, 3, and 4.

GDNF is found in nodose/petrosal target tissues, including the carotid body, at the same time as initial innervation by the neurons and coincident with neuronal dependence on GDNF.[50,181,230] GDNF receptors are found in the nodose ganglion during embryologic development.[131] The mRNA levels of the GDNF receptors GFR-1 and Ret are two to three times greater than that of the GDNF receptor GFR-2 at E8 to E12.[62]

GDNF supports the survival of developing chick nodose sensory neurons,[25,230] particularly at early embryologic stages (E8 to E12).[62] GDNF also supports rat embryologic nodose and petrosal ganglion neuronal survival in culture.[50] Neurturin, although less potent than GDNF, also supports nodose ganglion neuronal survival at early embryologic stages.[62]

At middle chick embryologic stages (E13 and E16), there is neurite growth in the absence of neurotrophic factors.[131] Thus, GDNF is not necessary for nodose ganglion neuronal neurite outgrowth at any embryologic stage, but GDNF can stimulate the outgrowth of fibers in the chick embryonic nodose ganglion.[47] Addition of GDNF alone or GDNF plus the GDNF receptor GFR-1 to cultured chick nodose

ganglion neurons increases neurite growth at all stages.[131] Likewise, GDNF increases neurite outgrowth from E18 and P1 rat nodose ganglion explants but not from adult ganglia.[180]

Moore et al.[174] report that newborn (P0) mice deficient for GDNF have fewer neurons in the nodose and petrosal ganglia complex compared with wild-type. However, the absence of GDNF does not affect the nodose neuron number but does reduce the number of petrosal ganglion neurons suggesting that nodose neurons do not require GDNF for survival while petrosal ganglion neurons do require GDNF.[50] Moreover, no nodose ganglion neurons are lost in mice deficient in neurturin,[89] GRF-2,[198] or GFR-3.[179] It has been proposed that BDNF and/or NT-4 support the survival of GDNF-dependent neurons in these mutant mice or that some nodose ganglion neurons become dependent on GDNF during development.[112]

GDNF null mutant mice have reduced numbers of petrosal ganglion neurons.[50] The absence of GDNF produces a loss in dopaminergic petrosal ganglion neurons between E15.5 and E17.5.[50] GDNF is detected in petrosal ganglion targets at E15.5, at the same stage where petrosal neuron loss begins when the cells do not have GDNF, suggesting that it is a target-derived survival factor.[50]

GDNF increases nodose neuronal survival in dissociate cultures as well as total and TH-ir neuron number.[50] GDNF increases the total number of neurons and the number of TH-ir neurons in explant cultures of petrosal ganglia; however, the percentage of TH-ir cells remains constant, indicating that the increase in TH-ir is due to an increase in neuronal number and not an upregulation of TH.[50] BDNF and GDNF together cause an additive increase in the number of TH-ir cells in the petrosal ganglion when they are administered at subsaturating, but not saturating, concentrations.[50] In double knock-out (BDNF−/− and GDNF−/−) mice, 98% of TH-ir and RET-ir neurons are lost, showing that a large subset of dopaminergic petrosal ganglion neurons requires both BDNF and GDNF for survival *in vivo*.[50]

2.2.2.2 Ciliary Neurotrophic Factor (CNTF) Family

CNTF is structurally related to interleukin 6 (IL-6), interleukin 11 (IL-11), leukemia inhibitory factor (LIF), cardiotrophin-like cytokine (CL-1) and oncostatin M (OSM). The high affinity receptor complex, which mediates the biological action of CNTF, contains the ligand-binding subunit (CNTF R) and two signal-transducing proteins, LIF R and gp130. CNTF and LIF receptor components are present in both E16.5 and newborn ganglia.[221] Rat nodose and petrosal sections incubated with iodinated LIF have strong binding at E18 and P0, also indicating the presence of receptors for these factors.[190]

CNTF was initially shown to promote the survival of the chick ciliary ganglion neurons.[11,162] However, a study by Oppenheim[184] suggested that CNTF had no effect, good or bad, on nodose survival, while a study by Rudge et al.[199] suggested that CNTF increased nodose neuronal survival early in development. CNTF supports the survival of E16.5 but not neonatal rat nodose and petrosal ganglia neurons in dissociate cultures.[212,221] LIF supports the survival of dissociated embryonic nodose ganglion neurons in culture.[221] LIF appears to support a subset of nodose ganglion neurons that is also responsive to BDNF, NT-3, and NT-4.[221] Throughout development, nodose

ganglion neurons in culture survive better when in the presence of CNTF, LIF, OSM, and CT-1.[95,96] This effect, however, is not present at birth where only 10% of P0 neurons survive in the presence of LIF and CNTF. The neuronal survival benefits of IL-6 are seen in the later embryologic stages only where up to 45% of neurons survive in culture.[95,96] Dose response analysis indicates that, of these neurotrophic factors, CNTF is the most potent, followed by OSM, LIF, CT-1, and, lastly, IL-6.[95]

The positive effects of CNTF on nodose neuronal survival are abolished when agents that block or inhibit PI3 kinase or inhibit lipid kinase are added to the culture medium.[2] The positive effects of CNTF, LIF, and CT-1 on nodose neuronal survival are abolished when NFκ-B activity is blocked, suggesting that these factors work via a system that requires NFκ-B.[170] This idea is further supported by a decrease in nodose ganglion neuronal death as a result of NFκ-B activation with no neurotrophic support.[170] Normal expression of STAT3 in mouse nodose ganglion neurons produces greater neuronal survival in the presence of CNTF and LIF compared with defective STAT3 expression.[2] Mice deficient for p65 have less nodose neuronal survival in the presence of CNTF, LIF, CT-1, or IL-6 and an increased number of dying cells (measured by the presence of pyknotic nuclei) compared with wild-type.[170] There are no differences in the number of cytokine receptors between p65 deficient and wild-type mice.[170] Whereas p65 deficiency and blocking of NFκ-B activity prevent the positive effects of the cytokines CNTF, LIF, and CT-1 on neuronal survival, they have no effect on the increased neuronal survival produced by BDNF suggesting that BDNF does not act via a system that requires NFκ-B.[170]

2.2.3 ACTIVITY- AND ION CHANNEL-DEPENDENT PLASTICITY OF VAGAL GANGLIA IN DEVELOPMENT

Depolarizing concentrations of potassium increase neuronal survival in petrosal neurons from late embryologic (E19.5) and newborn (P0) cultures, but have no effect on the survival of nodose neurons at these, or any other, stages of development.[23]

Intracellular Ca^{2+} appears to play a role in neuronal survival before the chick nodose neurons have begun to express L-type Ca^{2+} channels. Addition of a cytosolic free Ca^{2+} chelator caused complete nodose neuronal death within 36 to 48 hours.[129] Chronic addition of caffeine, which depletes intracellular stores of Ca^{2+}, to the culture medium at 12, 24, and 48 hours causes complete neuronal loss by 48 hours after caffeine administration began. Simultaneous addition of KCl to these cultures at 12 hours increases neuronal survival to 10% after 48 hours. Simultaneous addition of KCl to these cultures at 24 hours increased neuronal survival to 30 to 40% after 48 hours. Simultaneous addition of KCl to these cultures at 48 hours prevented the caffeine-induced neuronal death. These data show the significance of the expression of the L-type Ca^{2+} channels and Ca^{2+} on neuronal survival.[129] BDNF can also prevent the neuronal death produced by caffeine if administered after the neurons become dependent on BDNF for survival.[129]

Stage 18 chick nodose neurons express L-type Ca^{2+} channels after 48 hours in culture and began to depend on BDNF for survival at 72 hours.[129] Addition of KCl to the culture medium of stage 18 chick nodose neurons increases neuronal survival even in the absence of neurotrophic factors. Addition of nifedipine and verapamil

(L-type Ca^{2+} channel antagonists) completely blocks the survival-promoting effect of the KCl, while addition of an L-type Ca^{2+} channel agonist increases the survival-promoting effect of KCl.[129] KCl and BDNF both promote nodose neuronal survival, although the culture receiving KCl had higher percentages of neurons surviving after 120 hours than BDNF.[129] Addition of L-type Ca^{2+} channel antagonists produced no change in the effect of BDNF, indicating that BDNF does not act via Ca^{2+} influx through L-type Ca^{2+} channels.[129]

Activity-related cues can change the neurotransmitter phenotype of a population of neurons of the nodose ganglion. The presence of KCl in culture medium increases the number of TH-ir cells in both the nodose and petrosal ganglia throughout embryologic and neonatal development.[23] KCl has no effect on the expression of SP in either the nodose or petrosal neurons.[23]

In the fetal petrosal ganglion, where only 10 to 20% of the neurons are TH-ir under basal conditions, the TH expression and the dopamine content are increased tenfold by potassium or veratridine-induced depolarization.[85] After 15 days in culture, the number of TH-ir neurons in E16.5 petrosal neuronal culture increases as the amount of time that KCl is administered increases. The timing of KCl administration appears to be important as cultures administered KCl for the final 3 days have more TH-ir neurons than when the KCl is administered for the initial 3 days.[23] Block of L-type Ca^{2+} channels, but not N-type, significantly inhibits the TH induction by KCl in the petrosal neuron cultures.[23]

Continuous exposure of KCl to newborn nodose/petrosal neurons induces the neurons to release BDNF as measured by the amount of extracellular BDNF levels compared with neurons with no KCl.[7] Certain patterns of electrical stimulation are even more effective at inducing nodose/petrosal neurons to release BDNF.[7]

2.2.4 Trophic Actions of Nonneuronal Cells Associated with Developing Nodose Ganglia

The presence of nonneuronal cells in the nodose ganglion appears to play an important role in the development of neuronal phenotype (dopaminergic vs. cholinergic) especially in the 2 weeks prior to the neurons becoming committed to a sensory phenotype.[33] When neonatal nodose neurons are cultured in the presence of nonneuronal satellite cells, the neurons develop typical nodose neuron phenotypes; however, when the nonneuronal cells are not present, the nodose neurons develop functioning cholinergic nicotinic synapses with each other.[33] In nodose neuronal cultures without ganglionic satellite cells, 60% of the neurons develop synapses with each other and 75% are acetylcholine-sensitive. In nodose neuronal cultures with ganglionic cells, few synapses are formed between the cells and only 15% are acetylcholine-sensitive.[34] Moreover, when neonatal nodose neurons are cultured in the presence of nonneuronal ganglion cells, NGF has no effect on the proportion of Acetylcholine-sensitive neurons or the density of acetylcholine receptors on individual neurons; however, when nonneuronal cells are not present, NGF increases both the proportion of sensitive neurons and the density of the receptors on individual neurons.[33]

2.3   EPIGENETIC INFLUENCES ON MAINTENANCE OF MATURE VAGAL AFFERENT NEURONS

2.3.1   EPIGENETIC INFLUENCES ON NEUROCHEMISTRY OF MATURE VAGAL AFFERENT NEURONS

Multiple neurotransmitters, neuropeptides, calcium binding proteins, and other neuroactive substances are associated with vagal afferent neurons of the nodose ganglion.[253] The neurochemistry of the nodose ganglion was initially studied with the histochemistry and immunoassay, and subsequently with immunohistochemistry, *in situ* hybridization histochemistry, and RT-PCR. Putative neurotransmitters (glutamate, catecholamines, serotonin, and acetylcholine), and numerous neuropeptides [substance P (SP), neurokinin A (NKA), vasoactive intestinal peptide (VIP), calcitonin gene-related peptide (CGRP), galanin, enkephalin (ENK), somatostatin (SOM), cholecystokinin (CCK), neuropeptide Y (NPY)], calcium binding proteins, and other neuroactive molecules (e.g., nitric oxide) are identified in the neurons of the nodose and petrosal ganglia.[31,38,39,77–79,102,103,118,150,163] Many neurons colocalize two or more neuroactive substances, creating the potential for complex interactions of neurochemical signals in the NTS. Neurons of the nodose ganglion also contain a variety of receptors that respond to transmitters, inflammatory mediators, and neurotrophic factors.[253]

The content and expression of these neurochemicals and receptors are not static. In response to epigenetic influences, such as axonal injury or transection, inhibited axonal transport, disease, alterations of the neuronal expression and content of specific neuroactive agents and proto-oncogenes are triggered in mature vagal afferent neurons.[80,97,254,255] The neurochemical changes in mature visceral afferent neurons include the downregulation of specific neuropeptides and neurotransmitter enzymes and the upregulation of some neuropeptides and protooncogenes.

Alterations in the presence and expression of neurotransmitter enzymes include changes in neuronal nitric oxide synthase (nNOS) and tyrosine hydroxylase (TH).[80,253–255]

2.3.1.1   Nitric Oxide

Neuronal nitric oxide synthase (nNOS)-immunoreactivity (ir), nNOS mRNA, and NADPH-diaphorase (a cofactor of NOS) are present in nodose ganglion neurons,[100,182,232] and increase following transection of the vagus nerve.[107,240] A crush lesion of the vagus nerve increases the expression of iNOS-ir in the nodose ganglion at a time course paralleling neuronal regeneration.[158] Induction of nNOS, the enzyme that synthesizes neuronal nitric oxide, is a sensitive marker of injury to sensory neurons.[59,232,236] Acute hypoxia also upregulates NADPH-d/nNOS-ir in the nodose ganglion.[29] If the increase in nNOS protein also represents an increase in enzyme activity, and if the cofactors and L-arginine are present in the neuron, the result would be elevated nitric oxide. Nitric oxide is detrimental to the neurons when it forms peroxynitrite with O_2^-.[28,168] In the presence of oxidative stress, e.g., diminished GSH or SOD, this process is increased.

Diabetic autonomic neuropathy profoundly alters autonomic reflexes, and is associated with morbidity and poor prognosis.[233] A component of this dysfunction is due to altered visceral afferent neurons of the vagus nerve.[69,70,132–134] The numbers of nNOS-ir neurons are increased in the nodose ganglion of diabetic compared with control rats at the 8- and 16-week time points, but not at the 24-week time point.[192] However, no change is noted in the nNOS mRNA content of the diabetic nodose ganglion at either time point. Because anterograde and retrograde axonal transport are affected in the diabetic vagus nerve,[127,133,134,229] the increase in the number of nNOS-ir cells in the neurons of the nodose ganglion may be attributed to a diabetes-induced inhibition of axonal transport that either causes a build up of protein in the cell body, interrupts neurotrophic support to the neurons, or both.

nNOS is bidirectionally transported in the vagus nerve as shown in studies wherein ligation-induced interruption of axonal transport resulted in an accumulation of nNOS in the nerve segments proximal and distal to the ligation.[61,149] Nerve transection abolishes NADPH-d labeling distal to the ligature, suggesting that the accumulation of NADPH-d in the nerve is due to altered axonal transport rather than to an acute local production of inducible NOS as a result of injury.[61]

2.3.1.2 Tyrosine Hydroxylase

Mature nodose and petrosal ganglia neurons express tyrosine hydroxylase (TH).[253] In the adult nodose and petrosal ganglia of the rat *in vitro*, potassium-induced neuronal depolarization doubles TH enzyme activity[115] suggesting an activity-dependent regulation in TH synthesis.

The numbers of TH-ir and mRNA containing neurons decrease shortly after axotomy or blockade of axonal transport.[80,254] The number of tyrosine hydroxylase mRNA-containing neurons is significantly reduced at 3, 7, and 14 days after axotomy-induced deafferentation compared with intact and sham-operated controls. Labeling density of tyrosine hydroxylase mRNA-containing neurons is significantly reduced at 3 and 7 days.[255] Thus, axotomy-induced deafferentation reduces the number of TH mRNA-containing cells in the nodose ganglion and the amount of mRNA in the remaining positive cells. Since cell area measurements show no significant differences between the population of labeled neurons in the intact and the axotomized groups, the decrease in labeling density cannot be attributed to the dilution of an equal amount of mRNA in an enlarged cell. Cell death is not likely to be the sole cause of this reduction. Sensory neurons do not die within 30 days, only a small cell loss (<20% of neurons) occurs by 60 days after axotomy,[220] and a partial recovery in the number of TH-ir[80] and TH mRNA-containing neurons is seen at 14 days after axotomy. Likewise, disconnection of petrosal ganglion neurons and their targets by transection of the carotid sinus nerve results in a transient decrease in TH catalytic activity and the TH-ir in the petrosal ganglia of young female rats.[116]

Inhibition of axonal transport with application of vinblastine to the cervical vagus nerve, decreases the number of TH mRNA-containing and TH-ir neurons in the nodose ganglion.[254] Likewise, blockade of axonal transport in the carotid sinus nerve decreases TH-ir in visceral sensory neurons of the petrosal ganglion.[116] The pattern of alterations in TH mRNAs and immunoreactivity resulting from the selective

inhibition of axonal transport in the vagus nerve is similar to that seen following the axotomy-induced deafferentation of the nodose ganglion.[80,255] Therefore, it is likely that the selective inhibition of axonal transport by application of vinblastine to the vagus nerve may have contributed to the actions of the axotomy-induced deafferentation on TH expression in nodose ganglion neurons.

Neither the numbers of TH-ir neurons nor the content of TH mRNA is altered in the nodose ganglion of diabetic rats at the 8- and 16-week time points.[192] However, 24 weeks of diabetes results in a reduction in the numbers of TH-ir neurons in the diabetic nodose ganglia when compared with control, an effect not seen in diabetic rats receiving insulin. The late onset (24-week time point) decrease in TH-ir in diabetic nodose ganglia may reflect either a diabetes-induced nerve injury (milder and later than that noted with axotomy) or the loss of an axonally transported regulatory factor such as NGF. Because NGF increases the numbers of TH-ir nodose ganglion neurons in culture,[81] it follows that the loss of NGF secondary to diabetes-induced reductions in axonal transport may diminish the numbers of TH-ir neurons. A decrease in TH mRNA levels is not seen in the diabetic nodose ganglia,[192] therefore it is possible that the decreased availability of retrogradely transported regulatory factors, e.g., neurotrophins, is either directly or indirectly affecting the post translational processing, and/or stability of the products rather than affecting the production of mRNA.

Studies of the epigenetic factors regulating nodose ganglion visceral afferent neurons benefit from *in vitro* approaches wherein environmental influences are more clearly defined and controlled. Helke and Verdier-Pinard[81] used cultures of dissociated mature nodose and petrosal ganglia neurons to evaluate the presence of TH in the absence of neurotrophic support or depolarizing influences. At each time point in culture (<1d with no preplating, 1, 5, 7 days after plating), TH-ir nodose/petrosal ganglia neurons are present. TH, downregulated in the nodose ganglion after vagus nerve transection or inhibition of axonal transport,[254,255] is somewhat surprisingly present in a greater percentage of neurons in culture than in intact nodose/petrosal ganglia (21% at 5d versus 9%). The percentage of TH-ir neurons in the nodose/petrosal ganglia cultures is similar to those obtained when each ganglion is cultured separately.

2.3.1.3 Neuropeptides

The content of neuropeptides and/or their mRNAs in the nodose or petrosal ganglia can be altered by injury, alterations in axonal transport, and disease. Whereas substance P (SP) and calcitonin gene-related peptide (CGRP)-containing visceral afferent petrosal ganglion neurons of the glossopharyngeal nerve are reduced in number by axotomy, comparable changes are not detected in nodose ganglion neurons.[80] However, this difference may reflect the lack of sensitivity resulting from the small number of SP and CGRP neurons in the nodose ganglion compared with the petrosal ganglion because reductions in the numbers of CGRP mRNA-containing neurons are reduced in each ganglion following peripheral deafferentation.[97] A role for neuronal activity in the regulation of SP is suggested by the findings that the synthesis and transport of SP in the nodose ganglion of guinea pigs is inhibited by veratridine,

an effect reversed by tetrodotoxin.[151,152] Peripheral axotomy also decreases the number of CCKA-receptor mRNA-expressing nodose ganglion neurons and conversely increases the number of CCKB-receptor, CCK mRNA, and preproCCK-like ir neurons.[22]

The selective inhibition of axonal transport in the vagus nerve increases the number of CGRP mRNA-containing and CGRP-ir neurons in the nodose ganglion,[254] whereas axotomy-induced deafferentation results in a decrease in the CGRP mRNA-containing neurons and no change in the CGRP-ir neurons.[80,97] The different results between the vinblastine treatment and the axotomy-induced deafferentation on the CGRP neurons are likely due to the different experimental procedures on the vagus nerve, resulting in a differential response of the CGRP neurons. Both procedures interrupt axonal transport, axotomy additionally injures the neuron and interrupts conduction of depolarizing impulses from the periphery to the cell body. The results of these studies suggest that neurons with distinct neurochemical natures may have differential reaction following the same kind of experimental treatment, and neurons with the same neurochemical nature may have different responses following different treatment.

Whereas blocked axonal transport increases CGRP-ir and mRNA[254] and vagotomy decreases both,[80,97] the absence of a change in the numbers of CGRP-ir neurons in diabetic rat nodose ganglion[192] could be interpreted as a result of the counteracting diabetes-induced alterations in axonal transport and of nerve injury. Alternatively, the apparent absence of changes in the diabetic ganglion may also reflect a lack of sensitivity of the approach of counting CGRP-ir neurons in detecting changes in the relatively small number of CGRP-ir neurons found in the rat nodose ganglion.

Allergic inflammation of the guinea pig airways induces SP and CGRP production in large-diameter vagal afferent neurons.[176] The number of SP/NKA-containing vagal afferent neurons of the guinea pig nodose ganglion is increased during respiratory viral infection leading to both small diameter nociceptive-like neurons and large diameter nonnociceptive neurons expressing tachykinins.[27] This abnormal pattern of tachykinin expression may contribute to the abnormal physiology associated with respiratory viral infections. Conversely, chronic administration of ACTH or corticosterone decreases the quantity of peripherally transported SP in the afferent vagus nerve.[151,153]

Relatively few neurons in the normal intact mature nodose ganglion contain vasoactive intestinal peptide (VIP).[253] Following axotomy, VIP-ir and VIP mRNA markedly increase, the number of VIP mRNA-containing neurons increases (from virtually undetectable to readily apparent) significantly at 3, 7, and 14 days, while the labeling density of vasoactive intestinal peptide mRNA-containing neurons also increases at 1, 3, 7, and 14 days.[80,97,254,255] These results suggest that there may be a peripherally derived inhibitory influence on VIP mRNA expression which is removed by axotomy-induced deafferentation. When axonal transport is blocked, the VIP immunoreactivity and mRNA content are also increased.[254] Vinblastine treatment of the vagus nerve increases the numbers of VIP mRNA-containing neurons and VIP-ir neurons in the nodose ganglion at 3, 7, and 14 days. The average labeling density of VIP mRNA-containing neurons also increases following vinblastine treatment.[254]

Because the pattern of alterations in VIP mRNA and immunoreactivity resulting from the selective inhibition of axonal transport in the vagus nerve is similar to that seen following the axotomy-induced deafferentation of the nodose ganglion,[80,255] it is likely that inhibition of axonal transport may contribute to the effects of axotomy on VIP expression in nodose ganglion neurons.

The function of the increased VIP mRNA and resultant VIP-ir in neurons of the nodose ganglion is of interest. One possibility is that VIP functions as a neurotransmitter/neuromodulator.[56] Consistent with this idea is the finding that VIP increases in central terminal fields in a coordinate fashion with the increase in cell body content.[209] VIP may also play a role in promoting cell survival after neuronal injury. When added to the culture medium of dorsal root ganglion and retinal cells, VIP delays tetrodotoxin-induced and glutamate analogue-induced cell death.[19,20,111]

Although VIP-ir and mRNA in the nodose ganglion neurons increase after vagotomy[80,255] and after axonal transport is blocked,[254] diabetes has no apparent effect on their levels in these neurons. It appears that either the nature or the extent of nerve injury resulting from the diabetic state is insufficient to trigger the pronounced increases in VIP noted in other situations. An alternate explanation may be that diabetes results in a reduced ability of the VIP gene to upregulate expression.

Although a few neurons of the intact nodose and petrosal ganglia express preproneuropeptide Y (NPY) mRNA,[38,39] the synthesis of NPY in the nodose and petrosal ganglia is upregulated in response to transection of the vagus nerve. The numbers of NPY-ir and NPY mRNA-containing neurons in the nodose ganglion are dramatically increased in response to cervical vagus nerve axotomy.[253] Reimer and Kanje[193] show that peripheral axotomy of the sensory neurons in the nodose ganglion increase the number of the C-terminal flanking peptide of neuropeptide Y, galanin, and VIP, whereas central axotomy does not. Zhang et al.[249] show that galanin, NPY, and VIP -ir and mRNA-containing neurons increase in the nodose ganglion after peripheral axotomy.

Helke and Verdier-Pinard (Reference 81 and unpublished data) used cultures of dissociated mature nodose and petrosal ganglia neurons to evaluate the presence of neuropeptide (VIP, CGRP, and NPY)-containing neurons *in vitro* in the absence of neurotrophic factors. At each time point in culture (<1d with no preplating, 1, 5, and 7 days after plating), VIP, CGRP, and NPY-ir nodose/petrosal ganglia neurons are present. VIP and NPY, agents that are upregulated in nodose ganglion neurons after vagus nerve transection and/or inhibition of axonal transport,[253,254] are also present in greater percentages of neurons at each time in culture than in tissue sections of ganglia from intact rats. VIP increases from < 10% *in situ* to >20% of labeled neurons in culture (elevated at all time points in culture, including <1d unenriched cultures).[81] The elevation in numbers of NPY-ir cells is less (12% *in situ* to 21% at 5 d in culture). The percentage of VIP-ir neurons in the nodose/petrosal ganglia cultures is similar to that obtained when each ganglion is cultured separately. CGRP is present in 21% of the combined nodose and petrosal ganglia cultures (5d), a similar percentage to that seen in tissue sections (20%) from intact ganglia. Given the larger numbers and significantly higher percentage of CGRP-ir neurons in the intact[80] or in the separately cultured petrosal ganglion compared with the nodose

ganglion (34% versus 14% of neurons), it is likely that the majority of CGRP-ir neurons are from the petrosal ganglion.

Pituitary adenylate cyclase-activating polypeptide (PACAP)-ir and mRNA-containing neurons also increase in the cultured nodose ganglion over time in culture.[194] PACAP is transported and released at the site of a crush injury to the vagus nerve.[194]

The functional significance of alterations in neuropeptide expression in nodose ganglion neurons after vagotomy is not clear. Certain peptides (e.g., galanin, VIP, CCK, and CCK-B receptors) whose expression is increased may have trophic functions during nerve regeneration and may protect against further injury.

2.3.1.4 *c-Jun*

Another neurochemical marker of injury is induction of the transcription factor c-Jun. The constitutive levels of c-Jun in the nodose ganglion are low; however, following vagotomy, there is a rapid (within 10 hours) and long-lasting (up to 100 days) induction of c-*jun* mRNA and c-Jun protein, which are closely linked to the intensity of the cell-body reaction.[83,84]

The number of nodose ganglion neurons labeled for c-Jun is slightly increased in the diabetic nodose ganglia at the 8-week time point and is reversed with insulin treatment.[192] The increase in c-Jun-ir neurons is not found at 16 or 24 weeks of diabetes.

Because of this short-lived response to diabetes, c-Jun may be transiently increased in an initial, nonsustained response to injury, and/or transient early changes in availability of NGF.

Because anterograde and retrograde axonal transport are affected in the diabetic vagus nerve,[127,133,134,229] the increase in the number of c-Jun-ir cells in the neurons of the nodose ganglion may be attributed to a diabetes-induced inhibition of axonal transport that either causes a build up of protein in the cell body, interrupts neurotrophic support to the neurons, or both.

Thus, although Regalia et al.[192] note that certain of the diabetes-induced changes noted in the content of specific neurochemical agents (nNOS, TH, c-Jun) are similar to those noted after nerve injury due to vagotomy or blocked axonal transport,[80,84,107,240,254] the diabetes-induced neurochemical responses of the vagal afferent neurons are not as large in magnitude, as extensive (e.g., no changes in VIP and CGRP), or reflected by changes in mRNA content as those noted after vagotomy or after blocked axonal transport.[80,97,254,255]

2.3.2 NEUROTROPHINS

The altered expression of neuropeptide and neurotransmitter enzyme mRNAs in mature nodose ganglion neurons by local inhibition of vagus nerve axonal transport suggested that a transported factor (perhaps a target-derived neurotrophic factor) is important for the regulation of neuropeptide and neurotransmitter enzyme mRNAs in visceral sensory neurons of the nodose ganglion.[254] Retrogradely transported neurotrophic factors influence the expression of transmitters in somatic sensory dorsal root ganglion (DRG) neurons.[72,140] However, because sensory neurons of the

neural crest-derived dorsal root ganglion differ from sensory neurons of the placode-derived nodose ganglion embryologically (placodal- versus neural crest-derived[6]), morphologically (absence of RT97 labeled large neurons, and distinct cell size distribution profile, Helke et al., unpublished), neurochemically (TH-ir neurons are primarily in the nodose ganglion[119,241]), and in trophic factor responsiveness during development,[140] it is necessary to evaluate neurotrophic factors, their transport, and receptors in vagal visceral sensory neurons.

In mature peripheral sensory neurons, neurotrophins are important for development and maintenance of morphological integrity, for physiologic and phenotypic differentiation (including transmitter phenotype), and neuronal response to injury.[21,37,138,147] Moreover, axonal caliber is maintained by retrogradely transported neurotrophins via regulation of neurofilament synthesis.[226] Neurotrophins bind to specific receptors, are retrogradely transported from target tissues to the cell body, and affect synthesis of neurochemicals and structural proteins.[10,37,42,124,161]

2.3.2.1   Neurotrophins Associated with Vagal Afferent Neurons

Wetmore and Olson[243] report that 25% of nodose ganglion neurons contained BDNF mRNA, and BDNF-ir but no NGF or NT-3 mRNA-containing neurons. Other studies show no NGF, BDNF, or NT-3 mRNA-containing neurons in either intact or vagotomized nodose ganglia.[134] NGF and NT-3 proteins are detected by ELISA in the intact vagus nerve trunk, where they are likely to represent neurotrophins that are axonally transported from target tissues.[133] However, NGF, BDNF, or NT-3 mRNA-containing neurons were detected in non-neuronal cells in the vagus nerve trunk after axotomy.[134]

Neurotrophins and their mRNAs are present in numerous peripheral tissues (including atrium, stomach, ileum) innervated by the vagus nerve.[113,132,160,200,205,225,251] For example, NT-3 is detected in visceral targets of the nodose ganglion including heart, liver, and pancreas.[113] Thus, through retrograde axonal transport (see below) of neurotrophins, intact mature vagal afferent neurons are exposed to endogenous neurotrophins *in vivo*.

2.3.2.2   Neurotrophin Receptors Associated with Vagal Afferent Neurons

Whereas mature visceral sensory neurons do not require exogenous neurotrophins for survival,[81,130,139,140] neurotrophin receptors are clearly present on mature vagal afferent neurons and likely play a role in the maintenance of neuronal functions.

Mature nodose ganglion neurons and the vagus nerve express two classes of transmembrane neurotrophin receptors that display pharmacologically distinct neurotrophin binding sites, the low-affinity receptor (p75) and higher-affinity Trk receptors (Figure 2.4).[231,243,253]

2.3.2.2.1   *Nodose Ganglion*

As presented earlier, all three Trks are present in nodose ganglion neurons in the early postnatal period; in adulthood, expression of TrkB is reduced, while that of
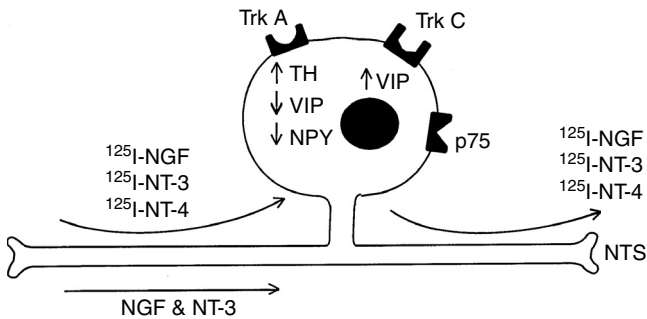
FIGURE 2.4 Schematic of a mature vagal afferent neuron in the nodose ganglion, the presence of TrkA, TrkC, and p75 neurotrophin receptors on neuronal perikarya, the ability of the cervical vagus nerve to retrogradely transport specific ^{125}I-labeled neurotrophins to the cell body and transganglionically to the CNS terminals in the nucleus of the solitary tract (NTS), the retrograde transport of endogenous NGF and NT-3 in cervical vagus nerve, and the ability of NGF and NT-3 to affect neurotransmitter/neuropeptide presence in the ganglia. (Based on data from Zhuo and Helke, 1996; Helke et al., 1998; Helke and Verdier-Pinard, 2000; Lee et al., 2001b.)

TrkC and TrkA remains.[53,76,232,252] In adult rats, the presence of mRNAs to the tyrosine kinase (Trk) receptors for neurotrophins was studied in visceral afferent neurons of the nodose and petrosal ganglia using *in situ* hybridization histochemistry (with oligonucleotide probes and with oligoprobes), immunocytochemistry and RT-PCR.[76,132,134,252]

Neurons containing TrkA mRNA are found in the intact adult nodose and petrosal ganglia. At least 10% of nodose ganglion neurons and 38% of petrosal ganglion neurons contain TrkA mRNA. TrkC mRNA is found in approximately 9% of nodose, and 11% of petrosal ganglion neurons of adult rats. Slightly more robust labeling for both TrkA and TrkC is noted with riboprobes than with oligonucleotide probes.[76,252] The cell size profiles of the TrkA and TrkC mRNA-containing nodose ganglion neurons were similar with average neuronal diameters of 35 ± 3 μm for each Trk. The presence of TrkA and TrkC mRNAs is verified in the nodose ganglion using RT-PCR.[132] Lamb and Beilefeldt[128] found a majority of rat nodose ganglion neurons express TrkA and TrkC receptor-ir after 1 day in culture, whereas Molliver et al.[173] found a small minority of nodose ganglion neurons were TrkA positive.

Ichikawa and Helke[101] defined the presence of the neurotrophin receptor, TrkA, in neurochemically identified vagal and glossopharyngeal sensory neurons of the adult rat. TrkA is colocalized with CGRP, and with the calcium-binding proteins, parvalbumin, or calbindin D-28k, in mature neurons of the rat nodose and petrosal ganglia. Although nearly one half of the TrkA-ir neurons in the nodose ganglion contain calbindin D-28k-ir, few or no TrkA-ir neurons in the petrosal ganglion are also labeled for either calcium binding protein. Conversely, whereas only a few of the numerous TrkA-ir neurons in the nodose ganglion contain CGRP-ir, about one half of the TrkA-ir neurons in the petrosal ganglion contained CGRP-ir. In contrast, no TrkA-ir neurons in these ganglia colocalize TH-ir. These data show

distinct colocalizations of TrkA with specific neurochemicals in vagal and glossopharyngeal sensory neurons, and suggest that nerve growth factor, the neurotrophin ligand for TrkA, plays a role in functions of specific neurochemically-defined subpopulations of mature vagal and glossopharyngeal sensory neurons. This study also shows the coexistence of TrkA with CGRP, parvalbumin, and calbindin D-28k, but not with TH, in neurons of the nodose, petrosal, and jugular ganglia.

Whereas TrkB mRNA is detected in 1-day-old neonatal nodose and petrosal ganglia, few or no TrkB mRNA-containing neurons were detected in the adult nodose and petrosal ganglia.[76,254] These data, obtained using two different approaches to *in situ* hybridization histochemistry (oligonucleotide probes and riboprobes), fit well with the absence of the retrograde transport of ^{25}I-BDNF by vagal afferent neurons[76] and absence of effects of exogenous BDNF on neuropeptides in nodose/petrosal ganglion cultures.[81] However, other studies using different probes report that a majority of intact nodose ganglion neurons contain TrkB.[112,243] Michael and Priestley[169] found that the majority of small visceral sensory neurons of the nodose ganglion express VR1 mRNA in conjunction with TrkB but not with TrkA. Moreover, mature nodose ganglion neurons in cultures or whole mounts show numerous TrkB containing neurons.[128,245]

The p75 receptor is also present in the nodose ganglion. A majority of the neurons of the nodose and petrosal ganglia contains p75^{NTR} mRNA or has p75^{NTR}-ir.[134,232,243,253] The presence of p75 mRNA in the ganglion is verified with RT-PCR.[132]

2.3.2.2.2   *Vagus Nerve Trunk*

In contrast to the neurons of the nodose ganglion, *in situ* hybridization histochemistry of the normal intact cervical vagus nerve trunk does not reveal mRNAs for Trk receptors. p75 mRNA is not found in non-neuronal elements of the vagus nerve either before or after injury.[134] However, using RT-PCR mRNAs of TrkA, TrkC and p75 are detected in the vagus nerve of normal adult rats.[132] The detection of TrkA and TrkC mRNAs in the nerve trunk using RT-PCR but not when using *in situ* hybridization histochemistry suggests a low level of activity that may not be histochemically localized in intact tissue but which can be detected and localized to non-neuronal elements after nerve injury (see the following).

2.3.2.3   Axonal Transport of Neurotrophins by Vagal Afferent Neurons

Neurotrophins initiate their effects, in part, by binding to high-affinity receptors, followed by uptake and retrograde transport to the cell body.[37] The ability of neurons to respond correlates with transport.[124,196] Likewise, retrograde transport may be predictive of neuronal types selectively responsive to NGF, BDNF, NT-3, or NT-4.[36,44] Neurons can transport neurotrophins by both Trk and p75-dependent mechanisms.[36,44]

Mature vagal afferent neurons retrogradely transport ^{125}I-NT-3, ^{125}I-NGF, and ^{125}I-NT-4 to perikarya in the ipsilateral nodose ganglion and transganglionically to the NTS.[76] More recently, the retrograde axonal transport of endogenous NGF and NT-3 was demonstrated.[132] The receptor mechanisms of axonal transport of

neurotrophins by nodose ganglion neurons are consistent with the expression of Trk and p75 receptors in these neurons. Moreover, vagal neurons have unique profiles of neurotrophin transport in comparison with somatic sensory and motor neurons.

^{125}I-NGF is retrogradely transported from the cervical vagus nerve to neuronal cell bodies in the ipsilateral but not the contralateral nodose ganglion.[76] The size of ^{125}I-NGF neuronal profiles is 499 ± 28 μm^2. The presence of excess unlabeled NGF diminishes the transport of ^{125}I-NGF to the nodose ganglion by >80%, whereas other unlabeled neurotrophins do not significantly alter the transport of ^{125}I-NGF. Autoradiographic grains are distributed in the NTS and the solitary tract after application of ^{125}I-NGF to the cervical vagus nerve, although considerably fewer are noted than with ^{125}I-NT-3. Retrograde axonal transport of endogenous NGF is also demonstrated in the cervical vagus nerve using a double-nerve ligation model and ELISA to measure accumulated NGF.[133] Little, if any, anterograde transport is noted using this approach. It is likely that the contributions of afferent versus efferent vagal fibers to the transport of endogenous NGF are similar to those noted with the exogenous iodinated NGF and thus reflex largely afferent vagal nerve transport.

^{125}I-NT-3 is retrogradely transported from the cervical vagus nerve to neuronal perikarya in the ipsilateral nodose ganglion.[76] The average cell size of ^{125}I-NT-3 neuronal profiles is 459 ± 38 μm^2 The transport of ^{125}I-NT-3 to the nodose ganglion is reduced by 85% in the presence of unlabeled NT-3 and by 30% in the presence of unlabeled NGF. Unlabeled BDNF and NT-4 had no significant effect on the transport of ^{125}I-NT-3 to the nodose ganglion. Autoradiographic grains are also present in the NTS and the solitary tract after application of ^{125}I-NT-3 to the cervical vagus nerve. The densest rostrocaudal labeling of the NTS is found at the level of the area postrema. Retrograde but not anterograde axonal transport of endogenous NT-3 is also demonstrated in the cervical vagus nerve using a double-nerve ligation model and ELISA to measure accumulated NT-3.[133] It is likely that the contributions of afferent versus efferent vagal fibers to the transport of endogenous NT-3 are similar to that noted with the exogenous iodinated NT-3 and thus reflect both afferent and efferent vagal nerve transport.

The content of ^{125}I-BDNF in the ipsilateral nodose ganglion after application to the cervical vagus nerve is not different from the content of ^{125}I-cytochrome C and is significantly less than the content of each of the other iodinated neurotrophins after similar application.[76] Autoradiography shows the presence of few labeled neurons scattered throughout the ipsilateral ganglion. No autoradiographic grains are accumulated in any NTS subnuclei subsequent to the application of ^{125}I-BDNF to the cervical vagus nerve. In contrast, ^{125}I-BDNF is retrogradely transported to CNS nuclei by efferent vagal axons.[76]

^{125}I-NT-4 is retrogradely transported from the cervical vagus nerve to neuronal perikarya in the ipsilateral nodose ganglion.[76] The presence of excess unlabeled NT-4 diminishes the transport of ^{125}I-NT-4 to the nodose ganglion by 86%. Interestingly, the presence of 22- to 25-fold excess of each of the other three unlabeled neurotrophins (NGF, BDNF, NT-3) also significantly alters the transport of ^{125}I-NT-4.

The studies using iodinated neurotrophins demonstrate the receptor-mediated retrograde transport of neurotrophins from axons of the afferent vagus nerve to

perikarya in the nodose ganglion, a profile of efficacy of NT-4>NT-3>NGF>>>BDNF, and the transganglionic transport to the central terminal fields of vagal afferent neurons in the NTS.

Based on evidence that NGF is the preferred ligand for TrkA, whereas TrkB is activated by both BDNF and NT-4, and NT-3 is the preferred ligand for TrkC and is a secondary ligand for TrkA,[30,68,122] the retrograde transport data are consistent with the demonstrated presence of TrkA and TrkC (but few TrkB) mRNA-containing neurons. Thus, the competition profile for ^{125}I-NT-3 transport (inhibition of transport by excess NT-3 and NGF) is consistent with the involvement of TrkC and to a lesser extent TrkA (Curtis and DiStefano, unpublished data). The competition profile for ^{125}I-NGF transport (significant inhibition of transport by excess NGF) is consistent with the involvement of TrkA. The absence of ^{125}I-BDNF transport is consistent with a minimal presence of TrkB in the adult nodose ganglion.[76,252] The finding that each of the excess unlabeled neurotrophins competed for the transport of ^{125}I-NT-4 to the nodose ganglion suggests a lack of involvement of specific Trk receptors in the transport of ^{125}I-NT-4 and is consistent with the minimal presence of TrkB mRNA. However, p75 may be involved in the transport of ^{125}I-NT-4. p75 binds all neurotrophins with comparable affinity[74,215] and is retrogradely transported.[109,121] The transport of NT-4 and BDNF (but not NGF) to the DRG is dependent on p75,[36] and p75 plays a role in regulating biological responsiveness to NT-4 but not to BDNF or NT-3.[203]

Thus, the presence of TrkA and TrkC and the retrograde transport of NGF and NT-3 suggested that mature nodose ganglion neurons are able to respond to NGF and NT-3, and perhaps NT-4, but they are unlikely to respond to BDNF.

2.3.2.4   Neurotrophins and Neurochemical Expression in Vagal Afferent Neurons

An established action of neurotrophins (NGF, BDNF, NT-3, and NT-4) is the maintenance of normal neurotransmitter and neuropeptide phenotype expression in mature neurons.[137,138,143,228]

After NGF injections into the tracheal wall, about 10% of the large diameter nodose neurofilament positive neurons projecting fibers to the trachea become SP-positive, suggesting that NGF not only increases SP expression in airway neurons, but changes the neuronal phenotype such that large, capsaicin-insensitive nodose neurons provide a component of the tachykininergic innervation.[99]

Helke and Verdier-Pinard[81] evaluated neurotrophin influences on the presence of neuropeptides and neurotransmitter enzymes in mature visceral sensory neurons. Exogenous NGF (10 to 100 ng/ml) increases the TH-ir and decreases VIP-ir neurons in the nodose/petrosal ganglia cultures over a 5-day period.[81] Given that *in vivo* NGF is a retrogradely transported target-derived neurotrophin, and that loss of contact with target (either through vagotomy or inhibition of axonal transport in the cervical vagus nerve) results in a decrease in TH and an increase in VIP neurons,[80,254,255] these data are consistent with a role for endogenous NGF *in vivo* to maintain normal neurotransmitter phenotype in nodose/petrosal ganglia neurons. These data, coupled

with the presence of TrkA mRNA and of the retrograde transport of NGF by vagal afferent neurons, indicate an important role for NGF in the functions (including maintenance of normal transmitter phenotype) of these visceral afferent neurons. The mechanism through which NGF alters the numbers of TH and VIP neurons is not known. One possibility is that NGF is acting directly through TrkA receptors on specific cultured nodose and petrosal ganglion neurons. Although we have pre-liminary evidence for the presence of TrkA mRNA in cultured nodose/petrosal ganglia neurons (Zhuo, Verdier-Pinard, and Helke, unpublished data), we do not know if the TrkA mRNA containing neurons are those in which the content of TH or VIP is altered. Moreover, TH-positive neurons of intact nodose and petrosal ganglia that co-expressed TrkA are not found.[101] NGF is also a ligand for p75 and nearly all nodose ganglion neurons contain p75.[232,243,253] Thus, the roles of neuronal TrkA, and p75, remain to be defined in this system. Likewise, the possibility that a non-neuronal cell type (e.g., fibroblasts) remaining in these neuronally enriched cultures responds to the addition of NGF with the secretion of a factor that second-arily alters neuronal phenotype requires additional studies.

Whereas NT-3 (up to 150 ng/ml) does not affect peptide expression in newborn DRG,[175] NT-3 does affect the numbers of VIP-ir neurons in the mature nodose/pet-rosal ganglia cultures.[81] NT-3 increases the number of VIP-ir neurons in the nodose/petrosal ganglia cultures and does not alter the numbers of TH- or CGRP-ir neurons. The addition of an NT-3 neutralizing antibody attenuates the effects of NT-3 on VIP-ir neurons. Because the increase in the numbers of VIP-ir neurons is the opposite effect noted in *in vivo* studies with removal of access to the target tissue, perhaps locally derived (not target derived) NT-3 is involved in the elevated VIP seen *in vivo* after injury or inhibition of axonal transport. The induction of NT-3 mRNA is noted in non-neuronal cells of the vagus nerve trunk immediately proximal and distal to a nerve lesion within 1 day after injury.[134] *In vivo* this non-neuronally derived NT-3 may have access to the injured neuron and, coupled with the loss of NGF, be involved in the elevation of neuronal VIP.

Although not required for survival, when adult murine nodose ganglion neurons are placed in culture, BDNF and NT-4 but not NGF or GDNF demonstrated the ability to stimulate axonal outgrowth. NT-3 showed weak stimulation of out-growth.[245] Likewise, neurite outgrowth from adult rat nodose ganglion placed in explant cultures is increased by BDNF but not by NGF, NT-3 or GDNF.[180]

2.3.3 OTHER NEUROTROPHIC FACTORS

Messenger RNAs for c-ret and GFR alpha 1, signaling receptors of GDNF family ligands, are found in 30 to 40% of nodose ganglion neurons, whereas GFR alpha 2 and GFR alpha 3 are not detected nodose ganglion neurons.[112] The latter finding suggests that mature nodose ganglion neurons do not respond to neurturin and artemin but have the capacity to respond to GDNF. Addition of GDNF to adult rat nodose ganglion neurons in culture rapidly increases cytosolic calcium due to release from intracellular stores.[128]

2.4   EFFECT OF VAGUS NERVE DAMAGE AND DISEASE ON NEUROTROPHINS ASSOCIATED WITH VAGAL AFFERENT NEURONS

2.4.1   NEUROTROPHIN AND NEUROTROPHIN RECEPTOR MRNAS AFTER VAGUS NERVE INJURY

Neurotrophins and neurotrophin receptors play an important role in survival and growth of injured peripheral nerves. The injury-mediated neurotrophic response in autonomic nerves has been investigated by studying changes in mRNA expression of neurotrophins and their receptors in the transected vagus nerve and nodose ganglion.[76,134] The presence and distribution of neurotrophin and neurotrophin receptor mRNAs in the nodose ganglion and in the cervical vagus nerve trunk after nerve injury were assessed at various time points (17 hours to 45 days). *In situ* hybridization histochemistry was used to detect mRNAs for the neurotrophins, NGF, BDNF, NT-3, and the neurotrophin receptors, TrkA, TrkB, TrkC, and p75[NTR] in the vagus nerve at multiple time points after axotomy and ELISA to detect NGF and NT-3 proteins at one time point after axotomy.

In nodose ganglion neurons at 17 hours after cervical vagotomy, there are no readily apparent differences in the numbers, distribution, or the labeling intensity of neurons containing TrkA, TrkB, or TrkC mRNA or p75-ir.[76] However, at more extended times after vagotomy, alterations in the expression of Trk receptors are noted in nodose ganglion neurons. By 48 hours after nerve injury, the numbers and labeling densities of TrkA and TrkC mRNA-containing neurons are reduced.[134] By 3 days, the receptor mRNA levels are nearly absent and remained markedly depressed for more than 28 days after the axotomy. Neuronal expression of the neurotrophins was also examined in intact and axotomized neurons to evaluate the potential of autocrine effects of neurotrophins in the injured nerve. No NGF, BDNF, or NT-3 mRNA-containing neurons are detected in intact or vagotomized nodose ganglia.[134]

Because vagal sensory neurons of the nodose ganglion can retrogradely transport ^{125}I-NGF and ^{125}I-NT-3[76] and endogenous NGF and NT-3,[133] it is likely that the transection-induced interruption of axonal transport of target-derived factors is involved in the decreased expression of TrkA, TrkC, and p75[NTR] in the nodose ganglia after nerve injury. However, it is also possible that a more generalized perikaryal reaction to the axonal injury resulted in the downregulation of the Trk mRNAs.

In contrast to the neurons of the nodose ganglion, the normal intact cervical vagus nerve trunk does not contain mRNAs for Trk receptors or neurotrophins. However, cervical vagotomy results in the expression of mRNAs for each neurotrophin, and for TrkA, TrkB, and TrkC receptors in non-neuronal cells at both the proximal and distal segments of the transected nerve.[134] The induction of each neurotrophin and Trk receptor mRNA is apparent within 1 day after the axotomy and is sustained at least 7 days. The increased neurotrophin and Trk receptor mRNAs in the proximal segments is limited to a short distance from the site of the transection, whereas in the distal segment the expression of these mRNAs is also noted at a greater distance from the transection. Moreover, NGF protein is increased in the distal end, and NT-3 protein is increased in both the distal and proximal ends of the

transected nerve 3 days after axotomy. The expression of neurotrophins and Trk receptors in the non-neuronal cells at or near the site of transection may be an attempt to compensate for the loss of target-derived trophic support and/or the injury-induced down-regulation of neuronal neurotrophin receptors.

The expression of mRNAs for neurotrophins and Trk receptors in the non-neuronal cells of the transected vagus nerve return to the normal control level 45 days after axotomy and coincide with regeneration of the nerve (as verified by retrograde transport of FluoroGold from the wall of the stomach to the ganglion). The return of the mRNA levels to the low pre-axotomy levels with reinnervation suggests that the restoration of target innervation either reduces the signals responsible for, or restores signals suppressive to, the induction of the neurotrophin and Trk mRNAs in the vagus nerve. In addition, the induction of individual neurotrophin mRNAs in the vagus nerve coincided with the increase of its preferred Trk receptor after axotomy.[134] This spatial and temporal co-localization of neurotrophin and Trk mRNA expression supports the idea that neurotrophins promote or guide axonal regeneration via their Trk receptor. Because the proximal end of a transected nerve no longer has access to target-derived trophic support, the injured vagus nerve may depend on local production of neurotrophin and their receptors resulting from the upregulation of their mRNA, for axonal survival and regrowth.

The induction of neurotrophin and Trk receptor mRNAs in the transected vagus nerve (but not in neuronal cell bodies) in proximity to the site of nerve transection and relation of the mRNA hybridization signals to underlying cellular elements suggests an injury-induced upregulation of mRNA expression in non-neuronal elements of the vagus nerve. Non-neuronal cells including Schwann cells and macrophages can produce neurotrophin and Trk mRNAs after nerve injury.[66,67,90,91,250] Schwann cells and macrophages are individually or cooperatively involved in Wallerian degeneration and regeneration.[71,183,187] Macrophages secrete a variety of proteins or factors that initiate and enhance proliferation of Schwann cells.[187] Schwann cells produce various cell adhesion molecules and neurotrophic factors that promote the outgrowth of regenerating axons[5,172,211,218,219] (see reviews by Ide[104] and Weinstein[242]).

p75 mRNA is not found in non-neuronal elements of the vagus nerve either before or after injury.[134] p75[NTR] can play a role as a positive regulator of Trk-mediated neurotrophin activity[12,159] and/or generate an apoptotic signal.[9,58,65] However, because cervical vagotomy fails to induce expression of p75[NTR] mRNA in the injured vagus nerve, expression of p75[NTR] mRNA at the site of the injury does not appear to be involved in the process of vagus nerve response to injury.

2.4.2 DIABETES AND NEUROTROPHINS ASSOCIATED WITH VAGAL AFFERENT NEURONS

2.4.2.1 Neurotrophins and Neurotrophin Receptors in Diabetes

The loss of neurotrophic support has several consequences to mature sensory neurons. Alterations in neurotransmitters and neuropeptides are key manifestations of

deficient neurotrophic support in injury or neuronal disease such as diabetic neuropathy.[227] Moreover, the neuropeptide changes in somatic sensory neurons and sciatic nerves of diabetic rats can be normalized by strict glycemic control, treatment with an aldose reductase inhibitor, or with exogenous NGF.[204,207,227,228] Deficient neurotrophic support may also be a factor in the defective neuronal repair and regeneration known to occur in diabetic neuropathy in humans and in animal models.[17,146,227] The established role for neurotrophins in nerve regeneration, and the finding that NGF assists sensory nerve regeneration in STZ diabetic rats[244] support this idea. Thus, even in the presence of other causative mechanisms (e.g., immunological, increased aldose reductase pathway activity, microvascular abnormalities) for the diabetic neuropathy, correction of an alteration in function or availability of the appropriate neurotrophic factors may enhance maintenance of normal transmitter phenotype, neuronal survival, and regeneration.[3,222,227]

Autonomic nerve dysfunction is a serious and common complication in diabetes mellitus[54,55,92,256] and contributes to the high risk of cardiovascular mortality and morbidity.[54,185,257] Cardiovascular reflex tests show the presence of autonomic neuropathy in 17 to 40% of diabetic patients, and 85% of diabetic patients with any peripheral neuropathy show evidence of autonomic neuropathy.[178,233] Diabetic cardiovascular autonomic neuropathy is associated with severe postural hypotension, exercise intolerance, impaired cardiac function, increased incidence of myocardial infarction and ischemia, and a poor prognosis.[178,234,256] Increased mortality is noted among diabetic patients with symptomatic autonomic neuropathy or with abnormal cardiovascular reflex tests.[157,233,256]

Whereas visceral afferent neurons, including those of the vagus nerve, are critical to autonomic reflexes including the baroreceptor reflex, our understanding of the involvement of specific reflex components in diabetes is incomplete. However, visceral afferent fibers appear to be implicated in the symptomatology of diabetic autonomic neuropathy, and their involvement considered part of the neuropathy.[4,92,189,224,256] For example, postural hypotension occurs because of an altered baroreceptor reflex and it has been suggested that damage to the afferent component of this reflex contributes to this deficit.[4] Low et al.[148] proposed that diabetes-induced postural hypotension results from degeneration of afferent baroreceptor fibers and of sympathetic neurons innervating the vasculature and the heart. Moreover, baroreceptor afferent nerve involvement in diabetic autonomic neuropathy is inferred from the postural hypotension and the altered circulatory reflexes in patients with intact efferent vasomotor pathways.[4,208] In addition, a component of abnormal baroreceptor afferent neurons could explain why parasympathetic responses in diabetic patients may be subnormal during increases of arterial baroreceptor input[48] but normal during increases of trigeminal nerve input provoked by face immersion.[14] Important to this premise is the recent demonstration of an impairment of the afferent limb of the baroreceptor reflex in experimental diabetes.[69,70]

In addition to the functional deficits mentioned above, morphologic, metabolic and neurochemical changes are found in diabetic vagal and/or baroreceptor afferent nerves. Marked lesions, demyelination and loss of myelinated axons in the vagus nerve, occur with symptomatic diabetic autonomic neuropathy.[46,73,125] Autonomic neuropathy affecting the vagus nerve is characterized by progressive axonal atrophy

of myelinated and unmyelinated fibers, which is preceded and accompanied by vagal dysfunction substantiated by impaired heart rate variability.[123,167,247,249] Diabetic gastroparesis has been associated with a marked reduction in the density of unmyelinated vagal axons.[73] Thus, it appears that both myelinated and unmyelinated vagal fibers and visceral afferent fibers are affected in diabetes. Diabetes-induced metabolic, oxidative, and neurochemical changes in the vagus nerve and nodose ganglion have been demonstrated.[133] The vagus nerves from STZ-induced diabetic rats had elevated glucose, fructose, and sorbitol, and decreased reduced glutathione. Diabetes-induced alterations in the neurochemical content of visceral afferent neurons are consistent with nerve injury (see above and Reference 192).

2.4.2.1.1   Neurotrophin Content of the Vagus Nerve

The vagus nerves have elevated NGF protein content at early stages of STZ-induced diabetes (Figure 2.5).[133] Cervical vagus nerves of streptozotocin (STZ)-induced diabetic rats were studied at 8, 16, and 24 weeks after the induction of diabetes. Elevations in vagus nerve hexose (glucose and fructose) and polyol levels (sorbitol), and their normalization with insulin treatment, verify that the STZ treatment results in hyperglycemia-induced metabolic abnormalities in the nerve. Intact right vagus nerves were used to determine whether STZ-induced diabetes altered the nerve content of endogenous NGF and NT-3.[133] The vagus nerves of diabetic rats have elevated NGF at 8 weeks (50%) and at 16 weeks (35%), but not at the 24-week time point, when compared with the control or the diabetic+insulin groups.[133] The intact cervical vagus nerve of the diabetic rats at each of the three time points (8, 16, and 24 weeks) show no significant changes in NT-3 compared with the control or the diabetic+insulin groups. The expression of NGF mRNA and NT-3 mRNA in the cervical vagus nerve, measured by RT-PCR, shows no significant differences in the relative levels of vagal nerve NGF or NT-3 mRNA from diabetic rats compared with the control or the diabetic+insulin rats at the 8- or 16-week time points.[133] The amounts of neurotrophin receptor (p75, TrkA, TrkC) mRNAs in the vagus nerve and vagal afferent nodose ganglion are not reduced in diabetic rats.[132]

Whether the elevated NGF at the early stages of diabetes is a regenerative response to an analogous hyperglycemia-induced injury to the nerve is not known. If it is, the loss of the elevated NGF at the later stages of diabetes may signal a failure of regenerative support of the neurons by locally produced neurotrophins. The elevation in vagal NGF at the early stages of STZ-induced diabetes is likely due to local production of the neurotrophin as other potential sources are not increased, e.g., there is no increase in transported NGF[133] nor is there an additional increase in NGF (above that seen in the nerve) in the nodose ganglia content of NGF (data not shown). Most likely the elevated NGF originated in non-neuronal cells such as Schwann cells and macrophages, as these non-neuronal cells have the ability to produce NGF after nerve injury.[24,90] The increase in NGF protein in the absence of elevations in vagus nerve NGF mRNA in diabetic rats may be due to an alteration in a post-transcriptional event. Regulation of NGF production can occur at a post-transcriptional level, e.g., increases in NGF protein can result from increases in NGF mRNA stability and/or an increased translational efficiency of NGF protein.[210] It is unclear whether increased levels of NGF present in the vagus nerve
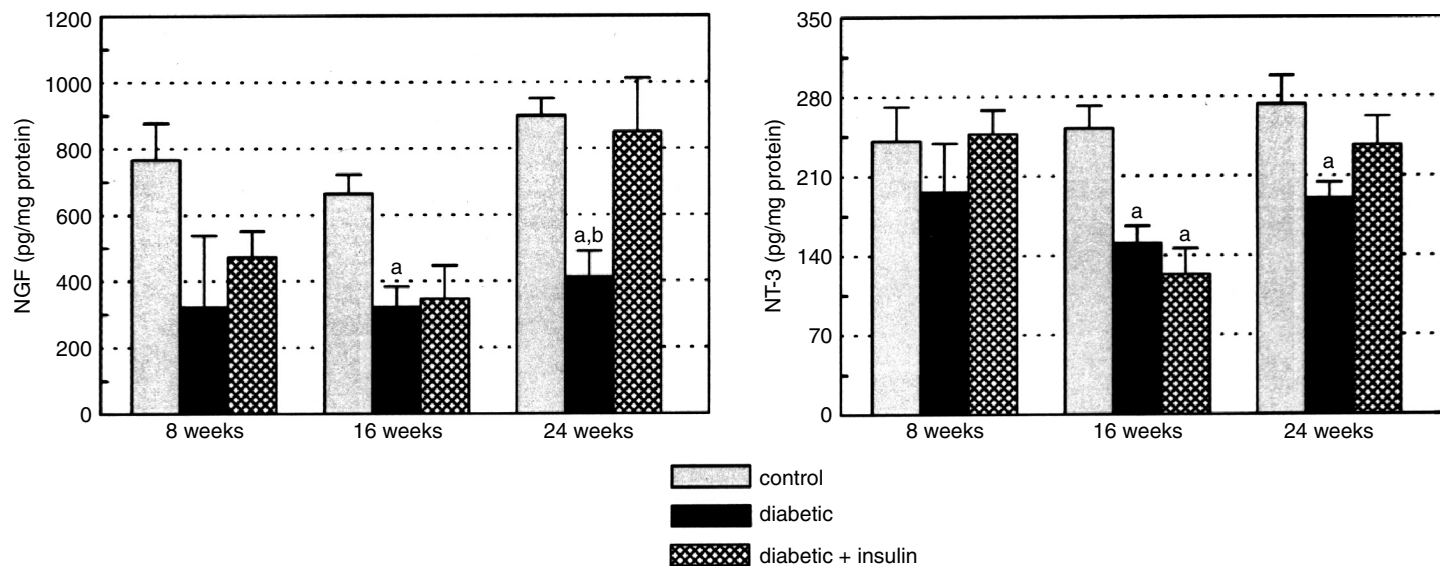
FIGURE 2.5 Bar graphs (grey bars = controls, black bars = diabetic, cross hatch bars = diabetic+insulin replacement) showing the effect of streptozotocin (STZ)-induced diabetes at the 8-, 16-, and 24-week time points on the retrograde transport of NGF and NT-3 in cervical vagus nerve segments 24 hours after placement of constricting double ligatures. The retrogradely transported NGF and NT-3 were calculated from the content in the distal segment minus the content in the intermediate segment of the double-ligated vagus nerve. a = P<0.05 compared with control, and b = P< 0.05 compared to diabetic+insulin-treated counterparts. (Adapted from Lee et al., 2001b.)

trunk during the early stages of diabetes results in an increased availability of the vagal afferent and/or efferent neuronal perikarya to NGF.

2.4.2.1.2 Neurotrophin Content in Peripheral Targets of the Vagus Nerve

The effects of diabetes on the contents of NGF and NT-3 protein and mRNAs are studied in tissues innervated by the vagus nerve (Reference 132 and Cai, Lee, and Helke, unpublished data). Using RT-PCR, NGF and NT-3 mRNAs are detected in multiple targets tissues of the vagus nerve, e.g., atrium, stomach and duodenum. At the 16-week time point, the expression of NT-3 mRNA in the right atrium, stomach and duodenum is not different among the control, diabetic or diabetic+insulin groups. At the 8-week time point, a small increase (22%) in the NT-3 mRNA in the diabetic right atrium compared with controls is noted but the increase is not reversed by insulin treatment. The expression of NT-3 mRNA in left ventricle, stomach and duodenum of diabetic rats at the 8-week time points is not different from control or from diabetic+insulin groups. Assessment of the neurotrophin protein content (using ELISA) in the stomach at the 16-week time point does not show differences in the content of NGF or NT-3 among control, diabetic, or diabetic+insulin groups.

2.4.2.1.3 Neurotrophin Receptors in the Vagus Nerve and Nodose Ganglion

To assess possible changes in the expression of the neurotrophin receptors (TrkA, TrkB, p75) in the diabetic vagus nerve, we used RT-PCR to measure the mRNAs for TrkA, full-length TrkC, and p75 in vagus nerves and nodose ganglia (Reference 132 and Cai et al. unpublished data). The mRNAs of TrkA, TrkC, and p75 are clearly detected in the nodose ganglia and the vagus nerve of normal adult rats by RT-PCR. After 8 weeks of STZ-induced diabetes, there are no differences in the mRNA levels of TrkA, full-length TrkC, and p75 in the nodose ganglia or the vagus nerves among control, diabetic, and diabetic+insulin groups. Likewise, at the 16-week time point, no reductions in the mRNA levels of TrkA, TrkC, or p75 are found in the nodose ganglia or the vagus nerves from diabetic rats. A modest increase (29%) in the expression of TrkA mRNA in vagus nerve, but not in the nodose ganglion, of diabetic rats is not reversed by insulin treatment.[13]

2.4.2.2 Axonal Transport of Neurotrophins in Diabetes

Using a double-ligation model to assess the transport of endogenous neurotrophins, the retrograde transport of both NGF and NT-3 is found to be significantly reduced in the cervical vagus nerve at later stages of streptozotocin (STZ)-induced diabetes (16 and 24 weeks).[133] Anterograde transport of NGF or NT-3 is not apparent in the vagus nerve of diabetic or control rats. The reduction in retrograde transport of endogenous NGF and NT-3 in the vagus nerve of diabetic rats could be due to a decline in the transport in the afferent and/or the efferent vagal nerve fibers. However, given that the vagal transport of both agents is altered in diabetic rats (this study), that the vagus nerve is more than 70% afferent,[1,60,188] and that iodinated NGF is retrogradely transported by the afferent but not the efferent vagus nerve,[76] it is likely

that the primary decrement of NGF and NT-3 transport is in the afferent component of the vagus nerve.

The finding that the retrograde transport of both NGF and NT-3 is affected suggests that diabetes may affect the transport of each agent by mechanisms that are shared by both. No changes in the NGF and NT-3 protein or mRNA levels in the stomach or atrium, two vagally innervated organs, are noted after 16 or 24 weeks of diabetes.[132] Moreover, the amounts of neurotrophin receptor (p75, TrkA, TrkC) mRNAs in the vagus nerve and vagal afferent nodose ganglion are not reduced in diabetic rats.[132] These data suggest that neither diminished access to target-derived neurotrophins nor the loss of relevant neurotrophin receptors accounts for the diabetes-induced alteration in the retrograde axonal transport of neurotrophins. However, the diabetes-induced reduction in retrogradely transported NGF and NT-3 by vagal nerve fibers at the later stages of diabetes suggests a deficit in the neurotrophin-dependent trophic support to vagal afferent and efferent neurons.

The possibility of more general diabetes-induced changes in the ability of the neuron to maintain machinery involved in retrograde transport is suggested by data showing that the anterograde transport of proteins (choline acetyltransferase, muscarinic and opioid receptors) is reduced in the vagus nerve of diabetic rats.[127,229] To assess whether diabetes causes a defect in axonal transport that may not be specific to neurotrophin transport, we studied the ability of a neuronal tracer (FluoroGold) to be retrogradely transported by vagal neurons of control and diabetic rats.[132] After 24 weeks of diabetes, FluoroGold is retrogradely transported from the stomach to more than 50% fewer afferent and efferent vagal neurons in the STZ-diabetic compared with control rats. The diabetes-induced deficit in retrograde axonal transport of FluoroGold is likely to reflect alterations in basic axonal transport mechanisms in both the afferent and efferent vagus nerve that contribute to the previously observed reductions in neurotrophin transport.

The interaction between neurotrophins and Trk receptors can activate the phosphatidylinositol-3 kinase (PI3 kinase)/Akt (protein kinase B) signal pathway which mediates neuron survival, differentiation, axon growth, protects neurons from apoptosis, and promotes nerve regeneration.[13,35,45,88,106,177,235] The PI3 kinase/Akt signal pathway located in the distal axon of neurons has a unique role in the retrograde transport of NGF and brain-derived neurotrophic factor (BDNF) in sympathetic, sensory neurons and motoneurons.[13,126,195,239] Inhibition of PI3 kinase in the distal axons of neurons attenuates the retrograde transport of NGF and also induces neuron apoptosis.[126] Furthermore, retrogradely transported neurotrophins play a critical role in the activation of downstream effectors of PI3 kinase/Akt in neuronal perikarya. Inhibition of the PI3 kinase/Akt signal pathway in distal axons attenuated the retrograde transport of NGF to the neuronal cell body, which reduced the activation of the Akt in the neuronal cell body.[126] Thus, it is plausible that impaired retrograde transport of neurotrophins,[43,82,206] deficits in nerve regeneration,[120,147] and neuronal apoptosis[201,202,216] in diabetes could be due to impairment in the PI3 kinase/Akt pathway in the neuronal perikarya and/or axons.

To assess the potential involvement of an impaired PI3 kinase/Akt signal pathway in the diabetes-induced reduction in retrograde axonal transport of neurotrophins in the vagus nerve, Cai and Helke[26] characterize diabetes-induced changes in the PI3

kinase/Akt signal pathway in the vagus nerve and vagal afferent neurons. Control and streptozotocin (STZ)-induced diabetic rats with a duration of 16 weeks, kinase assays, western blotting, and immunocytochemistry show that diabetes results in alterations in activity and protein expression of the PI3 kinase/Akt signal pathway in the vagus nerve and vagal afferent neurons. Diabetes causes a significant decrease in enzymatic activity of PI3 kinase and Akt (52% and 36% of control, respectively) in the vagus nerve. The reduced enzymatic activity is not associated with decreased protein expression of the p85 subunit of PI3 kinase, Akt and phosphorylation of Akt (ser473). In contrast, there is a significant increase in the phosphorylation of p70s6 kinase (thr421/ser424), along with a normal protein expression of p70s6 kinase in the vagus nerve of diabetic rats. However, diabetes induces an overall decrease in immunoreactivity of the p85 subunit of PI3 kinase, phospho-Akt (ser473) and phospho-p70s6/p85s6 kinase (thr421/ser424) in vagal afferent neurons. Thus, Cai and Helke[26] demonstrate that STZ-induced diabetes resulted in impairment in the PI3 kinase/Akt signal pathway in the vagal afferent neurons and the vagus nerve after 16 weeks of diabetes. The findings provide evidence to support previous observations that reduced retrograde transport of NGF and NT-3 in the vagus nerve of diabetic rats is not due to deficient neurotrophin production and neurotrophin receptors. The impaired PI3 kinase/Akt signal pathway could be, at least in part, responsible for the reduced retrograde transport of NGF and NT-3 in the vagus nerve.

ACKNOWLEDGMENTS

REFERENCES

1. Agostoni, E., Chinnock, J.E., Burgh Daluy, M.D., and Murray, J.G. Functional and histological studies of the vagus nerve and its branches to the heart, lungs, abdominal viscera in the cat, *J Physiol (Lond),* 135: 182, 1957.
2. Alonzi, T., Middleton, G., Wyatt, S., Buchman, V., Betz, U.A., Muller, W., Musiani, P., Poli, V., and Davies, A.M. Role of STAT3 and PI 3-kinase/Akt in mediating the survival actions of cytokines on sensory neurons, *Mol Cell Neurosci,* 18: 270, 2001.
3. Apfel, S.C., and Kessler, J.A. Neurotrophic factors in the therapy of peripheral neuropathy, *Bailliere's Clin. Neurol.,* 4: 593, 1995.
4. Appenzeller, O. Peripheral autonomic neuropathies, in *Disorders of the Autonomic Nervous System,* Robertson, D. and Biaggioni, I., Eds., Harwood Academic Publishers, New York, 1995: 141.
5. Araki, T. and Milbrandt, J. Ninjurin, a novel adhesion molecule, is induced by nerve injury and promotes axonal growth, *Neuron,* 17: 353, 1996.
6. Ayer-Le Lievre, C.S. and Le Douarin, N.M. The early development of cranial sensory ganglia and the potentialities of their component cells studied in quail-chick chimeras, *Dev Biol,* 94: 291, 1982.

7. Balkowiec, A. and Katz, D.M. Activity-dependent release of endogenous brain-derived neurotrophic factor from primary sensory neurons detected by ELISA *in situ*, *J Neurosci,* 20: 7417, 2000.

8. Baloh, R.H., Tansey, M.G., Lampe, P.A., Fahrner, T.J., Enomoto, H., Simburger, K.S., Leitner, M.L., Araki, T., Johnson, E.M. Jr., and Milbrandt, J. Artemin. A novel member of the GDNF ligand family, supports peripheral and central neurons and signals through the GFRalpha3-RET receptor complex, *Neuron,* 21: 1291, 1998.

9. Bamji, S.X., Majdan, M., Pozniak, C.D., Belliveau, D.J., Aloyz, R., Kohn, J., Causing, C.G., and Miller, F.D. The p75 neurotrophin receptor mediates neuronal apoptosis and is essential for naturally occurring sympathetic neuron death, *J Cell Biol,* 140: 911, 1998.

10. Barbacid, M. The Trk family of neurotrophin receptors, *J Neurobiol,* 25: 1386, 1994.

11. Barbin, G., Manthorpe, M., and Varon, S. Purification of the chick eye ciliary neuronotrophic factor, *J Neurochem,* 43: 1468, 1984.

12. Barker, P.A. and Shooter, E.M. Disruption of NGF binding to the low affinity neurotrophin receptor p75LNTR reduces NGF binding to TrkA on PC12 cells, *Neuron,* 13: 203, 1994.

13. Bartlett, S.E., Reynolds, A.J., Weible, M., Heydon, K., and Hendry, I.A. In sympathetic but not sensory neurones, phosphoinositide-3 kinase is important for NGF-dependent survival and the retrograde transport of ^{125}I-betaNGF, *Brain Res,* 761: 257, 1997.

14. Bennett, T., Farquhar, I.K., Hosking, D.J., and Hampton, J.R. Assessment of methods for estimating autonomic nervous control of the heart in patients with diabetes mellitus, *Diabetes,* 27: 1167, 1978.

15. Berkemeier, L.R., Winslow, J.W., Kaplan, D.R., Nikolics, K., Goeddel, D.V., and Rosenthal, A. Neurotrophin-5: a novel neurotrophic factor that activates trk and trkB, *Neuron,* 7: 857, 1991.

16. Borasio, G.D., Markus, A., Wittinghofer, A., Barde, Y.A., and Heumann, R. Involvement of ras p21 in neurotrophin-induced response of sensory, but not sympathetic neurons, *J Cell Biol,* 121: 665, 1993.

17. Bradley, J.L., Thomas, P.K., King, R.H.M., Muddle, J.R., Ward, J.D., Tesfaye, S., Boulton, A.J.M., Tsigos, C., and Young, R.J. Myelinated nerve fibre regeneration in diabetic sensory polyneuropathy: correlation with type of diabetes, *Acta Neuropathol,* 90: 403, 1995.

18. Brady, R., Zaidi, S.I., Mayer, C., and Katz, D.M. BDNF is a target-derived survival factor for arterial baroreceptor and chemoafferent primary sensory neurons, *J Neurosci,* 19: 2131, 1999.

19. Brenneman, D.E. and Eiden, L.E. Vasoactive intestinal peptide and electrical activity influence neuronal survival, *Proc Natl Acad Sci U.S.A.,* 83: 1159, 1986.

20. Brenneman, D.E., Nicol, T., Warren, D., and Bowers, L.M. Vasoactive intestinal peptide: a neurotrophic releasing agent and an astroglial mitogen, *J Neurosci Res,* 25: 386, 1990.

21. Brewster, W.J., Fernyhough, P., Diemel, L.T., Mohiuddin, L., and Tomlinson, D.R. Diabetic neuropathy, nerve growth factor and other neurotrophic factors, *Trends Neurosci (TINS),* 17: 321, 1994.

22. Broberger, C., Holmberg, K., Shi, T.J., Dockray, G., and Hokfelt, T. Expression and regulation of cholecystokinin and cholecystokinin receptors in rat nodose and dorsal root ganglia, *Brain Res,* 903: 128, 2001.

23. Brosenitsch, T.A., Salgado-Commissariat, D., Kunze, D.L., and Katz, D.M. A role for L-type calcium channels in developmental regulation of transmitter phenotype in primary sensory neurons, *J Neurosci,* 18: 1047, 1998.
24. Brown, M.C., Perry, V.H., Lunn, E.R., Gordon, S., and Heumann, R. Macrophage dependence of peripheral sensory nerve regeneration: possible involvement of nerve growth factor, *Neuron,* 6: 359, 1991.
25. Buj-Bello, A., Buchman, V.L., Horton, A., Rosenthal, A., and Davies, A.M. GDNF is an age-specific survival factor for sensory and autonomic neurons, *Neuron,* 15: 821, 1995.
26. Cai, F. and Helke, C.J. Abnormal PI3 kinase/Akt signal pathway in vagal afferent neurons and vagus nerve of streptozotocin-diabetic rats, *Mol Brain Res,* 110: 234, 2003.
27. Carr, M.J., Hunter, D.D., Jacoby, D.B., and Undem, B.J. Expression of tachykinins in nonnociceptive vagal afferent neurons during respiratory viral infection in guinea pigs, *Am J Respir Crit Care Med,* 165: 1071, 2002.
28. Chabrier, P.E., Demerle-Pallardy, C., and Auguet, M. Nitric oxide synthases: targets for therapeutic strategies in neurological diseases, *Cell Mol Life Sci,* 55: 1029, 1999.
29. Chang, H.M., Liao, W.C., Lue, J.H., Wen, C.Y., and Shieh, J.Y. Upregulation of NMDA receptor and neuronal NADPH-d/NOS expression in the nodose ganglion of acute hypoxic rats, *J Chem Neuroanat,* 25: 137, 2003.
30. Chao, M.V. Neurotrophin Receptors: A window into neuronal differentiation, *Neuron,* 9: 583, 1992.
31. Chery-Croze, S., Bosshard, A., Martin, H., Cuber, J.C., Chamay, Y., and Chayvialle, J.A. Peptide immunocytochemistry in afferent neurons from lower gut in rats, *Peptides,* 9: 873, 1988.
32. Conover, J.C., Erickson, J.T., Katz, D.M., Bianchi, L.M., Poueymirou, W.T., McClain, J., Pan, L., Helgren, M., Ip, N.Y., Boland, P., Friedman, B., Wiegand, S., Vejsada, R., Kato, A.C., DeChiara, T.M., and Yancopoulos, G.D. Neuronal deficits, not involving motor neurons, in mice lacking BDNF and/or NT4, *Nature,* 375: 235, 1995.
33. Cooper, E. Nicotinic acetylcholine receptors on vagal afferent neurons, *Ann N Y Acad Sci,* 940: 110, 2001.
34. Cooper, E. Synapse formation among developing sensory neurons from rat nodose ganglia grown in tissue culture, *J Physiol,* 351: 263, 1984.
35. Crowder, R.J. and Freeman, R.S. Phosphatidylinositol 3-kinase and Akt protein kinase are necessary and sufficient for the survival of nerve growth factor-dependent sympathetic neurons, *J Neurosci,* 18: 2933, 1998.
36. Curtis, R., Adryan, K.M., Stark, J.L., Park, J., Compton, D., Weskamp, G., Huber, L.J., Chao, M.V., Jaenisch, R., Lee, K., Lindsay, R.M., and DiStefano, P.S. Differential role of the low affinity neurotrophin receptor (p75) in retrograde axonal transport of the neurotrophins, *Neuron,* 14: 1201, 1995.
37. Curtis, R. and DiStefano, P.S. Neurotrophic factors, retrograde axonal transport and cell signaling, *Trends Cell Biol. (TICB),* 4: 383, 1994.
38. Czyzyk-Krzeska, M.F., Bayliss, D.A., Lawson, E.E., and Millhorn, D.E. Expression of messenger RNAs for peptides and tyrosine hydroxylase in primary sensory neurons that innervate arterial baroreceptors and chemoreceptors, *Neurosci Lett,* 129: 98, 1991.
39. Czyzyk-Krzeska, M.F., Bayliss, D.A., Seroogy, K.B., and Millhorn, D.E. Gene expression for peptides in neurons of the petrosal and nodose ganglia in rat, *Exp Brain Res,* 83: 411, 1991.

40. Davies, A.M., Minichiello, L., and Klein, R. Developmental changes in NT3 signalling via TrkA and TrkB in embryonic neurons, *EMBO J,* 14: 4482, 1995.

41. De Konnick, P., Carbonetto, S., and Cooper, E. NGF induces neonatal rat sensory neurons to extend dendrites in culture after removal of satellite cells, *J Neurosci,* 13: 577, 1993.

42. Dechant, G., Rodriguez-Tebar, A., and Barde, Y. Neurotrophin receptors, *Prog Neurobiol,* 42: 347, 1994.

43. Delcroix, J.D., Tomlinson, D.R., and Fernyhough, P. Diabetes and axotomy-induced deficits in retrograde axonal transport of nerve growth factor correlate with decreased levels of p75LNTR protein in lumbar dorsal root ganglia, *Mol Brain Res,* 51: 82, 1997.

44. DiStefano, P.S., Friedman, B., Radziejewski, C., Alexander, C., Boland, P., Schick, C.M., Lindsay, R.M., and Wiegand, S.J. The neurotrophins BDNF, NT-3, and NGF display distinct patterns of retrograde axonal transport in peripheral and central neurons, *Neuron,* 8: 983, 1992.

45. Dolcet, X., Egea, J., Soler, R.M., Martin-Zanca, D., and Comella, J.X. Activation of phosphatidylinositol 3-kinase, but not extracellular-regulated kinases, is necessary to mediate brain-derived neurotrophic factor-induced motoneuron survival, *J Neurochem,* 73: 521, 1999.

46. Duchen, L.W., Anjorin, A., Watkins, P.J., and Mackay, J.D. Pathology of autonomic neuropathy in diabetes mellitus, *Ann Intern Med,* 92: 301, 1980.

47. Ebendal, T., Tomac, A., Hoffer, B.J., and Olson, L. Glial cell line-derived neurotrophic factor stimulates fiber formation and survival in cultured neurons from peripheral autonomic ganglia, *J Neurosci Res,* 40: 276, 1995.

48. Eckberg, D.L., Harkins, S.W., Fritsch, J.M., Musgrave, G.E., and Gardner, D.F. Baroreflex control of plasma norepinephrine and heart period in healthy subjects and diabetic patients, *J Clin Invest,* 78: 366, 1986.

49. El Shamy, W.M. and Ernfors, P. Brain-derived neurotrophic factor, neurotrophin-3, and neurotrophin-4 complement and cooperate with each other sequentially during visceral neuron development, *J Neurosci,* 17: 8667, 1997.

50. Erickson, J.T., Brosenitsch, T.A., and Katz, D.M. Brain-derived neurotrophic factor and glial cell line-derived neurotrophic factor are required simultaneously for survival of dopaminergic primary sensory neurons *in vivo*, *J Neurosci,* 21: 581, 2001.

51. Erickson, J.T., Conover, J.C., Borday, V., Champagnat, J., Bardacid, M., Yancopoulos, G., and Katz, D. Mice lacking brain-derived neurotrophic factor exhibit visceral sensory neuron losses distinct from mice lacking NT-4 and display a severe developmental deficit in control of the breathing, *J Neurosci,* 16: 5361, 1996.

52. Ernfors, P., Lee, K., Kucera, J., and Jaenisch, R. Lack of neurotrophin-3 leads to deficiencies in the peripheral nervous system and loss of limb proprioceptive afferents, *Cell,* 77: 503, 1994.

53. Ernfors, P., Merlio, J.P., and Persson, H. Cells expressing mRNA for neurotrophins and their receptors during embryonic rat development, *Eur J Neuorsci,* 4: 1140, 1992.

54. Ewing, D.J., Campbell, I.W., and Clarke, B.F. The natural history of diabetic autonomic neuropathy, *Q J Med,* 49: 95, 1980.

55. Ewing, D.J., Martyn, C.N., Young, R.J., and Clarke, B.F. The value of cardiovascular autonomic function tests: 10 years experience in diabetes, *Diabetes Care,* 8: 491, 1985.

56. Fahrenkrug, J. Transmitter role of vasoactive intestinal peptide, *Pharmacol Toxicol,* 72: 354, 1993.

57. Farinas, I., Jones, K.R., Backus, C., Wang, X., and Reichardt, L.F. Severe sensory and sympathetic deficits in mice lacking neurotrophin-3, *Nature,* 369: 658, 1994.

58. Ferri, C.C., Moore, F.A., and Bisby, M.A. Effects of facial nerve injury on mouse motoneurons lacking the p75 low-affinity neurotrophin receptor, *J Neurobiol,* 34: 1, 1998.

59. Fiallos-Estrada, C.E., Herdegen, T., Kummer, W., Mayer, B., Bravo, R., and Zimmerman, M. Long-lasting increase of nitric oxide synthase immunoreactivity, NADPH-diaphorase reaction and c-JUN co-expression in rat dorsal root ganglion neurons following sciatic nerve transection, *Neurosci Lett,* 150: 169, 1993.

60. Foley, J. and DuBois, F.S. Quantitative studies of the vagus nerve in the cat, *J Comp Neurol,* 67: 49, 1937.

61. Fong, A.Y., Talman, W.T., and Lawrence, A.J. Axonal transport of NADPH-diaphorase and [^{3}H]nitro-L-arginine binding, but not [^{3}H]cGMP binding, by the rat vagus nerve, *Brain Res,* 878: 240, 2000.

62. Forgie, A., Doxakis, E., Buj-Bello, A., Wyatt, S., and Davies, A.M. Differences and developmental changes in the responsiveness of PNS neurons to GDNF and neurturin, *Mol Cell Neurosci,* 13: 430, 1999.

63. Forgie, A., Kuehnel, F., Wyatt, S., and Davies, A.M. *In vivo* survival requirement of a subset of nodose ganglion neurons for nerve growth factor, *Eur J Neurosci,* 12: 670, 2000.

64. Fox, E.A., Phillips, R.J., Baronowsky, E.A., Byerly, M.S., Jones, S., and Powley, T.L. Neurotrophin-4 deficient mice have a loss of vagal intraganglionic mechanoreceptors from the small intestine and a disruption of short-term satiety, *J Neurosci,* 21: 8602, 2001.

65. Frade, J.M., Rodriguez-Tebar, A., and Barde, Y.A. Induction of cell death by endogenous nerve growth factor through its p75 receptor, *Nature,* 383: 166, 1996.

66. Frisen, J., Verge, V.M., Fried, K., Risling, M., Persson, H., Trotter, J., Hokfelt, T., and Lindholm, D. Characterization of glial trkB receptors: differential response to injury in the central and peripheral nervous systems, *Proc Natl Acad Sci U.S.A.,* 90: 4971, 1993.

67. Funakoshi, H., Frissen, J., Barbany, G., Timmusk, T., Zachrisson, O., Verge, V.M.K., and Persson, H. Differential expression of mRNAs for neurotrophins and their receptors after axotomy of the sciatic nerve, *J Cell Biol,* 123: 455, 1993.

68. Glass, D.J. and Yancopoulos, G.D. The neurotrophins and their receptors, *Trends Cell Biol,* 3: 262, 1993.

69. Gouty, S., Regalia, J., Cai, F., and Helke, C.J. alpha-Lipoic acid treatment prevents the diabetes-induced attenuation of the afferent limb of the baroreceptor reflex in rats, *Auton Neurosci,* 108: 32, 2003.

70. Gouty, S., Regalia, J., and Helke, C.J. Attenuation of the afferent limb of the baroreceptor reflex in streptozotocin-induced diabetic rats, *Auton Neurosci,* 89: 86, 2001.

71. Griffin, J.W., George, R., and Ho, T. Macrophage systems in peripheral nerves. A review, *J Neuropathol Exp Neurol,* 52: 553, 1993.

72. Grothe, C. and Unsicker, K. Neuron-enriched cultures of adult rat dorsal root ganglia: establishment, characterization, survival, and neuropeptide expression in response to trophic factors, *J Neurosci. Res,* 18: 539, 1987.

73. Guy, R.J.C., Dawson, J.L., Garrett, J.R., Laws, J.W., Thomas, P.K., Sharma, A.K., and Watkins, P.J. Diabetic gastroparesis from autonomic neuropathy: surgical considerations and changes in vagus nerve morphology, *J Neurol Neurosurg Psychiatry,* 47: 686, 1984.

74. Hallböök, F., Ibanez, C.F., and Persson, H. Evolutionary studies of the nerve growth factor family reveal a novel member abundantly expressed in Xenopus ovary, *Neuron,* 6: 845, 1991.

75. Hallböök, F., Ayer-Lelievre, C., Ebendal, T., and Persson, H. Expression of nerve growth factor receptor mRNA during early development of the chicken embryo: emphasis on cranial ganglia, *Development,* 108: 693, 1990.

76. Helke, C.J., Adryan, K.M., Fedorowicz, J., Zhuo, H., Park, J.S., Curtis, R., Radley, H.E., and Distefano, P.S. Axonal transport of neurotrophins by visceral afferent and efferent neurons of the vagus nerve of the rat, *J Comp Neurol,* 393: 102, 1998.

77. Helke, C.J. and Hill, K.M. Immunohistochemical study of neuropeptides in vagal and glossopharyngeal afferent neurons in the rat, *Neuroscience,* 26: 539, 1988.

78. Helke, C.J., and Niederer, A.J. Studies on the coexistence of substance P with other putative transmitters in the nodose and petrosal ganglia, *Synapse,* 5: 144, 1990.

79. Helke, C.J., O'Donohue, T.L., and Jacobowitz, D.M. Substance P as a baro- and chemo-receptor afferent neurotransmitter: immunocytochemical and neurochemical evidence in the rat, *Peptides,* 1: 1, 1980.

80. Helke, C.J. and Rabchevsky, A. Axotomy alters putative neurotransmitters in visceral sensory neurons of the nodose and petrosal ganglia, *Brain Res,* 551: 44, 1991.

81. Helke, C.J. and Verdier-Pinard, D. Neurotrophins alter the numbers of neurotransmitter-ir mature vagal/glossopharyngeal visceral afferent neurons *in vitro*, *Brain Res,* 884: 206, 2000.

82. Hellweg, R. and Hartung, H.D. Endogenous levels of nerve growth factor (NGF) are altered in experimental diabetes mellitus: a possible role for NGF in the pathogenesis of diabetic neuropathy, *J Neurosci Res,* 26: 258, 1990.

83. Herdegen, T., Kummer, W., Fiallos, C.E., Leah, J., and Bravo, R. Expression of c-JUN, JUN B and JUN D proteins in rat nervous system following transection of vagus nerve and cervical sympathetic trunk, *Neuroscience,* 45: 413, 1991.

84. Herdegen, T., Skene, P., and Bahr, M. The c-Jun transcription factor-bipotential mediator of neuronal death, survival and regeneration, *Trends Neurosci (TINS),* 20: 227, 1997.

85. Hertzberg, T., Brosenitsch, T., and Katz, D.M. Depolarizing stimuli induce high levels of dopamine synthesis in fetal rat sensory neurons, *Neuroreport,* 7: 233, 1995.

86. Hertzberg, T., Fan, G., Finley, J.C., Erickson, J.T., and Katz, D.M. BDNF supports mammalian chemoafferent neurons in vitro and following Peripheral target removal *in vivo*, *Dev Biol,* 166: 801, 1994.

87. Hertzberg, T., Finley, J.C.W., and Katz, D.M. Trophic regulation of carotid body afferent development, *Adv Exp Med Biol,* 360: 305, 1993.

88. Hetman, M., Kanning, K., Cavanaugh, J.E., and Xia, Z. Neuroprotection by brain-derived neurotrophic factor is mediated by extracellular signal-regulated kinase and phosphatidylinositol 3-kinase, *J Biol Chem,* 274: 22569, 1999.

89. Heuckeroth, R.O., Enomoto, H., Grider, J.R., Golden, J.P., Hanke, J.A., Jackman, A., Molliver, D.C., Bardgett, M.E., Snider, W.D., Johnson, E.M. Jr., and Milbrandt, J. Gene targeting reveals a critical role for neurturin in the development and maintenance of enteric, sensory, and parasympathetic neurons, *Neuron,* 22: 253, 1999.

90. Heumann, R., Korsching, S., Bandtlow, C., and Thoenen, H. Changes of nerve growth factor synthesis in nonneuronal cells in response to sciatic nerve transection, *J Cell Biol,* 104: 1623, 1987.

91. Heumann, R., Lindholm, D., Bandtlow, C., Meyer, M., Radeke, M.J., Misko, T.P., Shooter, E., and Thoenen, H. Differential regulation of mRNA encoding nerve growth factor and its receptor in rat sciatic nerve during development, degeneration, and regeneration: role of macrophages, *Proc Natl Acad Sci (USA),* 84: 8735, 1987.

92. Hilsted, J. and Low, P.A. Diabetic autonomic neuropathy, Low, P.A., Ed., Little, Brown & Co., Boston, 1993: 423.

93. Hofer, M.M. and Barde, Y.-A. Brain-derived neurotrophic factor prevents neuronal death *in vivo*, *Nature,* 331: 261, 1988.

94. Hohn, A., Leibrock, J., Bailey, K., and Barde, Y.A. Identification and characterization of a novel member of the nerve growth factor/brain-derived neurotrophic factor family, *Nature,* 344: 339, 1990.

95. Horton, A.R., Barlett, P.F., Pennica, D., and Davies, A.M. Cytokines promote the survival of mouse cranial sensory neurons at different developmental stages, *Eur J Neurosci,* 10: 673, 1998.

96. Horton, A.R., Davies, A.M., Buj-Bello, A., Bartlett, P., and Murphy, M. Leukemia inhibitory factor and ciliary neurotrophic factor in sensory neuron development, *Perspect Dev Neurobiol,* 4: 35, 1996.

97. Huang, F.-L., Zhuo, H., Sinclair, C., Goldstein, M.E., McCabe, J.T., and Helke, C.J. Peripheral deafferentation alters calcitonin gene-related peptide mRNA in visceral sensory neurons of the nodose and petrosal ganglia, *Mol Brain Res,* 22: 290, 1994.

98. Huber, K., Kuehnel, F., Wyatt, S., and Davies, A.M. TrkB expression and early sensory neuron survival are independent of endogenous BDNF, *J Neurosci Res,* 59: 372, 2000.

99. Hunter, D.D., Myers, A.C., and Undem, B.J. Nerve growth factor-induced phenotypic switch in guinea pig airway sensory neurons, *Am J Respir Crit Care Med,* 161: 1985, 2000.

100. Ichikawa, H. and Helke, C.J. Coexistence of calbindin D-28k and NADPH-diaphorase in vagal and glossopharyngeal sensory neurons of the rat, *Brain Res,* 735: 325, 1996.

101. Ichikawa, H. and Helke, C.J. The coexistence of TrkA with putative transmitter agents and calcium-binding proteins in the vagal and glossopharyngeal sensory neurons of the adult rat, *Brain Res,* 846: 268, 1999.

102. Ichikawa, H. and Helke, C.J. Parvalbumin and calbindin D-28k in vagal and glossopharyngeal sensory neurons of the rat, *Brain Res,* 675: 337, 1995.

103. Ichikawa, H., Jacobowitz, D.M., Winsky, L., and Helke, C.J. Calretinin-immunoreactivity in vagal and glossopharyngeal sensory neurons of the rat: distribution and coexistence with putative transmitter agents, *Brain Res,* 557: 316, 1991.

104. Ide, C. Peripheral nerve regeneration, *Neurosci Res,* 25: 101, 1996.

105. Ip, N.Y., Maisonpierre, P., Alderson, R., Friedman, B., Furth, M.E., Panayotatos, N., Squinto, S., Yancopoulos, G.D., and Lindsay, R.M. The neurotrophins and CNTF: specificity of action towards PNS and CNS neurons, *J Physiol (Paris),* 85: 123, 1991.

106. Jackson, T.R., Blader, I.J., Hammonds-Odie, L.P., Burga, C.R., Cooke, F., Hawkins, P.T., Wolf, A.G., Heldman, K.A., and Theibert, A.B. Initiation and maintenance of NGF-stimulated neurite outgrowth requires activation of a phosphoinositide 3-kinase, *J Cell Sci,* 109: 289, 1996.

107. Jia, Y.S., Wang, X.A., and Ju, G. Nitric oxide synthase expression in vagal complex following vagotomy in the rat, *Neuroreport,* 5: 793, 1994.

108. Johnson, E.M. Jr., Gorin, P.D., Brandeis, L.D., and Pearson, J. Dorsal root ganglion neurons are destroyed by exposure *in utero* to maternal antibody to nerve growth factor, *Science,* 210: 916, 1980.

109. Johnson, E.M. Jr., Taniuchi, M., Clark, H.B., Springer, J.E., Koh, S., Tayrien, M.W., and Loy, R. Demonstration of the retrograde transport of nerve growth factor receptor in the peripheral and central nervous system, *J Neurosci,* 7: 923, 1987.

110. Jones, K.R., Farinas, I., Backus, C., and Reichardt, L.F. Targeted disruption of the BDNF gene perturbs brain and sensory neuron development but not motor neuron development, *Cell,* 76: 989, 1994.

111. Kaiser, P.K. and Lipton, S.A. VIP-mediated increase in cAMP prevents tetrodotoxin-induced retinal ganglion cell death *in vitro*, *Neuron,* 5: 373, 1990.

112. Kashiba, H., Uchida, Y., and Senba, E. Distribution and colocalization of NGF and GDNF family ligand receptor mRNAs in dorsal root and nodose ganglion neurons of adult rats, *Mol Brain Res,* 110: 52, 2003.

113. Katoh-Semba, R., Kaisho, Y., Shintani, A., Nagahama, M., and Kato, K. Tissue distribution and immunocytochemical localization of neurotrophin-3 in the brain and peripheral tissues of rats, *J Neurochem,* 66: 330, 1996.

114. Katz, D.M. A catecholaminergic sensory neuron phenotype in cranial derivatives of the neural crest: regulation by cell aggregation and nerve growth factor, *J Neurosci,* 11: 3991, 1991.

115. Katz, D.M., Adler, J.E., and Black, I.B. Expression and regulation of tyrosine hydroxylase in adult sensory neurons in culture: effects of elevated potassium and nerve growth factor, *Brain Res,* 385: 68, 1986.

116. Katz, D.M. and Black, I.B. Expression and regulation of catecholaminergic traits in primary sensory neurons: relationship to target innervation *in vivo*, *J Neurosci,* 6: 983, 1986.

117. Katz, D.M., Erb, M., Lillis, R., and Neet, K. Trophic regulation of nodose ganglion cell development: evidence for an expanded role of nerve growth factor during embryogenesis in the rat, *Exp Neurol,* 110: 1, 1990.

118. Katz, D.M. and Karten, H.J. Substance P in the vagal sensory ganglia: localization in cell bodies and pericellular arborizations, *J Comp Neurol,* 193: 549, 1980.

119. Katz, D.M., Markey, K.A., Goldstein, M., and Black, I.B. Expression of catecholaminergic characteristics by primary sensory neurons in the normal adult rat *in vivo*, *Proc Natl Acad.Sci (USA),* 80: 3526, 1983.

120. Kennedy, J.M. and Zochodne, D.W. The regenerative deficit of peripheral nerves in experimental diabetes: its extent, timing and possible mechanisms, *Brain,* 123: 2118, 2000.

121. Kiss, J., Shooter, E.M., and Patel, A.J. A low-affinity nerve growth factor receptor antibody is internalized and retrogradely transported selectively into cholinergic neurons of the rat basal forebrain, *Neuroscience,* 57: 297, 1993.

122. Klein, R., Lamballe, F., Bryant, S., and Barbacid, M. The trkB tyrosine protein kinase is a receptor for neurotrophin-4, *Neuron,* 8 : 947, 1992.

123. Kniel, P.C., Junker, U., Perrin, I.V., Bestetti, G.E., and Rossi, G.L. Varied effects of experimental diabetes on the autonomic nervous system of the rat, *Lab Invest,* 54: 523, 1986.

124. Koliatsos, V.E. and Price, D.L. Retrograde axonal transport, Vol. 25. Boulton, A., Baker, G., and Hefti, F., Eds., Totowa, Humana, 1993: 247.

125. Kristensson, K., Nordborg, C., Olsson, Y., and Sourander, P. Changes in the vagus nerve in diabetes mellitus, *Acta Pathol Microbiol Scand,* 79: 684, 1971.

126. Kuruvilla, R., Ye, H., and Ginty, D.D. Spatially and functionally distinct roles of the PI3-K effector pathway during NGF signaling in sympathetic neurons, *Neuron,* 27: 499, 2000.

127. Laduron, P.M. and Janssen, P.F. Impaired axonal transport of opiate and muscarinic receptors in streptozocin-diabetic rats, *Brain Res,* 380: 359, 1986.

128. Lamb, K. and Bielefeldt, K. Rapid effects of neurotrophic factors on calcium homeostasis in rat visceral afferent neurons, *Neurosci Lett,* 336: 9, 2003.

129. Larmet, Y., Dolphin, A.C., and Davies, A.M. Intracellular calcium regulates the survival of early sensory neurons before they become dependent on neurotrophic factors, *Neuron,* 9: 563, 1992.

130. Leal-Cardoso, H., Koschorke, G.M., Taylor, G., and Weinreich, D. Electrophysiological properties and chemosensitivity of acutely isolated nodose ganglion neurons of the rabbit, *J Auton Nerv Syst,* 45: 29, 1993.

131. Ledda, F., Paratcha, G., and Ibanez, C.F. Target-derived GFRalpha1 as an attractive guidance signal for developing sensory and sympathetic axons via activation of Cdk5, *Neuron,* 36: 387, 2002.

132. Lee, P.G., Cai, F., and Helke, C.J. Streptozotocin-induced diabetes reduces retrograde axonal transport in the afferent and efferent vagus nerve, *Brain Res,* 941: 127, 2002.

133. Lee, P.G., Hohman, T.C., Cai, F., Regalia, J., and Helke, C.J. Streptozotocin-induced diabetes causes metabolic changes and alterations in neurotrophin content and retrograde transport in the cervical vagus nerve, *Exp Neurol,* 170: 149, 2001b.

134. Lee, P.G., Zhuo, H., and Helke, C.J. Axotomy alters neurotrophin and neurotrophin receptor mRNAs in the vagus nerve and nodose ganglion of the rat, *Mol Brain Res,* 87: 31, 2001a.

135. LeMaster, A.M., Krimm, R.F., Davis, B.M., Noel, T., Forbes, M.E., Johnson, J.E., and Albers, K.M. Overexpression of brain-derived neurotrophic factor enhances sensory innervation and selectively increases neuron number, *J Neurosci,* 19: 5919, 1999.

136. Liebl, D.J., Tessarollo, L., Palko, M.E., and Parada, L.F. Absence of sensory neurons before target innervation in brain-derived neurotrophic factor-, neurotrophin 3-, and TrkC-deficient embryonic mice, *J Neurosci,* 17: 9113, 1997.

137. Lindsay, R.M. Role of neurotrophins and trk receptors in the development and maintenance of sensory neurons: an overview, *Phil Trans Roy Soc Lond,* 351: 365, 1996a.

138. Lindsay, R.M. Therapeutic potential of the neurotrophins and neurotrophin-CNTF combinations in peripheral neuropathies and motor neuron diseases, *Ciba Found Symp,* 196: 39, 1996b.

139. Lindsay, R.M., Evison, C.J., and Winter, J. Culture of adult mammalian peripheral neurons, Chad, J. and Wheal, H., Eds., IRL Press, New York, 1991: 3.

140. Lindsay, R.M. and Harmer, A.J. Nerve growth factor regulates expression of neuropeptide genes in adult sensory neurons, *Nature (Lond.),* 337: 362, 1989.

141. Lindsay R.M. and Rohrer, H. Placodal sensory neurons in culture: Nodose ganglion neurons are unresponsive to NGF, lack NGF receptors but are supported by a liver-derived neurotrophic factor, *Dev Biol,* 112: 30, 1985.

142. Lindsay, R.M., Thoenen, H., and Barde, Y.A. Placode and neural crest-derived sensory neurons are responsive at early developmental stages to brain-derived neurotrophic factor, *Dev Biol,* 112: 319, 1985a.

143. Lindsay, R.M., Wiegand, S.J., Altar, C.A., and DiStefano, P.S. Neurotrophic factors: from molecule to man, *TINS,* 17: 182, 1994.

144. Liu, X., Ernfors, P., Wu, H., and Jaenisch, R. Sensory but not motor neuron deficits in mice lacking NT4 and BDNF, *Nature,* 375: 238, 1995.

145. Liu, X. and Jaenisch, R. Severe peripheral sensory neuron loss and modest motor neuron reduction in mice with combined deficiency of brain-derived neurotrophic factor, neurotrophin 3 and neurotrophin 4/5, *Dev Dyn,* 218: 94, 2000.

146. Longo, F.M., Powell, H.C., LeBeau, J., Heckman, H., and Myers, R.R. Delayed nerve regeneration in streptozotocin diabetic rats, *Muscle Nerve,* 9: 385, 1986.

147. Love, A., Cotter, M.A., and Cameron, N.E. Effects of the sulphydryl donor N-acetyl-L-cysteine on nerve conduction, perfusion, maturation and regeneration following freeze damage in diabetic rats, *Europ J Clin Invest,* 26: 698, 1996.

148. Low, P.A., Walsh, J.C., Huang, C.Y., and McLeod, J.G. The sympathetic nervous system in diabetic neuropathy. A clinical and pathological study, *Brain,* 98: 341, 1975.

149. Lumme, A., Vanhatalo, S., and Soinila, S. Axonal transport of nitric oxide synthase in autonomic nerves, *J Auto Nerv Syst,* 56: 207, 1996.

150. Lundberg, J.M., Hokfelt, T., Nilsson, G., Terenius, L., Rehfeld, J., Elde, R., and Said, S. Peptide neurons in the vagus, splanchnic and sciatic nerves, *Acta Physiol Scand,* 104: 499, 1978.

151. MacLean, D.B. Adrenocorticotropin-adrenal regulation of transported substance P in the vagus nerve of the rat, *Endocrinology,* 121: 1540, 1987.

152. MacLean, D.B. Substance P and somatostatin content and transport in vagus and sciatic nerves of the streptozocin-induced diabetic rat, *Diabetes,* 36: 390, 1987.

153. MacLean, D.B., Bennett, B., Morris, M., and Wheeler, F.B. Differential regulation of calcitonin gene-related peptide and substance P in cultured neonatal rat vagal sensory neurons, *Brain Res,* 478: 349, 1989.

154. MacLean, D.B., Hayes, L., and Sasken, H. *In situ* hybridization of preprotachykinin mRNA in cultured vagal sensory neurons. The effect of nerve growth factor, *Ann NY Acad Sci,* 632: 229, 1991.

155. MacLean, D.B., Lewis, S.F., and Wheeler, F.B. Substance P content in cultured neonatal rat vagal sensory neurons: the effect of nerve growth factor, *Brain Res,* 457: 53, 1988.

156. MacLean, D.B., Wheeler, F., and Hayes, L. Basal and stimulated release of substance P from dissociated cultures of vagal sensory neurons, *Brain Res,* 519: 308, 1990.

157. Maeda, C.Y., Fernandes, T.G., Timm, H.B., and Irigoyen, M.C. Autonomic dysfunction in short-term experimental diabetes, *Hypertension,* 26: 1100, 1995.

158. Magnusson, S., Alm, P., and Kanje, M. Inducible nitric oxide synthase increases in regenerating rat ganglia, *Neuroreport,* 7 : 2046, 1996.

159. Mahadeo, D., Kaplan, L., Chao, M.V., and Hempstead, B.L. High affinity nerve growth factor binding displays a faster rate of association than p140trk binding. Implications for multi-subunit polypeptide receptors, *J Biol Chem,* 269: 6884, 1994.

160. Maisonpierre, P.C., Belluscio, L., Friedman, B., Alderson, R.F., Wiegand, S.J., Furth, M.E., Lindsay, R.M., and Yancopoulos, G.D. NT-3, BDNF, and NGF in the developing rat nervous system: parallel as well as reciprocal patterns of expression, *Neuron,* 5: 501, 1990.

161. Maness, L.M., Kastin, A.J., Weber, J.T., Banks, W.A., Backman, B.S., and Zadina, J.E. The neurotrophins and their receptors: structure, function, and neuropathology, *Neurosci Biobehav Rev,* 18: 143, 1994.

162. Manthorpe, M., Barbin, G., and Varon, S. Isoelectric focusing of the chick eye ciliary neurotrophic factor, *J Neurosci Res,* 8: 233, 1982.

163. Mantyh, P.W. and Hunt, S.P. Neuropeptides are present in projection neurones at all levels in visceral and taste pathways: from periphery to sensory cortex, *Brain Res,* 299: 297, 1984.

164. McCubbin, J.W. and Ferrario, C.M. Baroreceptor reflexes and hypertension, Genest, J. et al., Eds., McGraw Hill, New York, 1977: 128.

165. McDougall, A.J. and McLeod, J.G. Autonomic neuropathy, I: Clinical features, investigation, pathophysiology, and treatment, *J Neurol Sci,* 137: 79, 1996.

166. McDougall, A.J. and McLeod, J.G. Autonomic neuropathy, II: Specific neuropathies, *J Neurol Sci,* 138: 1, 1996.

167. McEwen, T.A. and Sima, A.A. Autonomic neuropathy in BB rat. Assessment by improved method for measuring heart-rate variability, *Diabetes,* 36: 251, 1987.

168. Melino, G., Catani, M.V., Corazzari, M., Guerrieri, P., and Bernassola, F. Nitric oxide can inhibit apoptosis or switch it into necrosis, *Cell Mol Life Sci,* 57: 612, 2000.

169. Michael, G.J. and Priestley, J.V. Differential expression of the mRNA for the vanilloid receptor subtype 1 in cells of the adult rat dorsal root and nodose ganglia and its downregulation by axotomy, *J Neurosci,* 19: 1844, 1999.

170. Middleton, G., Hamanoue, M., Enokido, Y., Wyatt, S., Pennica, D., Jaffray, E., Hay, R.T., and Davies, A.M. Cytokine-induced nuclear factor kappa B activation promotes the survival of developing neurons, *J Cell Biol,* 148: 325, 2000.

171. Middleton, G., Wyatt, S., Ninkina, N., and Davies, A.M. Reciprocal developmental changes in the roles of Bcl-w and Bcl-x(L) in regulating sensory neuron survival, *Development,* 128: 447, 2001.

172. Mirsky, R., Jessen, K.R., Schachner, M., and Goridis, C. Distribution of the adhesion molecules N-CAM and L1 on peripheral neurons and glia in adult rats, *J Neurocytol,* 15: 799, 1986.

173. Molliver, D.C., Radeke, M.J., Feinstein, S.C., and Snider, W.D. Presence or absence of TrkA protein distinguishes subsets of small sensory neurons with unique cytochemical characteristics and dorsal horn projections, *J Comp Neurol,* 361: 404, 1995.

174. Moore, M.W., Klein, R.D., Farinas, I., Sauer, H., Armanini, M., Phillips, H., Reichardt, L.F., Ryan, A.M., Carver-Moore, K., and Rosenthal, A. Renal and neuronal abnormalities in mice lacking GDNF, *Nature,* 382: 76, 1996.

175. Mulderry, P.K. Neuropeptide expression by newborn and adult rat sensory neurons in culture: effects of nerve growth factor and other neurotrophic factors, *Neuroscience,* 59: 673, 1994.

176. Myers, A.C., Kajekar, R., and Undem, B.J. Allergic inflammation-induced neuropeptide production in rapidly adapting afferent nerves in guinea pig airways, *Am J Physiol,* 282: L775, 2002.

177. Namikawa, K., Honma, M., Abe, K., Takeda, M., Mansur, K., Obata, T., Miwa, A., Okado, H., and Kiyama, H. Akt/protein kinase B prevents injury-induced motoneuron death and accelerates axonal regeneration, *J Neurosci,* 20: 2875, 2000.

178. Neil, H.A.W. The epidemiology of diabetic autonomic neuropathy, in *Autonomic Failure,* Bannister, R. and Mathias, C.J., Eds., Oxford University Press, New York, 1992: 682.

179. Nishino, J., Mochida, K., Ohfuji, Y., Shimazaki, T., Meno, C., Ohishi, S., Matsuda, Y., Fujii, H., Saijoh, Y., and Hamada, H. GFR alpha3, a component of the artemin receptor, is required for migration and survival of the superior cervical ganglion, *Neuron,* 23: 725, 1999.

180. Niwa, H., Hayakawa, K., Yamamoto, M., Itoh, T., Mitsuma, T., and Sobue, G. Differential age-dependent trophic responses of nodose, sensory, and sympathetic neurons to neurotrophins and GDNF: potencies for neurite extension in explant culture, *Neurochem Res,* 27: 485, 2002.

181. Nosrat, C.A., Tomac, A., Lindqvist, E., Lindskog, S., Humpel, C., Stromberg, I., Ebendal, T., Hoffer, B.J., and Olson, L. Cellular expression of GDNF mRNA suggests multiple functions inside and outside the nervous system, *Cell Tissue Res,* 286: 191, 1996.

182. Nozaki, K., Moskowitz, M.A., Maynard, K.I., Koketsu, N., Dawson, T.M., Bredt, D.S., and Snyder, S.H. Possible origins and distribution of immunoreactive nitric oxide synthase-containing nerve fibers in cerebral arteries, *J Cereb Blood Flow Metab,* 13: 70, 1993.

183. Olsson, Y., and Sjostrand, J. Origin of macrophages in Wallerian degeneration of peripheral nerves demonstrated autoradiographically, *Exp Neurol,* 23: 102, 1969.

184. Oppenheim, R.W., Prevette, D., Qin-Wei, Y., Collins, F., and MacDonald, J. Control of embryonic motoneuron survival *in vivo* by ciliary neurotrophic factor, *Science,* 251: 1616, 1991.

185. Orchard, T.J., LLoyd, C.E., Maser, R.E., and Kuller, L.H. Why does diabetic autonomic neuropathy predict IDDM mortality? An analysis from the Pittsburgh Epidemiology of Diabetes Complications Study, *Diabetes Res Clin Pract,* 34 Suppl:S165-171: 1996.

186. Pearson, J., Johnson, E.M., and Brandeis, L. Effects of antibodies to nerve growth factor on intrauterine development of derivatives of cranial neural crest and placode in the guinea pig, *Dev Biol,* 96: 32, 1983.

187. Perry, V.H., Brown, M.C., and Gordon, S. The macrophage response to central and peripheral nerve injury. A possible role for macrophages in regeneration, *J Exp Med,* 165: 1218, 1987.

188. Prechtl, J.C. and Powley, T.L. The fiber composition of the abdominal vagus of the rat, *Anat Embryol,* 181: 101, 1990.

189. Purewal, T.S. and Watkins, P.J. Postural hypotension in diabetic autonomic neuropathy: a review, *Diabetic Medicine,* 12: 192, 1995.

190. Qiu, L., Bernd, P., and Fukada, K. Cholinergic neuronal differentiation factor (CDF)/leukemia inhibitory factor (LIF) binds to specific regions of the developing nervous system *in vivo*, *Dev Biol,* 163: 516, 1994.

191. Raab, M., Worl, J., Brehmer, A., and Neuhuber, W.L. Reduction of NT-3 or TrkC results in fewer putative vagal mechanoreceptors in the mouse esophagus, *Auton Neurosci,* 108: 22, 2003.

192. Regalia, J., Cai, F., and Helke, C. Streptozotocin-induced diabetes and the neurochemistry of vagal afferent neurons, *Brain Res,* 938: 7, 2002.

193. Reimer, M. and Kanje, M. Peripheral but not central axotomy promotes axonal outgrowth and induces alterations in neuropeptide synthesis in the nodose ganglion of the rat, *Eur J Neurosci,* 11: 3415, 1999.

194. Reimer, M., Moller, K., Sundler, F., Hannibal, J., Fahrenkrug, J., and Kanje, M. Increased expression, axonal transport and release of pituitary adenylate cyclase-activating polypeptide in the cultured rat vagus nerve, *Neuroscience,* 88: 213, 1999.

195. Reynolds, A.J., Bartlett, S.E., and Hendry, I.A. Molecular mechanisms regulating the retrograde axonal transport of neurotrophins, *Brain Res Rev,* 33: 169, 2000.

196. Riccio, A., Pierchala, B.A., Ciarallo, C.L., and Ginty, D.D. An NGF-TrkA-mediated retrograde signal to transcription factor CREB in sympathetic neurons, *Science,* 277: 1097, 1997.

197. Robinson, M., Adu, J., and Davies, A.M. Timing and regulation of trkB and BDNF mRNA expression in placode-derived sensory neurons and their targets, *Europ J Neurosci,* 8: 2399, 1996.

198. Rossi, J., Luukko, K., Poteryaev, D., Laurikainen, A., Sun, Y.F., Laakso, T., Eerikainen, S., Tuominen, R., Lakso, M., Rauvala, H., Arumae, U., Pasternack, M., Saarma, M., and Airaksinen, M.S. Retarded growth and deficits in the enteric and parasympathetic nervous system in mice lacking GFR alpha2, a functional neurturin receptor, *Neuron,* 22: 243, 1999.

199. Rudge, J.S., Alderson, R.F., Pasnikowski, E., McClain, J., Ip, N.Y., and Lindsay, R.M. Expression of ciliary neurotrophic factor and the neurotrophins-nerve growth factor, brain-derived neurotrophic factor and neurotrophin–3 in cultured rat hippocampal astrocytes, *Eur J Neurosci,* 4: 459, 1992.

200. Rush, R.A., Mayo, R., and Zettler, C. The regulation of nerve growth factor synthesis and delivery to peripheral neurons, *Pharmacol Ther,* 65: 93, 1995.

201. Russell, J.W. and Feldman, E.L. Insulin-like growth factor-I prevents apoptosis in sympathetic neurons exposed to high glucose, *Horm Metab Res,* 31: 90, 1999.

202. Russell, J.W., Sullivan, K.A., Windebank, A.J., Herrmann, D.N., and Feldman, E.L. Neurons undergo apoptosis in animal and cell culture models of diabetes, *Neurobiol Dis,* 6: 347, 1999.

203. Ryden, M., Murrayrust, J., Glass, D., Ilag, L.L., Trupp, M., Yancopoulos, G.D., McDonald, N.Q., and Ibanez, C.F. Functional Analysis of mutant neurotrophins deficient in low affinity binding reveals a role for p75 (LNGFR) in NT-4 signaling, *EMBO J,* 14: 1979, 1995.

204. Sango, K., Verdes, J.M., Hikawa, N., Horie, H., Tanaka, S., Inoue, S., Sotelo, J.R., and Takenaka, T. Nerve growth factor (NGF) restores depletions of calcitonin gene-related peptide and substance P in sensory neurons from diabetic mice in vitro, *J Neurol Sci,* 126: 1, 1994.

205. Schmidt, R.E., Dorsey, D.A., Roth, K.A., Parvin, C.A., Hounsom, L., and Tomlinson, D.R. Effect of streptozotocin-induced diabetes on NGF, P75(NTR) and TrkA content of prevertebral and paravertebral rat sympathetic ganglia, *Brain Res,* 867: 149, 2000.

206. Schmidt, R.E., Plurad, S.B., Saffitz, J.E., Grabau, G.G., and Yip, H.K. Retrograde axonal transport of 125I-nerve growth factor in rat ileal mesenteric nerves. Effect of streptozocin diabetes., *Diabetes,* 34: 1230, 1985.

207. Schmidt, Y., Unger, J.W., Bartke, I., and Reiter, R. Effect of nerve growth factor on peptide neurons in dorsal root ganglia after taxol or cisplatin treatment and in diabetic (db/db) mice, *Exp Neurol,* 132: 16, 1995.

208. Sharpey-Schafer, E.P. and Taylor, P.J. Absent circulatory reflexes in diabetic neuritis, *Lancet,* 12: 331, 1960.

209. Shehab, S.A.S. and Atkinson, M.E. Vasoactive intestinal peptide (VIP) increases in the spinal cord after peripheral axotomy of the sciatic nerve originate from the primary afferent neurons, *Brain Res,* 372: 37, 1986.

210. Sherer, T.B., Neff, P.S., and Tuttle, J.B. Increased nerve growth factor mRNA stability may underlie elevated nerve growth factor secretion from hypertensive vascular smooth muscle cells, *Mol Brain Res,* 62: 167, 1998.

211. Shibuya, Y., Mizoguchi, A., Takeichi, M., Shimada, K., and Ide, C. Localization of N-cadherin in the normal and regenerating nerve fibers of the chicken peripheral nervous system, *Neuroscience,* 67: 253, 1995.

212. Smith, G.M., Hale, J., Pasnikowski, E.M., Lindsay, R.M., Wong, V., and Rudge, J.S. Astrocytes infected with replication-defective adenovirus containing a secreted form of CNTF or NT3 show enhanced support of neuronal populations in vitro, *Exp Neurol,* 139: 156, 1996.

213. Snider, W.D. Functions of the neurotrophins during nervous system development: what the knockouts are teaching us, *Cell,* 77: 627, 1994.

214. Springer, J.E., Mu, X., Bergmann, L.W., and Trojanowski, J.Q. Expression of GDNF mRNA in rat and human nerve tissue, *Exp Neurol,* 127: 167, 1994.

215. Squinto, S.P., Stitt, T.N., Aldrich, T.H., Davis, S., Biano, S.M., Radziejewski, C., Glass, D.J., Masiakowski, P., Furth, M.E., Valenzuela, D.M., and DiStefano, P.S.a.Y.G.D. trkB encodes a functional receptor for brain-derived neurotrophic factor and neurotrophin-3 but not nerve growth factor, *Cell,* 65: 885, 1991.

216. Srinivasan, S., Stevens, M., and Wiley, J.W. Diabetic peripheral neuropathy: evidence for apoptosis and associated mitochondrial dysfunction, *Diabetes,* 49: 1932, 2000.

217. Suter-Crazzolara, C. and Unsicker, K. GDNF is expressed in two forms in many tissues outside the CNS, *Neuroreport,* 5: 2486, 1994.

218. Taniuchi, M., Clark, H.B., and Johnson, E.M. Jr. Induction of nerve growth factor receptor in Schwann cells after axotomy, *Proc Natl Acad Sci U.S.A.,* 83: 4094, 1986.

219. Taniuchi, M., Clark, H.B., Schweitzer, J.B., and Johnson, E.M. Jr. Expression of nerve growth factor receptors by Schwann cells of axotomized peripheral nerves: ultrastructural location, suppression by axonal contact, and binding properties, *J Neurosci,* 8: 664, 1988.

220. Tessler, A., Himes, B.T., Krieger, N.R., Murray, M., and Goldberger, M.E. Sciatic nerve transection produces death of dorsal root ganglion cells and reversible loss of substance P in spinal cord, *Brain Res,* 332: 209, 1985.

221. Thaler, C.D., Suhr, L., Ip, N., and Katz, D.M. Leukemia inhibitory factor and neurotrophins support overlapping populations of rat nodose sensory neurons in culture, *Dev Biol,* 161: 338, 1994.

222. Thomas, P.K. Growth factors and diabetic neuropathy, *Diabet Med,* 11: 732, 1994.

223. Thomas, P.K. and Mathias, C.J. Diseases of the ninth, tenth, eleventh, and twelfth cranial nerves, in *Peripheral Neuropathy,* 3rd edition. Dyck, P.J. and Thomas, P.D., Eds., Saunders Press, Philadelphia, 1993: 869.

224. Thomas, P.K. and Tomlinson, D.R. Diabetic and hypoglycemic neuropathy, in *Peripheral Neuropathy,* Dyck, P.J. and Thomas, P.D., Eds., Saunders, Philadelphia, 1993: 1219.

225. Timmusk, T., Belluardo, N., Metsis, M., and Persson, H. Wide-spread and developmentally regulated expression of neurotrophin-4 mRNA in rat brain and peripheral tissues, *Eur J Neurosci,* 5: 605, 1993.

226. Tomlinson, D.R., Fernyhough, P., Diemel, L., Stevens, E., and Brewster, W. Biochemical pathogenesis of diabetic neuropathy, *Diab Nutr Metab,* 7: 335, 1994.

227. Tomlinson, D.R., Fernyhough, P., and Diemel, L.T. Neurotrophins and peripheral neuropathy, *Phil Trans R Soc Lond B,* 351: 455, 1996.

228. Tomlinson, D.R., Fernyhough, P., Mohiuddin, L., Delcroix, J.D., and Malcangio, M. Neurotrophic factors — Regulation of neuronal phenotype, *Neurosci Res Commun,* 21: 57, 1997.

229. Tomlinson, D.R., Townsend, J., and Fretten, P. Prevention of defective axonal transport in streptozocin-diabetic rats by treatment with "Statil" (ICI 128436), an aldose reductase inhibitor, *Diabetes,* 34: 970, 1985.

230. Trupp, M., Ryden, M., Jornvall, H., Funakoshi, H., Timmusk, T., Arenas, E., and Ibanez, C.F. Peripheral expression and biological activities of GDNF, a new neurotrophic factor for avian and mammalian peripheral neurons, *J Cell Biol,* 130: 137, 1995.

231. Verge, V.M.K., Merlio, J.-P., Grondin, J., Ernfors, P., Persson, H., Riopelle, R.J., Hokfelt, T., and Richardson, P.M. Colocalization of NGF binding sites, trk mRNA, and low-affinity NGF receptor mRNA in primary sensory neurons: responses to injury and infusion of NGF, *J Neurosci,* 12: 4011, 1992.

232. Verge, V.M.K., Xu, Z., Xu, X.J., Wiesenfeld-Hallin, Z., and Hokfelt, T. Marked increase in nitric oxide synthase mRNA in rat dorsal root ganglia after peripheral axotomy: *in situ* hybridization and functional studies, *Proc Natl Acad Sci (USA),* 89: 11617, 1992.

233. Vinik, A.I., Holland, M.T., Le Beau, J.M., Liuzzi, F.J., Stansberry, K.B., and Colen, L.B. Diabetic neuropathies, *Diabetes Care,* 15: 1926, 1992.

234. Vinik, A.I. and Milicevic, Z. Recent advances in the diagnosis and treatment of diabetic neuropathy, *The Endocrinologist,* 6: 443, 1996.

235. Virdee, K., Xue, L., Hemmings, B.A., Goemans, C., Heumann, R., and Tolkovsky, A.M. Nerve growth factor-induced PKB/Akt activity is sustained by phosphoinositide 3-kinase dependent and independent signals in sympathetic neurons, *Brain Res,* 837: 127, 1999.

236. Vizzard, M.A., Erdman, S.L., and De Groat, W.C. Increased expression of neuronal nitric oxide synthase (NOS) in visceral neurons after nerve injury, *J Neurosci,* 15: 4033, 1995.

237. Vogel, K.S. and Davies, A.M. The duration of neurotrophic factor independence in early sensory neurons is matched to the time course of target field innervation, *Neuron,* 7: 819, 1991.

238. Vogel, K.S., El-Afandi, M., and Parada, L.F. Neurofibromin negatively regulates neurotrophin signaling through p21ras in embryonic sensory neurons, *Mol Cell Neurosci,* 15: 398, 2000.

239. Wagey, R., Lurot, S., Perrelet, D., Pelech, S.L., Sagot, Y., and Krieger, C. Phosphatidylinositol 3-kinase activity in murine motoneuron disease: the progressive motor neuropathy mouse, *Neuroscience,* 103: 257, 2001.

240. Wang, X.-Y., Wong, W.-C., and Ling, E.-A. NADPH-diaphorase activity in the nodose ganglion of normal and vagotomized guinea-pigs, *Cell Tissue Res,* 285: 141, 1996.

241. Weil-Fugazza, J., Onteniente, B., Audet, G., and Philippe, E. Dopamine as trace amine in the dorsal root ganglia, *Neurochem Res,* 18: 965, 1993.

242. Weinstein, D. The role of Schwann cells in neural regeneration, *Neuroscientist,* 5: 208, 1999.

243. Wetmore, C. and Olson, L. Neuronal and nonneuronal expression of neurotrophins and their receptors in sensory and sympathetic ganglia suggest new intercellular trophic interactions, *J Comp Neurol,* 353: 143, 1995.

244. Whitworth, I.H., Terenghi, G., Green, C.J., Brown, R.A., Stevens, E., and Tomlinson, D.R. Targeted delivery of nerve growth factor via fibronectin conduits assists nerve regeneration in control and diabetic rats, *Eur J Neurosci,* 7: 2220, 1995.

245. Wiklund, P. and Ekstrom, P.A. Axonal outgrowth from adult mouse nodose ganglia *in vitro* is stimulated by neurotrophin-4 in a Trk receptor and mitogen-activated protein kinase-dependent way, *J Neurobiol,* 45: 142, 2000.

246. Williams, R., Backstrom, A., Ebendal, T., and Hallbook Molecular cloning and cellular localization of trkC in the chicken embryo, *Dev Brain Res,* 75: 235, 1993.

247. Yagihashi, S. and Sima, A.A. Diabetic autonomic neuropathy in BB rat. Ultrastructural and morphometric changes in parasympathetic nerves., *Diabetes,* 35: 733, 1986.

248. Zhang, W.X., Chakrabarti, S., Greene, D.A., and Sima, A.A. Diabetic autonomic neuropathy in BB rats and effect of ARI treatment on heart-rate variability and vagus nerve structure, *Diabetes,* 39: 613, 1990.

249. Zhang, X., Ji, R.R., Arvidsson, J., Lundberg, J.M., Bartfai, T., Bedecs, K., and Hokfelt, T. Expression of peptides, nitric oxide synthase and NPY receptor in trigeminal and nodose ganglia after nerve lesions, *Exp Brain Res,* 111: 393, 1996.

250. Zhou, X.F, Deng, Y.S., Chie, E., Xue, Q., Zhong, J.H., Mclachlan, E.M., Rush, R.A., and Xian, C.J. Satellite-cell-derived nerve growth factor and neurotrophin-3 are involved in noradrenergic sprouting in the dorsal root ganglia following peripheral nerve injury in the rat, *Eur J Neurosci,* 11: 1711, 1999.

251. Zhou, X.-F. and Rush, R.A. Peripheral projections of rat primary sensory neurons immunoreactive for neurotrophin 3, *J Comp Neurol,* 363: 69, 1995.

252. Zhuo, H. and Helke, C.J. Presence and localization of neurotrophin receptor tyrosine kinase (TrkA, TrkB, TrkC) mRNAs in visceral afferent neurons of the nodose and petrosal ganglia, *Mol Brain Res,* 38: 63, 1996.

253. Zhuo, H., Ichikawa, H., and Helke, C.J. Neurochemistry of the nodose ganglion, *Prog Neurobiol,* 52: 79, 1997.

254. Zhuo, H., Lewin, A.C., Phillips, E.T., Sinclair, C., and Helke, C.J. Inhibition of the axoplasmic transport in the vagus nerve alters the numbers of neuropeptide and tyrosine hydroxylase mRNA-containing and immunoreactive visceral afferent neurons of the nodose ganglion, *Neuroscience,* 66: 175, 1995.

255. Zhuo, H., Sinclair, C., and Helke, C.J. Plasticity of tyrosine hydroxylase and vasoactive intestinal peptide mRNAs in visceral afferent neurons of the nodose ganglion upon axotomy-induced deafferentation, *Neuroscience,* 63: 617, 1994.

256. Ziegler, D. Diabetic cardiovascular autonomic neuropathy: prognosis, diagnosis and treatment, *Diabetes Metab Rev,* 10: 339, 1994.

257. Ziegler, D., Dannehl, K., Muhlen, H., Spuler, M., and Gries, F.A. Prevalence of cardiovascular autonomic dysfunction assessed by spectral analysis, vector analysis, and standard tests of heart rate variation and blood pressure responses at various stages of diabetic neuropathy, *Diabet Med,* 9: 806, 1992.

258. Zucker, I.H. and Gilmore, J.P. Atrial receptor modulation of renal function in heart failure, in *Disturbances in Neurogenic Control of the Circulation,* Abboud, F.M., Fozzard, H.A., Gilmore, J.P., and Reis, D.J., Eds., Am. Physiol. Soc., Bethesda, 1981: 1.

Part II

Vagal Sensory Ganglion Neurons

3 Voltage-Gated Ion Channels in Vagal Afferent Neurons

J.H. Schild, K.D. Alfrey, and B.Y. Li

CONTENTS

3.1 INTRODUCTION

Numerous cellular and subcellular mechanisms contribute to the overall excitability of vagal afferent neurons. Those that alter the electrical state of charge across the plasma membrane can be broadly classified as either being functionally dependent upon transmembrane voltage or not. This chapter focuses upon the superfamily of voltage-gated ion channels expressed in the somata of vagal afferent neurons. Of particular interest here are the functional properties of the whole-cell currents that play a major role in setting the resting membrane potential, threshold for action

potential discharge, and voltage trajectory over the upstroke, downstroke, and initial afterhyperpolarization of the somatic action potential waveform.

Voltage-gated ion channels (VGC) are complex protein assemblies that function as specialized transmembrane conduits for ions flowing along a concentration gradient. Electrophysiological analyses of single VGC have demonstrated that these most often operate as unitary conductances, rapidly switching between a closed and open state in a voltage- and time-dependent manner. Underlying this bimodal transition in channel conductance are multiple molecular configurations of the protein complex most often described as nonconducting substates. The time a VGC spends occupying particular substates and the manner in which the transition or "gating" between these substates occurs can be influenced by a great many factors.[1] However, only when the VGC occupies a final open state will ions flow along the concentration gradient. This redistribution of ionic charge imparts a change in transmembrane potential, which, in turn, further influences the gating properties of the VGC. The net effect of a large population of these VGC is often described in terms of a single, whole-cell Na^+, K^+, or Ca^{+2} ion current or, in a few cases, as a mixed cation current such as with the family of hyperpolarization activated, cyclic nucleotide-gated cation channels (HCN). The whole-cell current may or may not be comprised of multiple current components arising from a superfamily of molecularly distinct VGC termed $Na_v X.Y$, $K_v X.Y$, and $Ca_v X.Y$, in which X and Y are integer classifiers for separate channel subtypes. (See the IUPHAR ion channel compendium at http://www.iuphar-db.org/iuphar-ic/ for an excellent summary) Another family of transmembrane proteins that can rapidly influence membrane excitability is ionic transporters such as the NaK and Ca^{2+} ATPases, Na^+-Ca^{2+} exchangers, and other mechanisms associated with ionic homeostasis. The net effect of a large population of these transporters is also most often described in terms of a single, whole-cell current. However, over the span of physiological membrane potentials associated with mammalian sensory neuron discharge (i.e., –90 to +60 mV), the amplitudes of these transmembrane currents are primarily dependent upon ionic concentration gradients across the cell membrane and are several orders of magnitude smaller than the peak, whole-cell currents arising from VGC over the course of action potential discharge.[2] Similar considerations exist for other classes of whole-cell currents arising from transient receptor potential (TRP), cyclic nucleotide-gated (CNG), and mixed classes of inward rectifier ($K_{IR}X.Y$ and $K_{2P}X.Y$) cation channels. Many of these are markedly influenced by transmembrane and subcellular signaling pathways and are most often associated with long-term modulation of neuronal excitability, especially when considering subthreshold membrane potentials.

Vagal afferent neurons are quiescent until depolarizing events drive membrane potential toward the threshold for action potential discharge. Once achieved, the neuron sequences through a stereotypical trajectory of membrane voltage that is delineated by a rapidly depolarizing upstroke, a slower repolarizing downstroke, and an afterhyperpolarization in membrane potential that is generally several times longer than the duration of the action potential waveform. This review will focus on those voltage-dependent Na^+, Ca^{+2}, or K^+ ionic currents that dominate the total transmembrane current over the time course immediately leading up to and for a few hundred milliseconds following a somatic action potential waveform. As there is no evidence

for any differences in the voltage- and time-dependent properties of ion channels expressed in myelinated or unmyelinated vagal afferents the data will be presented without regard to fiber type.

3.2 VOLTAGE-GATED SODIUM ION CHANNELS

To date, only four isoforms of the voltage-gated sodium ion channel family ($Na_v1.6$, $Na_v1.7$, $Na_v1.8$, and $Na_v1.9$) have been found in the peripheral nervous system.[3] Of these, the tetrodotoxin (TTX) sensitive $Na_v1.7$ and the TTX resistive $Na_v1.8$ are the most likely candidates expressed in vagal afferent neurons.[4] The $Na_v1.7$ whole-cell Na^+ current can be blocked by low nanomolar concentrations of TTX (TTX-sensitive, TTXS), while $Na_v1.8$ whole-cell current is unaffected by high micromolar concentrations of TTX (TTX-resistant, TTXR). Cellular observations suggest these two classes of Na_v are expressed at high densities (>100 channels/μm^2) in the nodose ganglia and are well suited for supplying the regenerative current flux necessary for the neural encoding of sustained physiological stimuli as repetitive patterns of action potential discharge.[5–9] Voltage and current clamp studies have also demonstrated that Na_v have the capacity to contribute much more to the dynamic neural encoding properties of vagal sensory afferents than simply helping to establish the number of action potentials produced per unit of physiological stimulation.[2,7,9–15]

3.2.1 TTX-Sensitive Na_v

Under voltage clamp conditions suitable for isolation of the whole-cell Na^+ current, rat nodose neurons exhibit an inward current transient that is reversibly blocked by submicromolar concentrations of TTX (I_{TTXS}). Under conditions of voltage clamp the I_{TTXS} has dynamic features that are typical of the large and fast TTXS inward Na^+ currents observed in other sensory neuron preparations. (Figure 3.1).[6,7,16–18] Numerical analysis of the current records reveals activation and inactivation kinetics that are typical of the voltage- and time-dependent properties of this current (Figure 3.2). Rapid activation begins as membrane potentials approach approximately -50 mV, with the amplitude of the current being highly dependent upon the rate of membrane depolarization relative to the magnitude of the inactivation time constants at that potential (see Section 3.5). Above approximately –10 mV the current follows an ohmic reduction in peak magnitude suggesting full availability of TTXS Na_v beyond this potential. The transmembrane voltage required for activation of one-half of the available population of TTXS Na_v ($V_{1/2}$) is in the range of approximately −40 to −30 mV, while the $V_{1/2}$ range for inactivation covers approximately −75 to −65 mV. At these respective half-activation potentials an analysis of chord conductance using a Boltzmann function reveals e-slope factors ($S_{1/2}$) in the range of −7 for activation and 6 for inactivation. The voltage-dependent profile of steady-state activation and inactivation of the available population of TTXS Na_v reveals a small Na^+ activation window (note arrow, Figure 3.2). The time-dependent profile of the whole-cell current shows time constants of activation (τ_m) and inactivation (τ_h) that are markedly voltage dependent and well below 10 msec for membrane potentials typical of somatic action potentials. Furthermore, under conditions of voltage clamp,
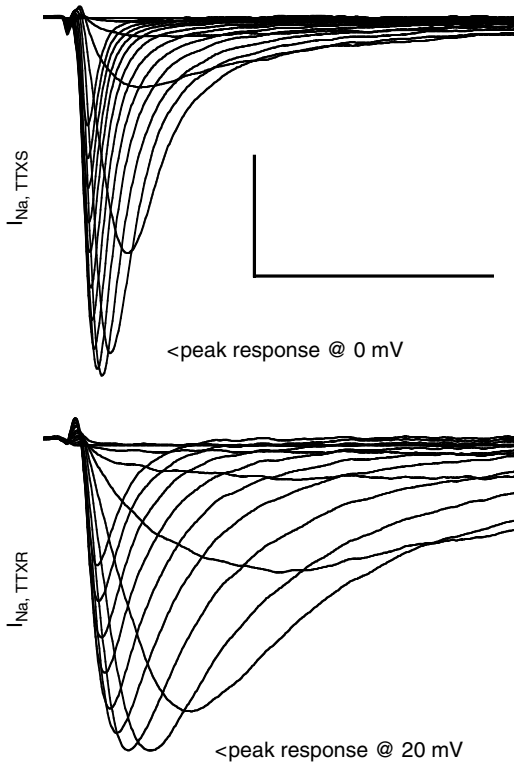
FIGURE 3.1 Two components of the whole cell Na^+ current in rat nodose neurons. The upper voltage clamp traces represent that component of the whole cell Na^+ current (I_{Na}) that is sensitive to submicromolar concentrations of tetrodotoxin (n.b. subtracted traces). The I_{TTXS} begins activation as membrane potentials approach -40 mV. Rapid inactivation follows a peak response, which generally occurs within a few milliseconds of the voltage clamp step. The lower voltage clamp traces represent that component of the I_{Na}, which remains in the presence of 10 μM tetrodotoxin. Here, membrane potentials must approach -20 mV to activate I_{TTXR}. While activation rates are comparable to those of I_{TTXS}, the I_{TTXR} rate of inactivation is markedly slower. Recording protocol consisted of 40 msec voltage steps from a holding potential of -90 mV, 5 mV increments up to 35 mV with an interstep interval of 3 sec. Solutions consisted of $[Na^+]_i = 7$ mM and $[Na^+]_o = 50$ mM. See Schild and Kunze[7] for complete details concerning the electrophysiological methods. The vertical scale bar is 1 nA for the TTXS and 0.5 nA for the TTXR Na^+ current records, respectively. The horizontal scale bar is 10 msec for both current recordings.

two pulse protocols have demonstrated that I_{TTXS} recovers from inactivation rather slowly, requiring more than 100 msec to return within 70 to 80% of control magnitudes, as is the case in dorsal root ganglion neurons.[7,18]

3.2.2 TTX-Resistant Na$_v$

In the presence of micromolar concentrations of TTX approximately 70 to 80% of adult vagal afferent neurons exhibit a large inward whole-cell Na^+ current (I_{TTXR})
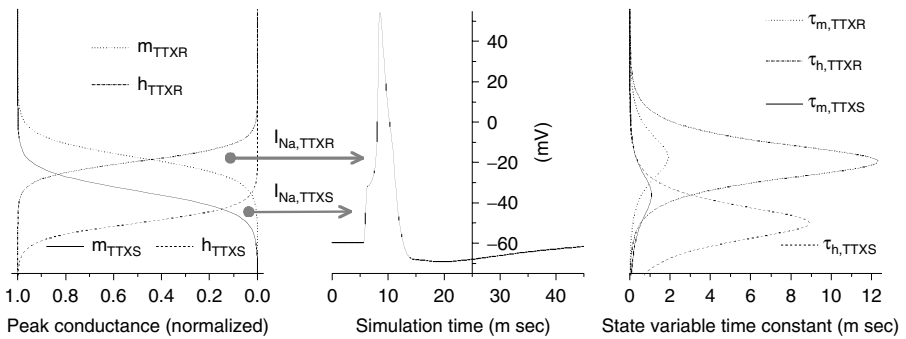
FIGURE 3.2 Voltage- and time-dependent channel gating for I_{TTXS} and I_{TTXR}. (Left) Hodgkin and Huxley (1952) ion channel gating variables can be derived from the voltage- and time-dependent activation and inactivation characteristics of I_{TTXS} and I_{TTXR}. Steady-state profiles of the (activation, inactivation) gating variables for I_{TTXS} (m_{TTXS}, h_{TTXS}) and I_{TTXR} (m_{TTXR}, h_{TTXR}) can reveal the region of the action potential waveform over which each inward current begins to contribute to membrane depolarization. Of particular importance are the "window currents" that result from an overlap in the voltage-dependent profiles of the activation and inactivation gating variables (i.e., the shaded arrows, see text). (Right) An examination of the voltage-dependent time constants (τ) for these gating variables provides insight into how quickly individual gating variables can respond to changes in membrane potential. (Center) C-type action potential waveform produced by a computational model utilizing the voltage-dependent gating variables and time constants presented in Figure 3.2, Figure 3.4, and Figure 3.6, a Hodgkin–Huxley model of the BK-type $I_{K,Ca}$ in Figure 3.7 and other currents as described in Schild et al.[2]

transient that is reversibly blocked by metals such as zinc, cadmium and cobalt.[5] The whole-cell I_{TTXR} has dynamic features that are typical of the slower inactivating TTXR Na^+ currents observed in other sensory neuron preparations (Figure 3.3).[17–19] Numerical analysis of the current records reveals activation and inactivation kinetics that are typical of the voltage- and time-dependent properties of this current (Figure 3.2). Rapid activation does not begin until membrane potentials approach approximately −30 mV. Above approximately 10 mV the current follows an ohmic reduction in peak magnitude suggesting full availability of TTXR Na_v beyond this potential. The $V_{1/2}$ of activation for the TTXR Na_v is in the range of approximately −15 to −5 mV, while the $V_{1/2}$ for inactivation ranges from approximately −35 to −25 mV. At this respective $V_{1/2}$ an analysis of chord conductance using a Boltzmann function reveals $S_{1/2}$ factors in the range of −5 for activation and 5 for inactivation. These modest slope factors coupled with the rather depolarized steady-state activation and inactivation profiles for I_{TTXR} result in a surprisingly large 40 mV Na^+ current activation window that is centered on a membrane potential of approximately −20 mV (note arrow, Figure 3.2). The voltage-dependent profile and magnitude of the τ_m and τ_h for I_{TTXR} are comparable to those of I_{TTXS}. However, because the peak values are 30 to 40 mV more depolarized than those for I_{TTXS}, over membrane potentials typical of somatic action potentials the activation rates for I_{TTXR} are moderately slower, but the inactivation rates are four to six times slower than those for I_{TTXS} (Figure 3.2). Interestingly, results of two pulse protocols demonstrate that
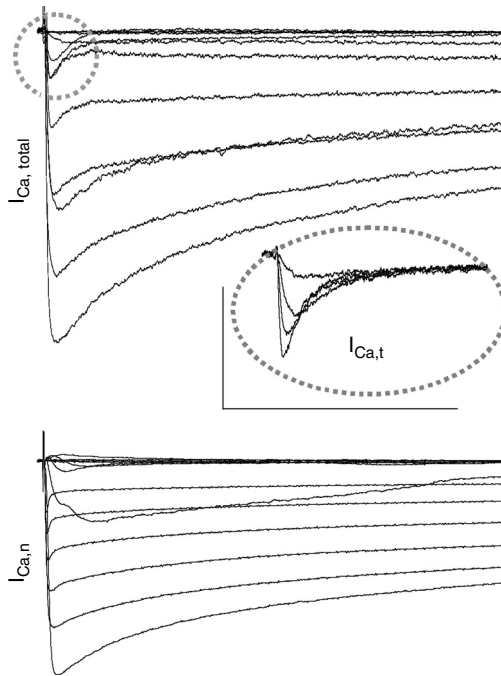
**FIGURE 3.3** The N- and T-type whole-cell Ca^{+2} currents in rat nodose neurons. The upper voltage clamp traces present the whole cell Ca^{+2} current ($I_{Ca,total}$), which presents distinct current components with either low-voltage or high-voltage activation thresholds. As membrane potentials approach -70 mV, a transient inward Ca^{+2} current ($I_{Ca,t}$) is observed with characteristics typical of members of the Ca_v3 family. On account of its small amplitude and rapid inactivation kinetics, this $I_{Ca,t}$ is obscured as membrane potential approaches the -30 mV threshold for the much larger magnitude high-voltage activated Ca^{+2} current components in $I_{Ca,total}$. In the presence of 1 μM ω-conotoxin, a selective blocker of the $Ca_v2.2$ Ca^{+2} channel, the $I_{Ca,total}$ is reduced by more than 70%. Subtraction of this remnant from $I_{Ca,total}$ reveals this N-type whole cell Ca^{+2} current ($I_{Ca,n}$). Recording protocol consisted of 400 msec voltage steps from a holding potential of -100 mV, 10 mV increments up to 40 mV with an interstep interval of 3 sec. The vertical and horizontal scale bars are 1 nA and 200 msec, respectively, for both recordings and 0.5 nA and 100 msec, respectively, for the inset. Solutions consisted of $[Ca^{+2}]_i = 100$ nM (BAPTA-K^+) and $[Ca^{+2}]_o = 2$ mM. See Mendelowitz and Kunze[21] for complete details concerning the electrophysiological methods.

I_{TTXR} recovers from complete inactivation quite rapidly, requiring less than 10 msec to return within 90% of control magnitudes, as is the case in dorsal root ganglion neurons.[7,18]

3.3 VOLTAGE-GATED CALCIUM ION CHANNELS

Voltage-gated calcium ion channels (Ca_v) are heterogeneous in molecular structure and endogenous regulation. Evidence for most isoforms of the Ca_v family has been found in the peripheral nervous system, in which multiple members often function

within a single cell type. The selective action of high-specificity calcium channel antagonists has led to the classification of five functionally distinct Ca_v subtypes, which are further identified as high-voltage activated (HVA) or low-voltage activated (LVA) on account of channel-gating thresholds in the range of -30 to -20 mV or -60 to -50 mV, respectively.[20–22] The HVA Ca_v exhibit selective IC_{50} values in the range of 100's nM to low μM for nifedipine (L-type, presumably $Ca_v1.2$), 10's nM to 100's nM for omega-conotoxin GVIA (N-type, presumably $Ca_v2.2$), subnanomolar to 10's nM for omega-agatoxin IVA (P-type, presumably $Ca_v2.1$), low 100's nM for omega-agatoxin IVA or low μM for omega-conotoxin MVIIC (Q-type, also presumably $Ca_v2.1$). Those Ca_v resistant (R-type, presumably $Ca_v2.3$) to all these antagonists may represent a single subtype or perhaps multiple, as yet unidentified Ca_v subtypes. The LVA Ca_v exhibit selective IC_{50} values in the low 10's nM for kurtoxin (T-type, the Ca_v3 family) with strong evidence for $Ca_v3.2$ in nodose neurons.[23]

Although the relative contribution of each Ca_v subtype to the I_{Ca} is quite variable across the general population of vagal afferent neurons, the majority of the whole-cell Ca^{+2} current (I_{Ca}) at the cell body arises from N-type Ca_v.[21,24] Our recordings from rat nodose neurons show that I_{Ca} peaks at approximately -10 mV within a few milliseconds of the voltage clamp step (Figure 3.3). The I_{Ca} decays along a multi-exponential time course for several hundred milliseconds before settling at a magnitude that is about one half the peak current magnitude for any particular clamp step beyond approximately -40 mV. From a holding voltage of -100 mV, 70 to 80% of the I_{Ca} is carried by a HVA N-type Ca_v that is completely blocked by 1 μM omega-conotoxin ($I_{Ca,n}$, Figure 3.3). This HVA Ca^{+2} current is responsible for the majority of the steady-state inward Ca^{+2} current in nodose neurons, giving rise to incomplete inactivation characteristics for $I_{Ca,n}$ (Figure 3.4). The total Ca^{+2} current that remains in the presence of ω–CTX exhibits comparable activation characteristics, but is far less inactivating and more sustained than the N-type current, common features of all the remaining four HVA Ca_v. Occasionally, a small LVA transient calcium current (<100-200 pA in 2 mM $[Ca^{+2}]_o$) is observed with activation and inactivation characteristics typical of a T-type Ca_v (Figure 3.3, inset). This current is completely inactivated at steady-state conditioning voltages more depolarized than -50 mV (Figure 3.3 and Figure 3.4).

Numerous aspects of neurobiological development and neuropathic injury responses are known to influence the relative expression of channel subtypes from the Ca_v1 and Ca_v2 families of HVA calcium channels.[24] Such dynamic distributions may be indicative of specialized functions for particular ion channel subtypes along the afferent fiber pathway (peripheral, somatic and central regions.) For example, the N-type Ca_v present in the cell body of nodose neurons are know to regulate synaptic transmission of vagal afferent information in the NTS, but a functional role is less apparent at the peripheral terminal ending.[25] The functional role of the Ca_v3 family of transient currents is less well understood. However, as the activation window for $I_{Ca,t}$ resides within the range of -70 to -60 mV there exists a small, but sustained inward Ca^{+2} current from these channels that may play an important role in establishing the resting membrane potential (Figure 3.4). Upon action potential discharge, a $Ca_v3.2$ current component may contribute over the time course of late
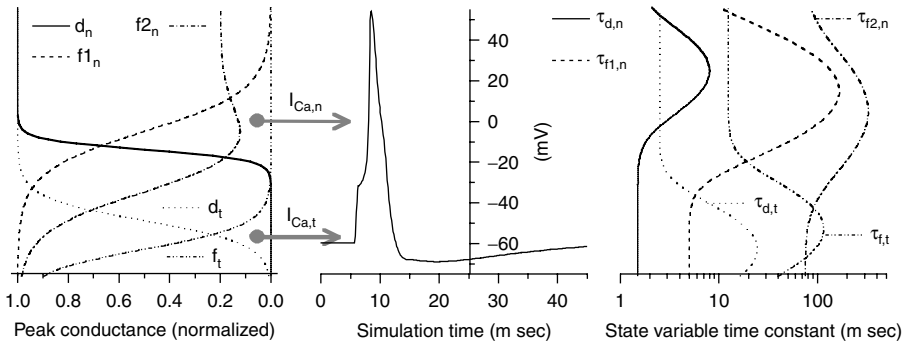
FIGURE 3.4 Voltage- and time-dependent channel gating for $I_{Ca,t}$ and $I_{Ca,n}$. (Left) Hodgkin and Huxley (1952) ion-channel gating variables derived from the voltage- and time-dependent activation and inactivation characteristics of $I_{Ca,t}$ and $I_{Ca,n}$. Steady-state profiles of the (activation, inactivation) gating variables for $I_{Ca,t}$ (d_t, f_t), and $I_{Ca,n}$ (d_n, $f1_n$, $f2_n$) reveal the region of the action potential waveform over which each inward current begins to contribute to membrane depolarization. Of particular importance are the "window currents" that result from an overlap in the voltage-dependent profiles of the activation and inactivation gating variables (i.e., the shaded arrows, see text). (Right) An examination of the voltage-dependent time constants (τ) for these gating variables provides insight into how quickly individual gating variables can respond to changes in membrane potential. (Center) The same as in Figure 3.2.

membrane repolarization and early afterhyperpolarization, which, in turn, may influence cell excitability of nodose neurons.[23]

3.4   VOLTAGE-GATED POTASSIUM ION CHANNELS

The considerable biological homology present across the superfamily of voltage-gated potassium channel (K_v) proteins has made it possible to demonstrate that only modest differences in molecular sequences, or perhaps membrane lipid dynamics, separate a disparate range of voltage- and time-dependent gating properties.[26,27] To date, the superfamily of K_v gives rise to the most functionally diverse and extensively studied class of transmembrane ion channel currents.[28] There exists a broad landscape of voltage- and time-dependent whole-cell K^+ currents that respond to the depolarizing action of the inward Na^+ and Ca^{+2} currents. The net effect of all these K_v channel subtypes is a total transmembrane outward K^+ current ($I_{K,total}$) that makes a critically important contribution in defining the membrane excitability characteristics of vagal afferent neurons. Evidence for many isoforms of the K_v family has been found in the central and, to a lesser extent, the peripheral nervous systems. The action of K_v antagonists has led to the broad classification of two functional forms of whole-cell K^+ currents, those that are noninactivating and those that rapidly inactivate.

Under conditions of voltage clamp and with K^+ as the major membrane permeant ion, the $I_{K,total}$ in rat nodose neurons exhibits threshold currents starting near −50 mV followed by a near ohmic current recruitment until presentation of a rather modest

transient outward peak at the highest clamp potentials (Figure 3.5). From this peak, the $I_{K,total}$ decays along a multiexponential time course toward a sustained activation that requires several seconds to achieve. Pharmacological dissection of the $I_{K,total}$ into specific VGC subtypes is limited by the selectivity of K^+ channel antagonists, most of which exhibit an overlapping concentration-dependent block of multiple K^+ current subtypes. The channel antagonists with the greatest specificity are those derived using recombinant techniques or from purified animal or plant neurotoxins such as the family of dendrotoxin peptides, which are highly selective for the $K_v1.1$, $K_v1.2$ and $K_v1.6$ subtypes with IC_{50}'s on the order of 1 to 10 nM.[29] At a concentration of 10 nM this whole-cell K^+ current (I_{DTX}), obtained by subtracting the current in the presence of α-dendrotoxin from that in its absence, exhibits rapid activation characteristics beyond a threshold of approximately -40mV and effectively no inactivation over the time course of 400 msec clamp steps. The voltage-dependent recruitment of I_{DTX} exhibits an e-fold slope (s = 7.5) and half activation ($V_{1/2} = -10mV$) that are comparable to the traditional delayed rectifier present in these cells (see below) but with an activation rate that is 5 to 10 times faster and, as a result, I_{DTX} contributes to setting discharge threshold from rest potentials (Figure 3.6).

In the presence of 10 nM α-dendrotoxin there is a component of the remaining $I_{K,total}$ that is sensitive to the K^+ channel antagonist 4-aminopyridine (4AP), that is presumed to be comprised of multiple, independent current components arising from members of the K_v1, K_v2, K_v3, and K_v4 families of K^+ VGC (Figure 3.5). Rapid activation (<10 msec) at low membrane potentials (<-50 mV) is a characteristic property of this whole-cell 4AP sensitive current (I_{4AP}), as is the complex inactivation profile that often follows a multiexponential time course of decay toward a sustained (or very slowly inactivating) outward current component. It is this multiexponential time course of decay that has led to the breakdown of I_{4AP} into transient (I_A) and delayed (I_D) 4AP sensitive current components. In some preparations it has been possible to discriminate these two current components based upon modest differences in sensitivity to 4AP and thresholds for voltage activation but further study is required for definitive classification of the VGC subtypes.[30] The I_A is likely comprised of $K_v1.4$ and members of the K_v3 and K_v4 families of VGC. The origins of the I_D component remain unclear although some members of the K_v1 and K_v2 families do exhibit the requisite insensitivity to α-dendrotoxin and an inactivation time constant large enough (> 3 sec) to account for the voltage- and time-dependent profile of this current.[29]

In the presence of 10 nM α-dendrotoxin and 5 mM 4AP there is a component of the remaining $I_{K,total}$ that is blocked by 15 mM of the ubiquitous K_v channel antagonist tetraethylammonium (TEA). This whole-cell current has voltage- and time-dependent features typical of a classical delayed rectifier current, I_K. Although at 15 mM TEA it is likely that at least some of this current, along with a significant component of the $I_{K,total}$ that remains in the presence of these three antagonists, is comprised of a calcium-activated K^+ current (K_{Ca}, see below). Threshold for voltage activation of I_K occurs at relatively depolarized membrane potentials greater than -30 mV ($V_{1/2}$ -5 mV) with an activation time constant greater than 30 msec and an extremely gradual e-fold slope of greater than 15 (Figure 3.6).

FIGURE 3.5 The α-DTX, 4-AP and TEA sensitive K^+ currents in rat nodose neurons. The upper voltage clamp traces present the whole cell K^+ current ($I_{K,total}$), which is comprised of multiple subtypes of K^+ currents that can only be separated through judicious application of selective channel antagonists. Alpha-dendrotoxin (α-DTX) has a high specificity for select members of the K_v1 family.[29] A 10 nM concentration of α-DTX reveals a K_v1 current (I_{DTX}) that is ~25% of $I_{K,total}$. At low millimolar concentrations 4-aminopyridine (4-AP) is moderately selective for members of the K_v1 family that exhibit both transient (I_A) and sustained (I_D) K^+ current components. A 5 mM concentration of 4-AP reveals a K^+ current (I_{4AP}) with peak and sustained responses that are ~25% and ~10% of $I_{K,total}$. Tetraethylammonium (TEA) blocks a broad spectrum of K_v channels in a concentration-dependent manner. A 15 mM concentration of TEA reveals a composite of K_v currents with delayed rectifier (I_K) characteristics that is ~25% of $I_{K,total}$. Recording protocol consisted of 400 msec voltage steps from a holding potential of –80 mV, 10 mV increments up to 40 mV with an interstep interval of 3 sec. $[K^+]_i$ = 140 mM, $[K^+]_o$ = 5.4 mM, $[Ca^{+2}]_i$ = 10 nM (BAPTA-K^+) and $[Ca^{+2}]_o$ = nominally, 1-10 μM. Agonist application was sequential and additive, i.e., 10 nM α-DTX, followed by 10 nM α-DTX and 5 mM 4-AP, followed by 10 nM α-DTX, 5 mM 4-AP and 15 mM TEA, in producing the subtracted traces. Vertical and horizontal scale bars are 2 nA and 100 msec, respectively, for all traces. See Schild et al.[2] and Glazebrook et al.[29] for complete details concerning the electrophysiological methods.
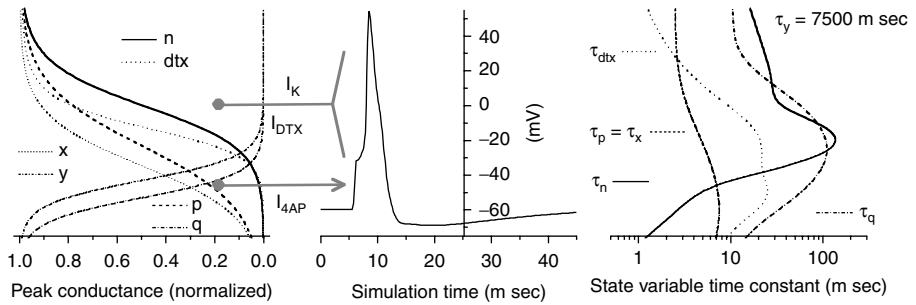
FIGURE 3.6 Voltage- and time-dependent channel-gating for I_K, I_{dtx} and I_{4AP}. (Left) Hodgkin and Huxley (1952) ion channel gating variables derived from the voltage- and time-dependent activation and inactivation characteristics of I_K, I_{DTX}, and I_{4AP} (I_A and I_D components). Steady-state profiles of the (activation, inactivation) gating variables for I_K (n), I_{DTX} (dtx), and the 4AP sensitive K^+ current components I_A (p, q) and I_D (x, y) reveal the region of the action potential waveform over which each inward current begins to contribute to membrane depolarization. Of particular importance are the "window currents" that result from an overlap in the voltage-dependent profiles of the activation and inactivation gating variables (i.e., the shaded arrows, see text). (Right) An examination of the voltage-dependent time constants (τ) for these gating variables provides insight into how quickly individual gating variables can respond to changes in membrane potential. (Center) The same as in Figure 3.2.

To date, calcium activated potassium channels that also exhibit voltage-dependent gating properties (K_{vCa}) are most often classified according to measures of single-channel conductance and pharmacological sensitivities. These include a large (>200 pS) and an intermediate (10 to 60 pS) K_{vCa} conductance that are blocked by low-nanomolar concentrations of charybdotoxin and, therefore, presumably members of the $K_{vCa}1$ and $K_{vCa}3$ families, respectively, and a small K_{vCa} conductance (<10 pS) that is blocked by low-nanomolar concentrations of apamin and presumably a member of the $K_{vCa}2$ family.[31–34]

Under conditions of voltage clamp, with potassium as the major membrane permeant ion and $[Ca^{+2}]_i$ buffered to 10 nM using BAPTA-K, the extracellular application of 10 nM charybdotoxin selectively blocks a whole-cell I_{KCa} in nodose neurons that is approximately one fourth of the peak magnitude of $I_{K,total}$. The voltage- and time-dependent activation characteristics are typical for this BK-type K_{vCa}. Beyond a −10 mV threshold, the $I_{KCa(BK)}$ achieves a sustained magnitude within 10 to 15 msec of the clamp step that scales in an ohmic manner with increasing potential (Figure 3.7).

3.5 DYNAMIC PROPERTIES OF IONIC CURRENTS IN VAGAL AFFERENT NEURONS

The voltage clamp technique has become the *de facto* standard for quantification of the voltage- and time-dependent properties of whole-cell ionic currents. When combined with molecular and pharmacological methodologies, it is possible to dissect out the individual contributions of particular VGC subtypes to the whole cell
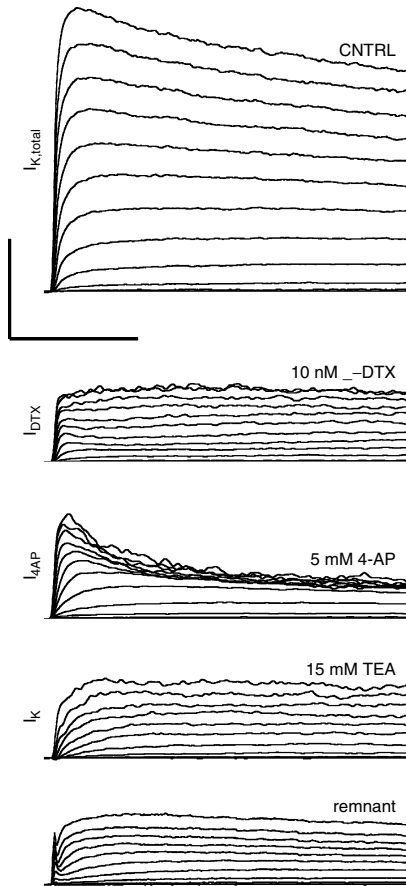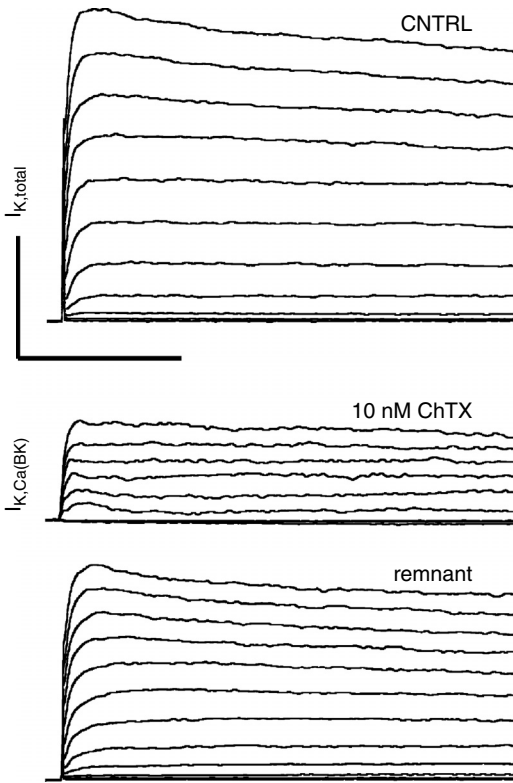
FIGURE 3.7 The charybdotoxin sensitive K_{Ca} current in rat nodose neurons. The upper voltage clamp traces present the whole cell K^+ current ($I_{K,total}$) of which a component is sensitive to the influx of Ca^{+2} (K_{Ca}). At nanomolar concentrations, charybdotoxin (ChTX) is a selective blocker of the large conductance $K_{Ca}3.1$ channel in neurons. A 10 nM concentration of ChTX reveals an $I_{K,Ca(BK)}$ that is ~25% of $I_{K,total}$ at a $[Ca^{+2}]_i$ of 10 nM. Recording protocol consisted of 400 msec voltage steps from a holding potential of -80 mV, 10 mV increments up to 40 mV with an interstep interval of 3 sec. $[K^+]_i = 140$ mM, $[K^+]_o = 5.4$ mM, $[Ca^{+2}]_i = 10$ nM (BAPTA-K^+) and $[Ca^{+2}]_o =$ nominally, 1-10 μM. Vertical and horizontal scale bars are 2 nA and 100 msec, respectively, for all traces.

transmembrane current (Figure 3.1 through Figure 3.7). Such data can provide insight concerning the impact of a particular ionic current upon membrane excitability, albeit under very limited and very contrived conditions. A more comprehensive assessment of ion channel function can be obtained through the application of pharmacological blockers of proven specificity and selectivity under conditions of current clamp, or through the use of antisense technologies in conjunction with more integrative experimental paradigms.[23,29,35] However, an interpretation of the functional consequences of the selective elimination or even over expression of a particular VGC subtype upon neural discharge can not follow the simple logic of superposition. The complex interplay of the transmembrane currents arising from the collective of VGC is inextricably bound to the magnitude and time course of

membrane potential. Therefore, it is not surprising that the changes in neuronal discharge properties observed in such deletion studies are often more subtle and less revealing than what might have been predicted based solely upon whole cell current magnitudes.[23,29] Computational models derived from a foundation of voltage and current clamp data from a single cell type can serve as a useful platform for studying the nonlinear ionic current dynamics underlying membrane excitability. However, even the most complex model of membrane excitability is, at best, only an approximation to the actual system or data under investigation. Although it generally presents but one abstract snapshot of highly integrated and nonlinear biophysical mechanisms the effort can reveal possibilities regarding ion channel function that are beyond the reach of existing experimental paradigms. For the computational simulations presented below the individual membrane currents were modeled using Hodgkin and Huxley (1952) formalisms that were parameterized through numerical fits to the voltage clamp data presented in this chapter (Figure 3.1 through Figure 3.6) with whole cell conductances scaled according to the relative contribution each individual current makes to the whole cell current (e.g., $I_{K,total}$, Figure 3.5).[2] The corresponding somatic action potential waveform is that of a C-type neuron as all the known ionic channel currents in rat nodose neurons are represented. Unlike the A-type, which do not exhibit I_{TTXR} and have an outward K^+ current that is dominated by the transient I_A.

3.5.1 NA⁺ AND CA⁺² CURRENT DYNAMICS

Over the course of a single action potential waveform I_{TTXS}, I_{TTXR}, and $I_{Ca,n}$ comprise the majority of the total inward ionic current. Of these, I_{TTXS} is the first to respond to a depolarizing event from resting membrane potential with a rapid inward current that reaches a maximum near 0 mV but quickly subsides as the overshoot approaches the reversal potential for Na^+ ions and the inactivation processes begin to dominate channel gating (Figure 3.8). Both I_{TTXR} and $I_{Ca,n}$ exhibit voltage-activation profiles that are considerably more depolarized and activation time constants that are slower than those for I_{TTXS} (Figure 3.2 and Figure 3.4). These factors substantially limit the recruitment of these currents over the rapid membrane depolarization leading up to the peak of the action potential waveform (Figure 3.8). Over the course of the action potential upstroke there is sufficient time and membrane depolarization to recruit a substantial $I_{K,total}$ (see below), which eventually results in a reversal in the trajectory of the action potential waveform. As repolarization proceeds, the membrane potential moves away from the reversal potential for both Na^+ and Ca^{+2} ions and back through the activation windows for I_{TTXR} and $I_{Ca,n}$ (Figure 3.2 and Figure 3.4). The time required to traverse from the action potential peak back toward threshold potentials for these currents is well below the magnitude of their activation time constants. This factor, combined with the slow rates of inactivation for these currents, results in a substantial I_{TTXR} and $I_{Ca,n}$ over the downstroke of the action potential waveform (Figure 3.8). The net magnitude of the inward Na^+ and Ca^{+2} currents are substantially less than the $I_{K,total}$ (see below) and, therefore, produce only a transient loss of total
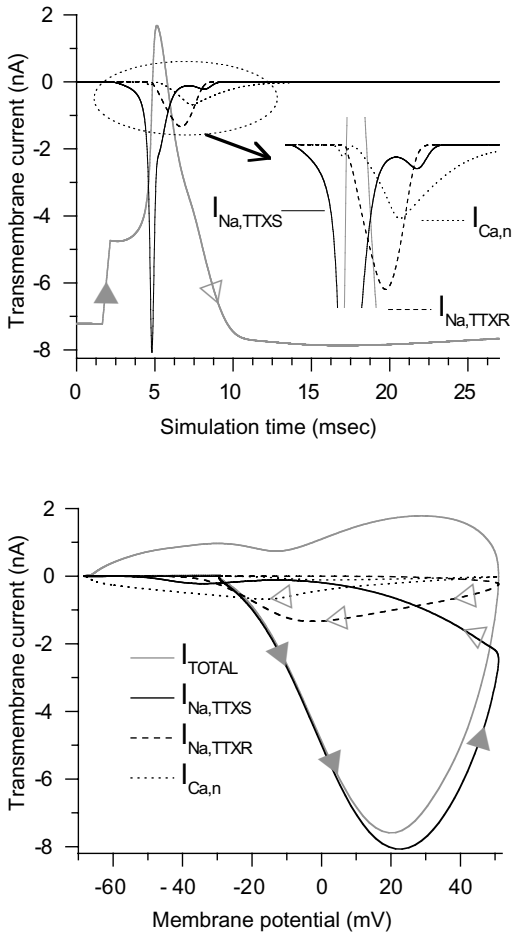
FIGURE 3.8 Dynamic aspects of the Na^+ and Ca^{+2} currents in membrane discharge. (Top) Magnitude of I_{TTXS}, I_{TTXR}, and $I_{Ca,n}$ over the time course of a simulated C-type action potential waveform (shaded trace). The inset clearly demonstrates that unlike I_{TTXS} the peak contribution of I_{TTXR} and $I_{Ca,n}$ to membrane depolarization occurs during the downstroke of the action potential waveform (see text). (Bottom) The functional impact of these late, inwardly flowing currents is most clearly demonstrated in a voltage phase plot of the total transmembrane current (shaded trace). Solid arrowheads (u) delineate a depolarizing trajectory in membrane potential over the course of an action potential. Open arrowheads (w) delineate a hyperpolarizing trajectory in membrane potential over the course of an action potential. See Schild et al.,[2], Schild and Kunze,[7] and Appendix for further explanation of this technique.

outward current but it is of sufficient magnitude to slow the progression of membrane voltage over the downstroke of the action potential waveform (Figure 3.8). This suggests that the counteractive influences of I_{TTXR} and $I_{Ca,n}$ upon the $I_{K,total}$ plays an important role in setting the duration of the action potential waveform, which further impacts the recruitment of the K_V VGC and, ultimately, neuronal excitability.

3.5.1.1 Functional Role of I_{TTXS} and I_{TTXR}

A-type nodose neurons, i.e., those with narrow (≤ 1 msec) somatic action potential waveforms and deep but short-lasting afterhyperpolarization transients, are known to give rise to myelinated axons.[36,37] The total inward Na^+ current in A-type neurons is comprised exclusively of I_{TTXS}. The characteristically low $V_{1/2}$ values, steep slope factors, small activation window and brief time constants coupled with a rather sluggish recovery from inactivation define the functional dynamics of I_{TTXS} over the range of membrane potentials typically exhibited by somatic action potentials. The I_{TTXS} is well suited for the low activation threshold and high discharge frequencies typically exhibited by myelinated vagal afferent fibers. In contrast, the rather depolarized activation profile of the I_{TTXR} in vagal afferents is not well suited for initiation of action potential discharge and is, therefore, always co-expressed with I_{TTXS}. Cells expressing both I_{TTXS} and I_{TTXR} are often classified as C-type, exhibiting broad (2 msec or more) somatic action potential waveforms with a hump or delay in repolarization phase and a shallow afterhyperpolarization transient that requires nearly 100 msec to return to baseline. These C-type nodose neurons are known to give rise to unmyelinated axons.[36,37] The physiological rationale behind the functional expression of two distinctly different Na^+ currents in a single nodose neuron remains unresolved. However, a closer examination of the dynamic profiles of I_{TTXS} and I_{TTXR} under conditions of both voltage and current clamp along with mathematical simulations offers some intriguing possibilities (Figures 3.1, 3.2, and 3.8).

Starting from a resting membrane potential of -60 mV, approximately 60% of the total population of TTXS Na_v in nodose neurons is available for action potential generation (Figure 3.2). Over the time course of repetitive discharge, the rather slow recovery from inactivation steadily reduces the peak magnitude of the regenerative I_{TTXS}, which, in turn, plays an important role in setting the maximum discharge frequency of vagal afferent neurons. In contrast, nearly 100% of the population of TTXR Na_v is available for action potential discharge from rest potentials on account of the depolarized activation and inactivation profiles for these VGC. Furthermore, the rapid recovery from inactivation exhibited by TTXR Na_v ensures that the peak magnitude of the regenerative I_{TTXR} remains essentially unchanged at discharge frequencies approaching 100 Hz. Therefore, neurons with an I_{TTXR} that comprises the majority of the total inward Na^+ current may be slowly adapting, assuming sufficient I_{TTXS} remains to drive membrane potential toward the activation threshold for TTXR Na_v. It would appear that the relative availability of the rapidly inactivating TTXS Na_v and the slowly inactivating TTXR Na_v is an important factor in defining the excitability, action potential waveshape, and capacity for repetitive discharge of vagal afferent neurons. There are multiple mechanisms that can influence this ratio of channel availability. Perhaps the simplest would be increasing the depth of the afterhyperpolarization in order to accelerate the recovery of the inactivated TTXS Na_v. Alternatively, neuropeptides, inflammatory mediators, and other chemical signaling agents are known to affect the voltage-dependent properties of TTXR Na_v, raising the possibility that the relative expression and availability of TTXS and TTXR Na_v may play an important role in the physiological response characteristics of vagal

afferents to (as an example) neuropathic injury or conditions of sustained inflammation.[8,14,38–40]

3.5.2 K⁺ CURRENT DYNAMICS

Over the course of a single action potential waveform I_A, I_D, I_{DTX}, I_K, and $I_{K,Ca}$ comprise the majority of the total outward ionic current. Each of these individual, pharmacologically identified whole-cell currents is comprised of multiple subtypes of K⁺ VGC, which are only beginning to be identified and characterized in vagal afferent neurons. Not surprisingly, I_A and I_D are the first to respond to a depolarizing event on account of the hyperpolarized activation profile and fast activation time constants for these currents (Figure 3.6 and Figure 3.9). As membrane potential enters into a phase of rapid depolarization there is a marked recruitment of I_{DTX} and $I_{K,Ca}$, which are the primary outward K⁺ currents responsible for terminating the action potential upstroke and initiating a reversal in the trajectory of the membrane potential. This effect is most apparent in the phase plot where beyond approximately 0 mV I_{DTX} dominates the outward current, being joined and eventually surpassed by $I_{K,Ca}$ near the peak of the action potential waveform (note shaded arrowheads, Figure 3.9). As repolarization proceeds from peak back toward 0 mV I_A, I_D, and I_K are recruited to a greater extent, eventually peaking near the midpoint of the action potential waveform. These three currents are slow to join I_{DTX} and $I_{K,Ca}$, but for different reasons. Both I_A and I_D are inactivating currents with gating profiles that are far more negative than those of the other K⁺ currents (Figure 3.6). The inactivation time constant for I_A is on the order of 10 to 15 msec over the more depolarized phases of the action potential waveform. This factor, coupled with a whole-cell conductance that is comparable to or just slightly smaller than for I_{DTX} and $I_{K,Ca}$ (see below), markedly restricts the peak whole-cell current from these transient VGC. This is in contrast to I_K and I_D, which are both considerably larger than I_A and present gradual current profiles that are quite similar in magnitude and time course (note inset, Figure 3.9). Interestingly, I_D has a whole-cell conductance that is nearly equal to that of I_A but only about one-third that of I_K (n.b. at the end of the I_{4AP} traces, Figure 3.5) I_A has nearly completely inactivated and the current that remains is I_D and this has a magnitude only one third that of I_K across all clamp voltages). The larger current magnitudes also come about because of the sustained nature of these currents, I_K is noninactivating and I_D has an inactivation time constant of 7500 msec.

By far the largest contributor to the total outward transmembrane current over the course of an action potential is $I_{K,Ca}$ (Figure 3.9).[2] This is best explained by first re-examining the voltage clamp response of this charybdotoxin-sensitive current (Figure 3.7). In voltage clamp, the $[Ca^{+2}]_i$ has been buffered to 10 nM, but more importantly the $[Ca^{+2}]_o$ is nominally calcium free with an unbuffered concentration on the order of 1 to 10 μM. While far below the influx of Ca^{+2} ions that give rise to the $I_{Ca,n}$ over the time course of a somatic action potential (Figure 3.8), this low micromolar concentration is sufficient to support the recruitment of a BK-type $I_{K,Ca}$ that is approximately one fourth of the $I_{K,total}$. Under conditions of normal $[Ca^{+2}]_o$ at 2 mM the $[Ca^{+2}]_i$ transient will be well above concentrations that have been shown
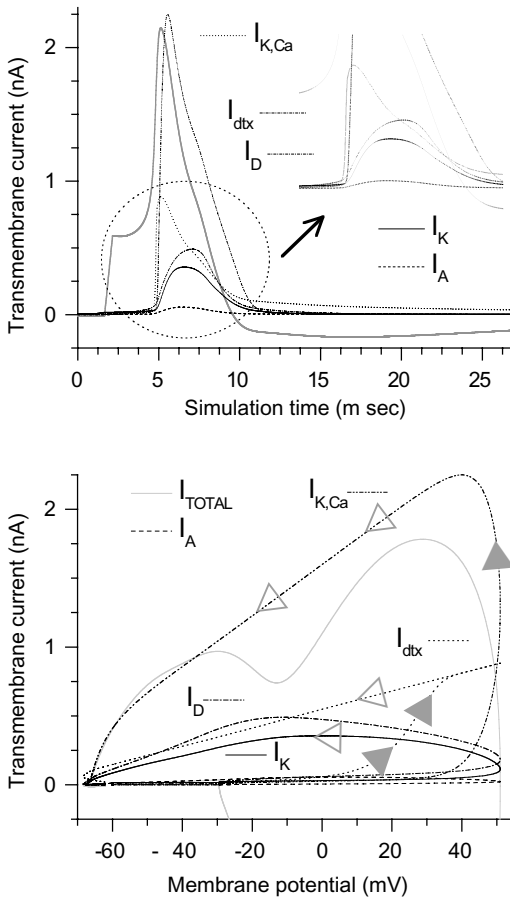
FIGURE 3.9 Dynamic aspects of the K+ currents in membrane discharge. (Top) Magnitude of I_K, I_{DTX}, I_A, I_D, and I_{KCa} over the time course of a simulated C-type action potential waveform (shaded trace). At all but the most depolarized membrane potentials the magnitude of these K+ currents is essentially unchanged from that at rest. The inset clearly demonstrates that the individual outward K+ currents are greatest and sustained throughout the downstroke of the action potential waveform. (Bottom) The functional impact of these late, outwardly flowing currents is most clearly demonstrated in a voltage phase plot of the total transmembrane current (shaded trace). Solid arrowheads (▲) delineate a depolarizing trajectory in membrane potential over the course of an action potential. Open arrowheads (Δ) delineate a hyperpolarizing trajectory in membrane potential over the course of an action potential. See Schild et al.,[2] Schild and Kunze,[7] and Appendix for further explanation of this technique.

to markedly increase single channel open probability.[34] Model predictions suggest that such a $[Ca^{+2}]_i$ would produce a voltage clamped $I_{K,Ca(BK)}$ several times larger than that presented in Figure 3.7, which is consistent with the simulations of the somatic action potential waveform (Figure 3.9).

3.5.3 Continued Study of the Ionic Currents Underlying Membrane Excitability

Knowledge of the molecular identity of the superfamily of VGC underlying the major transmembrane currents in vagal afferent neurons lags well behind that for somatic and central nervous system neurons. This, however, presents exciting opportunities for future scientific investigation of these afferents. When coupled with a definitive identification of sensory modality (e.g., through the use of fluorescent lipophilic tracers) such *in vitro* studies would advance the physiological relevance of using the cell body as a model system for investigating the molecular foundations of the ion channel currents participating in the neurosensory transduction and spike encoding processes.[11,41-43] Furthermore, there remain several identified subclasses of channel proteins in vagal afferents in which a functional interpretation of the impact of the corresponding whole-cell current upon membrane excitability is lacking. Two such subtypes are the K_{Ca} and hyperpolarization activated, cyclic nucleotide-gated cation (HCN) channels.

3.6 VOLTAGE DEPENDENT CALCIUM-ACTIVATED POTASSIUM ION CHANNELS

To date, the combined effects of $[Ca^{+2}]_i$ magnitude and transmembrane potential upon the availability of $K_{vCa(BK)}$ in vagal afferent neurons has not been well characterized. This is also true for the small fraction ($<5\%$) of the $I_{K,total}$ that is comprised of SK-type apamin sensitive and intermediate K_{vCa} current components. Both electrophysiological and computational studies have demonstrated that $I_{KCa(BK)}$ can have a significant impact upon action potential waveshape and repetitive discharge in vagal afferent neurons (Figure 3.9).[2,24,44] Further elucidation of the role of K_{Ca} dynamics in vagal afferent discharge will require a more intensive investigation of the subcellular mechanisms that can effect the transient change in $[Ca^{+2}]_i$ associated with membrane depolarization. A more comprehensive investigation of the gating properties of K_{vCa} channels along with molecular identification of K_{Ca} channel subtypes in vagal afferent neurons is needed. Likewise, existing mathematical models of the Ca^{+2}-dependent gating mechanisms of K_{Ca} channels must be advanced to include regional $[Ca^{+2}]_i$ dynamics that are influenced by both transmembrane and intracellular sources of Ca^{+2} ions.

3.7 HYPERPOLARIZATION ACTIVATED CYCLIC NUCLEOTIDE-GATED CATION CHANNELS

The channels underlying the HCN current (I_H) comprise four distinct subtypes that contribute to the oscillatory characteristics of neurons in the central nervous system, but differ with regard to cAMP sensitivity and activation dynamics.[45] Considerably less is known regarding the functional roles for HCN channels expressed in the normally quiescent cell bodies of vagal afferents, but as sustained suprathreshold stimulation can elicit repetitive discharge, a similar functional role is presumed.

Immunohistochemical studies have shown HCN2 and HCN4 immunoreactivity across all neurons in the rat nodose ganglia, but only 20% of these cells presented with immunoreactivity for HC1. Interestingly, HCN1 expression was present in nearly all neurons that carried positive for markers for myelination and was expressed at the mechanosensitive terminals of myelinated (A-type) but not unmyelinated (C-type) sensory fibers. In contrast, the HCN2 and HCN4 subtypes were found in the receptor terminals of both A- and C-type afferents.[35,46]

Glazebrook et al. (2002) demonstrated that under conditions of voltage clamp the capacitance normalized peak magnitude of the whole-cell mixed cation I_H in A-type nodose neurons was nearly ten times greater than that in C-type neurons.[29] In both cell types, I_H activated at potentials negative to –50 mV and developed slowly with time. At –120 mV I_H activated approximately twice as fast in A-type as compared with C-type neurons. Under current clamp conditions, I_H exhibits a time-dependent rectification in response to hyperpolarizing current injections from resting membrane potentials. Further experimental and computational study are required to resolve the differential role I_H may have across the population of A- and C-type vagal afferents such as active regulation of the resting membrane potential and limiting the substantial I_{KCa}-mediated hyperpolarization that can occur following periods of elevated membrane discharge.[44]

3.8 CONCLUSION

To this point we have focused on a select group of Na^+, Ca^{+2} and K^+ VGC whole-cell currents that make up the vast majority of the total transmembrane current over the course of a somatic action potential waveform. The magnitude of the whole-cell currents arising from these VGC is a direct reflection of the somatic expression density (i.e., channels/μm^2) and the nonlinear dynamic properties of channel gating (Figure 3.8 and Figure 3.9). Many questions remain concerning the molecular identity and functional distribution of these VGC subtypes along the vagal afferent pathway. Ion channel expression at the peripheral terminal ending is a critically important component of the sensory transduction process, while expression at synaptic terminations most certainly impacts the central integration of neurosensory information. Further *in vitro* study of the dynamic properties of particular subtypes of VGC can advance the understand of the role these transmembrane proteins play in neuronal excitability. Interpretation of these data in terms of issues relevant to health and disease of organ systems along the vagal afferent pathway will require more comprehensive molecular, electrophysiological and computational methodologies than can likely be provided by isolated cellular recordings alone.

REFERENCES

1. Hille, B., *Ion Channels of Excitable Membranes*, Sinauer Associates, Inc., 2001.
2. Schild, J. H. et al., A- and C-type rat nodose sensory neurons: model interpretations of dynamic discharge characteristics. *J. Neurophysiol.,* 71, 2338–2358, 1994.

3. Caldwell, J. H., Schaller, K. L., Lasher, R. S., Peles, E., and Levinson, S. R., Sodium channel Na(v)1.6 is localized at nodes of ranvier, dendrites, and synapses, *Proc. Natl. Acad. Sci. USA,* 97, 5616–5620, 2000.

4. Kerr, N. C., Holmes, F. E., and Wynick, D., Novel isoforms of the sodium channels Nav1.8 and Nav1.5 are produced by a conserved mechanism in mouse and rat, *J. Biol. Chem.,* 279, 24826–24833, 2004.

5. Ikeda, S. R. and Schofield, G. G., Tetrodotoxin-resistant sodium current of rat nodose neurones: monovalent cation selectivity and divalent cation block, *J. Physiol. (Lond),* 389, 255–270, 1987.

6. Ikeda, S. R., Schofield, G. G., and Weight, F. F., Na+ and Ca2+ currents of acutely isolated adult rat nodose ganglion cells, *J. Neurophysiol.,* 55, 527–539, 1986.

7. Schild, J. H. and Kunze, D. L., Experimental and modeling study of Na+ current heterogeneity in rat nodose neurons and its impact on neuronal discharge, *J. Neurophysiol.,* 78, 3198–3209, 1997.

8. Lancaster, E. and Weinreich, D., Sodium currents in vagotomized primary afferent neurones of the rat, *J. Physiol.,* 536, 445–458, 2001.

9. Bielefeldt, K., Ozaki, N., and Gebhart, G. F., Mild gastritis alters voltage-sensitive sodium currents in gastric sensory neurons in rats, *Gastroenterology,* 122, 752–761, 2002.

10. Bielefeldt, K., Ozaki, N., Whiteis, C., and Gebhart, G. F., Amitriptyline inhibits voltage-sensitive sodium currents in rat gastric sensory neurons, *Dig. Dis. Sci.,* 47, 959–966, 2002.

11. Bielefeldt, K., Ozaki, N., and Gebhart, G. F., Experimental ulcers alter voltage-sensitive sodium currents in rat gastric sensory neurons, *Gastroenterology,* 122, 394–405, 2002.

12. Fazan, R. J., Whiteis, C. A., Chapleau, M. W., Abboud, F. M., and Bielefeldt, K., Slow inactivation of sodium currents in the rat nodose neurons, *Auton. Neurosci.,* 87, 209–216, 2001.

13. Gebhart, G. F., Bielefeldt, K., and Ozaki, N., Gastric hyperalgesia and changes in voltage gated sodium channel function in the rat, *Gut,* 51 Suppl 1, i15–i18, 2002.

14. Li, Z. et al., Nitric oxide as an autocrine regulator of sodium currents in baroreceptor neurons, *Neuron,* 20, 1039–1049, 1998.

15. Bielefeldt, K., Differential effects of capsaicin on rat visceral sensory neurons, *Neuroscience,* 101, 727–736, 2000.

16. Bossu, J. L. and Feltz, A., Patch Clamp Study of the Tetrodotoxin-Resistant sodium Current in Group C Sensory Neurones, *Neuroscience Letters,* 51, 241–246, 1984.

17. Caffrey, J. M., Eng, D. L., Black, J. A., Waxman, S. G., and Kocsis, J. D., Three types of sodium channels in adult rat dorsal root ganglion neurons, *Brain Res.,* 592, 283–297, 1992.

18. Rush, A. M., Brau, M. E., Elliott, A. A., and Elliott, J. R., Electrophysiological properties of sodium current subtypes in small cells from adult rat dorsal root ganglia, *J. Physiol.,* 511 (Pt 3), 771–789, 1998.

19. Rizzo, M. A., Kocsis, J. D., and Waxman, S. G., Slow sodium conductances of dorsal root ganglion neurons: intraneuronal homogeneity and interneuronal heterogeneity, *J. Neurophysiol.,* 72, 2796–2815, 1994.

20. Rusin, K. I. and Moises, H. C., Mu-opioid and GABA(B) receptors modulate different types of Ca2+ currents in rat nodose ganglion neurons, *Neuroscience,* 85, 939–956 1998.

21. Mendelowitz, D. and Kunze, D. L., Characterization of calcium currents in aortic baroreceptor neurons, *J. Neurophysiol.,* 68, 509–517, 1992.

22. Catterall, W. A., Striessnig, J., Snutch, T. P., and Perez-Reyes, E., International Union of Pharmacology. XL. Compendium of voltage-gated ion channels: calcium channels, *Pharmacol. Rev.,* 55, 579–581, 2003.

23. Lambert, R. C. et al., Low-voltage-activated Ca2+ currents are generated by members of the CavT subunit family (alpha1G/H) in rat primary sensory neurons, *J. Neuroscience,* 18, 8605–8613, 1998.

24. Lancaster, E., Oh, E. J., Gover, T., and Weinreich, D., Calcium and calcium-activated currents in vagotomized rat primary vagal afferent neurons, *Journal of Physiology,* 540, 2–56, 2002.

25. Mendelowitz, D., Reynolds, P. J., and Andresen, M. C. Heterogeneous Functional Expression of Calcium Channels at Sensory and Synaptic Regions in Nodose Neurons, *Journal of Neurophysiology,* 73, 872–875, 1995.

26. Coetzee, W. A. et al.*,* Molecular diversity of K+ channels, *Ann. N. Y. Acad. Sci.,* 868, 233–285, 1999.

27. Oliver, D. et al., Functional conversion between A-type and delayed rectifier K+ channels by membrane lipids, *Science,* 304, 265–270, 2004.

28. Armstrong, C. M., Voltage-gated K channels, *Science STKE,* 2003, re10, 2003.

29. Glazebrook, P. A. et al., Potassium channels Kv1.1, Kv1.2 and Kv1.6 influence excitability of rat visceral sensory neurons, *J. Physiol.,* 541, 467–482, 2002.

30. McFarlane, S. and Cooper, E., Kinetics and voltage dependence of A-type currents on neonatal rat sensory neurons, *J. Neurophysiol.,* 66, 1380–1391, 1991.

31. Faber, E. S. and Sah, P., Calcium-activated potassium channels: multiple contributions to neuronal function, *Neuroscientist,* 9, 181–194, 2003.

32. Sah, P. and Faber, E. S., Channels underlying neuronal calcium-activated potassium currents, [Review] [94 refs], *Progress in Neurobiology,* 66, 345–353, 2002.

33. Faber, D. S., Young, W. S., Legendre, P., and Korn, H., Intrinsic quantal variability due to stochastic properties of receptor- transmitter interactions, *Science,* 258, 1494–1498, 1992.

34. Hay, M. and Kunze, D. L., Calcium-activated potassium channels in rat visceral sensory afferents, *Brain Res.,* 639, 333–336, 1994.

35. Doan, T. N. et al., Differential distribution and function of hyperpolarization-activated channels in sensory neurons and mechanosensitive fibers, *J. Neurosci.,* 24, 3335–3343, 2004.

36. Li, B. Y. and Schild, J. H., Patch clamp electrophysiology in nodose ganglia of adult rat, *J. Neurosci. Methods,* 115, 157–167, 2002.

37. Stansfeld, C. E. and Wallis, D. I., Properties of visceral primary afferent neurons in the nodose ganglion of the rabbit, *J. Neurophysiol.,* 54, 245–260, 1985.

38. Akopian, A. N., Sivilotti, L., and Wood, J. N., A tetrodotoxin-resistant voltage-gated sodium channel expressed by sensory neurons, *Nature,* 379, 257–262, 1996.

39. Gold, M. S., Levine, J. D., and Correa, A. M., Modulation of TTX-R INa by PKC and PKA and their role in PGE2-induced sensitization of rat sensory neurons in vitro, *J. Neurosci.,* 18, 10345–10355, 1998.

40. Lancaster, E., Oh, E. J., and Weinreich, D., Vagotomy decreases excitability in primary vagal afferent somata, *J. Neurophysiol.,* 85, 247–253, 2001.

41. Christian, E. P. et al. A retrograde labeling technique for the functional study of airway-specific visceral afferent neurons. *J. Neurosci. Methods,* 47, 147–160, 1993.

42. Flake, N. M., Lancaster, E., Weinreich, D. and Gold, M. S., Absence of an association between axotomy-induced changes in sodium currents and excitability in DRG neurons from the adult rat, *Pain,* 109, 471–480, 2004.

43. Doyle, M. W. *et al.,* Strategies for cellular identification in nucleus tractus solitarius slices, *J. Neurosci. Methods,* 137, 37–48, 2004.

44. Cordoba-Rodriguez, R., Moore, K. A., Kao, J. P., and Weinreich, D., Calcium regulation of a slow post-spike hyperpolarization in vagal afferent neurons, *Proc. Natl. Acad. Sci. U.S.A.,* 96, 7650–7657, 1999.

45. Accili, E. A., Proenza, C., Baruscotti, M., and DiFrancesco, D., From funny current to HCN channels: 20 years of excitation, *News Physiol. Sci.,* 17, 32–37, 2002.

46. Doan, T. N. and Kunze, D. L., Contribution of the hyperpolarization-activated current to the resting membrane potential of rat nodose sensory neurons, *J. Physiol. (Lond),* 514 (Pt 1), 125–138, 1999.

APPENDIX: TOTAL TRANSMEMBRANE CURRENT AS A FUNCTION OF MEMBRANE POTENTIAL

The "dynamics" of ionic current refers to how the current changes over the course of time and transmembrane voltage. An important objective of the mathematical theory of dynamical systems is to characterize and quantify system behavior by identifying critical interrelationships between system subcomponents.

The net transmembrane current functions electrically to alter the total charge of the whole cell capacitance which is most often observed as a change in membrane potential. As a result, the net ionic current flow can be calculated according to the product of whole-cell capacitance and the negative time derivative of membrane voltage (i.e., $-C_m dV/dt$). When presented as a function of membrane voltage, the ensuing phase plot forms a closed loop that makes possible detailed quantification of subtle changes in discharge threshold and waveshape over the more rapid phases of the action potential trajectory such as the upstroke and downstroke (Figure A.1). During the action potential upstroke, the net inward transmembrane current manifests as a downward trajectory in the phase plot, which rapidly returned to zero as the waveform peaked, i.e., total inward and total outward transmembrane currents were equal. The upward trajectory represents a net outward transmembrane current during the action potential downstroke, which was markedly distorted in neurons that exhibited delayed repolarization, i.e., a prominent "hump" over the time course of the action potential downstroke. On account of the temporal sensitivity of this and other dynamical systems analysis techniques, subtle changes in the action potential waveform as a result of experimental manipulation of whole cell transmembrane currents can be readily assessed.
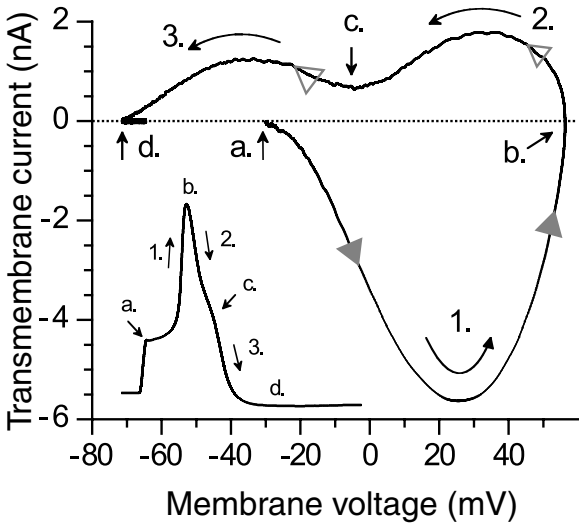
FIGURE A.1

4 Electrophysiological Studies of Target-Identified Vagal Afferent Cell Bodies

Danny Weinreich

CONTENTS

4.1 INTRODUCTION

The observation that cell bodies (somata) of primary sensory neurons are endowed with receptors similar to those that exist on their central or peripheral nerve terminals has been known for more than 30 years. Nishi et al.[50] demonstrated that activation of GABA receptors on somatosensory (dorsal root ganglion, DRG) neurons produced a membrane depolarization that is mediated by the efflux of chloride ions. From this observation, they proposed that the mechanism underlying GABA-evoked depolarization of primary afferent nerve terminals might also be due to an increase in chloride permeability. The correspondence between the chemosensitivity of vagal primary afferent nerve terminals and their cell bodies for a panel of excitatory/sensitizing substances and inflammatory mediators (serotonin, histamine, bradykinin, Substance P, and prostaglandins) was initially and elegantly delineated in a series of publications by Higashi and co-workers.[24] These results were derived from intracellular recordings of primary vagal afferent cell bodies in intact vagal ganglia, *in vitro*. Working with intact ganglia it was possible to measure conduction velocities of the impaled neurons and thus to correlate somal chemosensitivity with a neuronal phenotype, conduction velocity. Type A neurons have axons with conduction velocities 6 to 12 m/sec and somal action potentials that are completely blocked by tetrodotoxin (TTX, 0.1 to 0.5 FM). Type C neurons that have axons with conduction velocities 0.3 to 1.4 m/sec and somal action potentials resistant to TTX (1 to 5 μM). These two classes of neurons are also distinguished by their sensitivity to inflammatory mediators. Type C neurons are depolarized by serotonin, bradykinin or histamine, while type A neurons are relatively insensitive to these mediators. One drawback of this preparation is that intact vagal ganglion contain many different cell types besides primary afferent somata. Satellite cells, endothelial cells, and immune cells (macrophages and mast cells) are present in primary sensory ganglia[42] and may respond to inflammatory mediators and autacoids by releasing signal molecules that, in turn, alter the excitability of primary afferents.[23] Thus, when studying the actions of autacoids on neurons in intact vagal ganglia, interpretation of their site-of-action can be compromised by the heterogeneity of the tissue.

In 1983, two key papers were published that set the stage for using isolated primary afferent cell bodies as a tractable model for physiological and pharmacological studies of the primary afferent nerve terminal. Baccaglini and Hogan[2] reported that dissociated primary afferent somata (DRG neurons) maintained in culture expressed chemosensitive properties similar to those expressed by their peripheral nerve terminals and that these properties persisted in the absence of other cell types. In the same year, Belmonte and Gallego[3] reported that primary afferent somata with axons having different peripheral receptors had distinct electrophysiological properties. Cell bodies of chemoreceptor neurons had action potentials with prominent humps on their falling phase and a prolonged spike after-hyperpolarization, while the action potentials recorded in the cell bodies of baroreceptor neurons had action potentials with little or no deflections on their falling phase and they had much shorter duration spike after hyperpolarizations. Together, these two key papers revealed that somatic plasma membranes of primary afferent neurons possess distinct

sets of electrophysiological and chemosensitive properties that could reflect pharmacologic and biophysical properties of their nerve terminal membranes.

A third development that facilitated physiological studies of re-identifiable primary vagal afferent cell bodies was the introduction of fluorescent retrograde labeling techniques for the functional study of visceral-specific vagal afferent neurons. Mandelowitz and Kunze (1992)* were among the first investigators to combine axonal tracing methods, vital fluorescent dyes, with patch-clamp recording to examine electrophysiological and pharmacological properties of isolated, target-identified, primary afferent neurons. They measured whole-cell calcium currents from isolated aortic baroreceptor cell bodies that were identified by the fluorescent tracer, 4-(4-dihexadecylaminostyryl)-N-methylpyridinium iodine (DiA), previously applied to the uncut aortic nerve. A detailed methodological examination of the use of fluorescent dyes to study the electrophysiological properties and chemosensitivity of acutely isolated retrogradely labeled viscera-specific vagal afferent somata (nodose ganglion neurons) appeared the following year.[13]

The development of cell isolation techniques for adult primary sensory cell bodies and the application of retrograde fluorescent tracers to identify target-specific cell bodies have yielded a powerful technique to study numerous physiological, pharmacological and biophysical properties of vagal afferent nerve cells. This chapter deals with the attributes, limitations, and concerns about combining retrograde tracing techniques and sensory cell body isolation methods with intracellular recording methods for studying target-identified primary vagal afferents. It also considers several examples of how studies of target-identified vagal afferent cell bodies have furthered our understanding of the physiology and pathophysiology of the vagus nerve.

4.2   ANATOMY OF VAGAL AFFERENT CELL BODIES

A vagal primary afferent neuron is a pseudo-unipolar cell consisting of a spheroidal cell body (somata), an initial tract of axon (stem process) that extends from the cell body to a site of bifurcation (a distance ranging from a few μm to 100s of μm), and peripherally and centrally projecting processes.[42] The cell bodies of vagal primary afferents are housed in two separate vagal ganglia. Cell bodies in the superior vagal ganglion or jugular ganglion (JG), like neurons from spinal ganglia, are derived from the neural crest (see Chapter 1). Axons of JG neurons innervate the pharynx and larynx,[18] lower airways,[36,54] skin of the external acoustic meatus, and dura of the posterior cranial fossa.[4] The inferior vagal ganglion or nodose ganglion (NG) contains cell bodies that are derived from the placodal ectoderm (see Chapter 1), and innervate almost all viscera, including airways, heart, gastrointestinal tract, liver, thymus, uterus, neuro-epithelial bodies, and vagal paraganglia.[4,46]

---

* Though Mandelowitz and Kunze's 1992 paper appears to be the first report of electrophysiological studies of target-identified primary afferent cell bodies, a series of preliminary observations from Chuck deGroat's laboratory appeared in 1989 and 1990, detailing the application of fluorescent retrograde tracers with patchclamp recording to study isolated, target-identified dorsal root ganglion neurons; a full account of these observations did not appear until 1994 (Yoshimura et al., 1994).

There are approximately three times as many NG neurons as JG neurons (~25,000 vs 8,500 for vagal ganglia of the cat.[18] Based upon measurements of cross-sectional area, cell diameters, or membrane capacitance, the distribution of cell body sizes appears to be unimodally distributed for vagal ganglion neurons (VGNs). In rat, for example, NG neurons range in size from 56 μm^2 to 1631 μm^2 (mean, 595 μm^2), while JG cell body sizes varied between 80 μm^2 and 1288 μm^2 (mean, 391 μm^2).[29] Corresponding values for rat VGN size based upon membrane capacitance are: 20 pF to 60 pF (mean, 31 pF) for NG neurons, and 22 pF to 59 pF (mean, 32 pF) for JG neurons. Approximate mean cell body size based upon diameters measured from acutely isolated NG neurons for mouse, rat, guinea pig, rabbit, and ferret are: 33 μm, 35 μm, 39 μm, 61 μm, and 54 μm, respectively.

Like most sensory ganglia, detectable synaptic profiles have not been described in the adult JG or NG (Reference 42), although NG somata can chemically communicate with one another.[52] The nature of the mediator(s) supporting this form of neuronal communication remains to be identified.

4.3 DISSOCIATION OF VAGAL AFFERENT CELL BODIES FROM ADULT VAGAL GANGLIA

Ikeda and coworkers[30] initially developed an enzymatic dispersion procedure to isolate single nodose ganglion neurons from adult rats to study voltage-sensitive sodium and calcium currents with patch-clamp recording techniques. Their procedure used a combination of trypsin (type III, 1 mg/ml), collagenase (type 1A, 1mg/ml), and DNAase (type III, 0.1 mg/ml). General protocols for isolating adult primary sensory cell bodies have recently been published by Spigelman et al.[57] We have developed a relatively uncomplicated procedure for isolating nodose and jugular ganglion neurons from adult ganglia from various species (mouse, rat, guinea pig, rabbit, and ferret) using collagenase and dispase. This procedure consistently provides high yields of viable vagal cell bodies (in the case of rabbit > 90 % recovery of nodose neurons).[40]

After removing vagal ganglia, they are transferred to a dissecting chamber containing ice cold (4° C) calcium-free, magnesium-free Hank's Balanced Salt Solution (HBSS). Using a dissecting microscope, the adhering connective tissue, blood vessels, and other debris are removed from the ganglia with the aid of fine-sharpened watchmaker forceps and iris scissors. When suitably trimmed, it should be possible to visualize individual cell bodies with the dissecting microscope. What is visualized is a sack of cells surrounded by a thin transparent sheath. The reason for carefully trimming the ganglia is to reduce exposure time and concentration of digestive enzymes. In the case of larger nodose ganglia, those from guinea pig, rabbit, and ferret, nicks are made into the ganglia with iris scissors or the ganglia are cut into three to six segments.

The ganglia, or ganglion fragments, are transferred to a sterile 15 ml conical tube containing 5 ml cold, filter sterile (0.22 μm millex-Gs, Millipore) HBSS with 1 mg/ml collagenase (Type 1A, Sigma, C-9891) and 1 mg/ml dispase (grade II, Boehringer, Mannheim, A-7292). The tube containing the ganglia is either incubated

at 37° C for 2 hours, or placed in a 4° C refrigerator for 4 hours, or overnight. For the 37°C incubate, at 45 min, and 90 min the tissue is gently triturated with a fire-polished Pasteur pipette five times, taking care to avoid bubbles. At two hours the ganglia are triturated with a small-bore fire-polished Pasteur pipette. The orifice of the pipette should be just larger than the ganglia or ganglion segments. Only a few (3 to 8) triturations should be necessary to completely dissociate the neurons; the fewer the number of triturations, the less cell damage occurs. After trituration the neurons are centrifuged (700g, 45 sec) and the pelleted cells are resuspended in L15 media (GiBCO BRL containing heat-inactivated 10 % fetal bovine serum; JRH Biosciences). The neurons are washed two more times by centrifugation and then 150 μl aliquots of cells are transferred onto circular 15- or 25-mm glass cover slips coated with poly-D-lysine (0.1 mg/ml, Sigma) lying on the floor of 35 mm petri dishes. The cell bodies adhering to the cover slips are maintained for two hours after plating at 37° C and then they are used for recording or an additional 2 ml of culture medium is added to the petri dishes and the cells are transferred to a room-temperature incubator for storage. For the cold-incubated ganglia, at 4 hours, or longer, 4.5 ml of enzyme solution is removed and replaced with 4 ml of prewarmed enzyme solution and the tissues are incubated for 5 to 10 min at 37° C. After trituration (1 to 3 times) with a large-bore, fire-polished Pasteur pipette, the cells should dissociate completely. Then the cells are processed as described above for the 2-hour incubation. Though we have not performed a systematic investigation on the electrophysiological properties of the cell bodies prepared by these two methods, there do not appear to be any obvious differences in the passive or active membrane properties or to the responses to a panel of autacoids between the two procedures. The advantage of the cold incubation procedure is that tissue can be prepared in the evening then used the following morning. Isolated VGNs maintained at room temperature are used for recording for up to 48 hours.

We have not used antibiotics in our protocols because, with careful sterile technique, we have rarely encounter bacterial contamination. Over the years, we have found that the largest variable with the dissociation procedure is the activity of the collagenase. Adjustment between different lots can be made based upon specific activity and time of incubation. We have noted that once a suitable lot is optimized, then a year's supply is purchased and stored at –80°C. Manufacturers will often provide gratis small samples of different lots in order to choose an appropriate lot. A month's supply of enzyme solution can be prepared and divided aliquots stored at –20°C, facilitating the time necessary to prepare cells.

4.4   SELECTION OF DYE FOR RETROGRADE LABELING VAGAL GANGLION NEURONS

Honig and Hume[28] popularized the use of long-chain carbocyanine fluorescent dyes for neuronal labeling and pathway tracing. These dyes are ideal for retrogradely labeling neurons in intact tissues; they were essentially nontoxic, and there was no significant spread of dye from labeled cells to other cells. Subsequently, it was determined that there was no loss of label following acute dissociation of neurons

from primary sensory ganglia previously retrogradely labeled with fluorescent dyes.[13,47] A complete list of available fluorescent dyes and their attributes for retrograde labeling can be found in Handbook of Fluorescent Probes and Research Products.[48]

There are a large number of fluorescent tracers available for retrograde tracing; choosing the most suitable dye depends upon the end organ being labeled. Currently, the most commonly used dyes for retrograde labeling VGNs are long-chain lipophilic carbocyanine dyes (DiI, DiO, DiD, and DiR). In-depth information about the chemistry and use of these dyes can be found in chapter 14 of A Handbook of Fluorescent Probes and Research Products.[48] Because these dyes have a wide range of wavelength emission peaks, ranging from ~500 to 800 nm, it is possible to combine an appropriate retrograde dye with another fluorescent indicator. For example, simultaneous whole-cell patch-clamp and Fura-2 microfluorimetric recordings of Ca^{2+} currents and intracellular Ca^{2+} concentration can be accomplished from target-identified VGNs retrogradely labeled with DiD. In addition, because the carbocyanine dyes have absorption and fluorescence emission maxima separated by ~65 nm, several lipophilic carbocyanine dyes can be used to identify VGNs innervating two or more visceral organs or different areas within the same organ. Two newer dyes, Fast DiI and Fast DiO, have diunsaturated linolely ($C_{18:2}$) tails instead of saturated octadecyl tails (C_{18}). These chemical modifications are touted to substantially improve the rate of dye migration over that observed with DiI or DiO; however, little data is currently available about the migration rates of these dyes with respect to retrogradely labeling VGNs.[55]

Numerous methods exist for applying fluorescent tracers to tissues. Two of the most common are direct application of dye crystals to intact axons,[47] or injection of the tracer into organs or the vagus nerve. When injected, lipophilic carbocyanine dyes are dissolved in either dimethylsulfoxide, (up to 10 %), dimethylformamide (0.5 to 10%), or ethanol or methanol (2 to 5%). Usually multiple injections of (3–20 µl/site) are used. When labeling VGNs innervating lungs and airway much larger volumes of dye are used, 2×200 µl of 0.2 to 0.4 mg/ml DiI in 1% ethanol, in saline is instilled into the lumen of the airway.[13,37]

The time required to label VGNs with a retrograde tracer varies with target distance, nature of the dye, species, and age of the animal. In the adult rat (>150 gm), labeled nodose ganglion neurons innervating baroreceptors,[59] stomach,[17] or airways[37] with DiI dye was detected after 7 to 10 days.

One of the contentious problems generic to using retrogradely labeled somata for physiological studies of voltage-and ligand-gated channels is the argument that the properties of ion channels and chemoreceptors being studied may be altered by the labeling procedure. This problem is particularly applicable with the use of carbocyanine dyes because for injection they must be dissolved in methanol, DMSO, or other solvents that can cause localized inflammation or direct damage to the very cells that are being labeled. It is difficult to circumvent this argument directly. Several strategies are employed to minimize this argument. Waiting extended time periods (one to two weeks) after VGNs are retrogradely labeled before making physiological measurements should minimize injury- or inflammation-induced changes in the VGNs evoked by tracer application. In addition, it is possible to determine that the

electrical membrane properties (action potential waveform, chemosensitivity, resting conductance, etc.) of labeled VGNs are similar to those recorded from adjacent nonlabeled VGNs residing on the same coverslip.

4.5 PREPARATIONS USEFUL FOR STUDYING VAGAL AFFERENT CELL BODIES

There are a variety of experimental preparations that can be used when studying target-identified VGNs. These range from intact animals to acutely isolated somata. Though in principle there should be no experimental limitation in recording intracellularly from target-identified primary vagal afferent somata in intact animals, such recordings have not yet been reported. This is unfortunate because much could be learned from such preparations (e.g., testing the efficacy and magnitude of chemical communication between target-identified VGN somata labeled from different visceral).[52]

Recordings of target-identified VGNs in intact vagal ganglia either *in vivo* or *in vitro* have the advantage of correlating somatic electrical and chemical properties with action potential discharge patterns and conduction velocities in peripheral and central vagal axons. It has recently become feasible to apply whole-cell patch clamp recording techniques to adult intact nodose ganglia.[41] With this preparation it will be possible to classify somal voltage-and ligand gated ion channel types with action potential conduction velocities with target-identified vagal afferents.

Patch clamp recording has several advantages over "sharp" micropipettes: less shunting of the resting conductance yielding approximately an order-of-magnitude lower resting conductances; control of the internal ionic milieu for accurate determination of reversal potential values, or to isolate specific classes of ionic currents; the ability to introduce large molecular weight or nonionic substances (enzymes, antibodies, caged reagents, etc.) into somal compartments, and the capability to extract the intracellular milieu for studies of genes and gene products. The most common preparation utilizing target-identified VGNs is the acutely isolated VGN. Here investigators can combine the attributes of target-identified vagal somata with the methodological advantages afforded by using isolated primary afferent cell bodies; in particular, application of patch-clamp recording.

4.6 ATTRIBUTES, LIMITATIONS, AND CONCERNS WHEN STUDYING ISOLATED TARGET-IDENTIFIED VAGAL SENSORY CELL BODIES

4.6.1 ATTRIBUTES

Ikeda et al.[30] pioneered the use of primary vagal afferent cell bodies isolated from adult vagal ganglia for electrophysiological studies. They developed methods to enzymatically disperse nodose ganglion neurons with surface membranes sufficiently free of debris that it was possible to form giga-ohm seals, thereby allowing the application of patch-clamp techniques to VGNs. The same attributes associated

with patch-clamp recording from identified VGNs described earlier for studies of VGNs in the intact ganglia also hold for isolated VGNs with the additional experimental advantage that it is far easier to perform patch-clamp recordings with isolated VGNs.

Isolated VGNs possess many properties that make them very attractive for studying the electrical properties and chemosensitivity of vagal afferents. Anatomically, dissociated VGNs are isolated from satellite cells that normally surround each VGN in the intact ganglia. This situation is not only indispensable for patch-clamp recording and allowing rapid exchange of extracellular milieu, it is critical in for determining that drug- or pathology-induced changes in neuronal excitability are occurring directly from the neuron under study. It is known, for example, that satellite cells surrounding primary afferent cell bodies can release substances that alter the excitability of the primary afferent neuron. Bradykinin, for example, can exert a direct nociceptive effect on isolated NG neurons by blocking spike frequency adaptation[65] and by depolarizing the membrane potential by activating a chloride conductance.[53] It can also indirectly affect the excitability of primary afferent neurons by evoking an inward current that requires contact between the primary afferent somata and nonneuronal satellite cells.[23]

During the isolation procedure, the soma is sheared away from the stem process yielding nearly round neurons, a geometry that minimizes space-clamp errors. Isolated VGNs can be derived from adult animals, thereby obviating the reliance on the use of neurons derived from neonatal animals. Importantly, many voltage-gated currents as well as ionotropic and metabotropic receptors observed in the neurons from intact ganglia are not significantly altered by the isolation procedure. In an in-depth study, Leal-Cardoso et al.[40] compared the passive and active electrical membrane properties and the chemosensitivity of intact and acutely dissociated adult rabbit NG neurons (see Table 4.1, Table 4.2, and Table 4.3). Their results revealed

---

TABLE 4.1

Comparison of Passive Membrane Properties of Acutely Isolated Rabbit Nodose Neurons with Neurons from Intact Nodose Ganglion *In Vitro*

Parameter	Intact Ganglion	Acutely Dissociated
Resting Potential (mV)	-58 ± 0.6 (29)	-59 ± 0.6 (108)
Input Resistance (MΩ)	81 ± 4.4 (29)	80 ± 5.3 (104)
Time Constant (msec)	8.5 ± 0.8 (50)	5.7 ± 0.5 (47)
Membrane Resistance (kΩ/cm^2)	9.1	9.3
Membrane Capacitance (μF/cm^2)	0.92	0.78
Cell Diameter (μm)	60 ± 1.2 (35)	61 ± 1.6 (90)

Source: Data from Leal-Cardoso et al.[40] Values are means ±SEM. Numbers in parentheses are n values. All parameters were recorded at room temperature (21° to 23°C) with sharp micropipettes filled with 2 M KCl and 1 M K acetate. Recordings from isolated neurons were made between 2 to 4 hours after plating cells on glass coverslips. Recordings from intact nodose ganglion neurons were made between 1 to 2 hours after the nodose ganglion was *in vitro*.

---

essentially no differences between the membrane properties recorded from acutely isolated NG neurons and nodose neurons in intact vagal ganglia. Both ionotropic and metabotropic receptor-mediated ion channel function were unaffected by the isolation procedures. Noteworthy, the labile and metabolically dependent ($Q_{10} = 3$–4) slow spike afterhyperpolarization that is observed in ~ 40% of the rabbit NG neurons

TABLE 4.2

Comparison of Action Potential Properties of Acutely Isolated Rabbit Nodose Neurons with Neurons from Intact Nodose Ganglion *In Vitro*

Action Potential Parameter	Intact Ganglion	Acutely Dissociated
Amplitude (mV)	91 ± 0.7 (230	79 ± 1.2 (105)
Duration (msec)	3.5 ± 0.1 (23)	5.2 ± 0.1 (92)
Overshoot (mV)	26 ± 0.9 (23)	21 ± 1.0 (105)
Max. Rate of Rise (V/sec)	120 ± 9.4 (22)	52 ± 4.1 (80)
Spike Threshold (mV)	–41 ± 0.4 (23)	–38 ± 0.9 (98)
AHP$_{fast}$ Duration (msec)	89 ± 14.1 (16)	64 ± 3.8 (86)
Amplitude (mV)	13 ± 4.0 (20)	10 ± 0.5 (86)
AHP$_{slow}$ Duration (sec)	19.2 ± 0.8 (12)	13.1 ± 1.6 (23)
Amplitude (mV)	7.5 ± 0.3 (12)	9.5 ± 1.2 (23)

Source: Data from Leal-Cardoso et al.[40] Values are means ± SEM. Numbers in parentheses are n values. All parameters were recorded at room temperature (21° to 23°C) with "sharp" micropipettes filled with 2 M KCl and 1 M K acetate. Recordings from isolated neurons were made between 2 to 4 hours after plating cells on glass coverslips. Recordings from intact nodose ganglion neurons were made between 1 to 2 hours after the nodose ganglion was *in vitro*. AHP$_{fast}$ and AHP$_{slowt}$ are fast and slow spike afterhyperpolarizations, respectively. AHP$_{slow}$ elicited by four action potentials at 10 Hz.

TABLE 4.3

Chemosensitivity of Acutely Isolated Rabbit Nodose Neurons to Various Autacoids

Measurement	Serotonin	Bradykinin	Acetylcholine	Histamine
No. of Neurons Tested	28	21	23	23
Resting Potential (mV)	–58 ± 0.6	–59 ± 0.5	–59 ± 0.5	–58 ± 0.7
Input Resistance (Mohm)	67 ± 5.0	73 ± 6.6	71 ± 5.3	72 ± 5.2
Response (mV)	22 ± 2.1	3 ± 0.7	5 ± 0.8	4 ± 0.7
Percent Responding	79 (80)[a]	43 (36)	43 (33)	30 (24)

Source: Data from Leal-Cardoso et al.[40] Values are means ± SEM. All parameters were recorded at room temperature (21-23°C) with sharp micropipettes filled with 2 M KCl and 1 M K acetate. Recordings from isolated neurons were made between 2 to 4 hours after plating cells on glass coverslips.

[a] Values in parentheses are from data of Higashi et al.[25] obtained from intact ganglia.

in intact nodose ganglia[21] was not significantly altered in its magnitude, duration, or distribution in acutely dissociated NG neurons.

In many, but not all, respects acutely isolated somata of VGNs are convenient models for the less accessible, small, and morphologically complex peripheral and central nerve terminals. Voltage-gated ion channels (see Chapter 3), chemoreceptors, and physical transducers that exist in vagal afferent nerve terminals are also present and functional in the membranes of VGNs. Representative examples of somal receptors include: mechanoreceptors,[59] osmoreceptors,[15,17] TRV1 receptors,[5,43] Ca^{2+} sensing receptor/ion complex,[61] bradykinin receptors,[35,65] neurokinin receptors,[32,66] histamine H_1 receptors,[31,62] CCK-8 receptors,[19] serotonin receptors,[12,25] eicosanoid receptors,[56,62] and purinergic receptors.[27,33,34]

When considering the presence of functional autacoids and transmitter receptors in the membranes of VGNs, it is important to recognize that many agonists do not produce measurable changes, or only minimal changes, in excitability when recordings are carried out at room temperature (21° to 23°C) but do show prominent effects when recordings are made at physiological temperatures (33° to 37°C). Representative examples include: angiotensin,[67] bradykinin,[53] dopamine,[39] and Substance P.[64]

4.6.2 LIMITATIONS AND CONCERNS

There are a number of notable limitations and concerns when using acutely isolated vagal sensory cell bodies in general and target-identified VGNs in specific. By the very nature of isolating vagal afferent somata, these neurons have become axotomized. Axotomy can elicit a profound spectrum of morphological, physiological, and biochemical alterations in the nerve cell body, a process designated the retrograde response or the axon reaction. For example, vagotomy can dramatically decrease the excitability of NGNs, increasing action potential threshold by more than 200%, and reducing action potential discharge by up to 80% in response to a suprathreshold depolarizing stimuli.[38] These changes require >24 hours to develop. To minimize the effects of vagotomy, isolated VGNs are studied within a few hours after dissociation. The effects of vagotomy can also be minimized by maintaining neurons at room temperature. This has the effect of extending the useful life of the isolated neurons and reducing growth of neurites that can markedly affect the control of membrane voltages. VGNs can be maintained at room temperature (22°C) for several days, a procedure initially developed for isolated sympathetic neurons.[44]

A particularly confounding problem associated with the use of isolated VGNs is the potential redistribution of receptors upon cell isolation. There is a growing number of reports showing that some chemoreceptors, mechano- and thermo-transducers that reside in nerve terminals are not always present in membranes of cell bodies in the intact sensory ganglion, yet they become expressed and functional when the somata are isolated and held in culture. Cell bodies of primary afferent neurons do not ordinarily respond to mechanical stimulation, yet mechanosensitive currents can be readily recorded from these after a few days in culture.[45,59] Similarly, the excitatory actions of cold temperature are not observed in primary sensory somata

(trigeminal ganglion cells) but are evident at the level of the nerve terminal.[9] The discrepancy between the presence of chemoreceptors in isolated primary afferent somata but absent in cell bodies situated in sensory ganglia has also been noted. This problem was first revealed in the classic paper of Baccaglini and Hogan[2] in which they reported that the number of capsaicin-sensitive neurons and the fraction of neurons staining for Substance P were much larger for primary afferent neurons (dorsal root ganglion cells) in culture than was observed in intact ganglia. More recently Stebbing et al.[58] reported that < 6% of somata in intact dorsal root ganglia express functional purinoreceptors while ~ 90% of acutely dissociated somata responded to ATP with an inward current. These observations point out that caution should be exercised when studying receptor-mediated currents or voltages in isolated cell bodies and extrapolating this information to nerve terminals without information that the same receptors exist at the nerve terminals of the vagal afferents.

It is important to recognize that potential deleterious effects can occur when using fluorescent dyes to identify neurons for physiological studies. Protracted fluorescent excitation of labeled neurons can lead to profound changes in electrophysiological parameters, depending on the nature of the tracer, its concentration, excitation wavelength, and duration of epifluorescent illumination (see Table II and Figure 5 in Christian et al.[13], and also Figure 3 in Yoshimura et al.[69]). For example, when using dextran-tetramethylrhodamine, Fast Blue, or Fluorogold dyes, obvious signs of action potential broadening and depolarization of the membrane potential can occur with 30 to 40 sec of illumination. By contrast, when neurons are illuminated for a minimal amount of time to identify cell bodies with a fluorescent tracer (1 to 3 sec), neurons exhibited stable passive and active membrane properties similar to those recorded in nonlabeled neurons. The long-chain carbocyanine lipophilic neuronal tracer like DiA and other analogs appear to produce less deleterious membrane effects. To minimize the possibility of fluorescent tracers altering electrophysiological parameters, it would be prudent to restrict the duration of epifluorescent illumination to a minimal time necessary to identified labeled neurons. This process can be greatly facilitated by the use of an electronic shutter positioned between the epifluorescent illuminator and the microscope in conjunction with an inexpensive CCD camera.

4.7 PHYSIOLOGICAL STUDIES OF TARGET-IDENTIFIED VAGAL AFFERENT CELL BODIES

4.7.1 STUDIES OF BARORECEPTORS

The nerve terminals of baroreceptor neurons respond to increases in arterial blood pressure with a barrage of action potential activity triggering CNS-mediated reflexes vital to maintaining cardiovascular regulation. Nodose ganglion contain the cell bodies of aortic baroreceptors that contain transcripts for DEG/ENaC subunits, putative mechanosensitive ion channels.[17] By labeling baroreceptor endings in the aortic arch with DiI it is possible to isolate target-identified nodose ganglion

baroreceptor cell bodies for physiological and pharmacological studies with patch-clamp techniques.

Labeled baroreceptor cell bodies are significantly more sensitive to hypoosmotic stretch than nonlabeled nodose cell bodies. Hypoosmotic stretch produces an inward current with an increased membrane conductance and a reversal potential value consistent with the activation of a nonselective cation channel.[15] These electrophysiological observations suggest that these mechanosensitive ion channels may be involved in mechanoelectric transduction in baroreceptor nerve terminals.

Baroreceptor neurons possess a variety of low- and high-threshold calcium channels.[47] Low- voltage, T-type calcium channels likely contribute to activation of baroreceptors and support repetitive action potential activity in these neurons. High-voltage calcium channels are known to mediate many intracellular calcium-dependent processes in NGNs; in particular, they trigger activation of calcium-dependent calcium-release pools of intracellular calcium.[14] High-voltage calcium channels in target-identified nodose baroreceptor neurons are modulated by μ-opioid receptor activation perhaps contributing to the opioid-mediated attenuation of baroreflex activity.[22]

4.7.2 AIRWAY VAGAL AFFERENT C-FIBERS COMPRISE TWO DISTINCT PHENOTYPES

Using target-identified VGNs, Undem and his colleagues[54,60] applied immunocytochemistry, extracellular, and intracellular recording techniques to reveal that vagal C-fiber innervation of the intrapulmonary system is different from the extrapulmonary airways and that these two C-fiber populations represent distinct phenotypes. Retrograde tracing from the airways with fast blue showed that C-fibers innervating the pulmonary system are derived from vagal cell bodies situated in NG and JG. The nerve terminals of vagal afferents in the lungs can be activated by capsaicin and bradykinin but only the nodose C-fibers nerve terminals responded with action potential discharges following application of ATP or the P2X selective receptor agonist α,β-methylene ATP. Patch-clamp recordings from retrogradely labeled airway cell bodies revealed capsaicin responsive C-type cell bodies existed in both JG and NG. Lung-specific C-fiber nodose cell bodies expressed functional P2X receptors whereas lung-specific jugular C-fiber somata were categorically unresponsive to purinergic agonists. The nodose and jugular C-fibers projecting to the bronchopulmonary system are not only different with respect to their chemoresponsiveness but they also differ in their neuropeptide content.[54] Most Substance P containing vagal C-fiber somata innervating the airway reside in the JG. These data indicate that two classes of vagal C-fibers can be distinguished based upon their distribution within the lungs, their neuropeptide content, and their responsiveness to nociceptive substances. They also indicate that the chemosensitive properties of sensory airway nerve endings depend on the ganglionic origin of the supplying nerve fiber. These results illustrate how target-identified VGNs can be used to answer fundamental questions about the function of vagal sensory neurons.

4.7.3 ELECTROPHYSIOLOGICAL PROPERTIES AND CHEMICAL RESPONSIVENESS OF PARASYMPATHETIC AND SYMPATHETIC PRIMARY SENSORY NEURONS INNERVATING THE AIRWAYS

Visceral organs, including airway, are dually innervated by sympathetic and parasympathetic neurons Parasympathetic primary sensory neurons(vagal afferents) run through vagus nerves and have their cell bodies situated in NG and JG. The cell bodies of sympathetic airway sensory neurons (somatic afferents) reside in upper thoracic (T1-4) DRG. By contrast to the wealth of information about the physiology of parasympathetic airway sensory afferents, there is only limited amount of information about the function and cellular characteristics of sympathetic airway afferents. Oh et al.[51] utilized airway-identified sensory cell bodies isolated from NG, JG, and DRG to compare the electophysiological properties and chemosensitivity of sympathetic and parasympathetic airway afferent neurons.

Parasympathetic and sympathetic airway sensory neurons were comprised of both A- and C-type neurons as determined by neuronal size, action potential waveforms, and capsaicin sensitivity. Both parasympathetic and sympathetic afferent cell bodies fired tonically following a depolarizing current step regardless of ganglia and neuronal type. Thus, all airway primary sensory neurons could be classified as nonaccommodating or tonic neurons. Exogenously applied serotonin (5-HT, 10 μM) increased the excitability of airway sensory neurons from all three ganglia. However, the cellular mechanism underlying the actions of 5-HT differed depending upon the location of the primary afferents. In the majority of NG of neurons (78%) 5-HT evoked an inward current (~2.0 nA) that was associated with an increased membrane conductance. By contrast, 5-HT did not elicit measurable membrane currents in most of the airway sensory JG (72%) or DRG (68%) neurons. In these cells, 5-HT lowered the membrane potential for spike initiation (~4 mV) and reduced the current required to reach spike threshold.

ATP induced long-lasting (>10 sec) inward currents in 100% of airway-identified NG cell body tested. By contrast, ATP evoked relatively short duration responses (<1 sec) in 27% and 32% of airway JG and DRG cell bodies, respectively. These data show that airway primary afferent neurons existing in different sensory ganglia possess distinct cellular mechanisms underlying autacoid-induced changes in membrane excitability. These differences may reflect the existence of distinct receptors or second messenger pathways. Such differences may provide a basis to develop therapeutics that may be selective for different subpopulations of airway sensory neurons.

4.7.4 BRADYKININ EXCITES AIRWAY SENSORY NEURONS BY PROMOTING A CALCIUM-DEPENDENT CHLORIDE CURRENT

While studying the excitability changes produced by inflammatory mediators on isolated airway-identified sensory neurons, Oh and Weinreich[53] characterized a novel cellular mechanism underlying the excitatory action of bradykinin (BK), a nonapeptide inflammatory mediator. BK can alter the function of distinct populations of ion channels to exert increases in neuronal excitability. It can block a slowly activating

potassium current (M-current),[26] obtund a calcium-dependent potassium current (I_{AHP} current),[63,65] evoke an inward sodium current,[8] and activate nonselective cation channels via modification of TRPV1 receptors.[11] In airway-identified VGNs, BK causes a membrane depolarization, evokes action potential activity, and induces an inward ionic current (I_{BK}). Measurements of reversal potential values in conjunction with changes in extracellular and intracellular ion composition revealed that chloride ions were the major charge carriers for I_{BK}. Reducing the concentration of extracellular calcium had no effect on I_{BK} but buffering intracellular calcium with BAPTA or bath application of niflumic acid, a calcium-activated chloride channel blocker, inhibited I_{BK}. These results imply that the BK-evoked a chloride current that was dependent upon a rise in intracellular calcium concentration. These observations demonstrated, for the first time, that BK can excite primary afferent neurons by modifying an anion channel.

4.8 PATHOPHYSIOLOGICAL STUDIES OF TARGET-IDENTIFIED VAGAL AFFERENT CELL BODIES

Electrophysiological techniques have been widely used to examine how injury (physical, chemical, or immunological) produces changes in primary afferent neurons. Many injury-induced changes occur at or near the site of injury, often in the peripheral nerve terminals. The morphological complexity, small size, and inaccessability of nerve endings does not support the use of intracellular or patch-clamp recording techniques for direct cellular studies of injury-induced changes in these neurons. However, many injury-induced changes to primary afferent neurons are also reflected by alterations in electrophysiological properties of their cell bodies. It is often observed that voltage-sensitive currents are changed in somal membranes of neurons whose axons projects to a tissue that is inflamed. For example, chronic bladder inflammation sensitizes mechanosensitive afferents and increases the excitability of isolated bladder-identified afferent cell body, in part by suppressing an A-type, voltage-sensitive, potassium current.[68] The success of these experiments critically depended upon the ability to re-identify primary afferent cell bodies (DRG neurons) innervating the bladder. In this section, several examples are provided illustrating how studies of target-identified vagal afferent cell bodies have been used to gain insights into cellular basis of injury-provoked changes in excitation or sensitization.

4.8.1 GASTRIC INFLAMMATION

Gebhart and associates[6,16] used target-identified vagal cell bodies to study the mechanisms associated with excitability changes in primary afferents triggered by gastric inflammation. Using a rat model of gastric hyperalgesia, produced by multiple injections of acetic acid into the stomach wall, these investigators examined voltage-sensitive currents in isolated NG and DRG gastric-identified cell bodies. Patch-clamp recordings of retrogradely dye-labeled cells revealed that gastric inflammation altered both sodium and potassium currents. Sodium currents recovered significantly more rapidly from inactivation in neurons obtained from animals in the ulcer group compared with controls due, in part, to an enhanced contribution of the TTX-resistant

sodium current to the peak sodium current. The recovery kinetics of the TTX-sensitive sodium current was faster in the ulcer group. Gastric inflammation also reduced the density of A-type potassium current, shifted its steady-state inactivation to a more hyperpolarized membrane potential, and accelerated the inactivation kinetics. These changes in ionic currents are likely to contribute to the enhanced excitability of gastric afferents observed during gastric inflammation and perhaps during dyspeptic symptoms. An interesting observation from this work was that inflammation increased TTX-resistant current in both vagal and spinal afferents. Changes in TTX-resistant currents are often associated with the development and maintenance of pain, hyperalgesia, and allodynia, sensations not typically associated with parasympathetic afferents.

4.8.2   Airway Inflammation

Application of retrograde tracers to the airways of guinea pigs revealed that the cell bodies of the primary afferents innervating the airway are housed in two separate ganglia, the JG and the NG.[54] Though many of the cell bodies in both these ganglia contain tachykinins, such as Substance P and Neurokinin A, under normal conditions all the vagal tachykininergic fibers innervating the guinea pig airways are derived nearly exclusively from cell bodies in the JG.[54] Viral infection[10] or allergen-induced infection[20,49] of the airways causes an induction of tachykinin expression in NG cell bodies that innervate the airways. Interestingly, this phenotypic switch in the expression of tachykinins in NG neurons occurred in large, fast-conducting low-threshold mechanically sensitive Aδ-type neurons.[49] Electrophysiological studies of these airway-labeled Aδ-type somata revealed that they were insensitive to nociceptive stimuli such as capsaicin and bradykinin. Thus, it is possible that during airway inflammation non-noxious activation of low-threshold mechanosensory nerve terminals can cause tachykinin release that can contribute to exaggerated reflexes that accompany inflammatory diseases.

4.9   CONCLUSIONS AND FUTURE DIRECTIONS

It has been just over a decade since the first report was published describing the use of acutely isolated, target-identified, primary vagal afferent cell bodies for electrophysiological studies. It is now clear that this preparation is an invaluable model system for answering many fundamental physiological, pharmacological, and pathological questions about the vagus nerve. The ability to re-identify subpopulations of vagal sensory somata based upon the organs they innervate allows detailed cellular and molecular measurements to be made before and subsequent to brief and chronic manipulations of an end organ.

Most neuronal populations are heterogeneous with respect to the expression of plasma membrane proteins; primary vagal afferent neurons are no exception. To convert specific visceral modalities into electrical signals and pass these signals to the CNS, vagal sensory neurons have evolved a specific set of receptor proteins that are specialized to detect and transduce specific sensory stimuli. These vagal receptors include: mechanoreceptors (rapidly and slow adapting) chemoreceptors (alkali-and

acid sensitive receptors; amino acid receptors, glucoreceptors, autacoid receptors, etc.); thermoreceptors (cold and heat); osmoreceptors and nociceptors. Some of these transduction proteins are being identified and characterized. For example, the serpentine protein transient receptor potential V1 (TRPV1) is part of a receptor complex that responds to noxious stimuli, protons, heat, and endogenous ligands (fatty acids and eicosanoid derivatives); DEG/ENaC family of proteins (DEG-1, MEC-4, MEC-10, UNC-105, and UNC-8) may serve as mechanosensory channel proteins.[1] In the future, it should be possible to visually identify subpopulations of vagal afferent neurons based upon vital markers that can recognize these specialized receptor proteins or their distinct accessory proteins. Thus, functional subsets of vagal afferents innervating a given organ may be studied and manipulated for experimental and therapeutic purposes.

ACKNOWLEDGMENTS

REFERENCES

1. Askwith CC, Benson CJ, Welsh MJ, Snyder PM. (2001). DEG/ENaC ion channels involved in sensory transduction are modulated by cold temperature. *Proc. Natl. Acad. Sci.USA*, 98, 6459–6463.
2. Baccaglini PI, Hogan PG. (1983). Some rat sensory neurons in culture express characteristics of differentiated pain sensory cells. *Proc. Natl. Acad. Sci. U S A*, 80(2): 594–598.
3. Belmonte C, Gallego R. (1983). Membrane properties of cat sensory neurones with chemoreceptor and baroreceptor endings. *J. Physiol.,* 342: 603-14.
4. Berthoud HR, Neuhuber WL. (2000). Functional and chemical anatomy of the afferent vagal system. *Auton. Neurosci.*, 85(1–3):1–17.
5. Bielefeldt K. (2000) Differential effects of capsaicin on rat visceral sensory neurons. *Neuroscience*, 101 (3): 727–736.
6. Bielefeldt K, Ozaki N, Gebhart GF. (2002). Experimental ulcers alter voltage-sensitive sodium currents in rat gastric sensory neurons. *Gastroenterology*, 122(2): 394–405.
7. Bielefeldt K, Ozaki N, Gebhart GF. (2003). Role of nerve growth factor in modulation of gastric afferent neurons in the rat. *Am. J. Physiol. Gastrointest. Liver Physiol.*, 284(3): G499–507.
8. Burgess GM, Mullaney I, McNeill M, Dunn PM, Rang HP. (1989). Second messengers involved in the mechanism of action of bradykinin in sensory neurons in culture. *J. Neurosci.,* 9(9): 3314–2335.
9. Cabanes C, Viana F, Belmonte C. (2003). Differential thermosensitivity of sensory neurons in the guinea pig trigeminal ganglion. *J. Neurophysiol.,* 90(4): 2219–2231.

10. Carr MJ, Hunter DD, Jacoby DB, Undem BJ. (2002). Expression of tachykinins in nonnociceptive vagal afferent neurons during respiratory viral infection in guinea pigs. *Am. J. Respir. Crit. Care Med.,* 65(8): 1071–1075.

11. Carr MJ, Kollarik M, Meeker SN, Undem BJ. (2003). A role for TRPV1 in bradykinin-induced excitation of vagal airway afferent nerve terminals. *J. Pharmacol. Exp. Ther.,* 304(3): 1275–1279.

12. Christian EP, Taylor GE, Weinreich D. (1989). Serotonin increases excitability of rabbit C-fiber neurons by two distinct mechanisms. *J. Appl. Physiol.,* 67(2): 584–591.

13. Christian EP, Togo JA, Naper KE, Koschorke G, Taylor GA, Weinreich D. (1993). A retrograde labeling technique for the functional study of airway-specific visceral afferent neurons. *J. Neurosci. Methods*, 47(1–2): 147–160.

14. Cordoba-Rodriguez R, Moore KA, Kao JP, Weinreich D. (1999). Calcium regulation of a slow post-spike hyperpolarization in vagal afferent neurons. *Proc. Natl. Acad. Sci. U S A*, 96(14): 7650–7657.

15. Cunningham JT, Wachtel RE, Abboud FM. (1995). Mechanosensitive currents in putative aortic baroreceptor neurons in vitro. *J. Neurophysiol.*, 73(5): 2094–2098.

16. Dang K, Bielefeldt K, Gebhart GF.(2004). Gastric ulcers reduce A-type potassium currents in rat gastric sensory ganglion neurons. *Am. J. Physiol. Gastrointest. Liver Physiol.*, 286(4): G573–579.

17. Drummond HA, Price MP, Welsh MJ, Abboud FM. (1999). A molecular component of the arterial baroreceptor mechanotransducer. *Neuron*, 21(6): 1435–1441.

18. Dubois FS, Foley JO (1937). Quantitative studies of the vagus nerve in the cat II. The ratio of jugular to nodose fibers. *J. Comp. Neurol.*, 67: 39–87.

19. Dun NJ, Wu SY, Lin CW. (1991). Excitatory effects of cholecystokinin octapeptide on rat nodose ganglion cells in vitro. *Brain Res.,* 556(1): 161–164.

20. Fischer A, McGregor GP, Saria A, Philippin B, Kummer W. (1996). Induction of tachykinin gene and peptide expression in guinea pig nodose primary afferent neurons by allergic airway inflammation. *J. Clin. Invest.*, 98(10): 2284–2291.

21. Fowler JC, Greene R, Weinreich D. (1985). Two calcium-sensitive spike after-hyperpolarizations in visceral sensory neurones of the rabbit. *J. Physiol.*, 365: 59–75.

22. Hamra M, McNeil RS, Runciman M, Kunze DL. (1999). Opioid modulation of calcium current in cultured sensory neurons: mu-modulation of baroreceptor input. *Am. J. Physiol.,* 277(2 Pt 2): H705–713.

23. Heblich F, England S, Docherty RJ. (2001). Indirect actions of bradykinin on neonatal rat dorsal root ganglion neurones: a role for non-neuronal cells as nociceptors. *J. Physiol.*, 536(Pt 1): 111–121.

24. Higashi H. (1986). Pharmacological aspects of visceral sensory receptors. *Prog. Brain Res.*, 67: 149–162.

25. Higashi H, Ueda N, Nishi S, Gallagher JP, Shinnick-Gallagher P. (1982). Chemoreceptors for serotonin (5-HT), acetylcholine (ACh), bradykinin (BK), histamine (H) and gamma-aminobutyric acid (GABA) on rabbit visceral afferent neurons. *Brain Res. Bull.*, 8(1): 23–32.

26. Higashida H, Brown DA. (1986). Two polyphosphatidylinositide metabolites control two K^+ currents in a neuronal cell. *Nature*, 323(6086): 333–335.

27. Hoesch RE, Yienger K, Weinreich D, Kao JP. (2002). Coexistence of functional IP(3) and ryanodine receptors in vagal sensory neurons and their activation by ATP. *J. Neurophysiol.*, 88(3): 1212–1219.

28. Honig MG, Hume RI. (1989). Carbocyanine dyes. Novel markers for labelling neurons. *Trends Neurosci.* 12(9): 336–338.

29. Ichikawa H, Gouty S, Regalia J, Helke CJ, Sugimoto. (2004). Ca2+/calmodulin-dependent protein kinase II in the rat cranial sensory ganglia. *Brain Res.,* 1005(1-2): 36–43.

30. Ikeda SR, Schofield GG, Weight FF. (1986). Na$^+$ and Ca^{2+} currents of acutely isolated adult rat nodose ganglion cells. *J. Neurophysiol.,* 55(3): 527–539.

31. Jafri MS, Moore KA, Taylor GE, Weinreich D. (1997). Histamine H1 receptor activation blocks two classes of potassium current, IK(rest) and IAHP to excite ferret vagal afferents. *J. Physiol*., 503 (Pt 3): 533–546.

32. Jafri MS, Weinreich D. (1997). Substance P regulates Ih via a NK-1 receptor in vagal sensory neurons of the ferret. *J. Neurophysiol*., 79 (2): 769–777.

33. Khakh BS, Humphrey PP, Surprenant (1995). Electrophysiological properties of P2X-purinoceptors in rat superior cervical, nodose and guinea-pig coeliac neurones. *J. Physiol*., 484 (Pt 2): 385-95.

34. Krishtal OA, Marchenko SM, Pidoplichko VI. (1983). Receptor for ATP in the membrane of mammalian sensory neurones. *Neurosci. Lett.,* 35(1): 41–45.

35. Krstew E, Jarrott B, Lawrence AJ.(1998). Bradykinin B2 receptors in nodose ganglia of rat and human. *Eur. J. Pharmacol.*, 348(2–3): 175–80.

36. Kummer W, Fischer A, Kurkowski R, Heym C. (1992). The sensory and sympathetic innervation of guinea-pig lung and trachea as studied by retrograde neuronal tracing and double-labelling immunohistochemistry, *Neuroscience*, 49(3): 715–737.

37. Kwong K, Lee LY. (2002). PGE(2) sensitizes cultured pulmonary vagal sensory neurons to chemical and electrical stimuli. *J. Appl. Physiol*., 93(4): 1419–1428.

38. Lancaster E, Oh EJ, Weinreich D. (2001). Vagotomy decreases excitability in primary vagal afferent somata. *J. Neurophysiol*., 85(1): 247–253.

39. Lawrence AJ, Krstew E, Jarrott B. (1995) Functional dopamine D2 receptors on rat vagal afferent neurones. *Br. J. Pharmacol.,* 114(7): 1329–1334.

40. Leal-Cardoso H, Koschorke GM, Taylor G, Weinreich D. (1993). Electrophysiological properties and chemosensitivity of acutely isolated nodose ganglion neurons of the rabbit. *J. Auton. Nerv. Syst*., 45(1): 29–39.

41. Li BY, Schild JH. (2002). Patch clamp electrophysiology in nodose ganglia of adult rat. *J. Neurosci. Methods*, 115(2): 157–167.

42. Lieberman AR (1976). Sensory ganglia*, In: *The Peripheral Nerve*, Ed. DN Landon, John Wiley & Sons, Inc., New York, pp. 188–278.

43. Marsh SJ, Stansfeld CE, Brown DA, Davey R, McCarthy D. (1987). The mechanism of action of capsaicin on sensory C-type neurons and their axons in vitro. *Neuroscience*, 23(1): 275–278.

44. Magee JC, Schofield GG. (1991). Room temperature culture extends the useful life of adult neurons for voltage-clamp experiments. *J. Neurosci. Methods*, 38(2–3): 201–208.

45. McCarter GC, Reichling DB, Levine JD. (1999). Mechanical transduction by rat dorsal root ganglion neurons *in vitro. Neurosci. Lett*., 273(3): 179–182.

46. Mei, N. (1983). Sensory structures in the viscera*. In: *Progress in Sensory Physiology 4*. Eds. J. Antrum, D Ottoson, ER Perl, RF Schmidt, H Shimazu, WD Willis, Springer Verlag, New York, pp. 1–42.

47. Mendelowitz D, Kunze DL. (1992). Characterization of calcium currents in aortic baroreceptor neurons. *J. Neurophysiol*., 68(2): 509–517.

48. Molecular probes (2002). *Handbook of Fluorescent Probes and Research Products, 9th ed.*, Chapter 14. (http://www.probes.com/handbook/).

49. Myers AC, Kajekar, R, Undem BJ. (2002). Allergic inflammation-induced neuropeptide production in rapidly adapting afferent nerves in guinea pig airways. *Am. J. Physiol. Lung Cell Mol. Physiol.,* 284 (4): L775–781.

50. Nishi S, Minota S, Karczmar AG. (1974). Primary afferent neurones: the ionic mechanism of GABA-mediated depolarization. *Neuropharmacology*, 13(3): 215–219.

51. Oh EJ, Mazzone SB, Canning BS, Weinreich D. (2003). Electrophysiological properties of DRG neurons mediating a sympathetic airway reflex. *Soc. for Neurosc.,* Abstract.

52. Oh EJ, Weinreich D. (2002). Chemical communication between vagal afferent somata in nodose ganglia of the rat and the Guinea pig in vitro. *J. Neurophysiol.*, 87(6): 2801–2807.

53. Oh EJ, Weinreich D. (2004). Bradykinin decreases K^+ and increases Cl^- conductances in vagal afferent neurones of the guinea pig. *J. Physiol.*, 558(Pt 2): 513–526.

54. Riccio MM, Kummer W, Biglari B, Myers AC, Undem BJ. (1996). Interganglionic segregation of distinct vagal afferent fibre phenotypes in guinea-pig airways. *J. Physiol.*, 496 (Pt 2): 521–530.

55. Sekizawa S, Joad JP, Bonham AC. (2003). Substance P presynaptically depresses the transmission of sensory input to bronchopulmonary neurons in the guinea pig nucleus tractus solitarii. *J. Physiol.*, 552(Pt 2): 547–559.

56. Smith JA, Amagasu SM, Eglen RM, Hunter JC, Bley KR. (1998). Characterization of prostanoid receptor-evoked responses in rat sensory neurones. *Br. J. Pharmacol.*, 124(3): 513–523.

57. Spigelman I, Gold, MS Light, AR. (2001). Electrophysiological recording techniques in pain research. In: *Methods in Pain Research* Ed. L Kruger. CRC Press, New York, pp. 147–168.

58. Stebbing MJ, McLachlan EM, Sah P. (1998). Are there functional P2X receptors on cell bodies in intact dorsal root ganglia of rats? *Neuroscience*, 86(4): 1235–1244.

59. Sullivan MJ, Sharma RV, Wachtel RE, Chapleau MW, Waite LJ, Bhalla RC, Abboud FM. (1997). Non-voltage-gated Ca^{2+} influx through mechanosensitive ion channels in aortic baroreceptor neurons. *Circ. Res.*, 80(6): 861–867.

60. Undem BJ, Chuaychoo B, Lee MG, Weinreich D, Myers AC, Kollarik M. (2004). Subtypes of vagal afferent C-fibres in guinea-pig lungs. *J. Physiol.*, 556(Pt 3): 905–917.

61. Undem BJ, Oh EJ, Lancaster E, Weinreich D. (2003). Effect of extracellular calcium on excitability of guinea pig airway vagal afferent nerves. *J. Neurophysiol.*, 89(3): 1196–1204.

62. Undem BJ, Weinreich D. (1993). Electrophysiological properties and chemosensitivity of guinea pig nodose ganglion neurons *in vitro*. *J. Auton. Nerv. Syst.*, 44(1): 17–33.

63. Weinreich D. (1986). Bradykinin inhibits a slow spike afterhyperpolarization in visceral sensory neurons. *Eur. J. Pharmacol.*, 132(1): 61–63.

64. Weinreich D, Moore KA, Taylor GE. (1997). Allergic inflammation in isolated vagal sensory ganglia unmasks silent NK-2 tachykinin receptors. *J. Neurosci.,* 17(20): 7683–7693.

65. Weinreich, D., Koschorke, GM., Undem, BJ., Taylor, GE. (1995). Prevention of the excitatory actions of bradykinin by inhibition of PGI2 formation in nodose neurones of the guinea-pig in nodose neurones of the guinea-pig. *J. Physiol.*, 483, 735–746.

66. Weinreich, D,. Moore KA, Taylor GE. (1997). Allergic inflammation in isolated vagal sensory ganglia unmasks silent NK-2 tachykinin receptors. *J. Neurosci.*, 17(20): 7683–7693.

67. Widdop RE, Krstew E, Jarrott B. (1990). Temperature dependence of angiotensin II-mediated depolarisation of the rat isolated nodose ganglion. *Eur. J. Pharmacol.*, 185(1): 107–111.

68. Yoshimura N, de Groat WC. (1999). Increased excitability of afferent neurons innervating rat urinary bladder after chronic bladder inflammation. *J. Neurosci.*, 19(11): 4644–4653.

69. Yoshimura N, White G, Weight FF, de Groat WC. (1994). Patch-clamp recordings from subpopulations of autonomic and afferent neurons identified by axonal tracing techniques. *J. Auton. Nerv. Syst.*, 49(1): 85–92.

Part III

Vagal Sensory Nerve Terminals

5 Advances in Neural Tracing of Vagal Afferent Nerves and Terminals

Terry L. Powley and Robert J. Phillips

CONTENTS

5.1 OVERVIEW: NEURAL TRACERS PROVIDE ASSIGNABLE PHENOTYPES

Experiments on vagal afferents are often hampered by a lack of information about the precise distributions, as well as the specialized terminal architectures, of the peripheral processes of the neurons. As discussed elsewhere,[30] full analysis of an afferent system and its transduction mechanisms is impractical under such conditions. When the precise locations of the peripheral terminals are unknown, when the structural characteristics of the terminals are uninvestigated, and when any juxtapositions of the neurites with accessory cells or tissues are unknown, physiological investigations are significantly curtailed. This principle is clear in the abstract: Where would visual or auditory neuroscience be if such information about the retina and the cochlea were missing? Nonetheless, experimental approaches to the vagus frequently proceed under such handicaps.

Traditionally, there were few, if any, practical means of recognizing and analyzing the peripheral processes of vagal afferents. The viscera that the vagus innervates are commonly innervated by other visceral afferents, by extrinsic — including vagal — efferents, and by intrinsic neural networks. The complexity and heterogeneity of such innervation patterns means that vagal afferents cannot be unequivocally recognized unless they can be discriminated by some particular feature(s) from other neurites in the target tissues. Though vagal neurons display a variety of consistent chemical phenotypes (see other chapters in this volume), no neurochemical marker is specific for only vagal afferents and is inclusively characteristic of all vagal afferents. Thus, investigators traditionally have not been able to readily identify the terminals of all vagal afferents in a target organ or tissue and distinguish them from other circuitry by any unique neurochemical signature.

Recent advances and applications of neural tracing techniques, however, have made it practical to label selectively vagal afferents so that they can be unequivocally recognized in any target tissue. The tracers delineate neuronal processes with sufficient fidelity, in many cases, that they also provide significant structural information about these different vagal afferent projections. These tracers are exogenous molecules that are internalized and transported by neurons. In effect, neural tracers can be used to assign a specifiable and unique phenotype to vagal neurons. Once labeled, the peripheral processes of the neurons can be readily identified *in situ* and then mapped, inventoried, and analyzed structurally.

The last two decades have seen the development of a number of tracers and the proliferation of processing protocols for these labels (for reviews see, for example, References 18, 36, and 42). This armamentarium has become so extensive, it can be unclear which compound might be most promising for a particular application. Choosing processing protocols that are especially well suited to vagal afferents, as well as to a given tracer compound, also becomes an issue. In the present survey, we describe four different tracer strategies that we have found to be particularly suitable and powerful for labeling the peripheral processes and terminals of nodose neurons. Though this set is by no means complete, it offers a place to start if one does not want to screen through the entire list of candidate tracers. The survey also discusses some of the distinctive strengths and limitations of the four tracers, thus

underscoring issues an investigator might want to consider in choosing among the four for a given application or for evaluating additional tracer candidates. This overview also considers some of the control observations that should be used to validate a tracer protocol in a particular situation.

5.2   TRACERS AND TRACER PROTOCOLS FOR VAGAL AFFERENTS

We have found the four tracers described here to be exceptionally useful for analyses of vagal afferents in the gastrointestinal tract. They have also been used individually or in different combinations by different labs to describe vagal afferent projections to the heart, lungs, liver, and abdominal paraganglia as well. These different compounds meet a set of critical requirements for successful *in vivo* labeling of the peripheral neurites and terminals of the vagus. For example, the compounds are all readily incorporated by vagal neurons, they all (though not all of their solvents — cf. the carbocyanine dyes) appear to be tissue nonreactive, and they all are transported over at least the substantial distances from the nodose to the distal gastrointestinal tract of the rat (~15 cm).

For illustration and to provide some starting points for those interested in using the tracers, we also describe protocols for the four tracers that we have found effective in work on the rat gastrointestinal tract. The parameters reported would need, of course, to be adjusted for other species and other organ systems. In the case of the dextran amines, we also include examples of variations on the protocol in which counterstaining and immunohistochemistry are added to the basic procedures.

We should repeat, however, that each of the four tracers can be employed with a very large number of different protocols that might capitalize on the tracer's strengths, while optimizing them for other applications. There are far too many protocol variants to discuss in a short review, but investigators wishing to adapt one of the tracers we review (or others, for that matter) would want to consider utilizing some of the myriad different protocols that can be used with the labels.[18,36] A partial list of such variants would include the use of alternate chromagens in processing, the different intensification and amplification methods that have been developed, photostabilization or photoconversion strategies to stabilize the fluorescent labels, and immunohistochemistry with antibodies directed against the less stable tracers.

5.2.1   WHEATGERM AGGLUTININ-HORSERADISH PEROXIDASE (WGA-HRP)

The complex of wheatgerm agglutinin and horseradish peroxidase has been used extensively for neural tracing[18,21,22,32] and applied to the vagus.[17,24] WGA is a lectin that appears to be universally bound to membrane glycoproteins on vagal afferents (as well as many other cell types). When the lectin is conjugated to the enzyme HRP, neurons actively bind, incorporate, and then transport this complex throughout their neurites. Subsequent processing with a chromogen (TMB, DAB, etc.) developed by the HRP then labels the neuron. The glycoprotein binding sites are found particularly on somata, as opposed to neurites, thus nodose injections label vagal

afferents without concomitantly labeling *en passage* the efferent axons coursing through the nodose ganglion. Because the WGA conjugate capitalizes on this active binding mechanism to facilitate incorporation into cells, WGA-HRP injection provides much stronger labeling than administration of free or unconjugated HRP.

Our research group has used a WGA-HRP strategy extensively to inclusively label vagal afferents to an organ in order to appreciate the complete innervation pattern of vagal afferents.[27,30,40] Figure 5.1, for example, is a low-power view of a whole mount of the proximal duodenum of the rat that illustrates the pattern of afferent vagal axons in the smooth muscle wall of the intestine. The course of the fibers in the myenteric plexus connectives can be clearly traced. Figure 5.2 is a somewhat higher-power view that illustrates vagal afferent projection patterns in the wall of the stomach. At this magnification, one can see individual bundles of axons in connectives and even the vagal terminal apparatuses in smooth muscle (i.e., intraganglionic laminar endings and intramuscular arrays). Using such material, it has been possible to inventory and map the different types of vagal afferents to GI tract smooth muscle.[28,30]

5.2.1.1 WGA-HRP Protocol

- The nodose ganglion is exposed and injected with WGA-HRP (3 µl; 4%; Vector Laboratories, Burlingame, CA)
- At 72 hrs post injection, the animal is overdosed with a lethal injection of sodium pentobarbital and injected in the left ventricle of the heart with 0.25 ml Heparin (1,000 units/ml; Elkins-Sinn, Inc., Cherry Hill, NJ) to prevent coagulation and 0.25 ml propranolol (Ayerst Laboratories, Inc., Philadelphia, PA) to produce vasodilation
- The animal is perfused transcardially with 200 ml 0.9% saline at 40°C followed by 500 ml 3% paraformaldehyde and 0.4% glutaraldehyde in 0.1 M sodium phosphate buffer saline (PBS), pH 7.4, at 4ºC
- Whole mounts of the circular and longitudinal smooth muscle, containing the myenteric plexus, are prepared by removing the mucosal and submucosal layers
- Tissue is then processed with 3,3,5,5-tetramethylbenzidine (TMB; Sigma, St. Louis, MO) according to the protocol of Mesulam[20,21]
  - Buffer at pH 3.3: Add 200 ml of 1.0 M sodium acetate to 200 ml distilled water; add 190 ml of 1.0 M HCL; make up the volume to 1 L with distilled water. Titrate with concentrated acetic acid or sodium hydroxide in order to bring the final pH to 3.3
  - Solution A: Mix 92.5 ml of distilled water, 5 ml of the pH 3.3 buffer and 50 mg of sodium nitroferricyanide (Sigma)
  - Solution B: Add 5 mg of TMB to 2.5 ml absolute ethanol, which has been heated to 37º to 40ºC to dissolve the TMB
  - Mix solutions A and B and incubate the tissue for 20 min
  - Add 2.0 ml 0.3% H_2O_2 per 50 ml incubation solution and let react for 15 min
  - 6×5 min rinses in a post-reaction buffer consisting of 50 ml of the sodium acetate buffer, pH 3.3, in 950 ml distilled water
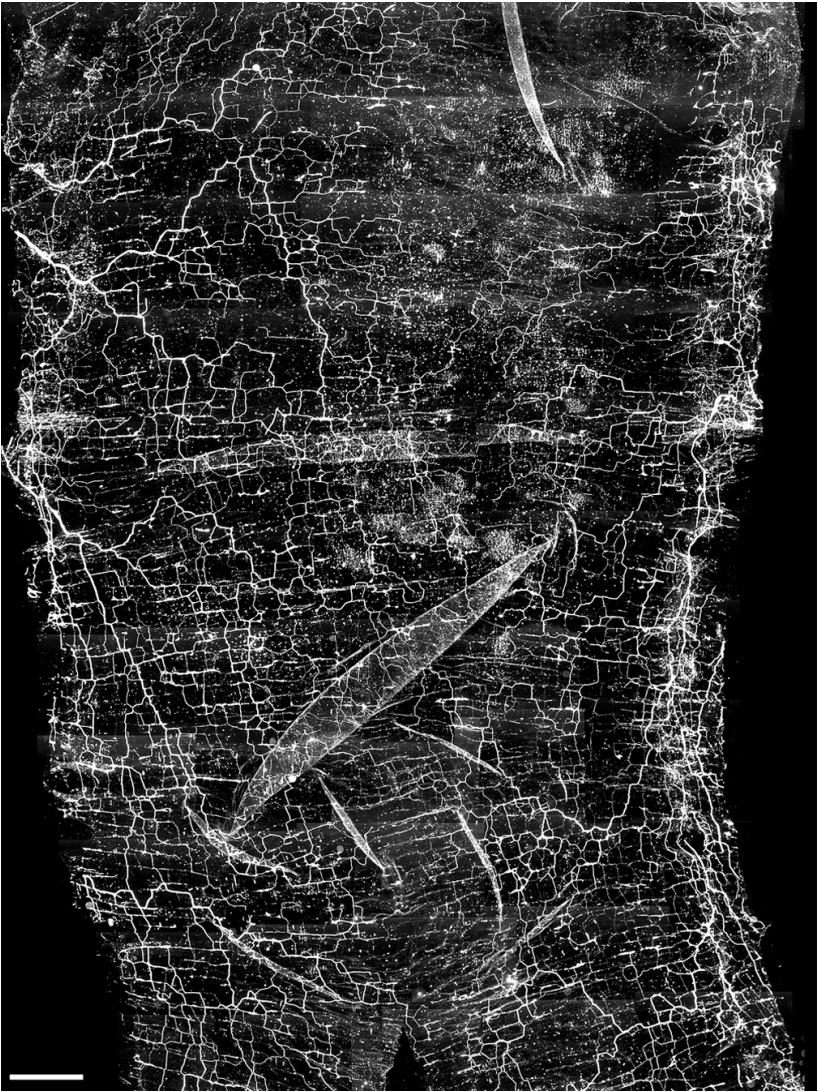
FIGURE 5.1 A photomontage of a duodenal whole mount from a rat that had received a left nodose injection of wheatgerm agglutinin-horseradish peroxidase (WGA-HRP). The intestinal segment was opened with a longitudinal cut along the mesenteric attachment, and large bundles of axons can be seen entering from the mesenteric attachment (left and right sides of the whole mount) and traveling both parallel to the mesenteric border and radially toward the antimesentery (center of the montage). The completeness of the label and the ability to view the label at low power magnification makes WGA-HRP a useful tracer for making both qualitative and quantitative descriptions of the vagal afferent innervation of the GI tract smooth muscle. Scale bar = 2 mm.

- Mount the tissue on gelatin coated slides and air dry overnight
- 2×30 min in xylene and coverslip using DPX (Aldrich, Milwaukee, WI)

FIGURE 5.2 A higher power view than that shown in Figure 5.1 of WGA-HRP labeled vagal afferents in the smooth muscle wall of the rat stomach. At this magnification, one can see, in addition to bundles, individual axons in the connectives and both types of vagal afferent terminals located in the smooth muscle wall [i.e., intraganglionic laminar endings (IGLEs) and intramuscular arrays (IMAs)]; see the legend for Figure 5.3 for a description of both endings. Scale bar = 320 μm.

5.2.1.2 Notes on WGA-HRP Protocols

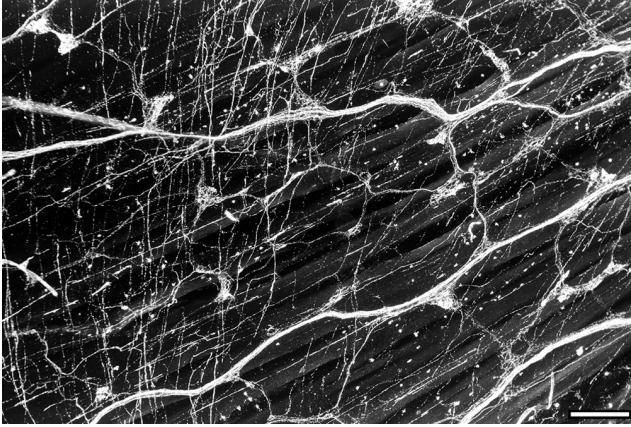Such injections tend to yield only afferent labeling and to label effectively all the afferents. Larger injections or larger pipettes (we use pulled glass pipettes with IDs of 25 μm and ODs of ~35–40 μm) that produce more mechanical disruption of the ganglion, however, tend to produce some efferent labeling *en passage* as well as the afferent labeling[17] and should generally be adopted cautiously.

To map the vagal afferent terminals in gastrointestinal smooth muscle, we typically employ a survival time of 72 hours in the rat or 24 hours in the mouse. By adjusting the timing slightly for transport, it is possible to maximize the labeling for a particular caliber of axon or a particular site within the GI tract, but transport times are similar enough and WGA-HRP accumulated in the terminals is stable enough that the survival times mentioned are typically satisfactory.

Much of the success of the WGA-HRP technique seems to be in the preparation of the target organ tissues. In the case of the vagal afferent innervation of the GI smooth muscle, we have found it particularly effective to work with whole mounts, to separate the tissue into layers to improve visibility and focus, and to mount the tissue so that it can be viewed from a perspective perpendicular to the plane(s) in which the afferent terminals lie.

5.2.2 CARBOCYANINE DYES

"DiI" (1,1-dioctadecyl-3,3,3,3-tetramethylindocarbocyanine) and the other compounds (e.g., "DiA" and "DiO") of the carbocyanine tracer family have been used extensively to label neuronal neurites or projections in fixed tissues.[16,37] Since the strong lipophilia and hydrophobia of the carbocyanines cause them to intercalate in

membrane and then to diffuse passively within the membrane, long incubations (e.g., weeks) of fixed tissue can eventually label neurons in their entirety (at least over a few millimeters). The technique has also been widely used as a vital dye for labeling developing neurons and cells in culture and then following their histories.

Our research group[1,3,6-8,24,27,40] and others[2,4,5,19,25,38] have, however, also used the carbocyanine dyes as *in vivo* anterograde and retrograde tracer to label over long distances (centimeters — e.g., nodose to the intestines). When a solution of DiI or other carbocyanine dye is injected into neuronal tissue, the dye dissolves in the membrane at the injection site. It appears that this labeled membrane is then slowly incorporated and recycled through endocytotic processes and intracellular vesicular membrane trafficking. Eventually, through such membrane exchange, the entire cellular membranes tend to accumulate the dye.

Utilizing this strategy, it is possible to label strongly a large number of neurons. Because endocytosis tends to occur at cell bodies (and axon terminals), nodose ganglion injections of DiI will selectively label vagal afferents and not label vagal efferents *en passage* (any label diffusing into the axonal membrane of vagal efferents traversing the nodose can spread locally slowly along that membrane by the passive diffusion process, but does not reach distal tissues over the distances and transport times employed).

5.2.2.1 DiI Protocol

- The nodose ganglion is exposed and injected with DiI (1 µl; 4% 1,1-dioctadecyl-3,3,3,3-tetramethylindocarbocyanine in methanol; Molecular Probes, Eugene, OR)
- At 3 to 4 weeks post injection, the animal is overdosed with a lethal injection of sodium pentobarbital
- The animal is perfused transcardially with 200 ml 0.9% saline at 40ºC followed by 500 ml 10% formalin in 0.1 M PBS, pH 7.4, at 4ºC
- Whole mounts of the tissue specimen are prepared
- Tissue is dehydrated through a graded series (70, 90, 100, and 100%) of glycerins
- The tissue is mounted and coverslipped using 100% glycerin and n-propyl gallate (5%; Sigma) to prevent fading

5.2.2.2 Notes on DiI Protocols

Though the DiI protocol is extremely simple, the solubility of the dye in solvents routinely used in histology makes the processing somewhat demanding. For example, all the carbocyanine dyes are so soluble in detergents that even trace amounts of the agents on glassware or slides will dissolve the dye from the tissue. Ethanol and most other alcohols will also degrade the label. Xylenes will also solubilize the label.

Another factor that can complicate work with the carbocyanines is that the compounds tend to continue to diffuse in a tissue specimen once it is fixed. DiI was originally used for its ability to diffuse in such fixed tissue, and if a specimen is not sufficiently well fixed (and particularly if the cell membranes have been damaged

and/or juxtaposed by mechanical stresses during processing), the dye will continue to migrate within the tissue. Whereas the dextran amines, in contrast, can be obtained with lysine fixable residues that anchor the label within the fixed tissue, the carbocyanine dyes are not always well stabilized in tissue samples.

5.2.3 DEXTRAN AMINES

Dextran amines conjugated with fluorochromes (Fluoro-ruby; Fluoro-emerald, Micro-ruby, Mini-ruby and other variants — see the Molecular Probes catalog) have also been extensively used as cell markers.[11-13,18,23,24] They are thought to be incorporated by intact neurons through an active endocytotic process. Since the uptake of the dextran amines, like that of the lectin WGA-HRP, does involve endocytosis, which occurs at somata and terminals, injections into the nodose typically do not label the efferent axons of passage. Once internalized, the dextran complex is distributed throughout the neuron in both retrograde and anterograde directions. As typically used in neuronal tracing, the dextran amine contains lysine residues that are cross-linked to cellular proteins by standard fixation protocols, thus leaving a stable fluorescent marker in fixed tissues. These lysine-fixable dextran amines remain stable through a variety of subsequent processing and counterstaining strategies. Further facilitating neuronal tracing, the dextran amines can be obtained in a variety of different molecular weights (commonly 3K and 10K), which influence the rate at which they are incorporated and transported by living cells as well as their relative storage stabilities, with a range of different fluorophores conjugated with them.

5.2.3.1 Dextran, Tetramethylrhodamine (TMR or "Fluoro-Ruby") Protocol

- The nodose ganglion is exposed and injected with TMR (3 µl; 7 to 15%; in distilled water; Molecular Probes)
- At 12 to 15 d post injection, the animal is overdosed with a lethal injection of sodium pentobarbital
- The animal is perfused transcardially with 200 ml 0.9% saline at 40ºC followed by 500 ml 4% paraformaldehyde in 0.1 M PBS, pH 7.4, at 4ºC
- Whole mounts of the tissue specimen are prepared
- Mount the tissue on gelatin coated slides and air dry overnight
- Run the tissue through an ascending series of alcohol (70, 90, 100, and 100%) for 2 min each followed by 2×5 min in xylene
- Coverslip using Cytoseal XYL (Richard-Allan Scientific, Kalamazoo, MI)

5.2.3.1.1   *TMR with the Putative Pan Neuronal Marker Fluoro-Gold*
- 5 d post TMR injection, the animal receives an i.p. injection of 1 mg/1 ml saline of Fluoro-Gold (Fluorochrome, Inc., Englewood, CO) to label all of the enteric neurons in the gut

5.2.3.1.2   TMR and Immunocytochemistry

- After perfusion the tissue is placed for 1 to 12 h in a blocking buffer (2% bovine serum albumin, 0.5% Triton X-100, 10% normal goat serum in 0.1 M PBS)
- 24 h in the primary antibody of choice (diluted with 2% bovine serum albumin, 0.3% Triton X-100, 2% normal goat serum in 0.1 M PBS)
- 3 × 10 min rinses in the same diluent as the primary 2 h in goat anti-rabbit FITC or goat anti-mouse FITC (1:100; Jackson ImmunoResearch, Laboratories, Inc., West Grove, PA) diluted with the same diluent
- 4 × 5 min PBS rinses
- Mount the tissue on slides and coverslip using VectaShield mounting medium (Vector Laboratories)

5.2.3.2   Notes on TMR Protocols

The fluorescent dextran amines yield excellent, high-definition labeling of vagal afferent axons and terminals (see, for example, Figure 5.3). Though, compared with some other fluorochromes, they are relatively stable when coverslipped with a mounting medium containing an antifade agent, the dextran amines will fade with protracted illumination. The tracer is also subject to the usual limitations of fluorescent markers: There is some degradation of the tracer fluorescence with long term storage, and autofluorescence of the tissue specimen tends to increase with storage. Other strengths and weaknesses of the fluorescent dextran amines are mentioned below in Section 5.4.2

5.2.4   BIOTIN CONJUGATED DEXTRAN AMINES

The dextran amines are also available with biotin conjugated to the appropriate complexes in order that investigators can capitalize simultaneously on the incorporation efficiency of the dextrans and the exceptional affinity of avidin and biotin for each other to yield a strong and permanent label. They too are widely used in neural tracing applications.[9,18,31,35,41,42]. The neuronal binding, incorporation, and transport characteristics of biotinylated dextran amines appear to be identical to those of the corresponding dextran amine without the biotin conjugate. Once the material has been transported to the target sites, however, the post-perfusion processing protocol involves the formation of the avidin-biotin complex and subsequent processing with a chromogen that will yield a light-stable permanent marker.

5.2.4.1   Dextran, Tetramethylrhodamine, and Biotin (TMR-B or 10K "mini-ruby" and 3K "micro-ruby") Protocol

- The nodose ganglion is exposed and injected with TMR-B (3 μl; 7 to 15%; in distilled water; Molecular Probes, Eugene, OR)
- At 12 to 15 days post injection, the animal is overdosed with a lethal injection of sodium pentobarbital
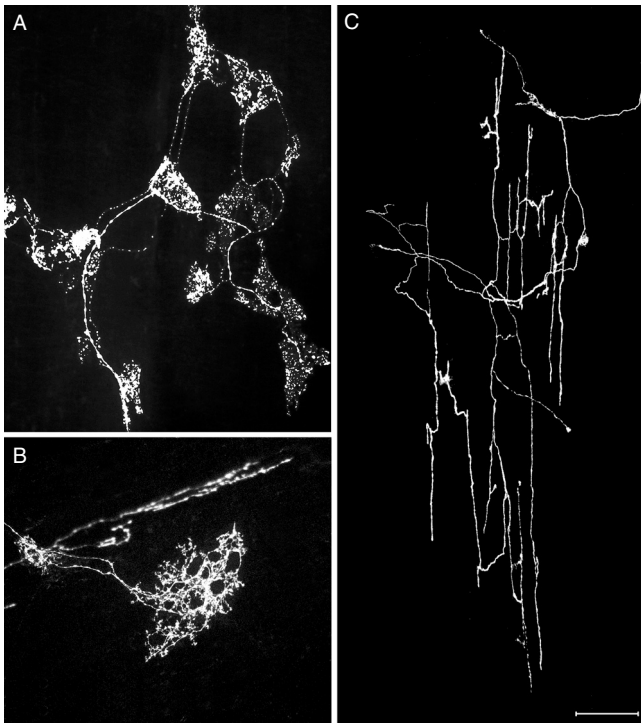
FIGURE 5.3 Labeling of the vagal afferent terminals in the smooth muscle wall of the rat gastrointestinal tract using either 1,1-dioctadecyl-3,3,3,3-tetramethylindocarbocyanine (DiI; panel **A**) or dextran-tetramethylrhodamine (TMR; panels **B** and **C**). Both tracers allow for high-power viewing of the structure of individual endings with either a fluorescent or confocal microscope; however, both are limited by the constraints of fluorescent microscopy (e.g., fading). **A, B**: The structures of IGLEs consist of vagal axons entering a myenteric ganglion and terminating as highly arborized laminar endings upon neurons (unlabeled) within the ganglion. **C**: IMAs originate from a parent axon (see upper right-hand corner) that typically branches several times before terminating within a smooth muscle layer. Upon entering the sheets of muscle, these individual terminals run for several millimeters, creating a distinct pattern of parallel elements. An out-of-focus element of an IMA also appears in the background of panel **B**. Scale bar = 100 μm for **A**, 100 μm for **B**, and 200 μm for **C**.

- The rat is perfused transcardially with 200 ml 0.01 M PBS at 40ºC followed by 500 ml 4% paraformaldehyde in 0.1 M PBS, pH 7.4, at 4ºC
- Whole mounts of the tissue specimen are prepared
- 3×5 min PBS rinses
- 15 min endogenous peroxidase block (methanol:3% H_2O_2; 4:1)
- 3×5 min PBS rinses
- Overnight in PBS with 0.5% Triton X-100 (PBST)
- 6×5 min PBS rinses
- 60 min in ABC (prepared as per the directions provided with the VECTASTAIN *ELITE* ABC kit; Vector Laboratories)

- 6 × 5 min PBS rinses
- 10 min DAB reaction
- 6 × 5 min distilled water rinses
- Mounted on slides and air dried overnight
- 4 × 2 min in ascending series of alcohols
- 2 × 8 min xylene
- Coverslip using Cytoseal

5.2.4.1.1   TMR-B with Cuprolinic Blue Counterstaining of Neurons

- Prior to the overnight soak in PBST, 3 × 5 min rinses in distilled water
- 4 h in a humidified slide warmer (38ºC) with 0.5% Cuprolinic Blue (quinolinic phthalocyanine; Polysciences, Inc., Warrington, PA) in 0.05 M sodium acetate buffer containing 1.0 M $MgCl_2$, pH 4.9. Protocol adapted from Holst and Powley[14]
- 3 × 5 min distilled water rinses
- 1 to 2 min differentiation in 0.05 M sodium acetate buffer containing 1.0 M $MgCl_2$, pH 4.9
- 3 × 5 min distilled water rinses
- 3 × 5 min PBS rinses

5.2.4.1.2   TMR-B with NADPHd Histochemistry or Counterstaining of Neurons

- Prior to the endogenous peroxidase block, 3 × 5 min rinses in 0.1 M Tris-HCl; pH 7.9
- 30 to 60 min soak in 0.1 M Tris-HCl (pH 7.6) containing 1.0 mg/ml -NADPH (Sigma), 0.33 mg/ml nitroblue tetrazolium (Sigma), and 0.5% Triton X-100 at 37ºC. Protocol adapted from Scherer-Singer et al.[33]
- 3 × 5 min 0.1 M Tris-HCl (pH 7.9) rinses

  Note: Use VectaMount (Vector Laboratories) instead of Cytoseal to coverslip TMR-B/NADPHd labeled tissue

5.2.4.1.3   TMR-B and Immunocytochemistry

- Following the overnight soak in PBST, 1 h in a blocking buffer (2% bovine serum albumin, 0.5% Triton X-100, 10% normal goat serum in 0.1 M PBS)
- 24 h in the primary of choice (diluted with 2% bovine serum albumin, 0.3% Triton X-100, 2% normal goat serum in 0.1 M PBS)
- 3 × 10 min PBS rinses
- 60 min in ABC solution
- 6 × 5 min PBS rinses

- 10 min DAB reaction
- 3 × 5 min distilled water rinses
- 3 × 5 min rinses in the primary diluent
- 60 min in the appropriate species specific biotinylated secondary raised in goat (Vector Laboratories or Jackson ImmunoResearch, Laboratories, Inc.) diluted with the same diluent used for the primary
- 6 × 5 min PBS rinses
- 60 min in ABC solution
- 6 × 5 min PBS rinses
- 5 min reaction in either Vector NovaRED or Vector VIP substrate kits (Vector Laboratories)
- 3 × 5 min distilled water rinses
- Mounted on slides and air dried overnight
- 4 × 2 min in ascending series of alcohols
- 2 × 6 min in xylene
- Coverslip using VectaMount

5.2.4.2   Notes on TMR-B Protocols

Biotinylated dextran amines generally provide excellent, high-definition labels for vagal afferents. One feature that can limit the use of this family of tracers is the requirement that the ABC processing or avidin binding step requires that the tissue specimen be sufficiently thin and permeable to allow ready penetration. (By comparison, the fluorescent dextran amines and carbocyanine dyes have no such constraints: the signal or fluorophore is part of labeling molecule and thus no penetration issue arises.) Combining TMR-B processing with immunohistochemical protocols similarly requires good tissue penetration by the antibodies in order to achieve staining of additional tissue elements. As an illustration, we have found that it is frequently necessary to separate the circular and longitudinal muscle layers of the GI smooth muscle wall in order to get effective antibody penetration in our immunohistochemical protocols.

Since the organs the vagus innervates are large and complex, vagal axons regularly project over circuitous paths (e.g., Figure 5.1 and Figure 5.2), vagal afferent terminals are structurally and spatially complex (e.g., Figure 5.3, Figure 5.4, and Figure 5.5), and success in analyzing the geometry of such endings can often hinge on the use of large blocks of tissue or whole mounts in particular orientations, strategies for achieving adequate penetration are often key to the successful use of the biotin-conjugated dextrans. Other strengths and limitations of this family of tracers are considered below in Section 5.4.

5.3   CONTROLS AND VALIDATIONS

Applications of neural tracers can lead to a variety of false positive and false negative outcomes (see Fox and Powley[10], for a detailed discussion). Many of
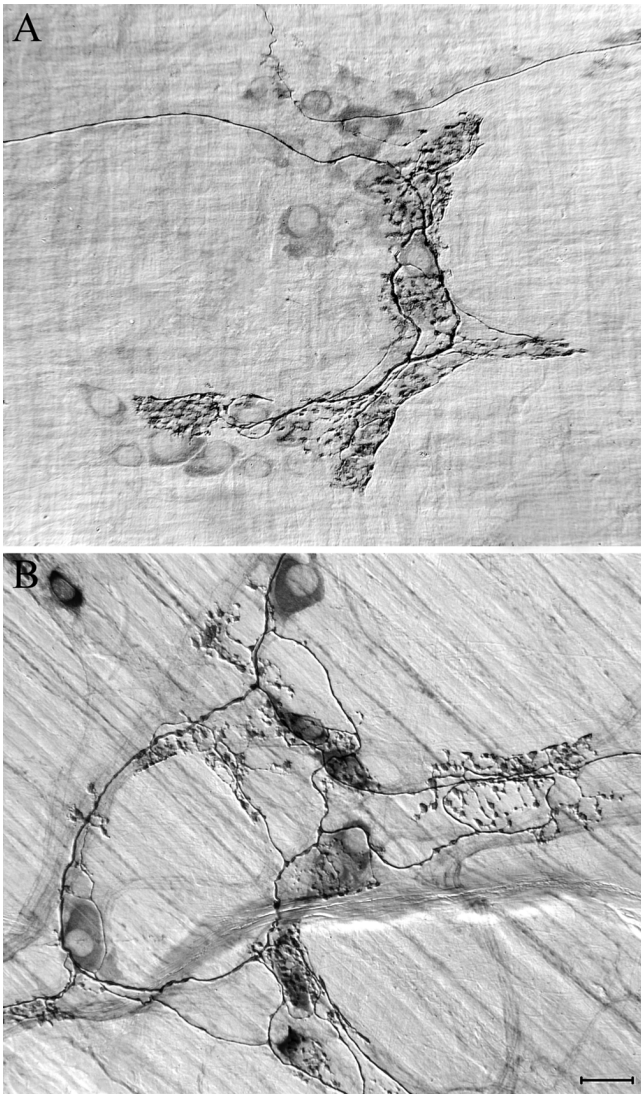
FIGURE 5.4 *(A color version of this figure follows page 236.)* Biotin-conjugated dextran-tetramethylrhodamine (TMR-B) is compatible with neuronal stains, allowing for permanent visualization of vagal terminals and myenteric neurons. (**A**) An IGLE (golden brown; TMR-B stained with a DAB reaction) is seen in close approximation to several neurons (light blue; stained with the putative pan-neuronal stain cuprolinic blue) within a myenteric ganglion. (**B**) TMR-B (golden brown) is also compatible with nicotinamide adenine dinucleotide phosphate diaphorase (NADPHd; dark blue) staining. In the myenteric plexus, neurons that produce nitric oxide synthase can be demonstrated histochemically in aldehyde-fixed tissue using a histochemical reaction for NADPHd. Note the disparate relationship of the IGLEs to the NADPHd-positive and NADPHd-negative (unstained) neurons. Mouse stomach whole mounts; scale bar = 25 μm.
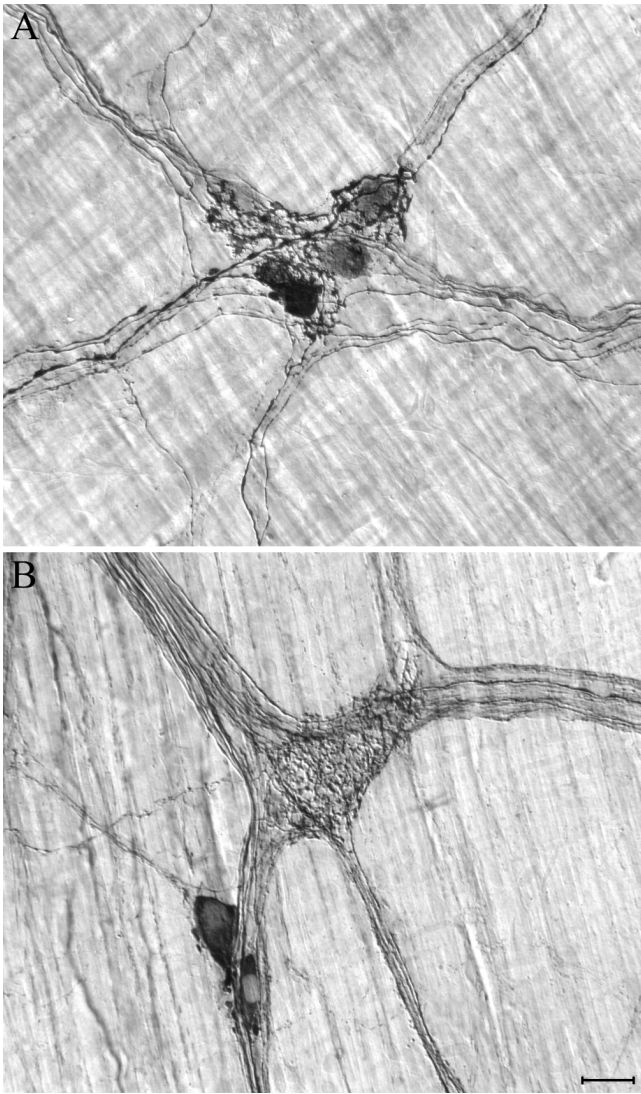
FIGURE 5.5 *(A color version of this figure follows page 236.)* The durability of the TMR-B molecule makes it an excellent choice for lengthy staining protocols, such as immunocytochemistry, that typically require exposure of the tissue to harsh detergents such as Triton X-100. (**A**) An IGLE (dark brown) visualized using TMR-B stained with a DAB reaction can be seen in close association with several myenteric neurons (stained red using Vector NovaRED) positive for the calcium-binding protein calbindin, which was labeled using a polyclonal antibody to calbindin. (**B**) TMR-B can also be used in conjunction with both a histochemical reaction and an immunocytochemical reaction. An IGLE is labeled brown using the tracer TMR-B stained with DAB, while two different nonoverlapping phenotypes of myenteric neurons are labeled different colors. A nitric oxide synthase producing neuron is labeled dark blue using an NADPHd reaction, while a calbindin-positive neuron is labeled red using NovaRED. Mouse stomach whole mounts; scale bar = 25 μm.

these complications are minimized in the case of vagal afferent labeling experiments by the facts that:

- Vagal afferents to more distal organs, such as the stomach and intestines, are relatively compactly organized in the nodose ganglion or, for the more cranial organs, in some instances in the jugular ganglion.
- The nodose is well encapsulated and thus possesses a natural limiting barrier that contains even large injections.
- The target tissues are not adjacent to the ganglion where leakage by diffusion could become an issue.

The anatomical organization of the vagus does not, however, mitigate all control issues in tracing analyses. From the perspective of investigations of the vagal afferents, the most problematic feature stems from the fact that the axons of vagal efferents course through (in some species, somewhat superficially to one side of) the nodose. There is always the prospect that injections of tracers will also label *en passage* the efferent axons. Even when experimental circumstances strongly favor selective labeling of afferents (e.g., tracer compounds such as lectins or dextrans that are selectively bound by somata rather than axons; minimal mechanical damage to the ganglion, small injections, etc.), there remains the prospect that efferent axons can be labeled and that any putative afferent ending in the periphery is actually a motor process.

The procedure that constitutes the "gold standard" for addressing this prospect is a preparation in which the efferents have been eliminated from the vagal trunk and the nodose is then injected. Complete and selective chemical lesions of all vagal efferents in the periphery are presently impractical, so surgical strategies are probably the most feasible means of achieving such controls. Furthermore, since the somata of vagal efferents are distributed centrally in two long and thin columnar bilateral cell groupings (i.e., the dorsal motor nucleus of the vagus and the nucleus ambiguus) and extensive lesions of the brainstem are not readily tolerated, CNS lesions of all efferents are not practical. One strategy for eliminating efferents is to perform an extracranial supranodose vagotomy, to wait for the peripheral efferent axons to undergo dissolution, and then to inject the nodose with tracer. Such an experiment is relatively simple in terms of surgical requirements, but it runs very substantial risks of damaging the nodose. The nodose is situated so close to the jugular foramen (at least in smaller mammals) that a transection above the ganglion must almost invariably damage the rostral pole of the ganglion either by direct mechanical damage or by disruptions of the local circulation.

The alternative to an extracranial supranodose vagotomy to eliminate efferent fibers is an intracranial transection of the motor roots of the vagus, just as they exit the medulla and span towards the jugular foramen. This strategy has proved practical from both a ventral[26] and a dorsal[39] approach. Conveniently too, from the perspective of tracer experiments, there are simple adaptations of the tracers such as HRP and FluoroGold that make it possible to verify the completeness of such selective efferent vagotomies.[39]

The complementary manipulation that makes the recognition of afferents unambiguous is to label the efferents coursing in the vagus in animals that have had the

afferents transected. Experimentally this is most readily achieved by injecting the motor neurons in the brainstem after the vagal afferent rootlets have been cut between the medulla and the jugular foramen. Identifying the motor profiles in the tissues of interest and formally comparing these efferent profiles with the afferent endings makes it practical to subsequently recognize any efferents inadvertently labeled after nodose injections in animals that do not have selective rhizotomies.

Such surgical manipulations and verification strategies are time-consuming, and would be especially tedious if they were routinely and continuously needed. In our experience with the vagal innervation of the heart,[6,8] as well as the GI tract,[1,3,15] though, afferents and efferents differ categorically in their target and accessories tissues and in their morphologies. Once afferents and efferents have been distinguished and characterized with the subtractive surgical analysis to validate the discriminations, it is possible to classify and identify vagal afferents and to distinguish them from any efferent profiles that may occasionally be labeled incidentally.

The issue of efferent profiles raises another point pertaining to a potential false positive analysis. If one regularly checks the dorsal motor nucleus of the vagus and the nucleus ambiguus in the brainstem after tracer injections in the nodose ganglion, it is common to see a small number (or with particularly large injections, a proportionately larger number) of neurons retrogradely labeled with the tracer. These retrogradely labeled somata typically appear without any corresponding labeling of efferent profiles in the periphery. It appears that any efferent axons interrupted or transected by the pipette when the nodose was impaled will effectively take up the tracer and transport it retrogradely. Just as in a classic cut-nerve-soak study, though, when the axons have been transected there is no mechanism for the tracer to be transported into the peripheral efferent terminals, hence the absence of efferent labeling in the periphery.

On the other hand, a second process, though it is more hypothetical, may also occur in some preparations. It is possible that some of the retrogradely labeled motor neurons one can observe possess transiently damaged but not destroyed peripheral axons. In these hypothetical cases, subsequent anterograde transport of the tracer might label efferent terminals in the periphery. Indeed, this mechanism seems likely to be responsible for the motor profiles we have observed occasionally in peripheral target organs after nodose injections. It might also be the case that different combinations of protocol manipulations (e.g., larger pipette tips, more mechanical damage, more chemical injuries from nonoptimal solvents, different survival periods tailored for the longer time course of retrograde then anterograde transport, etc.) might substantially increase the amount of adventitial efferent labeling one obtained. At any rate, the rhizotomy control experiments outlined earlier unequivocally eliminate such a source of erroneous labeling.

5.4 SELECTING TRACERS FOR PARTICULAR APPLICATIONS

With the extensive battery of tracers available, choosing the most useful compound for a particular experimental design can be a challenge. As outlined earlier, we have

found the four tracer protocols described in this chapter to be particularly successful in inventories and characterizations of vagal afferents. Each of the tracer strategies has distinct advantages and disadvantages when compared with the others. Their complementarities mean that they serve collectively as a useful arsenal of techniques that can be substituted for one another, depending upon the details of the experimental application. These complementarities, discussed below, also underscore some of the issues that one might consider when selecting and adapting additional tracer protocols.

5.4.1 ISSUES OF FIELD OF VIEW, MAGNIFICATION, AND POPULATION SURVEYS

The proportion of the entire vagal afferent population that the different tracers label is one such issue. WGA-HRP will label virtually the entire population of nodose neurons. The enzyme is highly soluble in aqueous solutions, it is delivered in distilled water or a buffer or solvent with an osmolarity similar to that of extracellular fluids, and the solution appears to readily diffuse throughout the ganglion, delivering the enzyme to all nodose neurons. Furthermore, vagal afferent neurons all apparently express binding sites for the lectin. The net effect is that WGA-HRP serves as a particularly powerful marker when one is seeking to label the entire afferent population. When processed with a chromogen such as TMB that amplifies the signal, the compound can be observed in whole mounts at even low power (e.g., Figure 5.1), and we think it is the method of choice for this purpose.

In contrast, the carbocyanine dyes will label extensively, but they are not ideal in applications requiring labeling of the entire population. Being lipophilic and hydrophobic, the carbocyanine dyes must be dissolved in methanol or other solvents that tend to damage cells. Furthermore, when the injected solution contacts extracellular fluids, the carbocyanine dyes tend to rapidly precipitate out of solution and produce a depot of dye at the injection site, rather than diffusing through the ganglion. For some applications where tracer spread is a problem this is a decided advantage, but for labeling a large population of neurons, it is a disadvantage. To distribute the carbocyanine material throughout the ganglion, multiple injections may be required, but then the risk of tissue damage and potential destruction of some afferents is greatly increased.

The dextran amines, with or without biotin conjugated, are soluble in aqueous media and can be easily injected throughout the ganglion (gauged by visible monitoring of the colored solution), and they do not produce any observable necrosis in the ganglion. Nonetheless, the dextran amines only label a small percentage of all neurons. This selectivity is unrelated to particular classes of neurons. Though the mechanism of the selectivity has not been established, the injected dextrans effectively label only those neurons located in close proximity to the injection sites. Typically, one finds a number of afferents strongly labeled (those immediately proximal to the pipette tip), a larger number that are relatively lightly labeled (those less proximal, but still close to the tip), and a still larger population of essentially unlabeled neurons (those a significant distance from the injection site, perhaps where the effective concentration of the dextran falls below a threshold level). Multiple

injections increase the number of labeled neurons, but it is impractical to label the entire nodose population this way.

5.4.2 RESOLUTION OR DEFINITION OF ENDINGS

A second issue that might influence any tracer selection relates to whether the intended application will involve relatively low-power surveys or higher-power, higher-definition analyses of individual endings. WGA-HRP is particularly effective for evaluating large fields or whole mounts, in part because, as mentioned earlier, the enzyme can label the entire population of vagal afferents. Additionally, WGA-HRP lends itself to wide-field inventories, in part because the signal can readily be amplified with TMB processing to generate a darkfield-compatible label that accentuates the endings. Neither the carbocyanine dyes nor the fluorescent dextran amines are as useful for low-power surveys. In these latter cases, the effective signal is limited both because fluorescent labels tend to label only a percentage of the neurons and because fluorescent emission signals are not sufficiently strong or stable to yield a robust signal through low-power optics of relatively low numerical aperture. Of the two limitations that plague the fluorescent labels, the first also applies to biotinylated dextran amines, though the second does not limit the permanent labeling strategies for dextrans.

At the other end of the magnification range, different considerations determine the relative strengths of the different tracers. The dextran amines produce high-definition smooth and continuous labeling of neurites that compares favorably with the benchmarks of neural tracing such as PHA-l processing. Where long-term stability and nonfading signals are not essential, the fluorescent dextran amines can be readily photographed (cf. Figure 5.3) or used for confocal microscopy. Where stability and fading are issues, permanent labeling with the biotinylated dextrans is particularly practical (cf. Figure 5.4 and Figure 5.5). Carbocyanine labeling of vagal afferents is frequently more grainy and less continuous or smooth than the dextrans (compare for example, Figure 5.3A and Figure 5.3B), but, at its best, carbocyanine labeling provides almost the same quality of fine-process definition. In contrast, WGA-HRP labeling provides a much less satisfactory image for high-definition analyses of individual endings. HRP labeling is typically grainy, and with TMB processing, the crystalline reaction product tends to aggregate on the ending without continuously and smoothly labeling only the axoplasm or membrane of the neurite.

5.4.3 COMPATIBILITY WITH IMMUNOHISTOCHEMISTRY AND COUNTERSTAINING

A third issue on which the four tracing techniques have different strengths is in their relative compatibility with immunohistochemistry and other techniques for double labeling. The dextran amines are in general the most compatible with such additional processing. Indeed, they produce exceptional results. The fixation protocols and tissue preparations for the dextrans are readily compatible with both immunohistochemistry (e.g., Figure 5.4 and Figure 5.5) and counterstaining methods (e.g.,

Figure 5.4). Furthermore, the dextran amines can be used for fluorescence or permanent-label immunohistochemistry and counterstaining.

In contrast, both WGA-HRP and the carbocyanine dyes are somewhat less satisfactory for routine double and triple staining protocols. WGA-HRP seldom can match the definition and quality of neurite filling seen readily with the dextrans (or with the carbocyanine labels). In addition, when TMB is used as the chromagen for WGA-HRP processing, the crystals are less stable and more subject to fading and to being dissolved when exposed to some of the reagents employed for immunohistochemistry and some counterstaining. The carbocyanine dyes are notoriously soluble in detergents and agents used to enhance penetration for immunohistochemistry. In addition, as commonly used, the carbocyanine dyes are limited to fluorescence and subject to the fading and oxidation that limit some applications. To date, with only a few limited exceptions, the successes in routinely combining the carbocyanine labels with immunohistochemistry have been modest (e.g., see discussion in Berthoud[4]).

5.4.4 DOUBLE OR MULTIPLE TRACER INJECTIONS

In a variety of experiments, tracer protocols that simultaneously distinguish two (or more) different subpopulations can be very powerful. For example, the separate peripheral innervation fields, as well as the target regions of overlap of the left and right nodose ganglion projections, can be distinguished with injections of different tracers into the two sides. Similarly, double tracer experiments provide practical means of comparing the projections of vagal afferents and efferents in the same tissue specimen, or the distinct projection fields of the rostral and caudal pole of the nodose ganglion, or the patterns of inputs of vagal versus dorsal root ganglion afferents. The carbocyanine dyes and dextran amines are readily adaptable for such experiments insofar as both families of tracers are available with several different fluorochromes conjugated to the basic complex. WGA-HRP and biotinylated dextran are somewhat less versatile in this regard, although protocols have been devised for combining other conjugates of HRP (e.g., WGA-HRP vs. cholera-toxin-HRP or free HRP) and different dextrans (e.g., a simple dextran amine vs. biotin-conjugated dextran amine). Though the fluorescent markers appear to be somewhat more practical in this type of double labeling experiment, it should be mentioned that the different variants within a marker family do not all appear to label neurons equally strongly. For example, the rhodamine-related forms of the fluorochromes (DiI and Fluoro-ruby, respectively) generally produce stronger labeling (or detectability) than the FITC variants, thus producing a need to counterbalance the different labels across the different injection sites.

5.4.5 PERMANENCE OF THE LABELING

Permanence of the different labels is another factor that has to be considered in selecting a tracer for a particular application. Of the four candidates under discussion, permanently labeled biotinylated dextrans appear to be the most stable for long-term storage. They are not affected by light, and they do not obviously deteriorate in

long-term storage (when they are well fixed prior to processing). WGA-HRP also does not fade when illuminated, and it is relatively stable, though even under ideal conditions (stored refrigerated in the dark), it does deteriorate slowly over several months. The quality of the initial fixation is important in ensuring the relatively long-term stability of the TMB reaction product. Both the carbocyanine family of dyes and the fluorescent dextran amines fade with sustained illumination. Furthermore, both of the types of fluorescent labels do tend to lose intensity in long-term storage, to diffuse into surround connectives and tissue if the fixation is sub-optimal, and to slowly become masked by the autofluorescence of the surrounding tissues that evolves over weeks or months of storage.

5.4.6 Transport Time

Transport (and incorporation) times vary widely and constitute another factor that, given the constraints of a particular experiment, might clearly dictate the use of one or another of the four tracers we have discussed. WGA-HRP is rapidly incorporated and transported to the peripheral terminals of vagal afferents. For the rat, we typically allow 72 hours between the injection of WGA-HRP into the nodose and the perfusion step; for the mouse, we typically use 24 hours. The dextran amines (both free and biotin-conjugated) are considerably slower. Typical survival periods for optimal dextran amine labeling of vagal afferents in the GI tract of the rat would be 14 days and of the mouse would be 7 days. This interval varies somewhat depending upon which compartment of the organ system is being investigated and which type of afferent terminal is of more interest. Optimal labeling with the carbocyanine tracers is still much slower. For analyses of the GI tract innervation, we typically wait three to four weeks between injection and perfusion.

5.5 SUMMARY

The development, over the last two decades, of powerful neural tracers and sensitive processing protocols for these labels has made it practical to investigate the distributions and finer structural details of vagal afferents. Such information is needed if the understanding of vagal sensory processes is going to progress toward parity with that of other sensory systems. Particularly effective tracers for the nodose neurons include WGA-HRP, carbocyanine dyes, dextran amines, and biotinylated dextran amines. These families of tracers have different and complementary strengths and weaknesses as well as specific control considerations, and such factors should shape decisions or choices of labeling strategies for different experimental applications.

ACKNOWLEDGMENTS

REFERENCES

1. Berthoud, H.R., Jedrzejewska, A., and Powley, T.L., Simultaneous labeling of vagal innervation of the gut and afferent projections from the visceral forebrain with diI injected into the dorsal vagal complex in the rat, *J. Comp. Neurol.*, 301, 65–79, 1990.
2. Berthoud, H.R., Kressel, M., and Neuhuber, W.L., An anterograde tracing study of the vagal innervation of rat liver, portal vein and biliary system, *Anat. Embryol. (Berl.)*, 186, 431–442, 1992.
3. Berthoud, H.R. and Powley, T.L., Vagal afferent innervation of the rat fundic stomach: morphological characterization of the gastric tension receptor, *J. Comp. Neurol.*, 319, 261–276, 1992.
4. Berthoud, H.R., Anatomical demonstration of vagal input to nicotinamide acetamide dinucleotide phosphate diaphorase-positive (nitrergic) neurons in rat fundic stomach, *J. Comp. Neurol.*, 358, 428–439, 1995.
5. Berthoud, H.R., Kressel, M., and Neuhuber, W.L., Vagal afferent innervation of rat abdominal paraganglia as revealed by anterograde DiI-tracing and confocal microscopy, *Acta Anat. (Basel)*, 152, 127–132, 1995.
6. Cheng, Z., Powley, T.L., Schwaber, J.S., and Doyle, F.J., 3rd, Vagal afferent innervation of the atria of the rat heart reconstructed with confocal microscopy, *J. Comp. Neurol.*, 381, 1–17, 1997.
7. Cheng, Z., Powley, T.L., Schwaber, J.S., and Doyle, F.J., 3rd, Projections of the dorsal motor nucleus of the vagus to cardiac ganglia of rat atria: an anterograde tracing study, *J. Comp. Neurol.*, 410, 320–341, 1999.
8. Cheng, Z. and Powley, T.L., Nucleus ambiguus projections to cardiac ganglia of rat atria: an anterograde tracing study, *J. Comp. Neurol.*, 424, 588–606, 2000.
9. Dolleman-Van der Weel, M.J., Wouterlood, F.G., and Witter, M.P., Multiple anterograde tracing, combining Phaseolus vulgaris leucoagglutinin with rhodamine- and biotin-conjugated dextran amine, *J. Neurosci. Methods*, 51, 9–21, 1994.
10. Fox, E.A. and Powley, T.L., False-positive artifacts of tracer strategies distort autonomic connectivity maps, *Brain Res. Brain Res. Rev.*, 14, 53–77, 1989.
11. Fritzsch, B. and Wilm, C., Dextran amines in neuronal tracing, *Trends Neurosci*, 13, 14, 1990.
12. Fritzsch, B. and Sonntag, R., Sequential double labelling with different fluorescent dyes coupled to dextran amines as a tool to estimate the accuracy of tracer application and of regeneration, *J. Neurosci. Methods*, 39, 9–17, 1991.
13. Fritzsch, B., Fast axonal diffusion of 3000 molecular weight dextran amines, *J. Neurosci. Methods*, 50, 95–103, 1993.
14. Holst, M.C. and Powley, T.L., Cuprolinic blue (quinolinic phthalocyanine) counterstaining of enteric neurons for peroxidase immunocytochemistry, *J. Neurosci. Methods*, 62, 121–127, 1995.
15. Holst, M.C., Kelly, J.B., and Powley, T.L., Vagal preganglionic projections to the enteric nervous system characterized with Phaseolus vulgaris-leucoagglutinin, *J. Comp. Neurol.*, 381, 81–100, 1997.
16. Honig, M.G. and Hume, R.I., Dil and diO: versatile fluorescent dyes for neuronal labelling and pathway tracing, *Trends Neurosci.*, 12, 333-335, 340–331, 1989.
17. Kalia, M. and Sullivan, J.M., Brainstem projections of sensory and motor components of the vagus nerve in the rat, *J. Comp. Neurol.*, 211, 248–265, 1982.
18. Kobbert, C., Apps, R., Bechmann, I., Lanciego, J.L., Mey, J., and Thanos, S., Current concepts in neuroanatomical tracing, *Prog. Neurobiol.*, 62, 327–351, 2000.

19. Kressel, M., Berthoud, H.R., and Neuhuber, W.L., Vagal innervation of the rat pylorus: an anterograde tracing study using carbocyanine dyes and laser scanning confocal microscopy, *Cell Tissue Res.*, 275, 109–123, 1994.

20. Mesulam, M.M., Tetramethyl benzidine for horseradish peroxidase neurohistochemistry: a non-carcinogenic blue reaction product with superior sensitivity for visualizing neural afferents and efferents, *J. Histochem. Cytochem.*, 26, 106–117, 1978.

21. Mesulam, M.M., Principles of horseradish peroxidase neurohistochemistry and their applications for tracing neural pathways — axonal transport, enzyme histochemistry and light microscopic analysis, in *Methods in the Neurosciences: Tracing Neural Connections with Horseradish Peroxidase*, Mesulam, M.M., Ed., John Wiley & Sons, New York, 1982, chap. 1.

22. Mesulam, M.M. and Mufson, E.J., The rapid anterograde transport of horseradish peroxidase, *Neuroscience*, 5, 1277–1286, 1980.

23. Nance, D.M. and Burns, J., Fluorescent dextrans as sensitive anterograde neuroanatomical tracers: applications and pitfalls, *Brain Res. Bull.*, 25, 139–145, 1990.

24. Neuhuber, W.L., Sensory vagal innervation of the rat esophagus and cardia: a light and electron microscopic anterograde tracing study, *J. Auton. Nerv. Syst.*, 20, 243–255, 1987.

25. Neuhuber, W.L., Kressel, M., Stark, A., and Berthoud, H.R., Vagal efferent and afferent innervation of the rat esophagus as demonstrated by anterograde DiI and DiA tracing: focus on myenteric ganglia, *J. Auton. Nerv. Syst.*, 70, 92–102, 1998.

26. Norgren, R. and Smith, G.P., A method for selective section of vagal afferent or efferent axons in the rat, *Am. J. Physiol.*, 267, R1136–1141, 1994.

27. Phillips, R.J., Baronowsky, E.A., and Powley, T.L., Afferent innervation of gastrointestinal tract smooth muscle by the hepatic branch of the vagus, *J. Comp. Neurol.*, 384, 248–270, 1997.

28. Phillips, R.J., Baronowsky, E.A., and Powley, T.L., Long-term regeneration of abdominal vagus: Efferents fail while afferents succeed, *J. Comp. Neurol.*, 455, 222–237, 2003.

29. Powley, T.L., Holst, M.C., Boyd, D.B., and Kelly, J.B., Three-dimensional reconstructions of autonomic projections to the gastrointestinal tract, *Microsc. Res. Tech.*, 29, 297–309, 1994.

30. Powley, T.L. and Phillips, R.J., Musings on the wanderer: what's new in our understanding of vago-vagal reflexes? I. Morphology and topography of vagal afferents innervating the GI tract, *Am. J. Physiol. Gastrointest. Liver Physiol.*, 283, G1217–1225, 2002.

31. Reiner, A., Veenman, C.L., Medina, L., Jiao, Y., Del Mar, N., and Honig, M.G., Pathway tracing using biotinylated dextran amines, *J. Neurosci. Methods*, 103, 23–37, 2000.

32. Rosene, D.L. and Mesulam, M.M., Fixation variables in horseradish peroxidase neurohistochemistry. I. The effect of fixation time and perfusion procedures upon enzyme activity, *J. Histochem. Cytochem.*, 26, 28–39, 1978.

33. Scherer-Singler, U., Vincent, S.R., Kimura, H., and McGeer, E.G., Demonstration of a unique population of neurons with NADPH-diaphorase histochemistry, *J. Neurosci. Methods*, 9, 229–234, 1983.

34. Schmued, L., Kyriakidis, K., and Heimer, L., In vivo anterograde and retrograde axonal transport of the fluorescent rhodamine-dextran-amine, Fluoro-Ruby, within the CNS, *Brain Res.*, 526, 127–134, 1990.

35. Veenman, C.L., Reiner, A., and Honig, M.G., Biotinylated dextran amine as an anterograde tracer for single- and double-labeling studies, *J. Neurosci. Methods*, 41, 239-254, 1992.

36. Vercelli, A., Repici, M., Garbossa, D., and Grimaldi, A., Recent techniques for tracing pathways in the central nervous system of developing and adult mammals, *Brain Res. Bull.*, 51, 11–28, 2000.

37. Vidal-Sanz, M., Villegas-Perez, M.P., Bray, G.M., and Aguayo, A.J., Persistent retrograde labeling of adult rat retinal ganglion cells with the carbocyanine dye diI, *Exp. Neurol.*, 102, 92–101, 1988.

38. von Bartheld, C.S., Cunningham, D.E., and Rubel, E.W., Neuronal tracing with DiI: decalcification, cryosectioning, and photoconversion for light and electron microscopic analysis, *J. Histochem. Cytochem.*, 38, 725–733, 1990.

39. Walls, E.K., Wang, F.B., Holst, M.C., Phillips, R.J., Voreis, J.S., Perkins, A.R., Pollard, L.E., and Powley, T.L., Selective vagal rhizotomies: a new dorsal surgical approach used for intestinal deafferentations, *Am. J. Physiol.*, 269, R1279–1288, 1995.

40. Wang, F.B. and Powley, T.L., Topographic inventories of vagal afferents in gastrointestinal muscle, *J. Comp. Neurol.*, 421, 302–324, 2000.

41. Wouterlood, F.G. and Jorritsma-Byham, B., The anterograde neuroanatomical tracer biotinylated dextran-amine: comparison with the tracer Phaseolus vulgaris-leucoagglutinin in preparations for electron microscopy, *J. Neurosci. Methods*, 48, 75–87, 1993.

42. Wouterlood, F.G., Vinkenoog, M., and van den Oever, M., Tracing tools to resolve neural circuits, *Network*, 13, 327–342, 2002.

6 Mechanotransduction by Vagal Tension Receptors in the Upper Gut

Simon J.H. Brookes, Vladimir P. Zagorodnyuk, and Marcello Costa

CONTENTS

6.1   INTRODUCTION

Vagal afferents to the gut form at least three different morphological types of endings: mucosal endings, intraganglionic laminar endings in myenteric ganglia, and intramuscular arrays in the muscularis externa. Electrophysiologically, two functional types of vagal afferents have been identified in most preparations from the upper gut: mucosal afferents, which respond to mucosal stroking and various chemical stimuli, and muscle afferents, which appear to function largely as in-series tension receptors. Few would dispute that mucosal endings probably correspond to the units that are activated by mucosal stroking. Intraganglionic laminar endings have been shown to correspond to the transduction sites of tension receptors. The role of intramuscular arrays is currently unclear; it has been argued that they may be length receptors, but physiological evidence for a specialized population of length receptors is currently lacking. Intraganglionic laminar endings respond on

147

a millisecond timescale to distortion and their ability to transduce mechanical stimuli is not blocked in calcium-free solution. These observations suggest that they probably transduce mechanical stimuli directly, rather than being activated indirectly by mediators released from other cells. The mechanosensitive ion channels responsible for transduction by IGLEs remain to be identified. A variety of substances released from various cells in the gut wall, including ATP and glutamate, may modulate their integrative properties, as can a number of exogenous neurochemicals, opening possibilities for pharmacological manipulation of mechanoreceptor activity in gastrointestinal disorders.

Vagal afferent nerve fibers innervating the upper gastrointestinal tract have been divided into two basic functional types; mucosal receptors, which respond to chemical or mechanical stimulation of the mucosa but not to stretch of the gut wall, and muscle receptors, which respond to stretch but are not activated by mucosal stimuli.[1,2] In the ferret esophagus, a third type of vagal afferent has been described with intermediate properties, the so-called tension-mucosal (TM) receptors.[3] Muscle receptors, which we will interchangeably refer to as vagal mechanoreceptors, have been extensively studied by many groups in a large number of preparations. They are functionally important as they underlie the sensations of esophageal and gastric distension and are the afferent limb of reflexes such as receptive relaxation and gastric accommodation. The first single unit recordings[4] were made using the fiber-teasing technique developed by Adrian (1933), which was shown to be capable of recording the smallest diameter axons.[5] In 1955, Iggo demonstrated that vagal mechanoreceptors in the goat stomach behaved as if they were in-series tension receptors. They increased their firing to both stretch and contractile activity in the muscular wall of the stomach, indicating that their firing did not simply reflect unidirectional length changes of their receptive fields.[6] Since then, a number of studies have confirmed this basic finding: vagal mechanoreceptors appear to function largely as tension receptors in the ferret stomach,[7] sheep stomach,[8] rat,[9] mouse,[10] dog,[11] and guinea pig esophagus and stomach.[12,13]

The observation that vagal mechanoreceptors behave as if they were in-series tension receptors is, at least anatomically, surprising. The concept of in-series tension receptors arose from studies of Golgi tendon organs. These are encapsulated structures located at the junction between skeletal muscle fibers and the tendon proper and thus are truly in-series with the muscle. Contraction of the muscle stretches the Golgi tendon organ and this leads to firing of group Ib somatic afferents. It has been hypothesized that linear stretch of the receptor by muscle contraction straightens out collagen fibrils within the tendon organ. These then squeeze and distort mechanosensitive branches of the afferent fiber, which intertwine between them.[14] In the gut wall, there are, of course, no tendons and the muscle layers form a continuous ring. Afferent fibers cannot, therefore, be aligned solely in-series with the muscle; they must always be aligned in parallel to it. This then raises questions as to how an in-parallel arrangement could give rise to mechanoreceptors being sensitive to tension rather than length. For this, one needs to consider the morphology of the nerve endings, their transduction sites and their relationship with the surrounding tissue.

In the skin and other organs of the body, identifying the morphology of physiologically characterized afferent fibers was relatively straightforward. Hunt in 1961 identified Pacinian corpuscles as the endings of specialized, rapidly adapting, vibration-sensitive mechanoreceptors.[15] This was made possible by locating the receptive fields of an afferent unit with the appropriate physiological activity, marking it in the tissue, and identifying the associated neuronal structures in either stained or unstained tissue. This is possible when receptors have a relatively low density in the tissue and when the density of all types of motor and sensory innervation is similarly low. In most viscera, the latter condition is not met; there is extensive innervation, both efferent and afferent, by autonomic neurones (sympathetic, parasympathetic, and intrinsic) as well as extrinsic sensory neurones. This makes it difficult to identify which particular structures are likely to correspond to a marked receptive field when all nerve fibers are stained in the tissue.

A modified dye-filling technique was reported in 1999, which allowed selective filling, via anterograde transport, of extrinsic axons innervating a piece of tissue from a single fine-nerve trunk.[16] This meant that extrinsic nerve fibers from a single nerve trunk could be labeled without labeling either axons of intrinsic origin, or extrinsic axons that reach the tissue via other nerve trunks. Using this technique, it became possible to correlate dye-filled structures with mechanically sensitive sites in the guinea-pig esophagus[12] and upper stomach.[13] This technique has subsequently revealed comparable specialized flattened endings in the guinea pig rectum.[17]

Specialized vagal afferent endings, now known as Intraganglionic Laminar Endings (IGLEs), were first described by Lawrentjew (1929) using silver staining.[18] Rodriguo and colleagues demonstrated that these endings were of vagal origin as they disappeared following subnodose vagotomy.[19] IGLEs are located within the myenteric ganglia of the esophagus and stomach, but are found in decreasing densities throughout the small and large intestine.[20,21] A second class of vagal afferent endings were described more recently following anterograde labeling from the nodose ganglion of the rat.[22] These endings had quite different morphological features and were called intramuscular arrays (IMAs).[21] These have a much more restricted distribution, being concentrated in the upper stomach and the lower esophageal sphincter and pylorus.[21, 23] There are also vagal afferent nerve endings in the inner layers of the gut including the mucosa.[22,24] However, mechanoreceptors activated by stretch of the gut wall do not generally respond to mucosal stroking[3,10,25] and removal of the mucosa does not interfere with vagal fiber responses to stretch.[26,27] This means that either IGLEs or IMAs are likely to be the endings of vagal mechanoreceptors.

6.2 IDENTIFICATION OF THE MORPHOLOGICAL STRUCTURE OF VAGAL TENSION RECEPTORS

The existence of three morphological types of vagal afferent endings in the upper gut (mucosal, IGLEs, IMAs), but only two major electrophysiologically characterized classes is problematic. Identifying the functions of IGLEs and IMAs became feasible when techniques to combine extracellular recording and dye filling were

developed. This required making recordings from fine nerve trunks close to the target tissue, rather than at remote sites far up the vagus nerve. Such recordings made in isolated preparations of guinea pig esophagus[12] and stomach[13] showed mechanoreceptors with very similar characteristics to those recorded *in vivo*. Typically, mechanoreceptors showed slow rates of spontaneous firing, had low thresholds to stretch, a wide dynamic range, and adapted slowly during maintained distension. In addition, units typically showed increased firing rates during spontaneous and evoked muscle contractions. This was the case even when the preparation was maintained at a constant length, indicating that the units were behaving similarly to the "in-series tension receptors" described by Iggo and subsequent investigators.

The small, *in vitro* preparations differed in two important aspects from the *in vivo* preparations that had previously been used so widely. First, it was possible to remove the mucosa and submucosa from *in vitro* preparations and thus reduce contamination from other classes of mucosal afferents. Secondly, the preparations could be studied at higher resolution, attaching transducers close to the receptive fields to closely monitor changes in both length and tension at the transduction sites, and probe systematically to identify mechanosensitive sites. Using light von Frey hairs, it was possible to show that nearly all of the mechanosensitive afferents had one or more small sites at which they could be powerfully activated by radial compression. These so-called "hotspots" were marked on the tissue by applying carbon particles on the tip of the von Frey hair, followed by photography. A clear pattern emerged from these studies. Each tension sensitive afferent had from 1 to 6 hotspots, each of which was surrounded by an area of much lower sensitivity. Dye fills from the recorded nerve trunk consistently revealed intraganglionic laminar endings close to, or directly under, each hotspot. While IMAs and viscerofugal nerve cell bodies were also labeled in the anterograde dye fills, these showed no significant association with hotspots. These studies led to the conclusion that vagal afferent mechanoreceptors, at least the slowly adapting, wide dynamic range tension receptors, have transduction sites that correspond to IGLEs and that the parent axons are not themselves mechanosensitive.[12,13]

The role of IMAs was not determined in the study of Zagorodnyuk and colleagues even though they were anterogradely filled from many of the nerve trunks from which recordings were made. No evidence was seen that IMAs were sensitive to probing with a von Frey hair. Mapping receptive fields failed to reveal the extensive structures extending in parallel to either longitudinal or circular smooth muscle layers, as would be expected for IMAs. The possibility that IMAs are transduction sites for length or stretch receptors has been strongly argued in several publications.[28,29] This possibility cannot be refuted on the present evidence. The studies of Zagorodnyuk et al. were not carried out to search systematically for a role for IMAs. There may have been selection bias in the units chosen for study; many of the units subsequently shown to have IGLEs had relatively large amplitude action potentials. It is possible that, while IMAs were present in the preparations studied, they may have represented a very small proportion of the total filled fibers and hence been missed in recordings. In support of this, we have seen several IMAs, extending over many square millimeters, arising from a single parent axon, suggesting that the total number of vagal axons giving rise to IMAs may be relatively small relative to

IGLE-bearing tension receptors. Thirdly, it is possible that IMAs are not activated by focal distortion — their adequate stimulus may stretch along their entire length. Lastly, the mucosa and submucosa was always removed from the preparations used in this study.[13] This meant that a restricted range of stretches had to be used to avoid irreversibly damaging the preparation.

It is possible that IMAs are activated only with large-amplitude distensions. Bearing in mind these limitations to the study, no evidence was seen for stretch activated afferents that lacked hotspots. Of 46 units in the stomach that could be activated by stretch, 6 units appeared to lack focal hotspots, of which four of these were rapidly adapting. The other two slowly adapting units were indistinguishable from IGLE-bearing units and probably had inaccessible transduction sites. If IMAs are transduction sites of vagal mechanoreceptors, it would seem that under the conditions used here, they acted as rapidly adapting units and are unlikely to function as length receptors. Nevertheless, the role of IMAs will only be determined by systematically attempting to record from their parent axons and applying a range of mechanical and chemical stimuli until their adequate stimulus is identified.

6.3   MECHANOTRANSDUCTION

The question then arises as to how IGLEs, which are located in parallel to the muscular elements of the muscularis externa, can transduce tension, when elsewhere in the body this is mediated by in-series structures. Two very different mechanisms appear to underlie mechanotransduction by afferent neurones in different systems. The first, which we will refer to as chemical transduction, involves chemicals, released from physically distorted non-neuronal cells, that increase the excitability of afferent nerve endings, beyond the threshold for action potential generation. For example, in slowly adapting mechanoreceptor corpuscles, Merkel cells make ultra-structurally identifiable synapse-like contacts onto afferent nerve fibres.[30] It is believed that release of a transmitter substance, possibly glutamate,[31] may activate the nerve fiber, with the Merkel cell being the actual site of transduction. Likewise, glutamate acting on AMPA receptors probably mediates transmission from mechanotransducing inner hair cells of the cochlea to spiral ganglion neurones.[32] Chemical transduction can be considered to occur when the released substance drives the afferent nerve fiber's entire response to the mechanical stimulus. This should be distinguished from substances released from damaged, inflamed or distorted tissue that only modify the firing rate of sensory nerve endings by changing their excitability. Thus prostaglandins, histamine, bradykinin, serotonin, ATP, proteases, and protons can all act on receptors or ion channels on afferent nerve endings to modulate their responses to mechanical stimuli. The difference between chemical transduction and modulation of excitability is one of degree. Suffice it to say that to qualify as a chemical transduction mechanism, the release of chemical should be both necessary and sufficient to account for the stimulus/response relationship of the afferent fiber.

The second mechanism, which we will refer to as direct mechanotransduction, is characterized by having all of the essential molecular elements located in the afferent nerve ending, without extracellular mediators being involved. This mechanism does not rely on other cell types except as mechanical anchor points for the

transduction complex. Direct mechanotransduction is believed to be mediated by specific mechanically gated ion channels, which open when the nerve ending is distorted.[33] The resulting ion fluxes produce a generator potential, which then gives rise to a train of action potentials. This is believed to be the case for many types of cutaneous mechanoreceptors to which putative mechanosensitive ion channels are transported.[34] Modulatory mechanisms can affect direct mechanotransduction at multiple points, by altering the function of mechano-gated ion channels, by altering the excitability of the nerve endings via other ion channels, by changing the mechanical activity of surrounding tissues (e.g., smooth muscle), or in the longer term by re-modeling the mechanical coupling to adjacent structures.

For vagal intraganglionic laminar endings the mechanisms of transduction have not yet been positively identified. Nevertheless, evidence is accumulating that direct mechanotransduction is likely to be involved,[35] but the molecular nature of the mechanotransduction complex is yet to be discovered.

6.4 MECHANICAL ACTIVATION OF MUSCLE MECHANORECEPTORS

Vagal tension receptors make intraganglionic laminar endings (IGLEs) located in the myenteric ganglia, within the external muscle layers of the gut wall. They appear to be activated by any stimulus that distorts the IGLE. Thus, stretch in either longitudinal or circumferential axes of the gut wall powerfully activates these endings (Figure 6.1). This occurs even if the gut wall is an intact tube, if the mucosa and submucosa are removed, or if the preparation is prepared as a flat sheet. Significantly, IGLEs are also exquisitely sensitive to compression by a von Frey hair applied perpendicular to the preparation. The lightest von Frey hair that can penetrate the surface tension of the bathing solution (which in our hands exerts a force of 0.08mN over an area of approximately 0.03 mm^2) can evoke brisk firing of a vagal afferent when positioned precisely on an IGLE. However, IGLEs do not only respond to externally imposed stretches — they are also powerfully activated by contractions of the wall musculature under isometric conditions (Figure 6.2). This gave rise to the description that they behave as in-series tension receptors[6] — although, as discussed earlier, this description cannot be anatomically accurate.

The responses of primary afferent neurones to mechanical stimuli are substantially affected by the physical environment surrounding the transduction site. This was elegantly demonstrated in Pacinian corpuscles, in which intact corpuscles give rapidly adapting responses to both the onset and offset of a mechanical deformation. In contrast, removal of part or all of the corpuscle (i.e., non-neuronal material) changes the response to a more slowly adapting response that extends further throughout the stimulus,[36] A recent ultrastructural study of Meissner corpuscles provides a convincing explanation of how the mechanical coupling between the terminal axons and surrounding tissue, mediated via collagen fibrils, and enveloping Schwann cells, could explain the rapidly adapting responses to cutaneous indentation,[37] It is likely that the details of the mechanical environment surrounding IGLEs may also strongly influence their firing patterns.
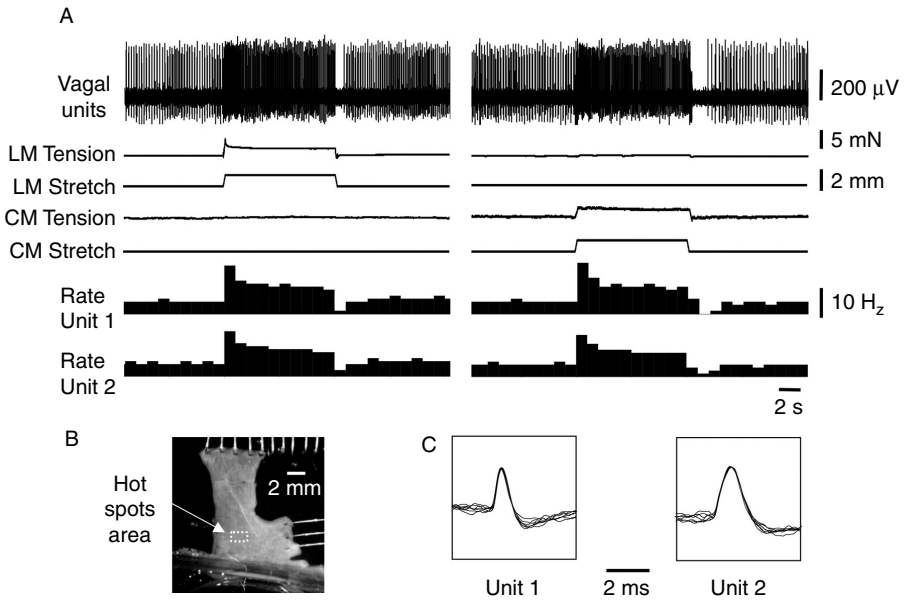
FIGURE 6.1 An L-shaped preparation of guinea pig esophagus is used to examine the effects of both longitudinal and circumferential stretch on two vagal mechanoreceptors. (**A**) Longitudinal stretch (1 mm for 10 s, left hand traces) evokes brisk firing of both units during the stretch, followed by a silent period after removal of the stimulus. Similarly, circumferential stretch (1 mm, 10 s) also evokes firing of both units (distinguishable by their height in the raw trace), again followed by a silent period. (**B**) The receptive fields of both units are located in the stretched area. (**C**) Superimposed action potentials show the different waveforms that distinguish the two units.
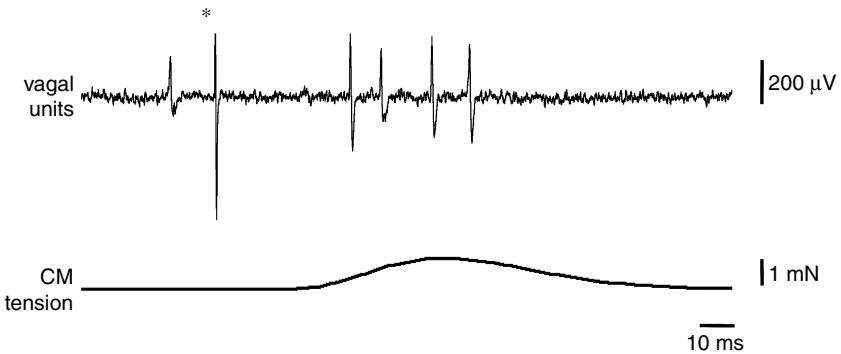

FIGURE 6.2 A single electrical stimulus applied to the guinea pig esophagus, maintained at constant length, evokes a rapid twitch in the striated muscle (lower trace). At least two tension-sensitive units are activated during the twitch (upper trace), demonstrating that they behave as if they were in-series tension receptors. The stimulus artifact is marked with an asterisk.

Two questions arise. First, what are the features of the mechanical microenvironment that give rise to this gross pattern of responsiveness? Secondly, what are the molecular mechanisms that convert forces or movements of tissue into electrical signals?

To answer the first question it is necessary to consider the fine structure of IGLEs. They arise from a parent axon via branches, which then typically subdivide and form flattened plate-like structures. Analysis with light microscopy reveals that these laminar endings are most dense close to the surface of the myenteric ganglia; there are few within the neuropil. A single IGLE often supplies laminar endings on both the mucosal surface of the ganglion sheath, and on the serosal surface, typically with endings also wrapping around one edge of the ganglion. In a large ganglion, several IGLEs may be present, arising from the same or different parent axons. Ultrastructurally, IGLEs appear to make junctional contacts with some enteric neurones, with small clear vesicles distributed in a fashion that suggests that these could be sites of transmitter release. However, studies of fos expression following afferent activation suggests that this is unlikely to be a major role for these endings.[38] In addition, the flattened structures of IGLEs are anchored to the ganglion and overlying muscle layer and have a close association with glial processes, which have been hypothesized to allow them to transduce shearing forces associated with change in tension and length.[28,39]

It would appear then that the location of IGLEs would be suitable to detect distortion of myenteric ganglia, caused by both passive stretch and by active contraction of the muscle layers. How this occurs requires further consideration. IGLEs, the muscle surrounding them and the ganglia are all fluid-filled structures and incompressible, therefore, it is unlikely that the volume of any of the structures changes when force is applied. Given the great sensitivity of IGLEs to radial compression of the ganglia (i.e., perpendicular to the plane of the muscle) it is tempting to speculate that this could be the major type of distortion that physiologically activates the endings during both stretch and contraction. This idea extends the analogy with Golgi tendon receptors, in which straightening of collagen fibrils by external force leads to compression of the branching nerve fibers coursing through the capsule. This idea could, we believe, explain how passive stretch of the tissue activates IGLEs.

During either circumferential or longitudinal stretch of a rectangular flat sheet of gut tissue, the gross surface area of the tissue increases, but as volume must be conserved, the thickness reduces. This is obvious as "pinching" in the middle of a flat sheet preparation. In the pinched region, there must be considerable distortion of the myenteric ganglia, including radial compression, which might be expected to activate IGLEs. In tubular preparations of gut, distension by a balloon inflated in the lumen (or infusion of fluid, or arrival of a semi-solid bolus) would lead to an equivalent reduction in wall thickness and radial compression of ganglia. The question then arises as to how isometric contractions, during which the dimensions of the tissue grossly remain constant, could also activate IGLEs. Typically, under isometric conditions, the overall dimensions of the tissue change very little during contraction, but there is still considerable movement on fine scale, readily visible under a dissecting microscope and recordable with a video camera. As individual

muscle cells contract, they inevitably shorten and increase in diameter as well as becoming more rigid. Compensatory stretching of the passive extracellular matrix presumably takes place, thus allowing the tissue to maintain constant length. The change in muscle cell shape and rigidity may be sufficient to apply radial compression to myenteric ganglia, and thereby activate the IGLEs. In a tubular preparation, the effect of circular muscle contractions may be further enhanced by the radius of curvature, which would tend to evoke a force with a radial vector acting against the resistance of the gut contents.

6.4.1 Activation of Mechanoreceptors in Intact Organs

This crude model, in which IGLEs are activated by radial distortion, can also account for the effects of muscle relaxants that are known to reduce the firing of mechanoreceptors to constant amplitude stretches, since their effect would be to reduce the rigidity of individual muscle cells, and hence their tendency to exert radial compressive forces on ganglia.

The stomach functions as two different organs in terms of motility: the proximal stomach acts as a low pressure reservoir, whereas the antrum acts as a pump, mill, and aliquotting device.[40] The reflex control of the two regions reflect these different functions: Cannon first described receptive relaxation, in which distension of the esophagus leads to relaxation of the upper stomach, in preparations for the arrival of contents.[41] Once food arrives in the stomach a vago-vagal reflex ("gastric accommodation"), activated by gastric distension, leads to further relaxation of the upper stomach and simultaneous excitation of the antral pump[42,43] The extrinsic accommodatory reflex is supplemented by an intrinsic reflex that can be recorded in the isolated stomach[44,45] Importantly, these two functions are also mirrored by the myogenic activity of the stomach, in which slow-wave mediated rhythmic activity starts weakly in the upper stomach and gains both force and velocity as it propagates toward the pylorus.[46,47] These reflex pathways have important consequences for the activation of gastric mechanoreceptors. Vagal mechanoreceptors in the two functional regions of the stomach typically have different patterns of firing, either firing rhythmically, in time with gastric peristaltic contractions or independently of them.[48,49] This may well be due to the different local mechanical environment surrounding IGLEs in the different regions. It is interesting that while both types exist in the antrum, there appear to be more nonrhythmic units in the upper stomach.[49]

During normal gastric filling, most of the contents tend to accumulate in the low tone-region of the fundus and corpus, with about 20% entering the antrum.[50] Under these conditions, food entering the stomach should cause stretch of the fundus wall with a resulting reduction in wall thickness and tonic radial compression of IGLEs in this region. In the antrum, the waves of propagating contraction activate IGLEs in a rhythmic fashion. Thus the mechanical environment surrounding IGLEs could explain how a single type of receptor may signal to the central nervous system, both the contractile state of the lower stomach and the state of distension of the upper stomach. Thus IGLEs in different parts of the stomach may be able to signal both hunger pangs and sensations of fullness after a large meal, without proposing the existence of a separate class of length receptor.

6.4.2 Receptive Fields of Mechanoreceptors

The functional significance of having multiple IGLEs arising from a single parent axon is worth considering. It is clear that each IGLE is capable of being mechanically activated by a von Frey hair.[12,13] and that it can interact with companion IGLEs, such that the fastest-firing IGLE determines the firing frequency of the whole unit. This was demonstrated by examining the firing of tension receptors during the adapted phase of a maintained distension. Under these conditions, afferents with multiple IGLEs fire at a highly constant rate, as long as spontaneous muscle activity is not present. Simple modeling revealed that such constant firing rate could not be reproduced by two IGLEs firing independently.[12] Rather, action potentials initiated from one IGLE appears to invade the others arising from the same parent axon and reset their excitability. Support for this idea was provided by the observation that activating a single IGLE strongly with a stiff von Frey hair reduced the response of the whole unit to a stretch stimulus applied moments later.[12,13] Clearly, the IGLEs that had not been activated by the von Frey hair were unable to respond normally to the subsequent stretch stimulus. This mechanism may involve 4-aminopyridine-sensitive, voltage operated potassium channels, or calcium-activated potassium channels being opened following arrival of antidromic action potentials in the IGLEs.[51] It seems likely that the result of multiple IGLEs spread out over a small area is that the firing of the unit reflects the maximal wall tension anywhere within this overall receptive field.

Smooth muscle contraction in the stomach is determined by an interaction between myogenic and neurogenic mechanisms, which give rise to migrating Ca^{2+} waves associated with shortening.[52] In the stomach it has been shown that myogenic pacemaker potentials arise from Interstitial Cells of Cajal (ICCs) sandwiched between the longitudinal and circular muscle layers[53] While the longitudinal and circular muscle layers are innervated by separate populations of motor neurones, and can thus be activated independently,[54–56] the common pacemaker drive will tend to mean that contractions of one layer are in concert with those of the other. Thus IGLEs are likely to be squeezed from both sides by rhythmic contractions. When neuronal input differs between the longitudinal and circular muscle layers, shear forces may be generated across the myenteric ganglia. It is possible that IGLEs are sensitive to such forces,[29] although this has not been directly tested to date.

Multiple receptive fields have also been described for mucosal afferents, activated by light mucosal probing.[57] In the stomach, receptive fields from the same axons could be separated by up to 35mm. Thus some mucosal afferents are likely to sample simultaneously luminal stimuli in two or more widely separated regions of the stomach. Interactions between the different transduction sites were not studied in this investigation, but it would seem likely that the most active site drives the firing frequency of the parent axon, which could apply here too.

In many recordings from vagal muscle mechanoreceptors, spontaneous firing has been observed, even when the gut is in a "no-load" state (i.e., neither stretched nor compressed). It is clear that within the tissue of the gut wall, there may be considerable residual stresses, thus the mucosa of the esophagus is normally compressed, whereas the outer muscle layers are normally under slight tension.[58] This

is readily demonstrated by the tendency of tubular segments of tissue to flatten, or even curl inside out, when they are opened up into flat sheets. Spontaneous tone of the muscle may also contribute to resting tension around the IGLEs and thus add to their "resting" excitability. Blockers of channels or receptors coupled to contraction (e.g., L-type calcium channel antagonists, muscarinic receptors) often reduce spontaneous firing. Likewise, drugs that actively relax the smooth muscle, such as sodium nitroprusside or other nitric oxide donors, vasoactive intestinal polypeptide, or beta adrenergic agonists can also reduce spontaneous firing rates. These effects can be considered as an indirect form of modulation of mechanoreceptor responses, since they are mediated via changes in smooth muscle contractility or tone.

6.5 EVIDENCE THAT TRANSDUCTION IS NOT CHEMICALLY MEDIATED

A number of experimental approaches have been used to distinguish whether IGLEs are activated directly, via mechano-gated ion channels or whether they could be activated by chemicals released from another cell type that functions at the true mechanoreceptor. The first test of this was to determine how quickly IGLEs respond to mechanical deformation. This was achieved in one study[35] by placing a piezo-operated probe directly above an IGLE and measuring the latency to the first action potential. The probe was then replaced with a focal electrical stimulating electrode and a near-threshold electrical stimulus was given to determine the conduction delay. Typically, this evoked a burst of antidromic action potentials amongst which the particular single unit could not be discriminated, however, a minimum conduction delay could be determined (Figure 6.3). When the conduction delay was subtracted from the latency to the mechanical probe, a transduction delay of less than 5 ms was consistently observed. In several cases, the latency was considerably less than this. This indicates that transduction occurs over a millisecond time scale. However, mechanically activated ATP release from cells occurs over a time scale of seconds[59,60], even when this is mediated by "burst release."[61]

In the bladder, where ATP mediated mechanotransduction has been implicated in determining afferent excitability,[62,63] there is also no evidence for rapid ATP release on a millisecond timescale. It has been suggested ATP release from epithelial cells also occurs in the gut, where ATP released from epithelia could increase the excitability of visceral afferents.[64] However, this appears again to occur with a slow timescale. However, it is likely that ATP plays an important role in modulating primary afferent sensitivity in a variety of pathological circumstances.[65] A recent paper has elegantly demonstrated an alternative method of chemical transduction that may occur in epithelia.[66] This suggests that there may be ongoing tonic release of a compound into the lateral extracellular space. Mechanical deformation of the epithelium reduces the volume of the lateral extracellular space and thus raised the concentration of, in this case, an EGF-like ligand, sufficiently to evoke a cellular response. Again, this mechanism occurs over a time course of seconds rather than milliseconds and cannot explain the rapid transduction by IGLEs.
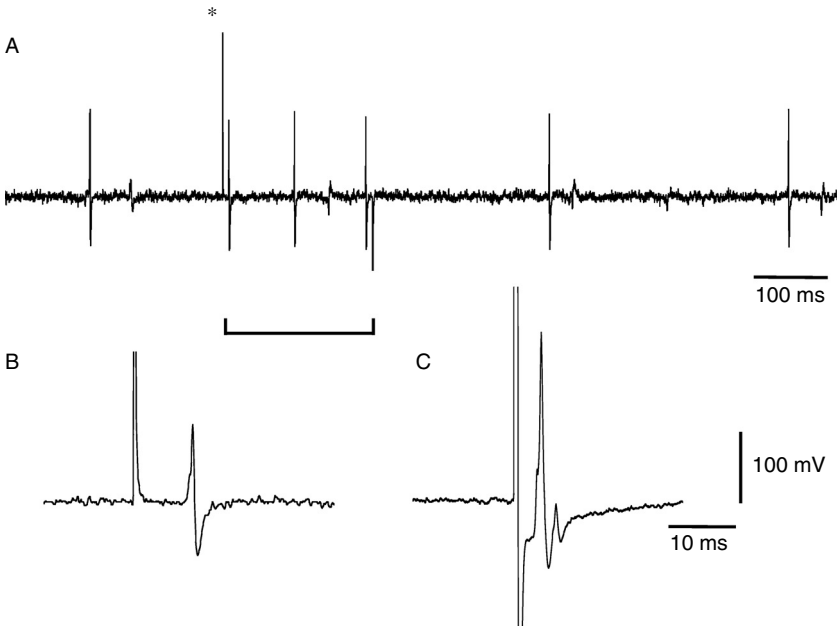
FIGURE 6.3 Calculating the minimum transduction delay for vagal mechanoreceptors. (**A**) A piezo-electric probe, with a response time of <20 μs was positioned directly above an IGLE of a vagal mechanoreceptor in the guinea pig esophagus. The unit showed slow, spontaneous firing. Immediately after the probe was advanced (stimulus artifact at asterisk) an action potential occurs with a latency of 7.85 ms. An increased rate of firing is also seen for the duration of the 200 ms stimulus (bar), followed by a silent period before spontaneous firing starts again. (**B**) The latency of the mechanically evoked response is shown on a faster timebase (**C**) A focal electrical stimulus, applied at the same site, evoked a compound action potential, which includes the recorded unit, with a delay of 3.3 ms. This indicates that the delay due to transduction was less than 4.55 ms.

ATP and other transmitters can be released very rapidly, during fast synaptic transmission[67] on a timescale well within the 5 ms latency that we identified. Rapid release is believed to be mediated by exocytotic release, which is a calcium-sensitive mechanism. It was of interest then to examine the effects of lowered $[Ca^{2+}]$ and raised $[Mg^{2+}]$, which blocks such exocytotic release. This did not block mechanotransduction by IGLE-bearing vagal mechanoreceptors. Rather, it increased both basal firing rate and stretch-activated responses,[35] possibly by reducing resting activation of calcium-dependent potassium channels, or by increasing membrane excitability through charge-mediated effects. The voltage-sensitive calcium channel blocker, Cd^{2+},[68] also failed to block IGLE activation by mechanical stimuli. This makes it unlikely that exocytotic release of a chemical mediator, ATP, glutamate, or any other transmitter from a second cell type, is involved in the rapid response of vagal muscle receptors to mechanoreceptors stimuli.

6.6 MODULATION OF VAGAL AFFERENT NERVE ENDINGS BY ENDOGENOUS CHEMICALS

Although ATP is unlikely to be responsible for mechanotransduction by IGLEs, it has potent effects on many primary afferent neurones.[65] It has been shown immunohistochemically that P_{2X2} purinoceptors are present on IGLEs[35,69] and ATP or its stable analogue, alpha beta methylene ATP strongly increase spontaneous firing of most vagal tension-sensitive afferents.[35] There appear to be striking differences between species. In the mouse, fewer than 50% of vagal mechanoreceptors were activated by ATP[10] and in the ferret, none were excited by it.[70] However, following acid-induced inflammation, many vagal mechanoreceptors in the ferret became sensitive to ATP, suggesting that this could be an important mechanism for inflammation-induced hypersensitivity.

Mouse vagal mechanosensitive afferents also responded to other chemicals such as bile and 5-HT, although typically after latencies of more than 10s, suggesting that other intermediate steps may have been involved. It has recently been reported that both colonic afferents[71] and vagal mechanoreceptors are sensitive to ionotropic glutamate agonists and that channel blockers of both NMDA and non-NMDA channels (memantine and CNQX respectively) can decrease the excitability of endings.[49] However it should be pointed out that mechanotransduction was not blocked even at the highest concentrations of these drugs, which may affect muscle contractility. This suggests that glutamate is neither necessary nor sufficient for mechanotransduction. Rather it appears to be a powerful modulator of mechanosensitive endings in the gut. Again, there are notable differences between species. In the guinea pig, glutamate and agonists did not affect the excitability of vagal mechanoreceptors.[35]

The effects of glutamate are interesting since much of the presynaptic apparatus required for glutamate release appears to be present in IGLEs. It is well established that vagal afferent neurones utilize glutamate as a primary transmitter[72] at their central endings. Several studies have recently shown the presence of vesicular glutamate transporters and elements of the SNARE complex that are involved in fast synaptic transmission, in IGLEs.[35,73] It is possible then that IGLEs release glutamate, which then acts in an autocrine fashion on ionotropic glutamate receptors on the same endings to increase their excitability. This does not appear to be the case in the guinea pig esophagus, where IGLEs appear to lack both ionotropic and metabotropic glutamate receptors[35] but it could occur in other species or regions.

A number of other neurotransmitters and hormones have been reported to modulate firing of vagal mechanoreceptors. These include cholecystokinin,[9] $GABA_B$ agonists,[74,75] metabotropic glutamate agonists,[76,77] bradykinin,[78] and nicotinic agonists.[79] In at least some cases, part or all of the effect of the agonist is mediated indirectly, via changes in muscle activity.[80] In other cases, the effects are probably direct and may reflect the presence of receptors that are functionally important on the central terminals of vagal afferents also being expressed on peripheral endings.

6.7 MOLECULAR BASIS OF TRANSDUCTION IN IGLES

It seems likely that mechanotransduction is directly mediated in IGLEs. The molecular basis of how mechanical deformation of nerve endings is converted into a cellular response has been the subject of intense interest for a number of years. Much of this has been driven by studies in invertebrates in which behavioral screens have been used to identify mutants with defects in mechanotransduction. Leading the way in this endeavor was the nematode *Caenorhabditis elegans*, or rather the investigators who study it. Studies have revealed twelve genes that are essential for normal mechanosensory function by six touch cells in body of C elegans.[81] Mec 4 and Mec 10 appear to be channel proteins, probably part of a heteromeric complex (Mec 2, a stomatin like protein) appears to be involved in intracellular tethering and is located in many mammalian sensory neurons[82] Mec 6, a homologue of mammalian paraoxonases, appears to be an essential part of the channel complex. Other mec genes appear to be largely involved in intracellular tethering to the cytoskeleton or extracellularly to the surrounding matrix. Mammalian mechanoreceptors probably also need equivalent tethering proteins. Thus, the tip links of mammalian hair cells are essential for transduction[83] and cadherin 23 has recently been shown to be one of the components.[84]

The ion channel subunits Mec4 and Mec10 are part of a class of ion channels called the degenerins, named after the effects of gain-of-function mutations that lead to selective death of the cells that express them. These channels share sequence homology with vertebrate epithelial sodium channels (ENaCs), a group of ion channels expressed in many cell types of the body. The Deg/ENaC family of ion channels are characterized by two membrane-spanning domains with a large extracellular loop and short intracellular n and c termini. Acid-sensing ion channels or ASICs are a subclass of the Deg/ENaC family, which are expressed in many mammalian sensory neurones[85] and which can be activated by reductions in pH. There is evidence that ASICs may be involved in mechanotransduction too. Thus ASIC2 knockout mice show reductions in sensitivity of low-threshold, rapidly adapting cutaneous mechanoreceptors,[86] although another study did not replicate this finding.[87] ASIC3 knockout mice showed increased sensitivity to light touch but decreased sensitivity to noxious pinch, suggesting that these channels may form a number of types of heteromeric complexes in different mechanosensory or mechano-nociceptive neurones. It should be pointed out, however, that there is some doubt about the exact role of ASICs in the mechanotransduction complex. It has been reported in cultured dorsal root ganglion cells, from ASIC2 and ASIC3 single and dual knockout mice, that the specific, mechanically activated currents, are unaffected.[88] This suggests that ASICs may, in fact, contribute to the integrative properties of afferent nerve endings rather than to mechanotransduction *per se*. It has recently been suggested that ASIC1 may be involved in mechanotransduction by vagal mechanoreceptors in the mouse esophagus, as in transgenic animals lacking this subunit, mechanosensitivity is enhanced[89] and benzamil sensitivity is altered. Visceral afferents in ASIC2 knockout mice appear to be normal, whereas in ASIC3 knockout mice, tension receptors may be less responsive.[90]

Another subfamily of the Deg/ENaCs, the mammalian ENaCs, has also been implicated for a role in mechanically sensitive primary afferent neurones in mammals, although direct functional evidence of its role is lacking. To date, transgenic mice lacking functional genes for these channels have not been reported. Both beta and gamma ENaC subunits have been localized immunohistochemically in the cell bodies of vagal afferent fibers that project to the aortic arch and gamma ENaC has been shown to be present in the terminal fibers in the aortic arch, in the carotid sinus[91] and in both Merkel cell complexes and Meissners corpuscles in the skin.[92] The role of ENaC subunits in vagal mechanoreceptor function is yet to be determined. Most ASICs and ENaCs are readily blocked by amiloride and its analogues. It is interesting that amiloride is not an effective blocker of IGLEs.[35] Benzamil, its more potent analogue is only effective at very high concentrations (100μM). These observations suggest either that ASICs and ENaCs are not the prime mechanosensitive ion channels in IGLEs, or that they form atypical, possibly heteromeric channel complexes with distinctive pharmacology.

A final set of candidates for mechanosensory channels belongs to a quite different class of ion channels, the Trp channels. Named after the original "transient receptor potential" ion channel located in light sensitive cells in Drosophila, this family of ion channels now has 29 mammalian members, divided into 6 subfamilies.[93] A number of members of the vanilloid receptor subfamily have been shown to be temperature-sensitive and one, TrpV4, can also be osmotically activated and can substitute for osm9 in touch-sensitive cells of *Caenorhabditis elegans*. A number of members of the TrpV family, including TrpV4 have been detected as mRNA transcripts in single nodose ganglion neurones projecting to the stomach.[94] In Drosophila, TRP family members *nompc*[95] and *Nanchung*[96] have been implicated in mechanotransduction in chordotonal organs and Johnston's organ respectively.

From this brief discussion, it is clear that a number of candidate ion channel subunits have been identified that are likely to be involved in mechanotransduction in mammalian and nonmammalian sensory neurones. One remaining challenge is to identify which are important in visceral mechanoreceptors from the vagus nerve. Furthermore, we need to understand how the presence of particular channels can be related to the sensory neurobiology of different functional regions of the gastrointestinal tract. This will require an account of how mechanosensitive ion channels are physically coupled to the surrounding structures. The mechanotransduction complexes represent potential targets for novel drugs that could selectively interfere with vagal afferent activity in a number of disease states.

ACKNOWLEDGMENTS

REFERENCES

1. Grundy, D. and T. Scratcherd, Sensory afferents from the gastrointestinal tract, in *Handbook of Physiology. Section 6. The gastrointestinal system*, J. Wood, Editor, American Physiological Society: Bethesda MD. p. 593–620. 1989.
2. Sengupta, J.N. and G.F. Gebhart, Gastrointestinal afferent fibers and sensation, in *Physiology of the gastrointestinal tract*, L.R. Johnson, Editor. Raven Press: New York. p. 483–519. 1994.
3. Page, A.J. and L.A. Blackshaw, An *in vitro* study of the properties of vagal afferent fibres innervating the ferret oesophagus and stomach. *J Physiol*. 512, 907–16. 1998.
4. Paintal, A.S., Impulses in vagal afferent fibres from stretch receptors in the stomach and their role in the peripheral mechanisms of hunger. *Nature*. 172, 1194–1195. 1953.
5. Adrian, E.D., Afferent impulses in the vagus and their effect on respiration. *J Physiol*. 79, 332–358. 1933.
6. Iggo, A., Tension receptors in the stomach and the urinary bladder. *J. Physiol*. 128, 593–607. 1955.
7. Blackshaw, L.A., D. Grundy, and T. Scratcherd, Vagal afferent discharge from gastric mechanoreceptors during contraction and relaxation of the ferret corpus. *J Autonom Nerv Syst*. 18, 19–24. 1987.
8. Falempin, M., N. Mei, and J.P. Rousseau, Vagal mechanoreceptors of the inferior thoracic oesophagus, the lower oesophageal sphincter and the stomach in the sheep. *Pflugers Archiv European Journal of Physiology*. 373, 25–30. 1978.
9. Davison, J.S. and G.D. Clarke, Mechanical properties and sensitivity to CCK of vagal gastric slowly adapting mechanoreceptors. *Am J Physiol*. 255, G55–61. 1988.
10. Page, A.J., C.M. Martin, and L.A. Blackshaw, Vagal mechanoreceptors and chemoreceptors in mouse stomach and esophagus. *J Neurophysiol*. 87, 2095–103. 2002.
11. Takeshima, T., Functional classification of the vagal afferent discharges in the dog's stomach. *Jap J Smooth Musc Res*. 7, 19–27. 1971.
12. Zagorodnyuk, V.P. and S.J.H. Brookes, Transduction sites of vagal mechanoreceptors in the guinea pig esophagus. *J Neurosci*. 20, 6249–6255. 2000.
13. Zagorodnyuk, V.P., B.N. Chen, and S.J. Brookes, Intraganglionic laminar endings are mechano-transduction sites of vagal tension receptors in the guinea-pig stomach. *J Physiol*. 534, 255–268. 2001.
14. Swett, J.E. and T.W. Schoultz, Mechanical transduction in the Golgi tendon organ: a hypothesis. *Arch Ital Biol*. 113, 374–382. 1975.
15. Hunt, C.C., On the nature of vibration receptors in the hind limb of the cat. *J Physiol*. 155, 175–186. 1961.
16. Tassicker, B.C., et al., Rapid anterograde and retrograde tracing from mesenteric nerve trunks to the guinea pig small intestine in vitro. *Cell Tiss Res*. 295, 437–452. 1998.
17. Lynn, P.A., et al., Rectal intraganglionic laminar endings are transduction sites of extrinsic mechanoreceptors in the guinea pig rectum. *Gastroenterology*. 125, 786–794. 2003.
18. Lawrentjew, B.J., Experimentell-morphologische Studien über den Aufbau des Ganglien des Spieserohre nebst einigen Bemerkungen über das Vorkommen und die Verteilung zweier Arten von Nervenzellen im autonomen Nervensystem. *Z Zellforsch Mikrosk Anat Forsch*. 18, 233–262. 1929.
19. Rodrigo, J., et al., Vegetative innervation of the esophagus. II. Intraganglionic laminar endings. *Acta Anat*. 92, 79–100. 1975.

20. Berthoud, H.R., et al., Distribution and structure of vagal afferent intraganglionic laminar endings (IGLEs) in the rat gastrointestinal tract. *Anat Embryol*. 195, 183–91. 1997.

21. Wang, F.B. and T.L. Powley, Topographic inventories of vagal afferents in gastro-intestinal muscle. *J Comp Neurol*. 421, 302–24. 2000.

22. Berthoud, H.R. and T.L. Powley, Vagal afferent innervation of the rat fundic stomach: morphological characterization of the gastric tension receptor. *J Comp Neurol*. 319, 261–76. 1992.

23. Kressel, M., H.R. Berthoud, and W.L. Neuhuber, Vagal innervation of the rat pylorus: an anterograde tracing study using carbocyanine dyes and laser scanning confocal microscopy. *Cell Tissue Res*. 275, 109–23. 1994.

24. Berthoud, H.R., et al., Vagal sensors in the rat duodenal mucosa: distribution and structure as revealed by in vivo DiI-tracing. *Anat Embryol*. 191, 203–12. 1995.

25. Lynn, P.A. and L.A. Blackshaw, In vitro recordings of afferent fibres with receptive fields in the serosa, muscle and mucosa of rat colon. *J Physiol*. 518, 271–82. 1999.

26. Iggo, A., Gastrointestinal tension receptors with unmyelinated afferent fibres in the vagus of the cat. *Q J Exp Physiol Cogn Med Sci*. 42, 130–143. 1957.

27. Davison, J.S., Response of single vagal afferent fibres to mechanical and chemical stimulation of the gastric and duodenal mucosa in cats. *Q J Exp Physiol Cogn Med Sci*. 57, 405–16. 1972.

28. Powley, T.L. and R.J. Phillips, Musings on the wanderer: what's new in our understanding of vago-vagal reflexes? I. Morphology and topography of vagal afferents innervating the GI tract. [Review] [36 refs]. *Am J Physiol*. 283, G1217–1225. 2002.

29. Phillips, R.J. and T.L. Powley, Tension and stretch receptors in gastrointestinal smooth muscle: re-evaluating vagal mechanoreceptor electrophysiology. *Brain Res Brain Res Rev*. 34, 1–26. 2000.

30. Iggo, A. and A.R. Muir, The structure and function of a slowly adapting touch corpuscle in hairy skin. *J Physiol*. 200, 763–796. 1969.

31. Fagan, B.M. and P.M. Cahusac, Evidence for glutamate receptor mediated transmission at mechanoreceptors in the skin. *Neuroreport*. 12, 341–347. 2001.

32. Ruel, J., et al., AMPA-preferring glutamate receptors in cochlear physiology of adult guinea-pig. *J Physiol*. 518, 667–80. 1999.

33. Hamill, O.P. and B. Martinac, Molecular basis of mechanotransduction in living cells. *Physiol Rev*. 81, 685–740. 2001.

34. Garcia-Anoveros, J., et al., Transport and localization of the DEG/ENaC ion channel BNaC1alpha to peripheral mechanosensory terminals of dorsal root ganglia neurons. *J Neurosci*. 21, 2678–2686. 2001.

35. Zagorodnyuk, V.P., et al., Mechanotransduction by intraganglionic laminar endings of vagal tension receptors in the guinea-pig oesophagus. *J Physiol*. 553, 575–587. 2003.

36. Loewenstein, W.R. and M. Mendelson, Components of receptor adaptation in a Pacinian corpuscle. *J Physiol*. 177, 377-397. 1965

37. Takahashi-Iwanaga, H. and H. Shimoda, The three-dimensional microanatomy of Meissner corpuscles in monkey palmar skin. *J Neurocytol*. 32, 363–371. 2003.

38. Zheng, H., et al., Limited excitatory local effector function of gastric vagal afferent intraganglionic terminals in rats. *Am J Physiol*. 273, G661-9. 1997.

39. Neuhuber, W.L. and N. Clerc, Afferent innervation of the esophagus in cat and rat, in *The Primary Afferent Neuron*, W. Zenker and W.L. Neuhuber, Editors. 1990, Plenum Press: New York. p. 93–107.

40. Malagelada, J.-R. and F. Azpiroz, Determinants of gastric emptying and transit in the small intestine*.*, in *Handbook of Physiology, Section 6: The gastrointestinal tract*, J.D. Wood, Editor. 1989, American Physiological Society: Bethesda. p. 909–937.

41. Cannon, W.B. and C.W. Lieb, The receptive relaxation of the stomach. *Am J Physiol.* 27. 1911.

42. Andrews, P.L., D. Grundy, and T. Scratcherd, Reflex excitation of antral motility induced by gastric distension in the ferret. *J Physiol.* 298, 79–84. 1980.

43. Andrews, P.L. and T. Scratcherd, The gastric motility patterns induced by direct and reflex excitation of the vagus nerves in the anaesthetized ferret. *J Physiol.* 302, 363–78. 1980.

44. Hennig, G.W., S.J.H. Brookes, and M. Costa, Excitatory and inhibitory motor reflexes in the isolated guinea-pig stomach. *J Physiol.* 501, 197–212. 1997.

45. Desai, K.M., W.C. Sessa, and J.R. Vane, Involvement of nitric oxide in the reflex relaxation of the stomach to accommodate food or fluid. *Nature.* 351, 477–479. 1991.

46. Kelly, K., C. Code, and L. Elveback, Patterns of canine gastric electrical activity. *Am J Physiol.* 217, 461-470. 1969

47. Szurszewski, J., Electrical basis for gastrointestinal motility, in *Physiology of the Gastrointestinal Tract.*, L. Johnson, Editor. 1981, Raven: New York. p. 1435–1466.

48. Peles, S., et al., Enhancement of antral contractions and vagal afferent signaling with synchronized electrical stimulation. *Am J Physiol.* 285, G577–585. 2003.

49. Sengupta, J.N., et al., Response properties of antral mechanosensitive afferent fibers and effects of ionotropic glutamate receptor antagonists. *Neuroscience.* 125, 711–723. 2004.

50. Andrews, P.L., D. Grundy, and T. Scratcherd, Vagal afferent discharge from mechanoreceptors in different regions of the ferret stomach. *J Physiol.* 298, 513–524. 1980.

51. Zagorodnyuk, V.P., et al., 4-aminopyridine- and dendrotoxin-sensitive potassium channels influence excitability of vagal mechano-sensitive endings in guinea-pig oesophagus. *Br J Pharmacol.* 137, 1195–1206. 2002.

52. Stevens, R.J., N.G. Publicover, and T.K. Smith, Induction and organization of Ca2+ waves by enteric neural reflexes. *Nature.* 399, 62–66. 1999.

53. Dickens, E.J., G.D. Hirst, and T. Tomita, Identification of rhythmically active cells in guinea-pig stomach. *J Physiol.* 514, 515–531. 1999.

54. Brookes, S.J., et al., Identification of motor neurons to the longitudinal muscle of the guinea pig ileum. *Gastroenterology.* 103, 961–973. 1992.

55. Brookes, S.J., P.A. Steele, and M. Costa, Identification and immunohistochemistry of cholinergic and non-cholinergic circular muscle motor neurons in the guinea-pig small intestine. *Neuroscience.* 42, 863–878. 1991.

56. Michel, K., D. Reiche, and M. Schemann, Projections and neurochemical coding of motor neurones to the circular and longitudinal muscle of the guinea pig gastric corpus. *Pflügers Archiv-European Journal of Physiology.* (in press).

57. Berthoud, H.R., P.A. Lynn, and L.A. Blackshaw, Vagal and spinal mechanosensors in the rat stomach and colon have multiple receptive fields. *Am J Physiol.* 280, R1371–1381. 2001.

58. Gregersen, H., Residual strain in the gastrointestinal tract: a new concept. *Neurogastroenterology & Motility.* 12, 411–414. 2000.

59. Birder, L., et al., Feline interstitial cystitis results in mechanical hypersensitivity and altered ATP release from bladder urothelium. *Am J Physiol.* 285, F423–F429. 2003.

60. Sauer, H., J. Hescheler, and M. Wartenberg, Mechanical strain-induced Ca2+ waves are propagated via ATP release and purinergic receptor activation. *Am J Physiol.* 279, C295–C307. 2000.

61. Arcuino, G., et al., Intercellular calcium signaling mediated by point-source burst release of ATP. *Proc Natl Acad Sci (USA)*. 99, 9840–9845. 2002.
62. Cockayne, D.A., et al., Urinary bladder hyporeflexia and reduced pain-related behaviour in P2X3-deficient mice *Nature*. 407, 1011–1015. 2000.
63. Rong, W., K.M. Spyer, and G. Burnstock, Activation and sensitisation of low and high threshold afferent fibres mediated by P2X receptors in the mouse urinary bladder. *J Physiol*. 541, 591--600. 2002.
64. Wynn, G., et al., Purinergic mechanisms contribute to mechanosensory transduction in the rat colorectum. *Gastroenterology*. 125, 1398–1409. 2003.
65. Burnstock, G., Purine-mediated signalling in pain and visceral perception. *Trends Pharmacol Sci*. 22, 182–188. 2001.
66. Tschumperlin, D.J., et al., Mechanotransduction through growth-factor shedding into the extracellular space. *Nature*. 429, 83–86. 2004.
67. Gao, C. and H. Gregersen, Biomechanical and morphological properties in rat large intestine. *J Biomech*. 33, 1089–1097. 2000.
68. Fox, A.P., M.C. Nowycky, and R.W. Tsien, Kinetic and pharmacological properties distinguishing three types of calcium currents in chick sensory neurones. *J Physiol*. 394, 149–172. 1987.
69. Castelucci, P., et al., The distribution of purine P2X(2) receptors in the guinea-pig enteric nervous system. *Histochem Cell Biol*. 117, 415–422. 2002.
70. Page, A.J., T.A. O'Donnell, and L.A. Blackshaw, P2X purinoceptor-induced sensitization of ferret vagal mechanoreceptors in oesophageal inflammation. *J Physiol*. 523, 403–411. 2000.
71. McRoberts, J.A., et al., Role of peripheral N-methyl-D-aspartate (NMDA) receptors in visceral nociception in rats. *Gastroenterology*. 120, 1737–1748. 2001.
72. Lawrence, A.J., Neurotransmitter mechanisms of rat vagal afferent neurons. *Clin Exp Pharmacol Physiol*. 22, 869–873. 1995.
73. Raab, M. and W.L. Neuhuber, Vesicular glutamate transporter 2 immunoreactivity in putative vagal mechanosensor terminals of mouse and rat esophagus: indication of a local effector function? *Cell Tissue Res*. 312, 141–148. 2003.
74. Page, A.J. and L.A. Blackshaw, GABA(B) receptors inhibit mechanosensitivity of primary afferent endings. *J Neurosci*. 19, 8597–8602. 1999.
75. Zagorodnyuk, V.P., et al., Functional GABAB receptors are present in guinea pig nodose ganglion cell bodies but not in peripheral mechanosensitive endings. *Autonom Neurosci*. 102, 20–29. 2002.
76. Page, A.J., C.M. Martin, and L.A. Blackshaw, Metabotropic glutamate receptors expressed on vagal afferents inhibit mechanosensitivity. *Gastroenterology*. 122, 58. 2002.
77. Young, R.L., et al., Metabotropic glutamate receptors expressed on vagal afferents inhibit mechanosensitivity. *Gastroenterology*. 122, T921. 2002.
78. Sengupta, J.N., J.K. Saha, and R.K. Goyal, Differential sensitivity to bradykinin of esophageal distension-sensitive mechanoreceptors in vagal and sympathetic afferents of the opossum. *J Neurophysiol*. 68, 1053–1067. 1992.
79. Jiang, W., et al., Effects of neuronal nicotinic acetylcholine receptor antagonists on jejunal mesenteric afferent firing evoked by nicotinic agonist DMPP. *Gastroenterology*. 122, S1087. 2002.
80. Grundy, D., V. Bagaev, and K. Hillsley, Inhibition of gastric mechanoreceptor discharge by cholecystokinin in the rat. *Am J Physiol*. 268, G355–360. 1995.
81. Goodman, M.B. and E.M. Schwarz, Transducing touch in Caenorhabditis elegans. *Ann Rev Physiol*. 65, 429–452. 2003.

82. Mannsfeldt, A.G., et al., Stomatin, a MEC-2 like protein, is expressed by mammalian sensory neurons. *Mol Cellular Neurosci.* 13, 391–404. 1999.

83. Pickles, J.O., S.D. Comis, and M.P. Osborne, Cross-links between stereocilia in the guinea pig organ of Corti, and their possible relation to sensory transduction. *Hearing Res.* 15, 103–112. 1984.

84. Siemens, J., et al., Cadherin 23 is a component of the tip link in hair-cell stereocilia.[see comment]. *Nature.* 428, 950–955. 2004.

85. Waldmann, R. and M. Lazdunski, H(+)-gated cation channels: neuronal acid sensors in the NaC/DEG family of ion channels. *Curr Opin Neurobiol.* 8, 418–424. 1998.

86. Price, M.P., et al., The mammalian sodium channel BNC1 is required for normal touch sensation. *Nature.* 407, 1007–1011. 2000.

87. Roza, C., et al., Knockout of the ASIC2 channel does not impair cutaneous mechanonociception, visceral mechanonociception and hearing. *J Physiol.* jphysiol.2004.066001. In press.

88. Drew, L.J., et al., Acid-sensing ion channels ASIC2 and ASIC3 do not contribute to mechanically-activated currents in mammalian sensory neurones. *J Physiol.* 556.3, 691–710. 2004.

89. Page, A.J., The ion channel ASIC1 contributes to visceral but not cutaneous mechanoreceptor function. *Gastroenterology.* 127, 1739–1747, 2004.

90. Blackshaw, L.A., Mechanotransduction in visceral afferents and its modulation: insights from genetic manipulation. *Autonom Neurosci Basic Clin.* 106, 8–9. 2003.

91. Drummond, H.A., M.J. Welsh, and F.M. Abboud, ENaC subunits are molecular components of the arterial baroreceptor complex. *Anns NY Acad Sci.* 940, 42–47. 2001.

92. Drummond, H.A., F.M. Abboud, and M.J. Welsh, Localization of beta and gamma subunits of ENaC in sensory nerve endings in the rat foot pad. *Brain Res.* 884, 1–12. 2000.

93. Chapman, D.E., TRP channels as cellular sensors. *Nature.* 426, 517–524. 2003.

94. Zhang, L., et al., thermosensitive transient receptor potential channels in vagal afferent neurons of the mouse. *Am J Physiol.* 286, G983–991. 2004.

95. Walker, R.G., A.T. Willingham, and C.S. Zuker, A Drosophila mechanosensory transduction channel. *Science.* 287, 2229–2234. 2000.

96. Kim, J., et al., A TRPV family ion channel required for hearing in Drosophila. *Nature.* 424, 81–84. 2003.